

UNIVERSITY OF YAOUNDE I

POSTGRADUATE SCHOOL OF SCIENCE TECHNOLOGY
AND GEOSCIENCE



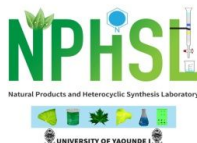
UNIVERSITE DE YAOUNDE I

CENTRE DE RECHERCHE ET DE FORMATION
DOCTORALES EN SCIENCES TECHNOLOGIES ET
GEOSCIENCES

DOCTORAL RESEARCH UNIT FOR CHEMISTRY AND APPLICATION
UNITE DE RECHERCHE ET DE FORMATION DOCTORALE EN CHIMIE ET APPLICATION

DEPARTMENT OF ORGANIC CHEMISTRY
DEPARTEMENT DE CHIMIE ORGANIQUE

NATURAL PRODUCTS
AND HETEROCYCLIC
SYNTHESIS LABORATORY



LABORATOIRE DE PRODUITS
NATURELS ET DE SYNTHESE DES
HETEROCYCLES

**CHEMICAL AND PHARMACOLOGICAL
STUDIES OF TWO MEDICINAL PLANTS:
TABERNAEMONTANA CONTORTA STAPF AND
TABERNAEMONTANA INCONSPICUA STAPF
(APOCYNACEAE)**

THESIS

Submitted and defended publicly in fulfilment of the requirements for the award of the
Doctorate /PhD degree in Organic Chemistry

By

FOUDJO MELACHEU Gertrude Laura

Reg.: 07T141

Master in Organic chemistry

Co-supervised By


WANDJI Jean
Professor

and

Elisabeth SEGUIN
Professor



2021

THE UNIVERSITY OF YAOUNDE I Faculty of Science Division of Programming and Follow-up of Academic Affairs		UNIVERSITÉ DE YAOUNDÉ I Faculté des Sciences Division de la Programmation et du Suivi des Activités Académiques
LIST OF PERMANENT TEACHING STAFF		LISTE DES ENSEIGNANTS PERMANENTS

ACADEMOC YEAR 2019/2020

(By Department and by Grade)

Last updated 03 march 2020

ADMINISTRATION

DEAN: TCHOUANKEU Jean- Claude, Associate professor

VICE-Dean in charge of Academic Affairs: ATCHADE Alex de Theodore, Associate professor

VICE-DOYEN in charge of Student Affairs: AJEAGAH Gideon AGHAINDUM, Professor

VICE-DOYEN in charge of Research and cooperation: ABOSSOLO Monique, Associate professor

Head of Administrative and Financial Division: NDOYE FOE Marie C. F., Associate professor

Head of Academic Affairs Division, Keeping of terms and research: MBAZE MEVA'A Luc Leonard, Professor.

1- DEPARTEMENT OF BIOCHEMISTRY (BC) (39)			
N°	NOMS ET PRÉNOMS	GRADE	OBSERVATIONS
1	BIGOGA DIAGA Jude	Professor	In service
2	FEKAM BOYOM Fabrice	Professor	In service
3	FOKOU Elie	Professor	In service
4	KANSCI Germain	Professor	In service
5	MBACHAM FON Wilfried	Professor	In service
6	MOUNDIPA FEWOU Paul	Professor	Head of Department
7	NINTCHOM PENLAP V. <i>épse</i> BENG	Professor	In service
8	OBEN Julius ENYONG	Professor	In service

9	ACHU Merci BIH	Associate Professor	In service
10	ATOGHO Barbara Mma	Associate Professor	In service
11	AZANTSA KINGUE GABIN BORIS	Associate Professor	In service
12	BELINGA née NDOYE FOE M. C. F.	Associate Professor	Chief DAF / FS
13	BOUDJEKO Thaddée	Associate Professor	In service
14	DJUIDJE NGOUNOUE Marcelline	Associate Professor	In service
15	EFFA NNOMO Pierre	Associate Professor	In service
16	NANA Louise épouse WAKAM	Associate Professor	In service
17	NGONDI Judith Laure	Associate Professor	In service
18	NGUEFACK Julienne	Associate Professor	In service
19	NJAYOU Frédéric Nico	Associate Professor	In service
20	MOFOR née TEUGWA Clotilde	Associate Professor	Inspector of Service MINESUP
21	TCHANA KOUATCHOUA Angèle	Associate Professor	In service
22	AKINDEH MBUH NJI	Senior Lecturer	In service
23	BEBOY EDZENGUELE Sara Nathalie	Senior Lecturer	In service
24	DAKOLE DABOY Charles	Senior Lecturer	In service
26	DJUIKWO NKONGA Ruth Viviane	Senior Lecturer	In service
27	DONGMO LEKAGNE Joseph Blaise	Senior Lecturer	In service
28	EWANE Cécile Anne	Senior Lecturer	In service
29	FONKOUA Martin	Senior Lecturer	In service
30	BEBEE Fadimatou	Senior Lecturer	In service
31	KOTUE KAPTUE Charles	Senior Lecturer	In service
32	LUNGA Paul KEILAH	Senior Lecturer	In service
33	MANANGA Marlyse Joséphine	Senior Lecturer	In service
34	MBONG ANGIE M. Mary Anne	Senior Lecturer	In service
35	PECHANGOU NSANGO Sylvain	Senior Lecturer	In service
36	Palmer MASUMBE NETONGO	Senior Lecturer	In service
37	MBOUCHE FANMOE Marcelline Joëlle	Assistant Lecturer	In service
38	OWONA AYISSI vincent Brice	Assistant Lecturer	In service
39	WILFRED ANGIE Abia	Assistant Lecturer	In service

2- DEPARTMENT OF ANIMAL BIOLOGY AND PHYSIOLOGY (ABP) (43)			
1	AJEAGAH Gideon AGHAINDUM	Professor	Vice-Dean / DSSE
2	BILONG BILONG Charles-Félix	Professor	Head of Department
3	DIMO Théophile	Professor	In service
4	DJIETO LORDON Champlain	Professor	In service
5	ESSOMBA née NTSAMA MBALA	Professor	Vice-Dean/FMSB/UII
6	FOMENA Abraham	Professor	In service
7	KAMTCHOUING Pierre	Professor	In service
8	NJAMEN Dieudonné	Professor	In service
9	NJIOKOU Flobert	Professor	In service
10	NOLA Moïse	Professor	In service
11	TAN Paul VERNYUY	Professor	In service
12	TCHUEM TCHUENTE Louis Albert	Professor	Service Inspector Coord. Progr. /MINSANTE
13	ZEBAZE TOGOUET Serge Hubert	Professor	In service
14	BILANDA Danielle Claude	Associate Professor	In service
15	DJIOGUE Séfirin	Associate Professor	In service
16	DZEUFUET DJOMENI Paul Désiré	Associate Professor	In service
17	JATSA BOUKENG Hermine épouse MEGAPTCHÉ	Associate Professor	In service
18	KEKEUNOU Sévilor	Associate Professor	In service
19	MEGNEKOU Rosette	Associate Professor	In service
20	MONY Ruth épouse NTONE	Associate Professor	In service
21	NGUEGUIM TSOFAK Florence	Associate Professor	In service
22	TOMBI Jeannette	Associate Professor	In service
23	ALENE Désirée Chantal	Senior Lecturer	In service
26	ATSAMO Albert Donatien	Senior Lecturer	In service
27	BELLET EDIMO Oscar Roger	Senior Lecturer	In service
28	DONFACK Mireille	Senior Lecturer	In service
29	ETEME ENAMA Serge	Senior Lecturer	In service
30	GOUNOUE KAMKUMO Raceline	Senior Lecturer	In service

31	KANDEDA KAVAYE Antoine	Senior Lecturer	In service
32	LEKEUFACK FOLEFACK Guy B.	Senior Lecturer	In service
33	MAHOB Raymond Joseph	Senior Lecturer	In service
34	MBENOUN MASSE Paul Serge	Senior Lecturer	In service
35	MOUNGANG LucianeMarlyse	Senior Lecturer	In service
36	MVEYO NDANKEU Yves Patrick	Senior Lecturer	In service
37	NGOUATEU KENFACK Omer Bébé	Senior Lecturer	In service
38	NGUEMBOK	Senior Lecturer	In service
39	NJUA Clarisse Yafi	Senior Lecturer	Chief Div. UBA
40	NOAH EWOTI Olive Vivien	Senior Lecturer	In service
41	TADU Zephyrin	Senior Lecturer	In service
42	YEDE	Senior Lecturer	In service
43	KOGA MANG DOBARA	Assistant Lecturer	In service

3- DEPARTMENT OF PLANT BIOLOGY AND PHYSIOLOGY (PBP) (25)			
1	AGWARA ONDOH Moïse	Professor	Vice Rector Univ. Bamenda
2	BELL Joseph Martin	Professor	In service
3	DJOCGOUE Pierre François	Professor	In service
4	MOSSEBO Dominique Claude	Professor	In service
5	YOUMBI Emmanuel	Professor	Head of Department
6	ZAPFACK Louis	Professor	In service
7	ANGONI Hyacinthe	Associate Professor	In Service
8	BIYE Elvire Hortense	Associate Professor	In Service
9	KENGNE NOUMSI Ives Magloire	Associate Professor	In Service
10	MALA Armand William	Associate Professor	In Service
11	MBARGA BINDZI Marie Alain	Associate Professor	CT/ MINESUP
12	MBOLO Marie	Associate Professor	In Service
13	NDONGO BEKOLO	Associate Professor	CE / MINRESI
14	NGONKEU MAGAPTCHE Eddy L.	Associate Professor	In Service
15	TSOATA Esaïe	Associate Professor	In Service
16	TONFACK Libert Brice	Associate Professor	In Service
17	DJEUANI Astride Carole	Senior Lecturer	In Service

18	GOMANDJE Christelle	Senior Lecturer	In Service
19	MAFFO MAFFO Nicole Liliane	Senior Lecturer	In Service
20	MAHBOU SOMO TOUKAM. Gabriel	Senior Lecturer	In Service
21	NGALLE Hermine BILLE	Senior Lecturer	In Service
22	NGOOU Lucas Vincent	Senior Lecturer	In Service
23	NNANGA MEBENGA Ruth Laure	Senior Lecturer	In Service
24	NOUKEU KOUAKAM Armelle	Senior Lecturer	In Service
25	ONANA JEAN MICHEL	Senior Lecturer	In Service

4- DEPARTMENT OF INORGANIC CHEMISTRY (IC) (32)			
1	AGWARA ONDOH Moïse	Professor	Vice Rector Univ. Bamenda
2	ELIMBI Antoine	Professor	In service
3	Florence UFI CHINJE épouse MELO	Professor	Rector Univ.Ngaoundere
4	GHO GOMU Paul MINGO	Professor	Minister in Charge of Miss. PR
5	NANSEU NJIKI Charles Péguy	Professor	In service
6	NDIFON Peter TEKE	Professor	CT MINRESI/Head of Department
7	NGOMO Horace MANGA	Professor	Vice Chancellor/UB
7	NDIKONTAR Maurice KOR	Professor	Vice-Dean Univ. Bamenda
8	NENWA Justin	Professor	In service
9	NGAMENI Emmanuel	Professor	Dean FS UDs
10	BABALE née DJAM DOUDOU	Associate Professor	Chargée Mission P.R.
11	DJOUFAC WOU MFO Emmanuel	Associate Professor	In service
12	KAMGANG YOUNBI Georges	Associate Professor	In service
13	KEMMEGNE MBOUGUEM Jean C.	Associate Professor	In service
14	KONG SAKEO	Associate Professor	In service
15	NDI NSAMI Julius	Associate Professor	In service
17	NJIOMOU C. épouse DJANGANG	Associate Professor	In service
18	NJOYA Dayirou	Associate Professor	In service
19	YOUNANG Elie	Associate Professor	In service
20	ACAYANKA Elie	Senior Lecturer	In service

21	BELIBI BELIBI Placide Désiré	Senior Lecturer	CS/ ENS Bertoua
22	CHEUMANI YONA Arnaud M.	Senior Lecturer	In service
23	EMADACK Alphonse	Senior Lecturer	In service
24	KENNE DEDZO GUSTAVE	Senior Lecturer	In service
25	KOUOTOU DAOUDA	Senior Lecturer	In service
26	MAKON Thomas Beauregard	Senior Lecturer	In service
27	MBEY Jean Aime	Senior Lecturer	In service
28	NCHIMI NONO KATIA	Senior Lecturer	In service
29	NEBA <i>née</i> NDOSIRI Bridget NDOYE	Senior Lecturer	CT/ MINFEM
30	NYAMEN Linda Dyorisse	Senior Lecturer	In service
31	PABOUDAM GBAMBIE A.	Senior Lecturer	In service
32	TCHAKOUTE KOUAMO Hervé	Senior Lecturer	In service

5- DEPARTMENT OF ORGANIC CHEMISTRY (OC) (32)			
1	DONGO Etienne	Professor	Vice-Dean / PSAA
2	GHOOMU TIH Robert Ralph	Professor	Dir. IBAF/UDA
3	NGOUELA Silvère Augustin	Professor	In service
4	NKENGFACK Augustin Ephreïm	Professor	Head of Department
5	NYASSE Barthélemy	Professor	In service
6	PEGNYEMB Dieudonné Emmanuel	Professor	Director/ MINESUP
7	WANDJI Jean	Professor	In service
8	Alex de Théodore ATCHADE	Associate Professor	DEPE/ Rectorat/UYI
9	EYONG Kenneth OBEN	Associate Professor	Chief Service DPER
10	FOLEFOC Gabriel NGOSONG	Associate Professor	In service
11	FOTSO WABO Ghislain	Associate Professor	In service
12	KEUMEDJIO Félix	Associate Professor	In service
13	KEUMOGNE Marguerite	Associate Professor	In service
14	KOUAM Jacques	Associate Professor	In service
15	MBAZOA <i>née</i> DJAMA Céline	Associate Professor	In service
16	MKOUNGA Pierre	Associate Professor	In service
17	NOTE LOUGBOT Olivier Placide	Associate Professor	Chief Service/MINESUP
18	NGO MBING Joséphine	Associate Professor	<i>Sous/Direct. MINERESI</i>

19	NGONO BIKOBO Dominique Serge	Associate Professor	In service
20	NOUNGOUE TCHAMO Diderot	Associate Professor	In service
21	TABOPDA KUATE Turibio	Associate Professor	In service
22	TCHOUANKEU Jean-Claude	Associate Professor	Dean /FS/ UYI
23	TIH née NGO BILONG E. Anastasie	Associate Professor	In service
24	YANKEP Emmanuel	Associate Professor	In service
25	AMBASSA Pantaléon	Senior Lecturer	In service
26	KAMTO Eutrophe Le Doux	Senior Lecturer	In service
27	MVOT AKAK CARINE	Senior Lecturer	In service
28	NGNINTEDO Dominique	Senior Lecturer	In service
29	NGOMO Orléans	Senior Lecturer	In service
30	OUAHOUE WACHE Blandine M.	Senior Lecturer	In service
31	TAGATSING FOTSING Maurice	Senior Lecturer	In service
32	ZONDENDEGOUNBA Ernestine	Senior Lecturer	In service

6- DEPARTMENT OF COMPUTER SCIENCE (CS) (25)			
1	ATSA ETOUNDI Roger	Professor	Chief Div.MINESUP
2	FOUDA NDJODO Marcel Laurent	Professor	Head of department ENS/Chief IGA.MINESUP
3	NDOUNDAM René	Associate Professor	In service
4	AMINOUE Halidou	Senior Lecturer	In service
5	DJAM XAVIERA YOUH - KIMBI	Senior Lecturer	In service
6	EBELE Serge Alain	Senior Lecturer	In service
7	KOUOKAM KOUOKAM E. A.	Senior Lecturer	In service
8	MELATAGIA YONTA Paulin	Senior Lecturer	In service
9	MOTO MPONG Serge Alain	Senior Lecturer	In service
10	TAPAMO Hyppolite	Senior Lecturer	In service
11	ABESOLO ALO'O Gislain	Senior Lecturer	In service
12	KAMGUEU Patrick Olivier	Senior Lecturer	In service
13	MONTHÉ DJIADEU Valéry M.	Senior Lecturer	In service
14	OLLE OLLE Daniel Claude Delort	Senior Lecturer	C/D Enset. Ebolowa

15	TINDO Gilbert	Senior Lecturer	In service
16	TSOPZE Norbert	Senior Lecturer	In service
17	WAKU KOUAMOU Jules	Senior Lecturer	In service
18	BAYEM Jacques Narcisse	Assistant Lecturer	In service
19	DOMGA KOMGUEM Rodrigue	Assistant Lecturer	In service
20	HAMZA Adamou	Assistant Lecturer	In service
21	JIOMEKONG AZANZI Fidel	Assistant Lecturer	In service
22	KAMDEM KENGNE Christiane	Assistant Lecturer	In service
23	MAKEMBE. S. Oswald	Assistant Lecturer	In service
24	MEYEMDOU Nadège Sylvianne	Assistant Lecturer	In service
25	NKONDOCK. MI. BAHANACK.N.	Assistant Lecturer	In service

7- DEPARTMENT OF MATHEMATICS (MA) (26)			
1	AYISSI Raoult Domingo	Associate Professor	Head of Department
2	EMVUDU WONO Yves S.	Associate Professor	CD Info/ Chief division MINESUP
3	NKUIMI JUGNIA Célestin	Associate Professor	In service
4	NOUNDJEU Pierre	Associate Professor	In service
5	MBEHOU Mohamed	Associate Professor	In service
6	TCHAPNDA NJABO Sophonie B.	Associate Professor	Director/AIMS Rwanda
7	AGHOUKENG JIOFACK Jean Gérard	Senior Lecturer	Chief Cell MINPLAMAT
8	CHENDJOU Gilbert	Senior Lecturer	In service
9	DJIADEU NGAHA Michel	Senior Lecturer	In service
10	DOUANLA YONTA Herman	Senior Lecturer	In service
11	FOMEKONG Christophe	Senior Lecturer	In service
12	KIANPI Maurice	Senior Lecturer	In service
13	KIKI Maxime Armand	Senior Lecturer	In service
14	MBAKOP Guy Merlin	Senior Lecturer	In service
15	MBANG Joseph	Senior Lecturer	In service
16	MBELE BIDIMA Martin Ledoux	Senior Lecturer	In service
17	MENGUE MENGUE David Joe	Senior Lecturer	In service
18	NGUEFACK Bernard	Senior Lecturer	In service

19	NIMPA PEFOUNKEU Romain	Senior Lecturer	In service
20	POLA DOUNDOU Emmanuel	Senior Lecturer	In service
21	TAKAM SOH Patrice	Senior Lecturer	In service
22	TCHANGANG Roger Duclos	Senior Lecturer	In service
23	TCHOUNDJA Edgar Landry	Senior Lecturer	In service
24	TETSADJIO TCHILEPECK M. E.	Senior Lecturer	In service
25	TIAYA TSAGUE N. Anne-Marie	Senior Lecturer	In service
26	MBIAKOP Hilaire George	Assistant Lecturer	In service

8- DEPARTEMENT OF MICROBIOLOGY (MIB) (12)

1	ESSIA NGANG Jean Justin	Professor	DRV/IMPM
2	BOYOMO ONANA	Associate Professor	In service
3	NWAGA Dieudonné M.	Associate Professor	In service
4	NYEGUE Maximilienne Ascension	Associate Professor	In service
5	RIWOM Sara Honorine	Associate Professor	In service
6	SADO KAMDEM Sylvain Leroy	Associate Professor	In service
7	ASSAM ASSAM Jean Paul	Senior Lecturer	In service
8	BODA Maurice	Senior Lecturer	In service
9	BOUGNOM Blaise Pascal	Senior Lecturer	In service
10	ESSONO OBOUGOU Germain G.	Senior Lecturer	In service
11	NJIKI BIKOÏ Jacky	Senior Lecturer	In service
12	TCHIKOUA Roger	Senior Lecturer	In service

9. DEPARTMENT OF PHYSICS (PHY) (40)

1	BEN- BOLIE Germain Hubert	Professor	In service
2	ESSIMBI ZOBO Bernard	Professor	In service
3	KOFANE Timoléon Crépin	Professor	In service
4	NANA ENGO Serge Guy	Professor	In service
5	NDJAKA Jean Marie Bienvenu	Professor	Head of Department
6	NOUAYOU Robert	Professor	In service
7	NJANDJOCK NOUCK Philippe	Professor	<i>Sous Directeur/ MINRESI</i>

8	PEMHA Elkana	Professor	In service
9	TABOD Charles TABOD	Professor	Dean Univ/Bda
10	TCHAWOUA Clément	Professor	In service
11	WOAFO Paul	Professor	In service
12	BIYA MOTTO Frédéric	Associate Professor	DG/HYDRO Mekin
13	BODO Bertrand	Associate Professor	In service
14	DJUIDJE KENMOE épouse ALOYEM	Associate Professor	In service
15	EKOBENA FOUA Henri Paul	Associate Professor	Chief Division. UN
16	EYEBE FOUA Jean sire	Associate Professor	In service
17	FEWO Serge Ibraïd	Associate Professor	In service
18	HONA Jacques	Associate Professor	In service
19	MBANE BIOUELE César	Associate Professor	In service
20	NANA NBENDJO Blaise	Associate Professor	In service
21	NDOP Joseph	Associate Professor	In service
22	SAIDOU	Associate Professor	MINERESI
23	SIEWE SIEWE Martin	Associate Professor	In service
24	SIMO Elie	Associate Professor	In service
25	VONDOU Derbetini Appolinaire	Associate Professor	In service
26	WAKATA née BEYA Annie	Associate Professor	Sous Directeur/ MINESUP
27	ZEKENG Serge Sylvain	Associate Professor	In service
28	ABDOURAHIMI	Senior Lecturer	In service
29	EDONGUE HERVAIS	Senior Lecturer	In service
30	ENYEGUE A NYAM épouse BELINGA	Senior Lecturer	In service
31	FOUEDJIO David	Senior Lecturer	Chief Cell. MINADER
32	MBINACK Clément	Senior Lecturer	In service
33	MBONO SAMBA Yves Christian U.	Senior Lecturer	In service
34	MELI'I Joelle Larissa	Senior Lecturer	In service
35	MVOGO ALAIN	Senior Lecturer	In service
38	OBOUNOU Marcel	Senior Lecturer	DA/Univ Inter Etat/Sangmalima
39	WOULACHE Rosalie Laure	Senior Lecturer	In service
40	CHAMANI Roméo	Assistant Lecturer	In service

10- DEPARTMENT OF EARTH SCIENCES (ES) (41)			
1	BITOM Dieudonné	Professor	Dean / FASA / Uds
2	FOUATEU Rose épouse YONGUE	Professor	In service
3	KAMGANG Pierre	Professor	In service
4	NDJIGUI Paul Désiré	Professor	Head of Department
5	NDAM NGOUPAYOU Jules-Remy	Professor	In service
6	NGOS III Simon	Professor	DAAC/Uma
7	NKOUMBOU Charles	Professor	In service
8	NZENTI Jean-Paul	Professor	In service
9	ABOSSOLO née ANGUE Monique	Associate Professor	Vice-Dean / DRC
10	GHOGOMU Richard TANWI	Associate Professor	CD/Uma
11	MOUNDI Amidou	Associate Professor	CT/ MINIMDT
12	NGUEUTCHOUA Gabriel	Associate Professor	CEA/MINRESI
13	NJILAH Isaac KONFOR	Associate Professor	In service
14	ONANA Vincent Laurent	Associate Professor	In service
15	BISSO Dieudonné	Associate Professor	Director/Projet Barrage Memve'ele
16	EKOMANE Emile	Associate Professor	In service
17	GANNO Sylvestre	Associate Professor	In service
18	NYECK Bruno	Associate Professor	In service
19	TCHOUANKOUE Jean-Pierre	Associate Professor	In service
20	TEMDJIM Robert	Associate Professor	In service
21	YENE ATANGANA Joseph Q.	Associate Professor	Chief Div. /MINTP
22	ZO'O ZAME Philémon	Associate Professor	DG/ART
23	ANABA ONANA Achille Basile	Senior Lecturer	In service
24	BEKOA Etienne	Senior Lecturer	In service
25	ELISE SABABA	Senior Lecturer	In service
26	ESSONO Jean	Senior Lecturer	In service
27	EYONG JOHN TAKEM	Senior Lecturer	In service
28	FUH Calistus Gentry	Senior Lecturer	Sec. D'Etat/MINMIDT
29	LAMILLEN BILLA Daniel	Senior Lecturer	In service

30	MBESSE CECILE OLIVE	Senior Lecturer	In service
31	MBIDA YEM	Senior Lecturer	In service
32	METANG Victor	Senior Lecturer	In service
33	MINYEM Dieudonné-Lucien	Senior Lecturer	CD/Uma
34	NGO BELNOUN Rose Noël	Senior Lecturer	In service
35	NGO BIDJECK Louise Marie	Senior Lecturer	In service
36	NOMO NEGUE Emmanuel	Senior Lecturer	In service
37	NTSAMA ATANGANA Jacqueline	Senior Lecturer	In service
38	TCHAKOUNTE J. <i>épse</i> NOUMBEM	Senior Lecturer	Chief cell / MINRESI
39	TCHAPCHET TCHATO De P.	Senior Lecturer	In service
40	TEHNA Nathanaël	Senior Lecturer	In service
41	TEMGA Jean Pierre	Senior Lecturer	In service

Classification of teaching staff by Department

Number of Lecturers					
Department	Professors	Associate Professors	Senior Lecturer	Assistant Lecturer	Total
BCH	8 (1)	13 (6)	15 (11)	1 (1)	37 (19)
BPA	13 (1)	9 (6)	18 (05)	1 (0)	41 (12)
BPV	6 (0)	10 (2)	10 (07)	0 (0)	26 (9)
CI	10 (1)	9 (2)	13 (3)	0 (0)	32 (6)
CO	7 (0)	17 (4)	8 (3)	0 (0)	32 (7)
IN	2 (0)	1 (0)	14 (0)	10 (3)	27 (3)
MAT	1 (0)	6 (1)	19 (1)	1 (0)	27 (2)
MIB	1 (0)	5 (2)	5 (1)	0 (0)	11 (3)
PHY	11 (0)	16 (2)	11 (3)	1 (0)	39 (5)
ST	9 (1)	14 (1)	20 (5)	0 (0)	43 (7)
	68 (4)		133 (37)	14 (4)	315(71)

Total **100 (26)**

A total of 315 (71) including :

- **Professors** **68 (4)**
- **Associate professors** **100 (25)**
- **Senior lecturers** **133 (39)**
- **Assistant Lecturers** **14 (5)**

() = No. of women

DEDICATION

To my grand father Melachio Mathias

ACKNOWLEDGEMENTS

My sincere appreciations go to:

- My supervisors, Pr. J. WANDJI and Pr. E. SEGUIN for their constant support, great patience, guidance, encouragement, constructive criticisms, advice and vast knowledge of Natural Product Chemistry have been invaluable.
- My academic mother Pr. C. D. MBAZOA for her support and encouragements.
- Pr. A. E. NKENGFAK, the Head of Department of Organic Chemistry, for his encouragements, dynamism and sound administration and to all the teachers of the Department of Organic chemistry for their support.
- Pr. Dr. Dr. M. SPITTELER and the Institute of Environmental Research, Department of Chemistry, TU Dortmund university, Germany, Pr. S. MICHEL, Pr. M. C. LALLEMAND, Dr. H. DUFAT of the University of Paris Descartes.
- Pr. W. Fei and the Key Laboratory of Natural Medicine and Clinical Translation, Chengdu Institute of Biology, Chinese Academy of Sciences, Chengdu, and Dr. E. MFOTIE NJOYA, of the Department of Biochemistry for running of tests.
- Dr. J.-B. JOUDA, Dr. J. CHI SHIRRI and Dr. S.V. FANNANG, for their co-operation and assistance.
- All the members of our research team especially K. B. WAKEU, V. W. CHIMEZE, M. R. TALLA for the memorable time spent in the laboratory.
- ALL my classe mates especially C. C. WALEGUELE and D. U. KAGHO for the unforgettable time spent on the bench and for their support.
- My husband R. M. TANEKEU and children T. A. FOPA, T. F. N. FOELEFACK and T. B. TSAYEM for their patience, concern, constant encouragement, financial and moral support.
- All the members of my family especially my mothers M. R. FOPA, M. Y. TSAYEM, J. DJUISSI, M. A. GUEMFO and fathers M. MELACHIO, G. CHANYON, S. NKENG NGAH for their patience, moral and financial support.

The realization of a work of this nature could not have been possible without many hands on the plough. Many thanks equally go to those not mentioned who contributed in one way or the other to the success of this work.

TABLE OF CONTENT

DEDICATION	xiv
ACKNOWLEDGEMENTS	xv
TABLE OF CONTENT	xvi
LIST OF ABBREVIATIONS	xx
LIST OF TABLES	xxii
LIST OF FIGURES	xxiv
LIST OF SCHEMES	xxviii
ABSTRACT	xxix
RESUME	xxx
GENERAL INTRODUCTION	1
CHAPTER I. LITERATURE REVIEW	3
I.1. BOTANICAL ASPECT OF <i>TABERNAEMONTANA CONTORTA</i> AND <i>TABERNAEMONTANA INCONSPICUA</i>	4
I.1.1. General information on the family Apocynaceae	4
I.1.2. General information on the genus <i>Tabernaemontana</i>	4
I.1.2. 1 General information on <i>Tabernaemontana contorta</i>	4
I.1.2.2 General information on <i>Tabernaemontana inconspicua</i>	5
I.1.3. Uses of plants of the genus <i>Tabernaemontana</i>	6
I.1.3.1. Medicinal uses	6
I.1.3.2. Economic uses	7
I.2. CHEMICAL AND BIOLOGICAL STUDIES OF THE GENUS <i>TABERNAEMONTANA</i>	7
I.2.1. Alkaloids	8
I.2.1.1. General information on alkaloids	8
I.2.1.2. Classification of alkaloids	9
I.2.1.3. Monoterpene indole alkaloids	9
I.2.1.4. Biosynthesis of monoterpene indole alkaloids	11
I.2.1.5. Monoterpene indole alkaloids isolated from plants of the genus <i>Tabernaemontana</i> ...	12

I.2.1.6. Biological activities of alkaloids from the genus <i>Tabernaemontana</i>	16
-Anticancer activity	16
I.2.2. Pentacyclic triterpenoids	18
I.2.2.1. General information on terpenes.....	18
I.2.2.2. Triterpenes	19
I.2.2.3. Biosynthesis of triterpenoids	20
I.2.2.4. Triterpenes isolated from plants of the genus <i>Tabernaemontana</i>	23
I.2.2.5. Biological activity of triterpenoids isolated from plants of the genus <i>Tabernaemontana</i>	25
I.3. CANCER	26
I.3.1. Definition	26
I.3.2. Causes of cancer.....	27
I.3.2.1. Life style and environment	27
I.3.2.2. Age	28
I.3.3 Types of cancer	29
I.3.4 Symptoms and signs of cancer.....	30
I.3.6 Treatment for cancer.....	32
I.3.7 Prevention of cancer	32
I.3.7 Anti-cancer and anti-inflammatory effect	33
CHAPTER II. RESULTS AND DISCUSSION	35
II.1. INTRODUCTION	36
II.2. CHARACTERIZATION OF ISOLATED COMPOUNDS	39
II.2.1. Alkaloids.....	39
II.2.1.1. Characterization of TCO ₃	39
II.2.1.2. Characterization of TCO ₅	46
II.2.1.3. Characterization of TiS ₅	53
II.2.1.4. Identification of TiS ₁₀	58
II.2.1.5. Identification of TiS ₆ = TCO ₇	63
II.2.1.6. Identification of TC ₅	68
II.2.1.7. Identification of TiS ₇	71
II.2.1.8. Identification of TC ₆	74
II.2.1.9. Identification of TiS ₈	79
II.2.2. Triterpenoids.....	83

II.2.2.1. Characterisation of TCO ₉	83
II.2.2.2. Identification of TC ₄ =TCO ₄	89
II.2.2.3. Identification of TiS ₃	92
II.2.2.4. Identification of TCO ₈	96
II.2.2.5. Identification of TiS ₉	99
II.2.2.6. Identification of TC ₃	102
II.2.2.7. Identification of TiS ₂	105
II.2.2.8. Identification of TiS ₄	107
II.2.3 Steroids.....	108
II.2.3.1 Identification of TCO ₁ =TC ₂ =TiS ₁	108
II.2.3.2. Identification of TCO ₁₈ =TC ₁₆	110
II.2.3.3. Identification of TiS ₁₄	111
II.2.4. Monoterpenes.....	112
II.2.4.1. Identification of TCO ₂	112
II.2.4 lipids.....	115
II.2.4.1. Characterization of TiS ₁₅	115
II.2.4.2.Characterisation of TCO ₁₉	120
II.2.4.3.Characterisation of TCO ₂₀	122
II.2.4.4 Characterisation of TC ₁₂	124
II.2.4.5.Characterisation of TCO ₁₄	127
II.2.4.6.Identification of TiS ₁₃ =TC ₇	129
II.2.4.7. Identification of TC ₁	131
II.3. BIOLOGICAL TESTS ON SOME ISOLATED COMPOUNDS.....	133
II.3.1. Cytotoxic effect.....	133
II.3.2. Anti-inflammatory assay.....	134
CONCLUSION AND PERSPECTIVES.....	135
CHAPTER III. GENERAL EXPERIMENT.....	137
III.1. GENERAL EXPERIMENTAL PROCEDURES.....	138
III.2. CHARACTERISTIC ANALYTICAL TESTS.....	138
III.3. MATERIALS.....	139
III.3.1. Plant material.....	139
III.4. EXTRACTION AND ISOLATION OF COMPOUNDS.....	140
III.4.1. Extraction.....	140

III.4.2. Isolation	140
III.5. BIOLOGICAL TESTS	149
0III.5.1. Cytotoxicity	149
III.5.1.1. Cytotoxic effect of compound TiS_5	149
III.5.2. Anti-inflammatory assay	150
III.5.2.1. Cell culture	150
III.5.2.2. Cell viability assay	150
III.5.2.3. Nitric Oxide measurement	150
III.6. PHYSICO-CHEMICAL PROPERTIES OF COMPOUNDS DESCRIBED	151
REFERENCES.....	157

LIST OF ABBREVIATIONS

DNA	Deoxyribonucleic acid
IC ₅₀	Half maximal inhibitory concentration
COX-2	cyclooxygenase
HIV	Human Immunodeficiency Virus
CNS	Cantral Nervous System
FDA	Food and Drug Adminidtration
CDC	Centers for Disease Control
NCI	International Cancer Institute
RT	Room temperature
DMSO	dimethylsulfoxide
EA	Ethylacetate
Hex	Hexane
EI	Electronic Impact
FAB	Fast Atom Bombardment
ev	Electron volts
MHz	megaHertz
UV	ultraviolet
SEM	Standard error of mean
HSQC	Heteronuclear single quantum coherence
HMBC	Heteronuclear multiple bond correlation
COSY	Correlation spectroscopy
HRESI-MS	High resolution electrospray ionization mass spectrum
TLC	Thin layer chromatography
J (Hz)	Coupling constant expressed in Hertz
m/z	Masse to charge ratio
ppm	Parts per million
ov	overlape
¹ H NMR	Proton Nuclear Magnetic Resonance
¹³ C NMR	Carbon-13 Nuclear Magnetic Resonance
s	Singlet
d	Doublet

dd	Doublet of doublets
ddd	Doublet of doublet of doublets
brs	Broad singlet
brd	Broad doublet
Δ^x	Double bond at position x

LIST OF TABLES

Table I: Distribution of <i>T. contorta</i> in Cameroon (Cameroon National Herbarium).....	5
Table II: Distribution of <i>T. inconspicua</i> in Cameroon (Cameroon National Herbarium).....	6
Table III: Monoterpene indole alkaloids isolated from plants of the genus <i>Tabernaemontana</i>	13
Table IV: Some triterpenes isolated from plants of the genus <i>Tabernaemontana</i>	23
Table V: Other biological activities of triterpenoids.....	25
Table VI: NMR data (DMSO- <i>d</i> ₆) of TCO ₃	45
Table VII: ¹ H and ¹³ C NMR data (DMSO- <i>d</i> ₆) of TCO ₅	53
Table VIII: ¹ H and ¹³ C NMR data (DMSO- <i>d</i> ₆) of TiS ₅	58
Table IX: ¹ H and ¹³ C NMR (DMSO- <i>d</i> ₆) data of TiS ₁₀ compared to the literature (Chen <i>et al.</i> , 2016).....	62
Table X: ¹ H and ¹³ C NMR (CDCl ₃) data of TiS ₆ compared to the literature (Pereira <i>et al.</i> , 2008).....	67
Table XI: ¹ H and ¹³ C NMR (DMSO- <i>d</i> ₆) data of TC ₅ compared to the literature (Gao <i>et al.</i> , 2015).....	70
Table XII: ¹³ C NMR data (Pyridine- <i>d</i> ₆) of TiS ₇ compared to the literature (Sheludko <i>et al.</i> , 2002).....	73
Table XIII: ¹ H and ¹³ C NMR (CDCl ₃) data of TC ₆ compared to those of the literature (Yaya <i>et al.</i> , 2014).....	79
Table XIV: ¹ H and ¹³ C NMR (CDCl ₃) data of TiS ₁₁ compared to the literature (Hasnah <i>et al.</i> , 2010).....	82
Table XV: ¹ H and ¹³ C NMR data (MeOD) of TCO ₉	89
Table XVI: ¹³ C NMR (DMSO- <i>d</i> ₆) data of TC ₄ compared to the literature (Seebacher <i>et al.</i> , 2003).....	92
Table XVII: ¹³ C NMR (pyridine- <i>d</i> ₅) data of TiS ₃ compared to those of the literature (Kwon <i>et al.</i> , 2009).....	95
Table XVIII: ¹³ C NMR (DMSO- <i>d</i> ₆) data of TCO ₈ compared to those of the literature (Collins <i>et al.</i> , 1992).....	99
Table XIX: ¹³ C NMR (DMSO- <i>d</i> ₆) data of TiS ₉ compared to the literature (Khan <i>et al.</i> , 1991)	101
Table XX: ¹³ C NMR (CDCl ₃) data of TC ₂ compared to the literature (Mahato and Kundu, 1994).....	104

Table XXI: ^1H and ^{13}C NMR (Pyridine- d_5) data of TCO_2 compared to the literature (Bianco <i>et al.</i> , 1984)	115
Table XXII: ^{13}C and ^1H NMR data for TiS_{15}	119
Table XXIII: ^{13}C NMR (MeOD) data for TiS_{13} compared to the literature (Choi <i>et al.</i> , 2012)	131
Table XXIV: Chromatogram of the crud extract of the fruits of <i>T. contorta</i>	140
Table XXV: Chromatogram of series B	141
Table XXVI: Chromatogram of series C	142
Table XXVII: chromatogram of series D	143
Table XXVIII: Chromatogram of the crud extract of the stem-bark of <i>T. contorta</i>	143
Table XXIX: Chromatogram of series B	144
Table XXX: Chromatogram of series C	145
Table XXXI: Chromatogram of series D.....	145
Table XXXII: Chromatogram of the crud extract of the stem of <i>T. inconspicua</i>	146
Table XXXIII: Chromatogram of series B	147
Table XXXIV: Chromatogram of series C	147
Table XXXV: Chromatogram of series D	148

LIST OF FIGURES

Figure 1: Fruits (1), leaves (2), branche (3) and trunk (4) of <i>Tabernaemontana contorta</i>	5
Figure 2: Plant (1), leaves (2), and fruits (3) of <i>Tabernaemontana inconspicua</i>	6
Figure 3: HRESI-MS of TCO ₃ (full Spectrum).....	40
Figure 4: ¹ H NMR spectrum (DMSO- <i>d</i> ₆ , 600 MHz) of TCO ₃	40
Figure 5: COSY Spectrum (DMSO- <i>d</i> ₆) of TCO ₃	41
Figure 6: COSY Spectrum (DMSO- <i>d</i> ₆) of TCO ₃	42
Figure 7: ¹³ C NMR spectrum (DMSO- <i>d</i> ₆ , 150 MHz) of TCO ₃	43
Figure 8: HMBC spectrum (DMSO- <i>d</i> ₆) of TCO ₃	44
Figure 9: HRESI-MS of TCO ₅	47
Figure 10: ¹ H NMR spectrum (600 MHz, DMSO- <i>d</i> ₆) of TCO ₅	48
Figure 11: COSY Spectrum (DMSO- <i>d</i> ₆) of TCO ₅	49
Figure 12: ¹³ C NMR spectrum (150 MHz, DMSO- <i>d</i> ₆) of TCO ₅	50
Figure 13: HMBC spectrum (DMSO- <i>d</i> ₆) of TCO ₅	51
Figure 14: NOESY Spectrum (DMSO- <i>d</i> ₆) of TCO ₅	52
Figure 15: HRESI-MS of TiS ₅	54
Figure 16: ¹ H NMR (600 MHz, DMSO- <i>d</i> ₆) of TiS ₅	55
Figure 17: COSY Spectrum (DMSO- <i>d</i> ₆) of TiS ₅	55
Figure 18: NOESY Spectrum (DMSO- <i>d</i> ₆) of TiS ₅	56
Figure 19: ¹³ C NMR spectrum (150 MHz, DMSO- <i>d</i> ₆) of TiS ₅	56
Figure 20: HMBC spectrum (DMSO- <i>d</i> ₆) of TiS ₅	57
Figure 21: HRESI-MS of TiS ₁₀	59
Figure 22: ¹ H NMR spectrum (DMSO- <i>d</i> ₆ , 600 MHz) of TiS ₁₀	60
Figure 23: COSY Spectrum (DMSO- <i>d</i> ₆ , 600 MHz) of TiS ₁₀	61
Figure 24: ¹³ C NMR spectrum (DMSO- <i>d</i> ₆ , 150 MHz) of TiS ₁₀	61
Figure 25: HMBC spectrum (DMSO- <i>d</i> ₆) of TiS ₁₀	62
Figure 26: HRESI-MS of TiS ₆	64
Figure 27: ¹ H NMR spectrum (CDCl ₃ , 600 MHz) of TiS ₆	65
Figure 28: COSY Spectrum (CDCl ₃ , 600 MHz) of TiS ₆	65
Figure 29: ¹³ C NMR Spectrum (CDCl ₃ , 150 MHz) of TiS ₆	66
Figure 30: HMBC Spectrum (CDCl ₃ , 600 MHz) of TiS ₆	66
Figure 31: ¹ H NMR Spectrum (DMSO- <i>d</i> ₆ , 600 MHz) of TC ₅	69
Figure 32: ¹³ C NMR Spectrum (DMSO- <i>d</i> ₆ , 150 MHz) of TC ₅	69

Figure 33: EI-MS of TiS ₇	71
Figure 34: ¹ H NMR Spectrum (Pyridine- <i>d</i> ₆ , 300 MHz) of TiS ₇	72
Figure 35: ¹³ C NMR Spectrum (Pyridine- <i>d</i> ₆ , 75 MHz) of TiS ₇	72
Figure 36: HRESI-MS of TC ₆	75
Figure 37: ¹ H NMR spectrum (CDCl ₃ , 400 MHz) of TC ₆	76
Figure 38: ¹³ C NMR spectrum (CDCl ₃ , 100 MHz) of TC ₆	76
Figure 39: COSY spectrum (CDCl ₃) of TC ₆	77
Figure 40: HMBC spectrum (CDCl ₃) of TC ₆	78
Figure 41: HRESI-MS of TiS ₈	80
Figure 42: ¹ H NMR spectrum (CDCl ₃ , 400 MHz) of TiS ₈	81
Figure 43: ¹³ C NMR spectrum (CDCl ₃ , 100 MHz) of TiS ₈	81
Figure 44: HRESI-MS of TCO ₉	84
Figure 45: ¹ H NMR spectrum (MeOD, 500 MHz) of TCO ₉	85
Figure 46: COSY spectrum (MeOD) of TCO ₉	85
Figure 47: ¹³ C NMR spectrum (MeOD, 125 MHz) of TCO ₉	86
Figure 48: HMBC spectrum (MeOD) of TCO ₉	87
Figure 49: NOESY spectrum (MeOD) of TCO ₉	88
Figure 50: ¹ H NMR spectrum (DMSO- <i>d</i> ₆ , 500 MHz) of TC ₄	90
Figure 51: ¹³ C NMR spectrum (DMSO- <i>d</i> ₆ , 125 MHz) of TC ₄	91
Figure 52: ¹ H NMR spectrum (pyridine- <i>d</i> ₅ , 400 MHz) of TiS ₃	93
Figure 53: ¹³ C NMR spectrum (pyridine- <i>d</i> ₅ , 100 MHz) of compound TiS ₃	94
Figure 54: HSQC spectrum (pyridine- <i>d</i> ₅) of TiS ₃	94
Figure 55: HMBC spectrum (pyridine- <i>d</i> ₅) of TiS ₃	94
Figure 56: HRESIMS of TCO ₈	97
Figure 57: ¹ H NMR spectrum (DMSO- <i>d</i> ₆ , 600 MHz) of TCO ₈	97
Figure 58: ¹³ C NMR spectrum (DMSO- <i>d</i> ₆ , 150 MHz) of TCO ₈	98
Figure 59: ¹ H NMR spectrum (pyridine- <i>d</i> ₅ , 400 MHz) of TiS ₉	100
Figure 60: ¹³ C NMR spectrum (pyridine- <i>d</i> ₅ , 100 MHz) of TiS ₉	101
Figure 61: ¹ H NMR spectrum (CDCl ₃ , 600 MHz) of TC ₃	103
Figure 62: ¹³ C NMR spectrum (CDCl ₃ , 150 MHz) of TC ₃	103
Figure 63: ¹ H NMR spectrum (CDCl ₃ , 400 MHz) of TiS ₂	106
Figure 64: ¹³ C NMR spectrum (CDCl ₃ , 100 MHz) of TiS ₂	106
Figure 65: ¹ H NMR spectrum (CDCl ₃ , 400 MHz) of TiS ₄	107
Figure 66: ¹³ C NMR spectrum (CDCl ₃ , 100 MHz) of TiS ₄	108

Figure 67: ¹ H NMR spectrum (CDCl ₃ , 400 MHz) of TCO ₁	109
Figure 68: ¹³ C NMR spectrum (CDCl ₃ , 100 MHz) of TCO ₁	109
Figure 69: ¹ H NMR spectrum (pyridine- <i>d</i> ₅ , 300 MHz) of TCO ₁₈	110
Figure 70: ¹³ C NMR spectrum (pyridine- <i>d</i> ₅ , 75 MHz) of TCO ₁₈	111
Figure 71: ¹ H NMR spectrum (pyridine- <i>d</i> ₅ , 400 MHz) of TS ₁₄	112
Figure 72: ¹³ C NMR spectrum (pyridine- <i>d</i> ₅ , 100 MHz) of TS ₁₄	112
Figure 73: EIMS of TCO ₂	113
Figure 74: ¹ H NMR spectrum (Pyridine- <i>d</i> ₅ , 400 MHz) of TCO ₂	114
Figure 75: ¹³ C NMR spectrum (Pyridine- <i>d</i> ₅ , 100 MHz) of TCO ₂	114
Figure 76: DEPT-135 spectrum (Pyridine- <i>d</i> ₅ , 100 MHz) of TCO ₂	114
Figure 77: HRESI-MS of TiS ₁₅	116
Figure 78: ¹ H NMR spectrum (DMSO- <i>d</i> ₆ , 600 MHz) of TiS ₁₅	117
Figure 79: ¹³ C NMR spectrum (DMSO- <i>d</i> ₆ , 150MHz) of TiS ₁₅	117
Figure 80: COSY spectrum (DMSO- <i>d</i> ₆) of TiS ₁₅	118
Figure 81: HMBC spectrum (DMSO- <i>d</i> ₆) of TiS ₁₅	118
Figure 82: HRESI-MS/MS of compound TiS ₁₅	119
Figure 83: HRESI- MS of TCO ₁₉	120
Figure 84: ¹ H NMR spectrum (Pyridine- <i>d</i> ₅ , 400 MHz) of TCO ₁₉	121
Figure 85: ¹³ C NMR spectrum ((Pyridine- <i>d</i> ₅ , 100 MHz) of TCO ₁₉	121
Figure 86: HRESI-MS of TCO ₂₀	123
Figure 87: ¹ H NMR spectrum (Pyridine- <i>d</i> ₅ , 400 MHz) of TCO ₂₀	123
Figure 88: ¹³ C NMR spectrum (Pyridine- <i>d</i> ₅ , 100 MHz) of TCO ₂₀	124
Figure 89: HRESI- MS of TC ₁₂	125
Figure 90: ¹ H NMR spectrum (DMSO- <i>d</i> ₆ , 500 MHz) of TC ₁₂	126
Figure 91: ¹³ C NMR spectrum (DMSO- <i>d</i> ₆ , 125 MHz) of TC ₁₂	126
Figure 92: HRESI- MS/MS of TC ₁₂	127
Figure 93: ¹ H NMR spectrum (Pyridine- <i>d</i> ₅ , 400 MHz) of TCO ₁₄	128
Figure 94: ¹³ C NMR spectrum (Pyridine- <i>d</i> ₅ , 100 MHz) of TCO ₁₄	129
Figure 95: ¹ H NMR spectrum (MeOD, 500 MHz) of TiS ₁₃	130
Figure 96: ¹³ C NMR spectrum (MeOD, 125 MHz) of TiS ₁₃	130
Figure 97: ¹ H NMR spectrum (CDCl ₃ , 500 MHz) of TC ₁	132
Figure 98: ¹³ C NMR spectrum (CDCl ₃ , 125MHz) of TC ₁	132
Figure 99: Cytotoxic effect of some isolated compounds on human breast cancer MDA-MB 231 cells	133

Figure 100: Cytotoxic effect of TiS₅ on human breast cancer MDA-MB 231 cells..... 134

Figure 101: Effect of compounds on nitric oxide inhibitory activity (A) on lipopolysaccharide (LPS)-stimulated RAW 264.7 cells and their cell viability (B). 134

LIST OF SCHEMES

Scheme 1: Biosynthesis of monoterpenoid indole alkaloids	11
Scheme 2: Biosynthesis of monoterpene indole alkaloids isolated from plants of the genus <i>Tabernaemontana</i>	12
Scheme 3: Biosynthesis of terpenes	19
Scheme 4: Biosynthesis of triterpenoids.....	23
Scheme 5: Extraction and isolation protocols of the fruits of <i>T. contorta</i>	36
Scheme 6: Extraction and isolation protocol of the stem-bark of <i>T. contorta</i>	37
Scheme 7: Extraction and isolation protocol of the stem of <i>T. inconspicua</i>	38

ABSTRACT

This work describes the isolation and structure elucidation of secondary metabolites from the fruits and stem-bark of *Tabernaemontana contorta* and stem *Tabernaemontana inconspicua*, as well as the evaluation of the anti-inflammatory and cytotoxicity potencies of some isolated compounds. In this study, a total of 28 compounds were isolated using chromatographic techniques and characterized using spectroscopic methods. These compounds were classified as: 9 alkaloids with 3 new derivatives, 8 triterpenoids with 1 new derivative, 1 monoterpene, 7 lipids with 1 new cerebroside and 3 sterioids.

Two of the new indole alkaloids (apparcine-21-one and 5,6-dioxo-11-methoxyvoacangine) were tested for their anti-inflammatory activity but no significant activity was observed.

The anticancer potency of eight of these compounds was carried on human breast cancer cells and 5,6-dioxo-11-hydroxy voacangine showed a significant activity. This compound inhibited the cell growth in both a concentration and time-dependent manner, and it therefore suggests that this compound be used as a chemotherapeutic agent since it was found to be more effective over time exposure.

Key words index: Apocynaceae, *Tabernaemontana contorta*, *Tabernaemontana inconspicua*, secondary metabolites, anti-inflammatory activity, anticancer effect.

RESUME

Ce travail porte sur l'isolement et l'élucidation structurale des métabolites secondaires des fruits et écorces du tronc de *Tabernaemontana contorta* et du tronc de *Tabernaemontana inconspicua* ainsi que l'évaluation des activités anti-inflammatoires et cytotoxicité de certains isolats. Ainsi, 28 composés ont été isolés à l'aide des techniques chromatographiques et caractérisés grâce aux techniques spectroscopiques. Ces composés ont été classifiés dans plusieurs groupes: 9 alcaloïdes avec 3 dérivés nouveaux, 8 triterpènes avec 1 dérivé nouveau, 1 monoterpène, 7 lipides avec 1 nouveau cébroside et 3 stéroïdes.

Huit composés ont été testés pour leurs effets antiprolifératifs sur les cellules cancéreuses MDA-MB 231 du sein et le composé 5,6-dioxo-11-hydroxyvoacangine a montré une activité significative.

Ce composé inhibe la croissance de ces cellules d'une manière dépendante de la concentration et du temps et suggère qu'il peut s'agir d'un agent chimiothérapeutique puisqu'il s'est révélé plus efficace dans le temps.

Deux de ces nouveaux alcaloïdes (apparicine-21-one et 5,6-dioxo-11-méthoxyvoacangine) ont été testés pour leur activité anti-inflammatoire mais aucune activité significative n'a été détectée.

Mot clés: Apocynaceae, *Tabernaemontana contorta*, *Tabernaemontana inconspicua*, métabolites secondaires, activité anti-inflammatoire, antiprolifératif.

GENERAL INTRODUCTION

Detailed investigation and documentation of plants used in local health traditions and their pharmacological evaluations have led to development of invaluable plant drugs for many dreaded diseases. This could be the case for cancer which is one of the leading causes of morbidity and mortality worldwide, with approximately 18.1 million new cases in 2018 (Chatterjee, 2000; WHO, 2018). The number of new cases is expected to rise by about 70% over the next 2 decades (Ferlay *et al.*, 2015). It is the second leading cause of death globally and was responsible for about 9.6 million deaths in 2018. Globally, one in 5 men and one in 6 women worldwide develop cancer during their lifetime, and one in 8 men and one in 11 women die from the disease. Approximately 70% of deaths from cancer occur in low- and middle-income countries (WHO, 2018) such as Cameroon with approximately 20745 new cases and 13199 deaths in 2020 (WHO, 2020).

The lung and breast cancer constitute a major portion of cancer in men and women, respectively (Siegel *et al.*, 2016; WHO, 2018). For children, the highest percentage types of cancer disease are blood cancer and cancers related to the brain and lymph nodes (Schottenfeld and Fraumeni, 2006; Yoo and Shin, 2003). Around one third of deaths from cancer are due to the leading behavioral and dietary risks: high body mass index, low fruit and vegetable intake, lack of physical activity, tobacco and alcohol use (WHO, 2018).

Therefore, cancer is a serious problem affecting the health of all human societies. Unfortunately, it is a variety disease at the tissue level and this variety is a major challenge for its specific diagnosis, followed by efficacy of treatment (Meacham and Morrison, 2013; Fisher *et al.*, 2013).

Even though some cancers can currently be prevented by avoiding risk factors and implementing existing evidence-based prevention strategies and its burden can also be reduced through early detection and management of patients (through surgery, chemotherapy, radiation therapy or a combination of the three treatments), the need for naturally occurring substances that can inhibit, reverse or retard the multistage carcinogenesis still arises.

Natural products could be a solution because it has proven to be powerful therapeutics for treatment of various human sufferings including cancer. It has been proven that natural products from medicinal plants, either as pure compounds or standardized extracts, provide unlimited opportunities for new drug leads because of the incomparable availability of chemical diversity (Cos *et al.*, 2006).

Due to an increasing demand for chemical diversity in screening programs and therapeutic drugs from natural products, interests particularly in edible plants has grown throughout the world. For these reasons, a special interest has been developed in species of the genus *Tabernaemontana* especially *Tabernaemontana contorta* and *Tabernaemontana inconspicua*, Cameroonian medicinal plants of the Apocynaceae family.

To the best of our knowledge, very little phytochemical and pharmacological investigations have been reported on these two plants. The widespread uses of plants of the genus *Tabernaemontana* in traditional medicine for the treatment of cancer and other diseases, the available literature data on anticancer activity of extracts and compounds from these plants and chemotaxonomic criteria justified our choice.

The aim of this work was to contribute to the identification of bioactive molecules of plants origin through the isolation of secondary metabolites which could serve as lead to production of drugs against cancer. To achieve this, the compounds were isolated, characterized and some were tested for their cytotoxic activity and others for anti-inflammatory activity.

This work is divided into three chapters: the literature review from family to species of the plants and the class of compounds isolated. In the second chapter, we present the results and discussion of our work; the experimental part is in the third chapter and finally the references.

CHAPTER I. LITERATURE REVIEW

I.1. BOTANICAL ASPECT OF *TABERNAEMONTANA CONTORTA* AND *TABERNAEMONTANA INCONSPICUA*

I.1.1. General information on the family Apocynaceae

Described for the first time in 1789 by Antoine-Laurent (Endress and Bruyns, 2000), the Apocynaceae forms a family of dicotyledonous plants. It consists of tropical trees, shrubs and vines. The characteristic features of the family are that almost all species are laticifers and usually produce milky sap; they usually have opposite leaves (Heywood *et al.*, 2007). With the inclusion of species of Asclepiadaceae, the family has now enlarged from two to five sub-families. The expanded family now comprises 366 genera and 4650 species (Endress *et al.*, 2014; Heywood *et al.*, 2007). A few of these genera are found in Cameroon including: *Alstonia*, *Catharanthus*, *Holarrhena*, *Picralima*, *Strophanthus*, *Voacanga*, *Rauvolfia* and *Tabernaemontana*, which is the object of this thesis.

I.1.2. General information on the genus *Tabernaemontana*

The genus *Tabernaemontana* was named after J. Th. Miiller, a German physician and botanist in 1590. It is a large genus, belonging to the Apocynaceae family and distributed throughout the tropical, as well as some subtropical parts of Africa, Asia, Pacific Islands and America (Van Beek *et al.*, 1984; Edith and Rosa, 2015). Mainly shrubs or small trees with white latex, this genus is made up of approximately 117 species including *T. inconspiciua* and *T. contorta* (Edith and Rosa, 2015).

I.1.2. 1 General information on *Tabernaemontana contorta*

T. contorta is a tree of about 3-10 m high with a trunk of about 10-25 cm of diameter. Its branches are stout and greenish. Leaves are elliptic or sub obovate, obtuse or sub acuminate and rounded or shortly contracted at the base. They are about 6 -20 cm long and 13-40 cm broad and sub-coriaceous; secondary nerves are 9-15 on each side. The midrib is much raised below and petiole is stout and about 6 -20 mm long. Inflorescences are sub-corymbs with very stout peduncle of about 4 inches long. Bracts are ovate and caduceus with stout pedicels of up to 9 mm long. The calyx is about 4-4.5 mm long with roundish-oblong sepals, and numerous small basal glands within. The corolla is white and sweet-scented with tube: stout, much twisted, sub-cylindrical and slightly widened near the base, 2-2.5 inches long, scantily pubescent within above the stamens, densely pubescent below towards the base and between the filamental ridges. Lobes are obovate-oblong, about as long as the tube. Stamens are inserted and 6-7 mm above the base of the corolla-tube.

Anthers are long-sagittate and 7-8 mm long. The style is up to 7 mm long. Fruits are tough with ovoid or globular follicles (Otto Stapf, 1904; Leeuvenberg, 1991).

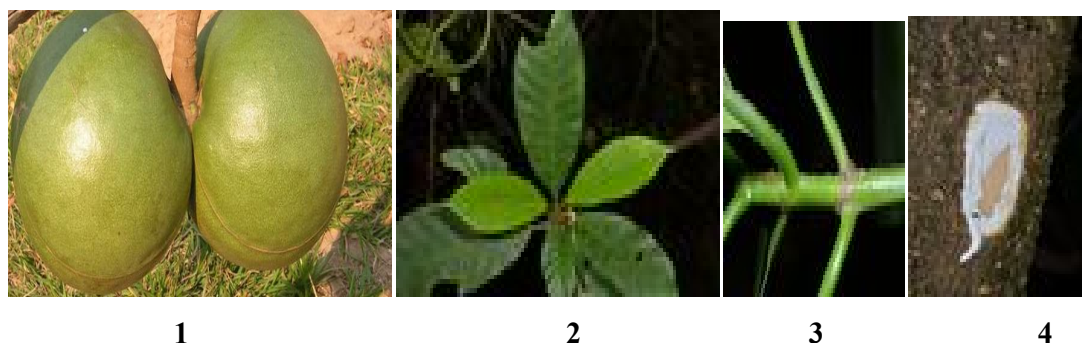


Figure 1: Fruits (1), leaves (2), branche (3) and trunk (4) of *Tabernaemontana contorta* (G. L. M. Foudjo; M. Walters)

In Cameroon, the specie *Tabernaemontana contorta* is distributed as shown in table 1 below (Cameroon National Herbarium).

Table I: Distribution of *T. contorta* in Cameroon (Cameroon National Herbarium)

Regions	Localities
West	Foumban, Banyo
Centre	Melen, Eloundem, Nkolbisson
Littoral	Masok-Kopongo, Dibombe, Loum, Yabassi.
Northwest	Wum, Baji, Chongbonbon
South west	Limbe, Buea
East	Ndokayo, Batouri, Yokadouma
Adamaoa	Yoko-Tibati

Synonyms:

Conopharyngia contorta (Stapf) Stapf

Sarcopharyngia contorta (Stapf) Boiteau

1.1.2.2 General information on *Tabernaemontana inconspicua*

T. inconspicua is a perfectly glabrous shrub of about 10 feet high with greyish or brown branches when dry. Its leaves are obovate-oblong to oblong, abruptly acuminate (acumen narrow, linear, up to 1 mm long), acute to cuneate at the base, very variable in size, 2-6 inches long, 1.25-2.5 inches broad, thin, dark-green above and paler beneath with slender secondary nerves of 8-10 on each side, oblique and curved. Veins are quite obscure

with petiole slender of up to 8 mm long. Inflorescence is about 1-1.5 inch long with peduncle of up to 0.5 inch long. Bracts are linear-lanceolate, inconspicuous with pedicels of up to 2.5 mm long. Its calyx is slightly over 1 mm long, persistent with sepals ovate-lanceolate and acute. Corolla-tube is about 3-4 mm long, delicately papillose below the stamens and otherwise quite glabrous with lobes obovate and about 2.5 mm long. Anthers are 1.5 mm. long. Mericarps are orange-colored, about 1 inch long, over 0.5 inch broad with wings of about 1 mm broad and fused towards the tip into a very broad obtuse short beak. Seeds are up to 4 mm long. (Otto Stapf, 1904).



Figure 2: Plant (1), leaves (2), and fruits (3) of *Tabernaemontana inconspicua* (G. L. M. Foudjo; M. Walters)

In Cameroon, the species *Tabernaemontana inconspicua* is distributed as shown in table 2 below (Cameroon National Herbarium).

Table II: Distribution of *T. inconspicua* in Cameroon (Cameroon National Herbarium)

Regions	Localities
Centre	Akonolinga, eseka
Littoral	Campo, Mouanko, Yabassi, Yingui
South	Ebolowa

I.1.3. Uses of plants of the genus *Tabernaemontana*

I.1.3.1. Medicinal uses

Various parts of plants of the genus *Tabernaemontana* are widely used in traditional medicine for the treatment of several sicknesses (Van Beek *et al.*, 1984). For instance in West Africa pulped leaves and latex from the stem and bark of *Tabernaemontana crassa* have several uses with the main ones being as a local anesthetic, e.g. to treat dislocated

bones or headache, for the treatment of wounds, sores, abscesses and to treat dermal infections such as filaria, ringworm and fungal infections. The latex is also applied as a hemostatic, as it forms a film over the wound and it is taken internally as an anthelmintic (Van Beek *et al.*, 1984). The root of *Tabernaemontana coronaria* is an aphrodisiac tonic especially to the brain, liver, spleen and it is also a purgative (Gupta *et al.*, 2004). The milky juice mixed with oil is rubbed on to the head to cure the pains in the eye. The milky juice is very useful in many eye infections, especially red eye. It kills intestinal worms, and its root when chewed, relieves tooth ache (Thambi *et al.*, 2006). The bark of *Tabernaemontana pachysiphon* is used as medicine for hypertension (Elia, 2006). In Cameroon, the leaves of *T. contorta* are used as antiseptic and to prevent keloid formation (Burkill, 1985). In addition to the medicinal uses, plants of the genus *Tabernaemontana* are cultivated for commercial purposes.

1.1.3.2. Economic uses

In eastern Congo, the wood of *T. stapfiana* is used for construction of local houses, combs spoons and handle for knives and swords (Lemmens, 2006). The greenish brown and slightly streaked wood of *T. psychotriifolia* is said to be used for making furnitures and musical instruments (Van Beek *et al.*, 1984). The sawdust of *T. salzmannii* is smoked to repel insects in Brazil (Van Beek *et al.*, 1984). *T. pachysiphon* has an abundance of white latex which does not coagulate and has been used to adulterate heavy rubber; its bark contain fiber which is used in southern Nigeria to make cloth (Elia, 2006). The tree has ornamental values because of its dark green shiny leaves and sweet-scented white flowers. The pulp of the pounded leaves is used to colour hair brown (Elia, 2006).

In order to confirm the various uses of plants of the genus *Tabernaemontana* in traditional medicine, many chemical and biological studies have been carried on some of these plants.

1.2. CHEMICAL AND BIOLOGICAL STUDIES OF THE GENUS *TABERNAEMONTANA*

Extracts from plants of the genus *Tabernaemontana* show important biological activities. For instance, *T. coronaria* has the potential to scavenge free radicals and act as a good antioxidant for treating various diseases (Surya *et al.*, 2011). The hydroalcoholic extract of *T. catherinensis* leaves and stem-bark showed cytotoxic activities (Bolygon and Athayde, 2012). *T. divaricata* extracts are known for their antimicrobial action against infectious diseases such as syphilis, leprosy and gonorrhoea; as well as its antiparasitic action against

worms, dysentery, diarrhea, and malaria (Van Beek *et al.*, 1984). Experimental studies on extract from leaves of *T. divaricata* exhibited considerable antidiabetic activity and low cytotoxicity (Masudur *et al.*, 2011). *T. alternifolia* including roots and leaves contains alkaloids which are found to be active against lymphocytic leukemia (Gorman *et al.*, 1960).

Plants of the Apocynaceae family are known for their high alkaloid content and the *Tabernaemontana* genus is not an exception. In as much as the largest part of chemical investigations carried on these plants is being focused on their alkaloids content and most traditional uses probably linked to the activities of these metabolites, non-alkaloidal secondary metabolites such as: triterpenoids, flavonoids, steroids and lipids have also been isolated from plants of the *Tabernaemontana* genus.

I.2.1. Alkaloids

I.2.1.1. General information on alkaloids

The term alkaloid (or alkali-like) was first and foremost proposed by the pharmacist, W. Meissner, in 1819, for the basic nitrogen-containing compounds of plant origin (Dewick 2009). This definition is now very reductive due to the fact that alkaloids are not only isolated from plants but also from fungi and animals. They do not necessarily have a basic character. Over several years and with the discovery of new alkaloids, the definition has evolved such that in 1896, Guareschi I. marked the term alkaloid as applicable to all basic organic compounds obtained from plants, animals or artificially prepared. From the biological point of view, the alkaloid is any biologically active and heterocyclic chemical compound which contains nitrogen and may have some pharmacological activity and in many cases, medicinal or ecological use (Aniszewski, 1994). This definition, as a relatively wide one based on application, can be criticized as inexact. However, it presents a general picture of what kinds of compound are under consideration. The biological and chemical nature of this group of compounds leads to the conclusion that each definition of alkaloids is either too broad or too narrow. A short exact definition is not possible without a long list of exceptions (Winterstein and Tier, 1910). In 2003, Sengbush simply stressed that alkaloids are a group of nitrogen-containing bases and that most of them are drugs.

More than 15,000 different alkaloids have been isolated up to date. Since the definition of alkaloids is already difficult, their classification is also not easy.

I.2.1.2. Classification of alkaloids

Alkaloids are generally classified according to the precursor through which they pass during their synthesis in a biological pathway. From a structural point of view, alkaloids are divided according to their shapes and origins. There are three main types of alkaloids: true-alkaloids, proto-alkaloids and pseudo-alkaloids. True-alkaloids and proto-alkaloids are derived from amino acids, whereas pseudo-alkaloids are not derived from these compounds (Aniszewski, 2007).

- True-alkaloids

True-alkaloids derive from amino acid and they share a heterocyclic ring with nitrogen. These alkaloids are highly reactive substances with biological activity even in low doses. All true-alkaloids have a bitter taste. True-alkaloids form water-soluble salts. Moreover, most of them are well-defined crystalline substances which unite with acids to form salts. True-alkaloids may occur in plants in the free state, as salts and as N-oxides. These alkaloids occur in a limited number of species and families. The primary precursors of true-alkaloids are such amino acids as l-ornithine, l-lysine, l-phenylalanine, l-tryptophan and l-histidine (Aniszewski, 2007).

- Proto-alkaloids

Proto-alkaloids are compounds whose nitrogen atom derived from an amino acid is not a part of the heterocycle. Such kinds of alkaloid include compounds derived from l-tyrosine and l-tryptophan. Proto-alkaloids are those with a closed ring, being perfect but structurally simple alkaloids. They form a minority of all alkaloids (Aniszewski, 2007).

-Pseudo-alkaloids

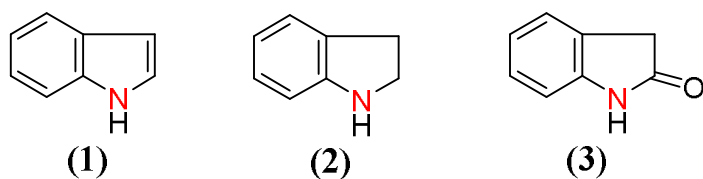
Pseudo-alkaloids are not derived from amino acids. They may, however, be indirectly linked to the amino acid pathway via one of their precursors or one of their postcursors (derivatives of the indegradation process). They may also result from amination or the transamination reaction in a pathway connected with amino acid precursors or postcursors (Aniszewski, 2007).

I.2.1.3. Monoterpene indole alkaloids

Indole alkaloids are compounds with an indole (**1**) nucleus in their basic skeletons. Indole (**1**) is an aromatic organic compound containing a nitrogen atom in its heterocycle. It can be described schematically as composed of a benzene ring and a pyrrole ring joined

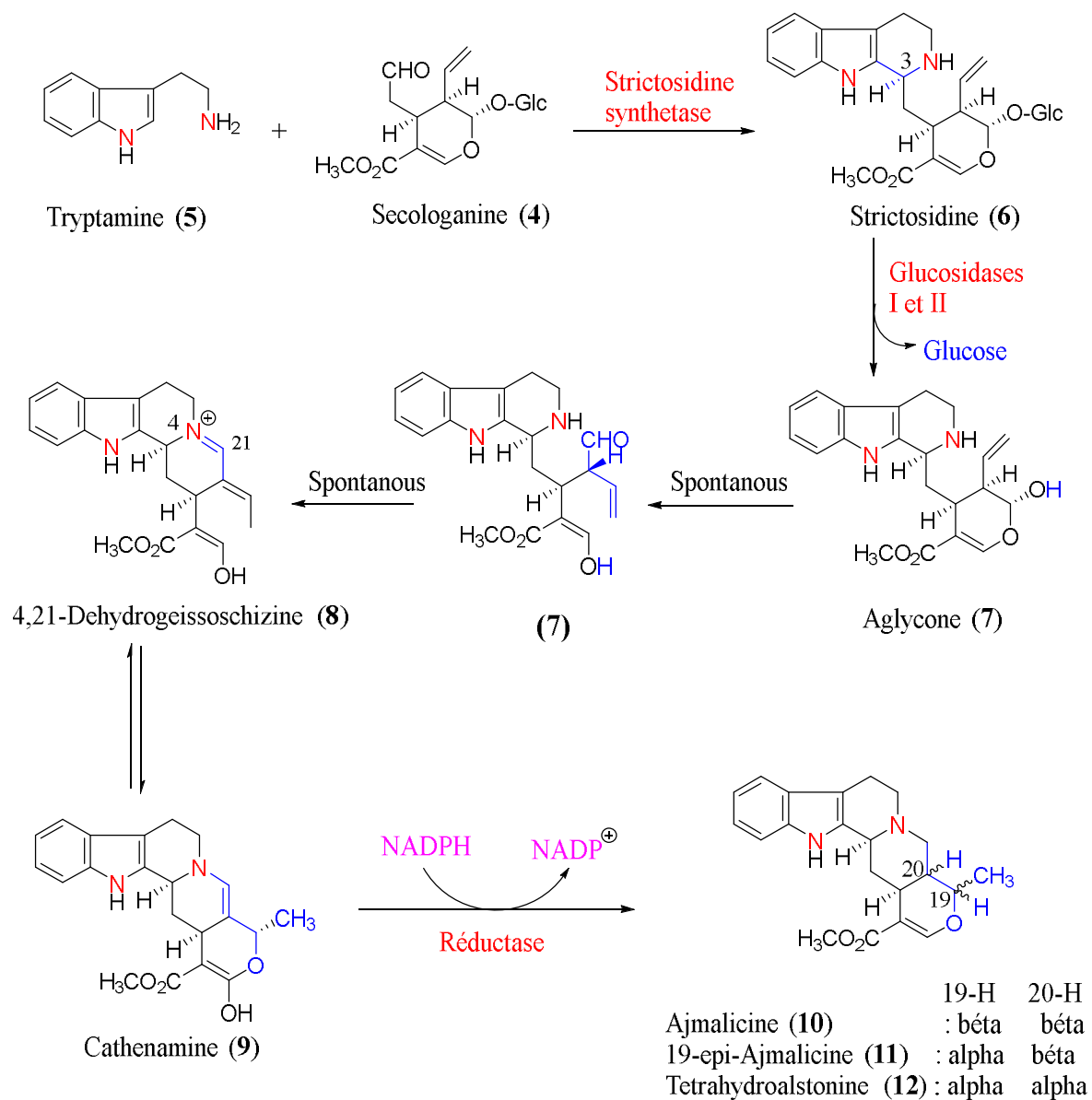
together. The electronic doublet carried by the nitrogen atom in the Lewis representation participates in the aromatic delocalization. The indole (**1**) may undergo an electrophilic aromatic substitution (substitution of a hydrogen atom by an electrophilic group). The most reactive position with respect to the aromatic electrophilic substitution is the C-3 position which is about 1000 times more reactive than those on the benzene ring (Möhlau, 1882). This group of nitrogen-containing compounds is not homogenous. Several subgroups of these compounds were distinguished, among them the following types: Strychnos alkaloids, yohimbans, heteroyohimbans, Vinca alkaloids, kratom alkaloids, tryptamines, ergolines alkaloids, and Tabernanthe iboga alkaloids.

Also, monoterpene indole alkaloids contain an indole (**1**), dihydroindole (**2**), or oxindole (**3**) skeleton coupled with a monoterpene unit derived from secologanine (**4**). They typically contain two nitrogen atoms, one indolic, and the second from the N1-position of the indole ring. Various groups of indole alkaloids have been isolated from more than thirty botanical families including the Apocynaceae, Rubiaceae, Loganiaceae, Passifloraceae, as well as several fungi (Kukula-Koch, 2017).



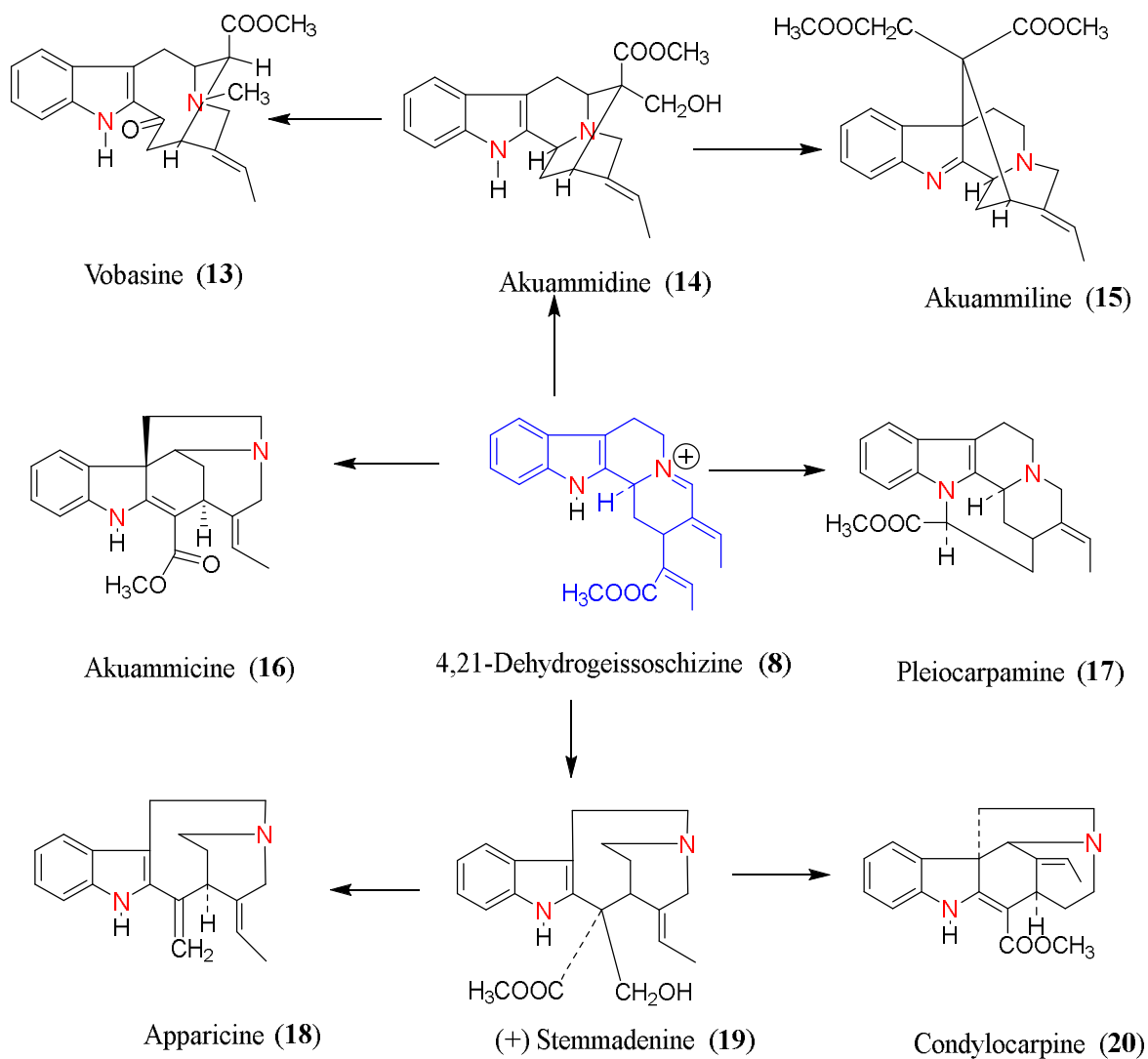
I.2.1.4. Biosynthesis of monoterpene indole alkaloids

This biosynthesis was first described by Rodney *et al.*, in the year 2000 as shown in Scheme 1.



Scheme 1: Biosynthesis of monoterpene indole alkaloids (Rodney *et al.*, 2000)

Scheme 2 describes the biosynthetic pathway of monoterpene indole alkaloids isolated from plants of the genus *Tabernaemontana*.

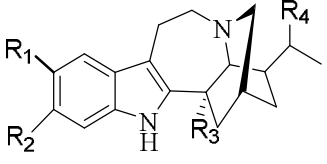
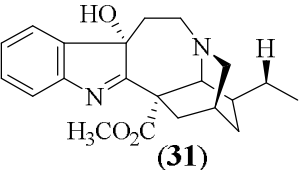


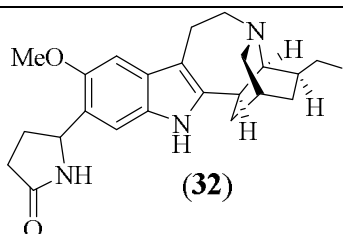
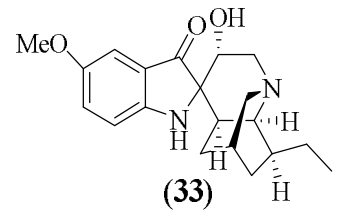
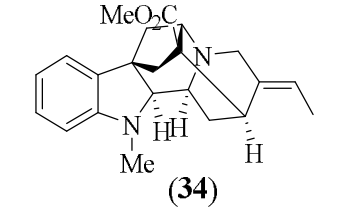
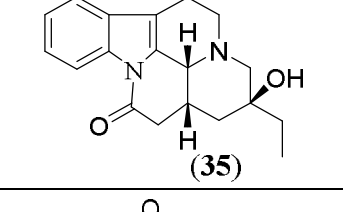
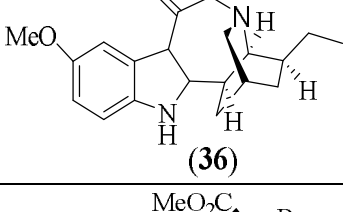
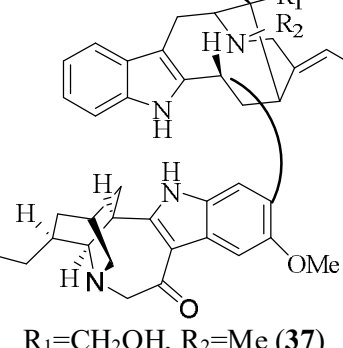
Scheme 2: Biosynthesis of monoterpene indole alkaloids isolated from plants of the genus *Tabernaemontana* (Van Beek *et al.*, 1984).

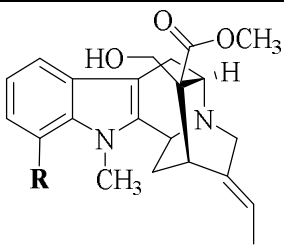
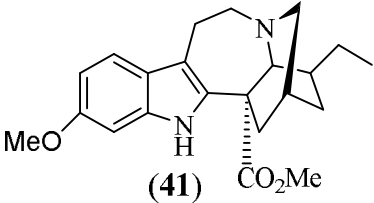
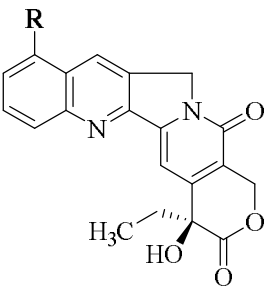
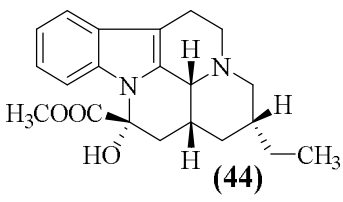
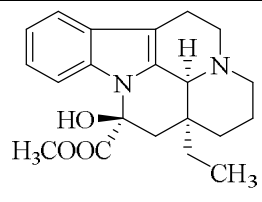
1.2.1.5. Monoterpene indole alkaloids isolated from plants of the genus *Tabernaemontana*

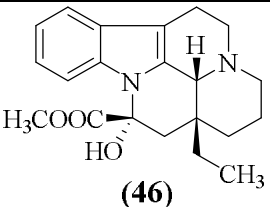
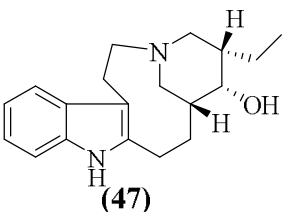
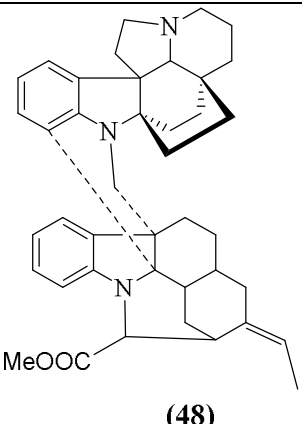
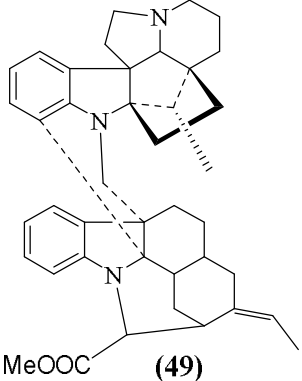
Table III regroups some monoterpene indole alkaloids isolated from the genus *Tabernaemontana*.

Table III: Monoterpene indole alkaloids isolated from plants of the genus *Tabernaemontana*

Structure	Name	Source	Reference
 <p>R₁=H, R₂=H, R₃=CO₂Me, R₄=H (21)</p>	Coronaridine (21)	<i>T. catharinensis</i> <i>T. cymosa</i>	(Pereira <i>et al.</i> , 2008) (Achenbach <i>et al.</i> , 1997)
R ₁ = OMe, R ₂ =H, R ₃ =CO ₂ Me, R ₄ =H (22)	Voacangine (22)	<i>T. catharinensis</i> <i>T. calcarea</i>	(Pereira <i>et al.</i> , 2008) (Prakash <i>et al.</i> , 2005)
R ₁ =H, R ₂ =H, R ₃ =H, R ₄ =H (23)	Ibogamine (23)	<i>T. catharinensis</i>	(Pereira <i>et al.</i> , 2008)
R ₁ =H, R ₂ = OMe, R ₃ =CO ₂ Me, R ₄ =H (24)	Isovoacangine (24)	<i>T. calcarea</i>	(Prakash <i>et al.</i> , 2005)
R ₁ =H, R ₂ =OH, R ₃ =CO ₂ Me, R ₄ =H (25)	11-hydroxycoronaridine (25)		
R ₁ = OMe, R ₂ =H, R ₃ =CO ₂ Me, R ₄ =OH (26)	Voacristine (26)		
R ₁ =H, R ₂ = OMe, R ₃ =CO ₂ Me, R ₄ =OH (27)	Isovoacristine (27)		
R ₁ =OMe, R ₂ =H, R ₃ =H, R ₄ =H (28)	10-methoxyibogamine (28)		
R ₁ =H, R ₂ =OMe, R ₃ =H, R ₄ =H (29)	11-methoxyibogamine (29)	<i>T. catharinensis</i> <i>T. cymosa</i>	(Pereira <i>et al.</i> , 2008) (Achenbach <i>et al.</i> , 1997)
R ₁ =H, R ₂ =COOCH ₃ , R ₃ =OH (30)	Heyneanine (30)		
 <p>(31)</p>	coronaridine hydroxyindolenine (31)	<i>T. catharinensis</i>	(Pereira <i>et al.</i> , 2008)

 <p>Cononusine (32)</p>		<i>T. corymbosa</i>	(Lim <i>et al.</i> , 2015)
 <p>Evaliteine (33)</p>		<i>T. corymbosa</i>	(Lim <i>et al.</i> , 2015)
 <p>Vincamajicine (34)</p>		<i>T. corymbosa</i>	(Lim <i>et al.</i> , 2015)
 <p>Tacamondine (35)</p>		<i>T. corymbosa</i>	(Lim <i>et al.</i> , 2015)
 <p>6-oxoibogaine (36)</p>		<i>T. corymbosa</i>	(Lim <i>et al.</i> , 2015)
 <p>ervatensines A (37) R₁=CH₂OH, R₂=Me (37)</p>		<i>T. corymbosa</i>	(Lim <i>et al.</i> , 2015)
<p>R₁=R₂=H (38)</p>		<i>T. corymbosa</i>	(Lim <i>et al.</i> , 2015)

 <p>R=H (39)</p>	Voachalotine (39)	<i>T. catharinensis</i> <i>T. cymosa</i>	(Milena <i>et al.</i> , 2011) (Achenbach <i>et al.</i> , 1997)
R=OCH ₃ (40)	12-Methoxy-N-MethylVoachalotine (40)	<i>T. catharinensis</i>	(Milena <i>et al.</i> , 2011)
 <p>(41)</p>	Isovoacangine (41)	<i>T. calcarea</i>	(Prakash <i>et al.</i> , 2005)
 <p>R=H (42)</p>	Camptothecin (42)	<i>T. heyneana</i>	(Van Beek <i>et al.</i> , 1984)
R=OCH ₃ (43)	9-MethoxyCamptothecin (43)	<i>T. heyneana</i>	(Van Beek <i>et al.</i> , 1984)
 <p>(44)</p>	Tacamine (44)	<i>T. eglandulosa</i>	(Van Beek <i>et al.</i> , 1984)
 <p>(45)</p>	(+)-Vincamine (45)	<i>T. rigida</i>	(Van Beek <i>et al.</i> , 1984)

 <p>(46)</p>	(-)-Vincamine (46)	<i>T. rigida</i>	(Van Beek <i>et al.</i> , 1984)
 <p>(47)</p>	Capurinine (47)	<i>T. capuronii</i>	(Van Beek <i>et al.</i> , 1984)
 <p>(48)</p>	nortartarine (48)	<i>T. contorta</i>	(Ndongo <i>et al.</i> , 2017)
 <p>(49)</p>	Pleiomutinine (49)	<i>T. contorta</i>	(Ndongo <i>et al.</i> , 2017)

1.2.1.6. Biological activities of alkaloids from the genus *Tabernaemontana*

-Anticancer activity and cytotoxic activity

Indole alkaloids such as voacangine (22), isovoacangine (24), coronaridine (21), 11-hydroxycoronaridine (25), voacristine (26), isovoacristine (27), ibogamine (23), 10-methoxyibogamine (28), 11-methoxyibogamine (29) and heyneanine (24), isolated from an alkaloid portion of dichloromethane/methanol extract of *T. calcarea* from the Madagascar rainforest exhibited cytotoxicity toward A2780 ovarian cancer cell line with IC₅₀ values ranging over 3.5-11 mg/mL (Prakash *et al.*, 2005). Heyneanine (24), coronaridine (21), and voacangine (22) isolated from *T. catharinensis* exhibited cytotoxicity against HeLa (human

cervix tumor), 3T3 (normal mouse embryo fibroblasts), Hep-2 (human laryngeal epithelial carcinoma), and B-16 (murine skin) cell lines with coronaridine (**21**), voacangine (**22**), and heyneanine (**24**) displaying respective IC₅₀ values of 54.47 mg/mL, 159.33 g/mL, and 689.45 mg/mL against Hep2 cell line. In addition, coronaridine (**21**) was reported to induce apoptosis in 3T3 and Hep-2 cell lines (Rizo *et al.*, 2003). Cononusine (**31**), ervaluteine (**32**), vincamajicine (**33**), tacamonidine (**34**), 6-oxoibogaine (**35**), and other alkaloids isolated from the stem-bark extract of *T. corymbosa* were tested for MDR reversal and cytotoxicity against vincristine-resistant KB cells, human KB cells, A549, MCF-7, MDA-468, HCT-116, and HT-29 cells. Vincamajicine (**33**) exhibited reversal of MDR in vincristine-resistant KB cells with IC₅₀ value of 2.62 mM whereas ervatensines A (**36**) and B (**37**) inhibited growth in human KB cells with IC₅₀<2 mM and in A549, MCF-7, MDA-468, HCT-116, and HT-29 cells with IC₅₀ value ranging over 0.70-4.19 mM via inducing apoptosis and necrotic cell death (Lim *et al.*, 2015).

-Neuroprotective and psychoactive

Indole alkaloids such as coronaridine (**21**), voacangine (**22**) (2.5 mL of each sample) from *T. australis* exhibited significant AChE inhibitory potential at the same level as the reference drugs physostigmine and galantamine (Andrade *et al.*, 2005). In another study, formulations containing the alkaloidal extract (0.1 mg/mL) from *T. divaricata* exhibited significant AChE inhibitory potential which was analyzed through in-vitro permeation study of microemulsions and liquid crystalline systems (Chaiyana *et al.*, 2013).

-antimicrobial activities

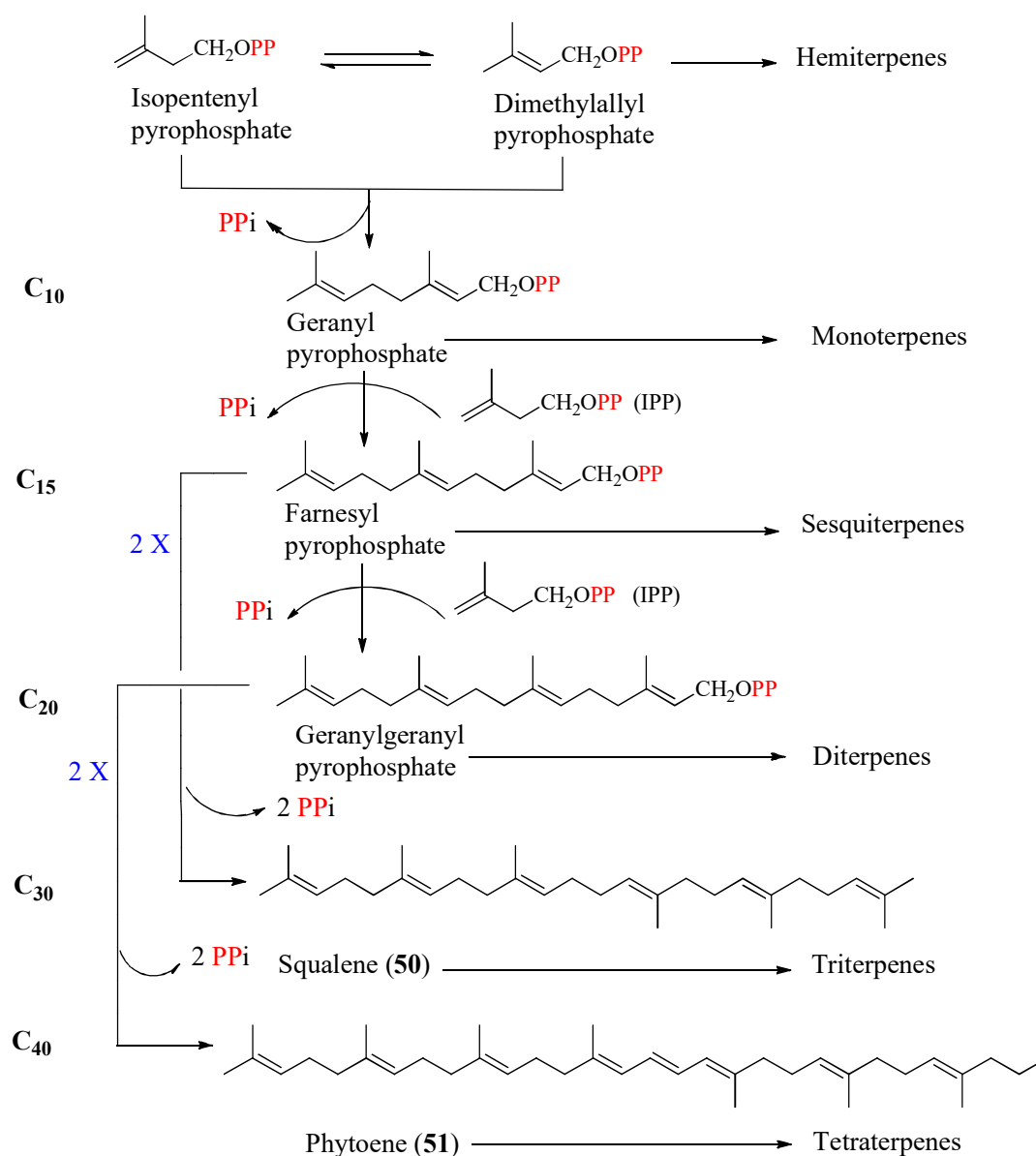
Alkaloidal (voacangine (**22**) etc.) fraction from the *T. elegans* root extract was noted to inhibit *M. tuberculosis* H37RV (ATCC 25177) and *M. smegmatis* (ATCC 14468) with MIC value of 32 mg/mL (against both mycobacteria) and minimum bactericidal concentration (MBC) value of 128 µg/mL (against *M. smegmatis*) (Pallant *et al.*, 2012). Corynanthean, ibogan, or bisindole alkaloids and 3-hydroxy derivatives of dimeric voacamine type alkaloids from *T. chippii* root-bark were tested for antimicrobial activities, and all dimeric alkaloids showed potent and moderate-to-less antimicrobial activities against gram-positive and gram negative bacteria (*B. subtilis*, *S. aureus*, *E. coli*, and *P. aeruginosa*), respectively. The MIC (mg/mL) values were found to be ranging over 4 to 60, 35 to 500, and 70 to >1000, 65 to >1000 (for the compounds and against the bacteria, respectively) (Van Beek *et al.*, 1984). *T. catharinensis* root-bark derived 12-methoxy-4-methylvoachalotine (**40**) when tested against the ATCC strains of *S. aureus*, *S. epidermidis*,

E. coli, and *P. aeruginosa*; resistant clinical isolated species of *Enterococcus sp.*, *K. oxytoca*, *Citrobacter*, *K. pneumoniae*, *P. mirabilis*, *S. aureus*, *S. epidermidis*, *E. coli*, and *P. aeruginosa*, exhibited antimicrobial properties with MIC value of 0.16 mg/mL (against the strains of *S. aureus* and *E. coli* ATCC) and MIC values ranging over 0.08 to 0.31 µg/mL (against *Enterococcus sp.*, *Citrobacter*, *S. aureus*, *S. epidermidis*, *E. coli*, and *P. aeruginosa*) (Medeiros *et al.*, 2011). Alkaloidal (voacangine (**22**) etc.) fraction of *T. elegans* root extract inhibited gram-positive bacteria [*B. subtilis* (ATCC 6633), *E. faecalis* (ATCC 29212), *S. aureus* (ATCC 12600), *S. aureus* (NHLS 363)] with MIC values ranging over 32 to 64 µg/mL and gram-negative bacteria [*E. coli* (ATCC 35218), *K. pneumoniae* (ATCC 13883), *P. aeruginosa* (ATCC 9027)] with MIC values of 512 µg/mL or more (Pallant *et al.*, 2012). Alkaloid-containing aqueous extracts of *T. alternifolia* stem-bark inhibited clinical isolates of methicillin resistant *Staphylococcus aureus* with MIC values ranging over 600 to 800 µg/mL (Marathe *et al.*, 2013).

I.2.2. Pentacyclic triterpenoids

I.2.2.1. General information on terpenes

The term terpene invented by Kekulé comes from their historical origin of the *Terebinth* tree: "*Pistacia terebinthus*" (Ruzica, 1953). Terpenes represent a group of natural products distributed among many botanical families. These organic substances are among the most common secondary metabolites in nature. They constitute a set of organic compounds derived from the rearrangements or cyclization of the basic structural unit called isoprene C₅H₉. Its multiple that is to say (C₅H₉)_n constitutes the basic formula of terpenes. They exist as hemiterpenes (C-5), monoterpenes (C-10), sesquiterpenes (C-15), diterpenes (C-20), and triterpenes (C-30) (Dewick, 2002; Banthorpe, 1991) as summarized in Scheme 3.



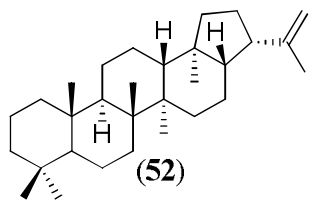
Scheme 3: Biosynthesis of terpenes

Terpenes have two fundamental properties: firstly, they constitute among others the odoriferous principle of plants. This odor is due to the release of highly volatile molecules containing 10, 15 and 20 carbon atoms. Then, because of the alternation of single and double bonds (conjugated bonds) in some molecules, they interact with light.

1.2.2.2. Triterpenes

These are one of the largest classes of plant natural products, with more than 20,000 different triterpenes reported to date (Hill and Connolly, 2012). The vast majority of triterpene diversity occurs in the plant kingdom, although other organisms also produce triterpenes. Examples include the synthesis of the simple triterpene hopene (52) from

squalene in bacteria (Ourisson and Albrecht, 1992) and the production of defense-related triterpene glycosides by sea cucumbers (Van Dyck *et al.*, 2010).



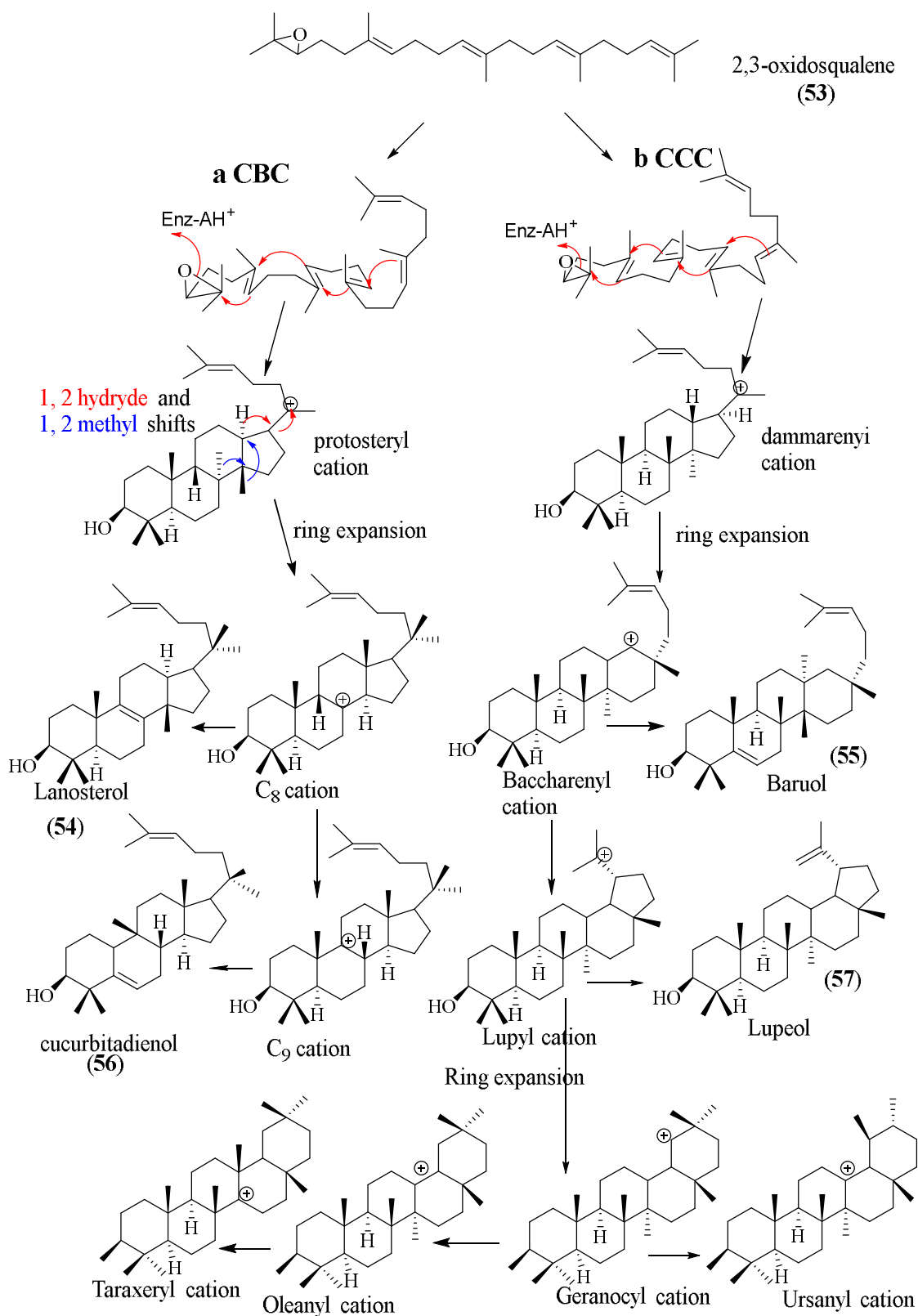
More than 100 different triterpene scaffolds are currently known in plants (Xu *et al.*, 2004). Triterpene cyclization can thus lead to a wide array of different triterpene structures, all derived from the simple and ubiquitous linear isoprenoid substrate 2,3-oxidosqualene (53). These triterpene scaffolds can then provide the foundation for further modification by triterpene-modifying (or tailoring) enzymes (e.g., cytochrome P450s, sugar transferases, and acyltransferases), thereby leading to enormous structural diversity. Nature's triterpene reservoir remains largely undiscovered, despite the considerable commercial interest in these compounds for a range of applications (Augustin *et al.*, 2011; Moses *et al.*, 2013; Osbourn *et al.*, 2011; Sawai and Saito, 2011). Major advances in our understanding of the genes, enzymes, and pathways required to synthesize these molecules are now opening up unprecedented opportunities for triterpene metabolic engineering and for the discovery of new pathways and chemistries, facilitated by the recent discovery that the genes for triterpene pathways are at least in some cases organized in biosynthetic gene clusters in plant genomes (Field *et al.*, 2011; Field and Osbourn, 2008; Kliebenstein and Osbourn, 2012; Krokida *et al.*, 2013; Qi *et al.*, 2004).

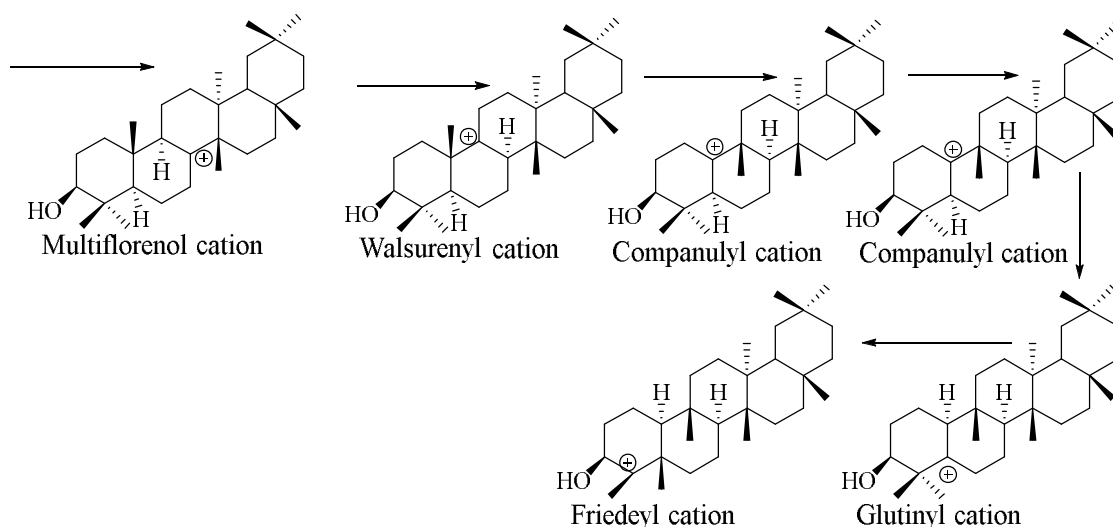
1.2.2.3. Biosynthesis of triterpenoids

Cyclization of 2,3-Oxidosqualene: One Substrate, an Array of Products

Cyclization of 2,3-oxidosqualene (53) is catalyzed by enzymes known as oxidosqualene cyclases (OSCs), which generate either sterol or triterpene scaffolds in a process involving substrate binding and pre-organization (folding), initiation of the reaction by protonation of the epoxide, cyclization and rearrangement of carbocation species and termination by deprotonation or water capture to yield a final terpene product (scheme 4). Although variation in carbocation cyclization and rearrangement steps contributes substantially to scaffold diversity, the initial substrate folding step is critical, because this predisposes the substrate to follow a particular cyclization pathway. For example, the chair-boat-chair (CBC) conformation organizes cyclization to form the protosteryl cation, which then gives rise to sterols, whereas the chair-chair-chair (CCC) conformation directs

cyclization into the dammarenyl cation, which then gives rise to a host of diverse triterpene scaffolds. In the synthesis of triterpenes, squalene (**50**) is cyclized to pentacyclic hopene (**52**) by squalene-hopene cyclases (SHCs). Following substrate folding, SHCs and OSCs initiate the cyclization reaction by protonation of the terminal double bond of squalene (**50**) and the epoxide of 2,3-oxidosqualene (**53**), respectively. This step defines SHC and OSC enzymes as class II terpene synthases. (Thimmappa *et al.*, 2014)





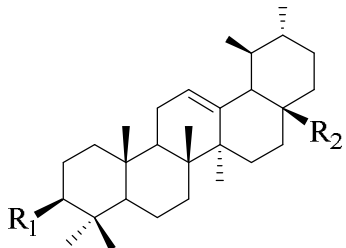
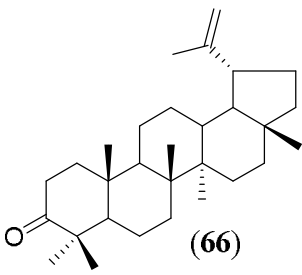
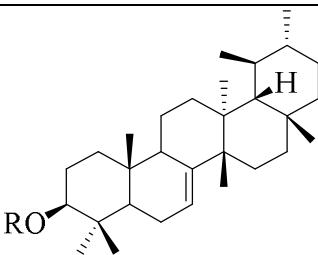
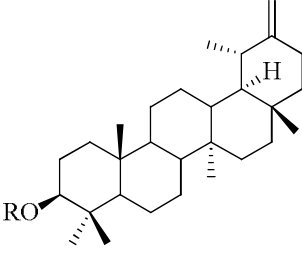
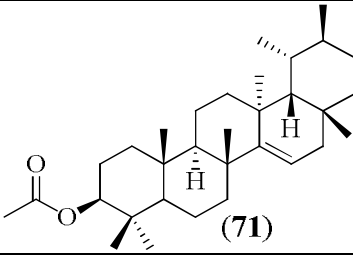
Scheme 4: Biosynthesis of triterpenoids (Thimmappa *et al.*, 2014)

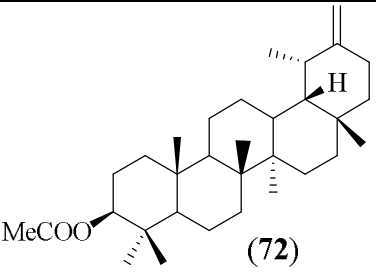
1.2.2.4. Triterpenes isolated from plants of the genus *Tabernaemontana*

The table below regroups some triterpenoids isolated from plants of the genus *Tabernaemontana*.

Table IV: Some triterpenes isolated from plants of the genus *Tabernaemontana*

Structure	Name	Source	Reference
<p>$R_1=OH, R_2=CH_3$ (57)</p>	Lupeol (57)	<i>T. affinis</i> , <i>T. crassa</i> and <i>T. catherinensis</i>	(Van Beek <i>et al.</i> , 1984; Pereira <i>et al.</i> , 2007 ; Pereira <i>et al.</i> , 2008)
$R_1=CO_2CH_3, R_2=CH_3$ (58)	Lupeyl Acetate (58)		
$R_1=OH, R_2=CO_2H$ (59)	Betulinic acid (59)		
<p>$R_1=OH, R_2=CH_3$ (60)</p>	β -Amyrine (60)	<i>T. crassa</i> , <i>T. heyneana</i> and <i>T. catherinensis</i>	(Van Beek <i>et al.</i> , 1984; Pereira <i>et al.</i> , 2007 ; Pereira <i>et al.</i> , 2008)
$R=CO_2CH_3, R_2=CH_3$ (61)	β -Amyrine Acetate (61)		
$R_1=OH, R_2=CO_2H$ (62)	Oleanolic acid (62)		

 $R_1=OH, R_2=CH_3$ (63)	α -Amyrine (63)	<i>T. crassa</i> , <i>T. heyneana</i> and <i>T. catharinensis</i>	(Van Beek <i>et al.</i> , 1984; Pereira <i>et al.</i> , 2007 ; Pereira <i>et al.</i> , 2008)
$R_1=CO_2CH_3, R_2=CH_3$ (64)	α -Amyrine Acetate (64)		
$R_1=OH, R_2=COOH$ (65)	Ursolic Acid (65)		
 (66)	Lupenone (66)	<i>T. pacifica</i>	(Van Beek <i>et al.</i> , 1984)
 $R=H$ (67)	Baurenol (67)	<i>T. markgrafiana</i> and <i>T. catharinensis</i>	(Nielsen <i>et al.</i> , 1994; Pereira <i>et al.</i> , 2008)
$R=MeCO$ (68)	Baurenyl acetate (68)		
 $R=H$ (69)	20(30)-taraxasten-3-ol (taraxasterol) (69)	<i>T. markgrafiana</i> and <i>T. catharinensis</i>	(Nielsen <i>et al.</i> , 1994; Pereira <i>et al.</i> , 2008)
$R=MeCO$ (70)	20(30)-taraxasten-3- acetate (70)		
 (71)	Isoursenyl acetate (71)	<i>T. markgrafiana</i> and <i>T. catharinensis</i>	(Nielsen <i>et al.</i> , 1994; Pereira <i>et al.</i> , 2008)

 <p>MeCOO (72)</p>	<p>20(30)-ursen-3-yl acetate (72)</p>	<p><i>T. markgrafiana</i></p>	<p>(Nielsen <i>et al.</i>, 1994)</p>
---	---------------------------------------	-------------------------------	--------------------------------------

1.2.2.5. Biological activity of triterpenoids isolated from plants of the genus *Tabernaemontana*

Anticancer activity

Triterpenoids play a very important role in the treatment of human affections and a subject of many biological activities. However, α -amyrin (63) induced proliferation of human keratinocytes (HaCaT) by about 18%. (Biskup *et al.*, 2012). The anticancer activities of lupeyl acetate (58), lupeol (57), and lupenone (66) were determined against breast cancer cells MCF-7 using neutral red assay, while their apoptotic activity were confirmed by flow cytometric analysis using annexin V-FTIC assay and DNA fragmentation. The IC₅₀ of lupeyl acetate (58), lupeol (57), and lupenone (66) were 48.79; 43.09; and 8.07 μ g/mL respectively. The results of flow cytometric analysis and DNA fragmentation showed the anticancer activity of the prepared compounds following apoptosis mechanism (Suwito *et al.*, 2016). Lupeyl acetate (60), betulinic acid (61), oleanolic acid (64) and ursolic acid (67) were evaluated in the A2780 cytotoxicity assay, oleanolic acid (62) and ursolic acid (65) were only very weakly cytotoxic, with IC₅₀ values of 20 μ g/mL. Lupeyl acetate (57) and betulinic acid (59) were more active (16.0) (Prakash *et al.*, 2003).

In addition to anticancer activity, triterpenes possess other biological activities with some presented in the following table.

Table V: Other biological activities of triterpenoids

Compound name	Activity	Reference
Oleanolic acid (62)	C3 convertase inhibition	(Kapil and Sharma, 1995; Kapil and Sharma, 1994)
	major COX-2 inhibition	(Subbaramaiah <i>et al.</i> , 2000; Ringbom <i>et al.</i> , 1998)
	Antiulcerogenic effect	(Rodriguez <i>et al.</i> , 2003; Farina <i>et al.</i> , 1998.)
	Inhibition of HIV-1 protease	(Quere <i>et al.</i> , 1996)

	Hepatoprotective activity	(Liu, 1995.)
Ursolic acid (67)	Inhibition of the production of reactive oxygen species	(Chen <i>et al.</i> , 2002)
	Antiulcerogenic effect	(Farina <i>et al.</i> , 1998)
	Inhibition of HIV-1 protease	(Quereet <i>et al.</i> , 1996)
	Hepatoprotective activity	(Liu <i>et al.</i> , 1993; Liu <i>et al.</i> , 1994)
	Analgesic effect	(Bhalla <i>et al.</i> , 1971; Tapondjou <i>et al.</i> , 2003)
Betulinic acid (59)	Phospholipase A2 inhibition	(Bernard <i>et al.</i> , 2001)
	Antiplasmodial activity	(Steele <i>et al.</i> , 1999)
	HIV replication activity	(Chou <i>et al.</i> , 2000)
Lupeol (57)	Inhibition of the production of reactive oxygen species	(Yamashita <i>et al.</i> , 2002; Geetha <i>et al.</i> , 1998)
	Hepatoprotective activity	(Liu <i>et al.</i> , 1993; Liu <i>et al.</i> , 1994)
α -Amyrin (63)	Inhibition of reactive oxygen species production	(Chen <i>et al.</i> , 2002)
	Analgesic effect	(Bhalla <i>et al.</i> , 1971; Tapondjou <i>et al.</i> , 2003)

I.3. CANCERS

I.3.1. Definition

Cancer occurs by a series of successive mutations in genes so that these mutations change cell functions. Chemical compounds have an obvious role of forming gene mutations and cancer cells (Aizawa *et al.*, 2016). It can therefore be defined as a disease in which a group of abnormal cells grow uncontrollably by disregarding the normal rules of cell division. Normal cells are constantly subjected to signals that dictate whether the cell should divide differentiate into another or die. Cancer cells develop a degree of autonomy from these signals, resulting in uncontrolled growth and proliferation (Momna heijmadi, 2010).

From the molecular prospective, it is the various genetic changes that lead to oncogene generation. These genetic disorders include chromosomal translocation (gene Bcr and oncogene Abl in chronic blood cancer), point mutation (Ras gene in coloncancer), deletion (Erb-B gene in breast cancer), amplification (N-myc in neuroblastoma), and insertion activation (C-myc in acute blood cancer). Chronic blood cancer often occurs in the elderly due to an exchange of genetic material between chromosomes 9 and 22. This condition leads to production of a biomarker called ph1, which is found in 95% of patients and can facilitate a correct diagnosis. The connection of Bcr gene to Abl oncogene results in

creation of a gene new combination that translated to protein with kinase activity (Joensuu *et al.*, 2001; King *et al.*, 1985; Heinrich *et al.*, 2002; Thomas *et al.*, 2007).

I.3.2. Causes of cancer

The initiation and progression of cancer depends on both external factors (tobacco, chemicals, radiation and infectious organisms) and internal factors (inherited mutations, hormones, immune conditions and mutations that occur from metabolism). These factors can act together or in sequence, resulting to abnormal cell behavior and proliferation. As a result, cell masses grow and expand, affecting surrounding normal tissues and can also spread to other locations in the body (metastasis). However, it is important to remember that most common cancer take months and years for these DNA mutations to accumulate and result to a detectable cancer (Momna heijmadi, 2010).

Which of the two, genes or the environment play a dominant role in developing cancer? While genes are distributed unequally across population, they do not explain the differences in cancer incidence rates in the world, but the risk of developing cancer seems largely environmental, accounting for more than 90% of all cancers caused (Momna heijmadi, 2010).

I.3.2.1. Life style and environment

The first known report linking the influence of life style on cancer was by John Hill, an English physician, who noted the link between nasal cancer and the use of tobacco snuff. In the late 18th century, Sir Percival Pott reported that scrotal cancer in chimney sweeps was links to poor hygiene and accumulation of cancer causing agents from soot. The Danish Chimney Sweeper's Guide recommended a daily bath which was the most likely reason for the dramatic reduction in scrotal cancer incidence rates in Europe (Momna heijmadi, 2010).

In 1950, compelling epidemiological evidence showed that cigarette smokers ran a 20 fold higher risk of developing lung cancer compared to non-smokers. Since then, tobacco and alcohol consumption have been linked to almost 170000 mouth throat cancer death per year in the US alone. Over half a million deaths every year are expected to be caused by life style choices such as obesity, physical inactivity, diet (low in vegetables, high in salt or nitrates are linked to stomach and esophageal cancers whereas high fat, low fiber diets are linked to bowel, pancreatic, breast and prostate cancer) (Momna heijmadi, 2010).

Risk of cancer are also increased by infectious agents including viruses (hepatitis B virus, human papilloma virus, human immunodeficiency virus increase risk of

nasopharyngeal, cervical carcinomas and Kaposi's sarcoma) and bacteria such as *Helicobacter pylori* (stomach cancer). Incidences of skin cancers (melanomas) are on the rise, especially in Australia, due to exposure to high levels of ultraviolet radiation in the sun's ray and popularity of tanning salons. However, the risk of developing some of these cancers can be reduced by changing lifestyles and vaccines (like Gardasil which reduces the risk of cervical carcinomas) (Momna heijmadi, 2010).

Initiation and progression of cancer is also due to exposure to cancer-causing agents (carcinogens, mutagens). These are present in food and water, in the air, chemicals and sunlight that people are exposed to. Since epithelia cells cover the skin, line the respiratory and alimentary tracks, and metabolize ingested carcinogens, it is not surprising that over 90% of cancer originates from epithelia. In less than 10% of cases, a genetic predisposition increases the risk of cancer developing a lot earlier (Momna heijmadi, 2010).

I.3.2.2. Age

Although cancer can occur in persons of every age, it is common among the aging population. Sixty percent of new cancer cases and two thirds of cancer deaths occur in persons older than 65 years. The incidence of common cancers (breast, colorectal, prostate, lung) increases with age. There are many several theories as to why cancer incidence increases in the elderly: age-related alterations in the immune system (decreased immune surveillances); accumulation of random genetic mutations or lifetime carcinogen exposure (especially for colorectal and lung cancers); hormonal alterations or exposure and long lifespans. Multiple genetic changes are necessary for the development of cancer, most clearly exemplified by the stepwise genetic changes shown by many colon polyps progressing to cancer. The exponential rise in many cancers with age fits with an increased susceptibility to the late ages of carcinogenesis by environmental exposures. Lifetime exposure to estrogen may lead to breast or uterine cancer; exposure to testosterone leads to prostate cancer. The decline in cellular immunity may also lead to certain types of cancer that are highly immunogenic. Accumulation of DNA mutations have to be amplified to constitute a cancer, therefore the longer the lifespan, the higher the risk of developing cancer (Momna heijmadi, 2010).

I.3.3 Types of cancer

There are over 200 types of cancer, below is a list of more specific types of cancers found in each general category; it is not all inclusive and the cancers listed in quotes are the general names of some cancers:

Carcinoma: Cancer that begins in the skin or in tissues that line or cover internal organs “skin, lung, colon, pancreatic, ovarian cancers”, epithelial, squamous and basal cell carcinomas, melanomas, papillomas, and adenomas (National Cancer Institute, 2014).

Sarcoma: Cancer that begins in bone, cartilage, fat, muscle, blood vessels, or other connective or supportive tissue "bone, soft tissue cancers," osteosarcoma, synovial sarcoma, liposarcoma, angiosarcoma, rhabdosarcoma, and fibrosarcoma (National Cancer Institute, 2014).

Leukemia: Cancer that starts in blood-forming tissue such as the bone marrow and causes large numbers of abnormal blood cells to be produced and enter the blood "leukemia," lymphoblastic leukemias, myelogenous leukemias, T-cell leukemia, and hairy-cell leukemia (National Cancer Institute, 2014).

Lymphoma and myeloma: Cancers that begin in the cells of the immune system- "lymphoma," T-cell lymphomas, B-cell lymphomas, Hodgkin lymphomas, non-Hodgkin lymphoma and lymphoproliferative lymphomas (Harvard Women’s Health Watch, 2006)

Central nervous system cancers: Cancers that begin in the tissues of the brain and spinal cord "brain and spinal cord tumors," gliomas, meningiomas, pituitary adenomas, vestibular schwannomas, primary central nervous system lymphomas, and primitive neuroectodermal tumors (National Cancer Institute, 2014).

Not included in the above types listed are metastatic cancers; this is because metastatic cancer cells usually arise from a cell type listed above and the major difference from the above types is that these cells are now present in a tissue from which the cancer cells did not originally develop. Consequently, if the terms "metastatic cancer" is used, for accuracy, the tissue from which the cancer cells arose should be included. For example, a patient may say they have or are diagnosed with "metastatic cancer" but the more accurate statement is "metastatic (breast, lung, colon, or other type) cancer which spread to the organ in which it has been found (National Cancer Institute, 2014).

I.3.4 Symptoms and signs of cancer

The symptoms and signs of cancer depend on the type of cancer, where it is located, and/or where the cancer cells have spread. For example, breast cancer may be present as a lump in the breast or as nipple discharge while metastatic breast cancer may present with symptoms of pain (if spread to bones), extreme fatigue (lungs), or seizures (brain). A few patients show no signs or symptoms until the cancer is far advanced (Devita *et al.*, 2005; Markowitz *et al.*, 2014).

The American Cancer Society describes seven warning signs and/or symptoms that a cancer may be present and which should prompt a person to seek medical attention. The word CAUTION can help you remember these (Markowitz *et al.*, 2014):

- Change in bowel or bladder habits;
- A sore throat that does not heal;
- Unusual bleeding or discharge (for example, nipple secretions or a "sore" that will not heal that oozes material);
- Thickening or lump in the breast, testicles, or elsewhere;
- Indigestion (usually chronic) or difficulty swallowing;
- Obvious change in the size, color, shape, or thickness of a wart or mole;
- Nagging cough or hoarseness ;
- Unexplained loss of weight or loss of appetite;
- A new type of pain in the bones or other parts of the body that may be steadily worsening, or come and go, but is unlike previous pains one has had before;
- Persistent fatigue, nausea or vomiting ;
- Unexplained low-grade fevers which may be either persistent or come and go;
- Recurring infections which will not clear with usual treatment.

Anyone with these signs and symptoms should consult their doctor; these symptoms may also arise from noncancerous conditions.

Many cancers will present some of the above general symptoms but often have one or more symptoms that are more specific for the cancer type. For example, lung cancer may present common symptoms of pain, but usually the pain is located in the chest. The patient may have unusual bleeding, but the bleeding usually occurs when the patient coughs. Lung cancer patients often become short of breath and then become very tired (Markowitz *et al.*, 2014).

I.3.5 Diagnosis of cancer

Some cancers are diagnosed during routine screening examinations. These are usual tests that are routinely done at a certain age. Many cancers are discovered when you present to your health care professional with specific symptoms.

A physical exam and medical history, especially the history of symptoms, are the first steps in diagnosing cancer. In many instances, the medical caregiver will order several tests, most of which will be determined by the type of cancer and where it is suspected to be located in or on the person's body. In addition, most caregivers will order a complete blood count, electrolyte levels and in some cases, other blood studies that may give additional information (Baron, 2005).

Imaging studies are commonly used to help physicians detect abnormalities in the body that may be cancer. X-rays, CT and MRI scans, and ultrasound are common tools used to examine the body. Other tests such as endoscopy, with which variations in the equipment used, can allow visualization of tissues in the intestinal tract, throat, and bronchi that may be cancerous. In areas that cannot be well visualized (inside bones or some lymph nodes, for example), radionuclide scanning is often used. The test involves ingestion or IV injection of a weakly radioactive substance that can be concentrated and detected in abnormal tissue (Baron, 2005).

The preceding tests can be very good at localizing abnormalities in the body; many clinicians consider that some of the tests provide presumptive evidence for the diagnosis of cancer. However, in virtually all patients, the definitive diagnosis of cancer is based on the examination of a tissue sample taken in a procedure called a biopsy from the tissue that may be cancerous, and then analyzed by a pathologist. Some biopsy samples are relatively simple to procure (for example, skin biopsy or intestinal tissue biopsy done with a device called an endoscope equipped with a biopsy attachment). Other biopsies may require as little as a carefully guided needle, or as much as a surgery (for example, brain tissue or lymph node biopsy). In some instances, the surgery to diagnose the cancer may result in a cure if all of the cancerous tissue is removed at the time of biopsy (Baron, 2005).

The biopsy can provide more than the definitive diagnosis of cancer; it can identify the cancer type (for example, the type of tissue found may indicate that the sample is from a primary or metastatic type of brain cancer) and thereby help to stage the cancer. The stage, or cancer staging, is a way for clinicians and researchers to estimate how extensive the cancer is in the patient's body (Baron, 2005).

I.3.6 Treatment for cancer

The cancer treatment is based on the type of cancer and the stage of the cancer. In some people, diagnosis and treatment may occur at the same time if the cancer is entirely surgically removed when the surgeon removes the tissue for biopsy (Baron, 2005).

Although patients may receive a unique sequenced treatment, or protocol, for their cancer, most treatments have one or more of the following components: surgery, chemotherapy, radiation therapy, or combination treatments (a combination of two or all three treatments) (Baron, 2005). Individuals obtain variations of these treatments for cancer. Patients whose cancer cannot be cured by surgery usually will get a combination therapy; the composition is determined by the cancer type and stage (Baron, 2005).

Palliative therapy (medical care or treatment used to reduce disease symptoms but unable to cure the patient) utilizes the same treatments described above. It is done with the intent to extend and improve the quality of life of the terminally ill cancer patient. There are many other palliative treatments to reduce symptoms such as pain medications and antinausea medications (Baron, 2005).

I.3.7 Cancer risk factors

Most experts are convinced that many cancers can either be prevented or the risk of developing cancers can be markedly reduced. Some of the methods are simple; others are relatively extreme, depending on an individual's view (Kaelin and Neugut, 2005, Markowitz *et al.*, 2014).

Prevention of cancer, by avoiding its potential causes, is the simplest method. First on most clinicians and researchers list is to stop (or better, never start) smoking tobacco. Avoiding excess sunlight and many of the chemicals and toxins are excellent ways to avoid cancers. Avoiding contact with certain viruses and other pathogens also are likely ways of prevention of some cancers. People who have to work close to cancer-causing agents should follow all safety precautions and minimize any exposure to such compounds. Although the FDA and the CDC suggests that there is no scientific evidence that definitively says cell phones cause cancer, other agencies call for more research or indicate that the risk is very low. Individuals who are concerned can limit exposure to cell phones by using an earpiece and simply make as few cell phone calls as possible (Kaelin and Neugut, 2005; Markowitz *et al.*, 2014).

There are two vaccines currently approved by the U.S. Food and Drug Administration (FDA) to prevent specific types of cancer. Vaccines against the hepatitis B virus, which is considered a cause of some liver cancers, and vaccines against human papillomavirus (HPV) types 16 and 18 are available. According to the NCI, these viruses are responsible for about 70% of cervical cancers. These viruses also play a role in cancers arising in the head and neck, as well as cancers in the anal region, and probably in others. Today, vaccination against HPV is recommended in teenagers and young adults of both sexes. The HPV virus is so common that by the age of 50, half or more people have evidence of being exposed to it. Sipuleucel-T is a new vaccine approved by the FDA to help treat advanced prostate cancer. Although vaccine does not cure prostate cancer, it has been shown to help extend the lifespan of individuals with advanced prostate cancer (Kaelin and Neugut, 2005; Markowitz *et al.*, 2014).

People with a genetic predisposition to develop certain cancers and others with a history of cancers in their genetically linked relatives currently cannot change their genetic makeup. However, some individuals who have a high possibility of developing genetically linked cancer have taken actions to prevent cancer development. For example, some young women who have had many family members develop breast cancer have elected to have their breast tissue removed even if they have no symptoms or signs of cancer development to reduce or eliminate the possibility of developing breast cancer. Some doctors consider this as an extreme measure to prevent cancer while others do not (Markowitz *et al.*, 2014).

Screening tests and studies for cancer are meant to help detect a cancer at an early stage when the cancer is more likely to be potentially cured with treatment. Such screening studies are breast exams, testicular exams, colon-rectal exams (colonoscopy), mammography, certain blood tests, prostate exams, urine tests and others. People who have any suspicion that they may have cancer should discuss their concerns with their doctor as soon as possible. Screening recommendations have been the subject of numerous conflicting reports in recent years. Screening may not be cost effective for many groups of patients or lead to unnecessary further invasive tests, but individual patients' unique circumstances should always be considered by doctors in making recommendations about ordering or not ordering screening tests (Markowitz *et al.*, 2014).

I.3.7 Anti-cancer and anti-inflammatory effect

There is a considerable evidence that reactive oxygen species (ROS) induce oxidative damage in biomolecules, causing atherosclerosis (Heinecke, 1998), hypertension

(Wilcox, 2005), diabetes (Niedowicz and Daleke, 2005), and cancer (Oikawa *et al.*, 2003). For example, the low-density lipoprotein (LDL) is subject oxidative modification due to its high content of unsaturated fatty acyl group (Kalyanaraman *et al.*, 1993). Consequently, free radicals existing in arterial wall have been known to be a crucial factor resulting to atherosclerosis (Heinecke, 1997). On the other hand, many literatures reported that dietary antioxidants (e.g. polyphenol and flavonoid) have some potentially protective effects against LDL oxidation (Fuhrman and Aviram, 2001). Epidemiological studies showed that diets rich in fruit and vegetables containing antioxidants are well associated with lower risk of cardiovascular diseases (Ness and Powles, 1997). Thus, the intake of dietary antioxidants may be a useful therapy to prevent LDL oxidation and the atherosclerotic progression.

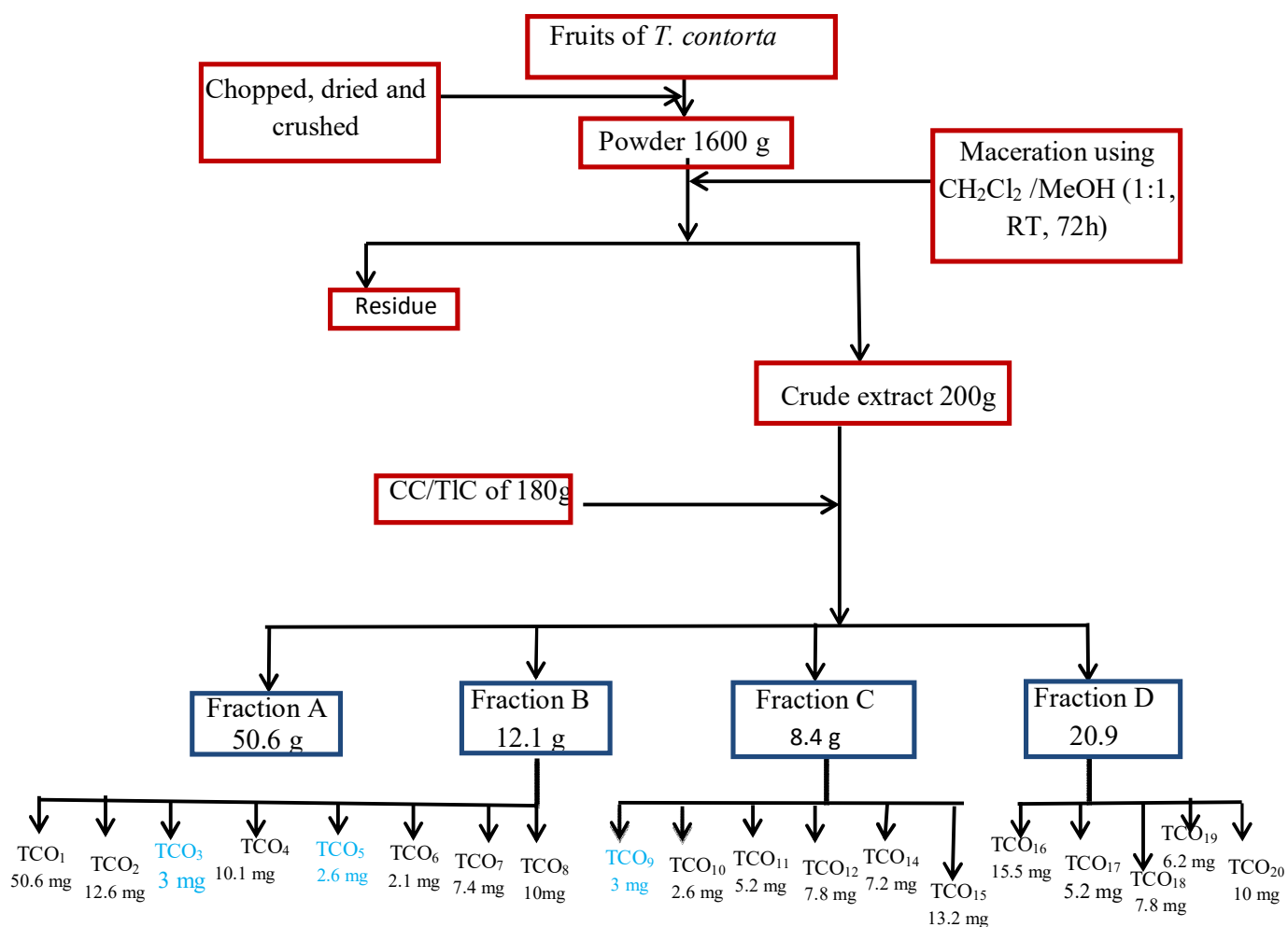
Nitric oxide (NO) is synthesized from amino acid, arginine, by nitric oxide synthase (NOS). Under normal physiological conditions, NO production is regulated by constitutive isoforms of NOS (eNOS), this nanomolar concentrations of NO plays an important role as a vasodilator, neurotransmitter and in the immunological system as a defense against tumor cells, parasites and bacteria (Nakagawa and Yokozawa, 2002). However, under pathological condition, NO production is increased by the inducible isoform of NOS (iNOS), subsequently, brings about cytotoxicity and tissue damage (Kim *et al.*, 1999). Therefore, much attention has focused on how to decrease the NO production generated by iNOS. For example, natural products with bioactive action inhibiting NO production have been reported (Kim *et al.*, 1998). And recently, several investigations have demonstrated the action mechanism of natural antioxidants on decreasing NO production (Sheu *et al.*, 2001). In addition, cyclooxygenase 2 (COX-2) is the rate limiting enzyme and responsible for the catalysis of prostaglandin E2 (PGE2) from arachidonic acid (Surh *et al.*, 2001). Chen *et al.* in 2006 noted that the induction of COX-2 activity and subsequent generation of PGE2 are closely related to the NO production. In other words, the overproduction of PGE2 mediated by COX-2 has been linked to the development of inflammation and carcinogenesis (Park *et al.*, 2004). Thus, reducing the levels of PGE2 and COX-2 may be an effective strategy for inhibiting the inflammation and carcinogenesis.

CHAPTER II. RESULTS AND DISCUSSION

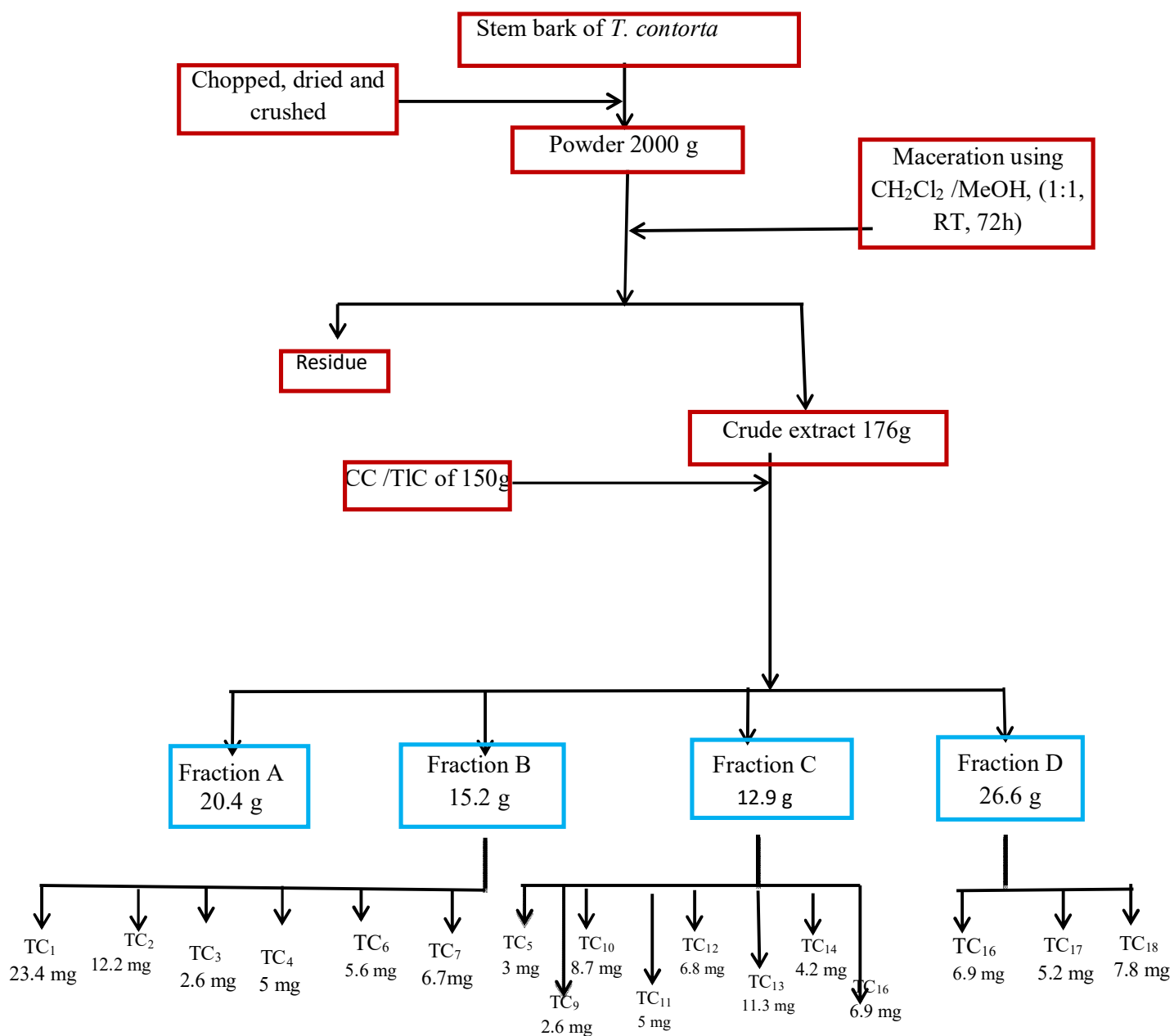
II.1. INTRODUCTION

The different parts of *T. contorta* (fruits and stem-bark) and *T. inconspicua* (stem) were collected in December 2013 at mount Elounden and Kalla respectively, locations of the central region of Cameroon. These plants were identified by Mr NANA Victor, a botanist at the National Nebaruim of Cameroon with identification numbers NHC 45445 for *T. contorta* and NHC 61026 for *T. inconspicua*. The different parts of the plants were chopped, dried and crushed. The powders obtained were macerated at room temperature in a mixture MeOH/CH₂Cl₂ (1:1) for 24×3 hours. After solvent evaporation, the extracts obtained were separated and purified using diverse chromatographic techniques. The obtained products are classified as follows: alkaloids, terpenoids, steroids and lipids.

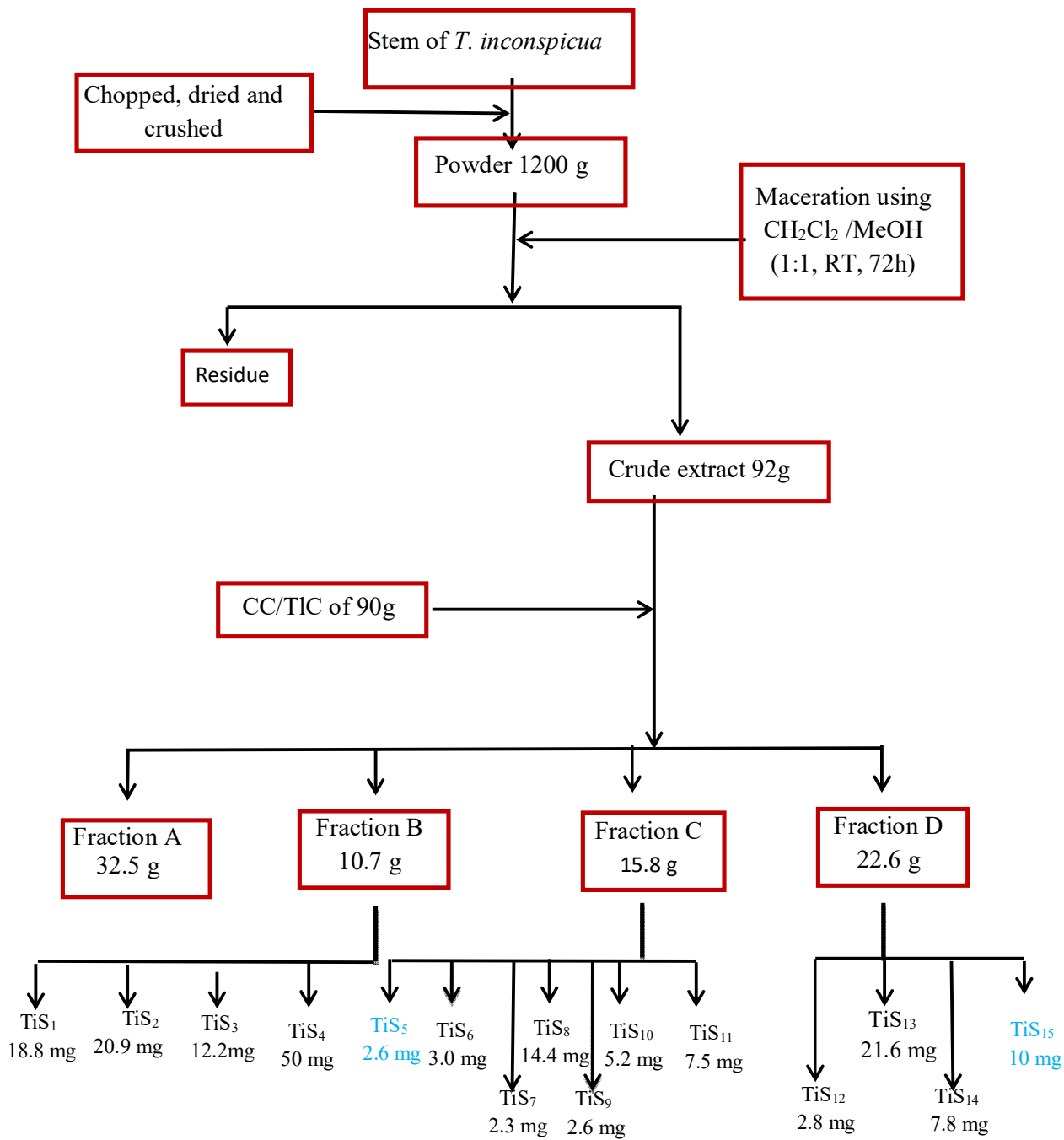
Scheme 5, 6 and 7 summarizes the extraction and isolation protocols.



Scheme 5: Extraction and isolation protocols of the fruits of *T. contorta*



Scheme 6: Extraction and isolation protocol of the stem-bark of *T. contorta*



Scheme 7: Extraction and isolation protocol of the stem of *T. inconspicua*

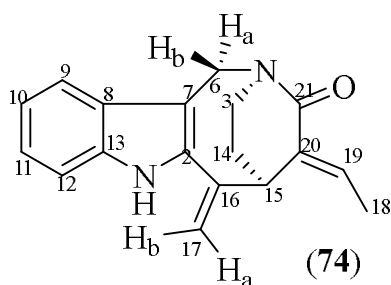
II.2. CHARACTERIZATION OF ISOLATED COMPOUNDS

II.2.1. Alkaloids

II.2.1.1. Characterization of TCO₃

TCO₃ was obtained from the fruits of *T. contorta* as a black powder in a mixture of Hex/AE 85/15. It is soluble in CHCl₃ and DMSO and responds positively to the Meyer's test giving a yellowish white precipitate and also to the Draggendorf's test giving a dark-red color characteristic of alkaloids.

From the spectroscopic data of TCO₃ such as HRESIMS, NMR 1D and 2D (including ¹H, ¹³C, COSY, NOESY, HSQC and HMBC), its structure was determined to be that of a monoterpene indole alkaloid:



The molecular formula of TCO₃ was determined to be C₁₈H₁₈ON₂ on the basis of the HRESI-MS (Figure 3) (m/z 279.1491 [M+H]⁺ calculated for 279.1497) indicating 11 double bond equivalents.

JW166 #710-755 RT: 10.98-11.69 AV: 46 NL: 1.39E8
F: FTMS + c ESI Full ms [100.00-2000.00]

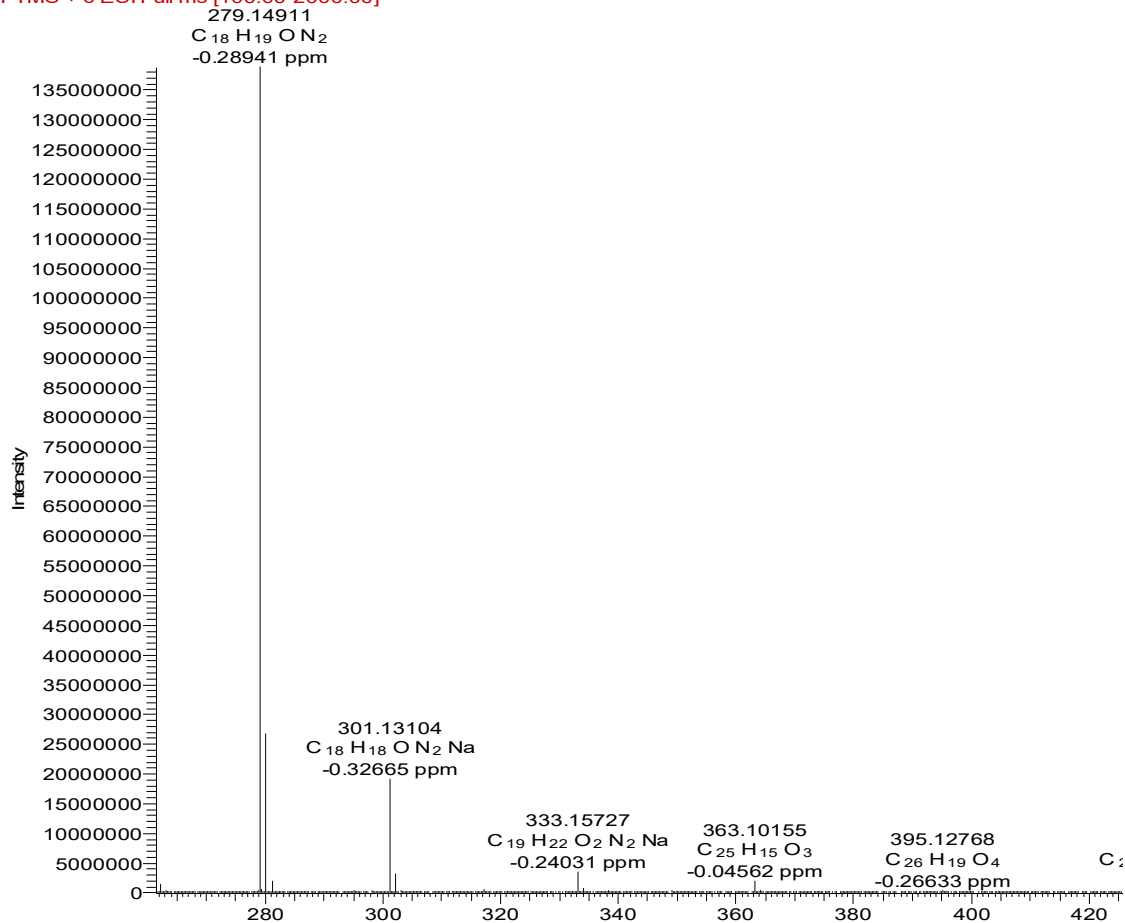


Figure 3: HRESI-MS of TCO₃ (full Spectrum)

The ¹H NMR spectrum (Figure 4) reveals the presence of aromatic protons sorted into two triplets at δ_H 6.96 (1H, t, 7.6 Hz, H-10) and δ_H 7.08 (1H, t, 7.6 Hz, H-11) and two doublets at δ_H 7.42 (1H, d, 7.8 Hz, H-9) and δ_H 7.28 (1H, d, 7.8 Hz, H-12). These protons correlate between themselves in the COSY spectrum (Figure 5) suggesting the presence of an unsubstituted indole aromatic ring.

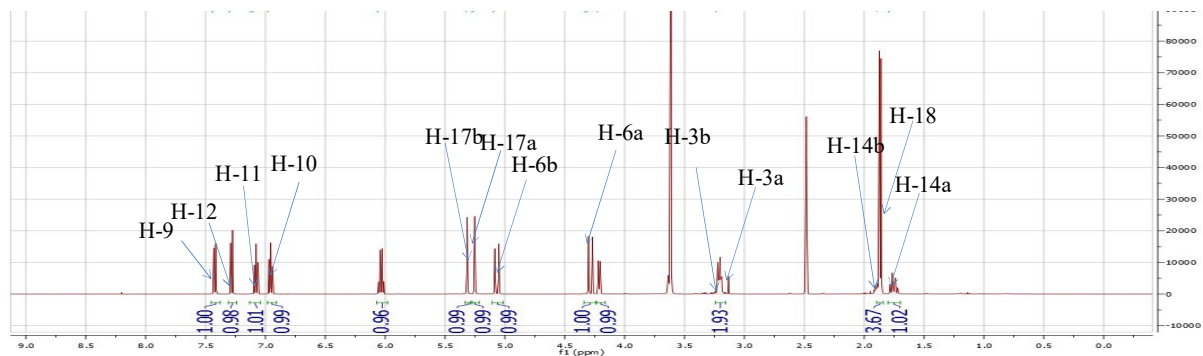


Figure 4: ¹H NMR spectrum (DMSO-*d*₆, 600 MHz) of TCO₃

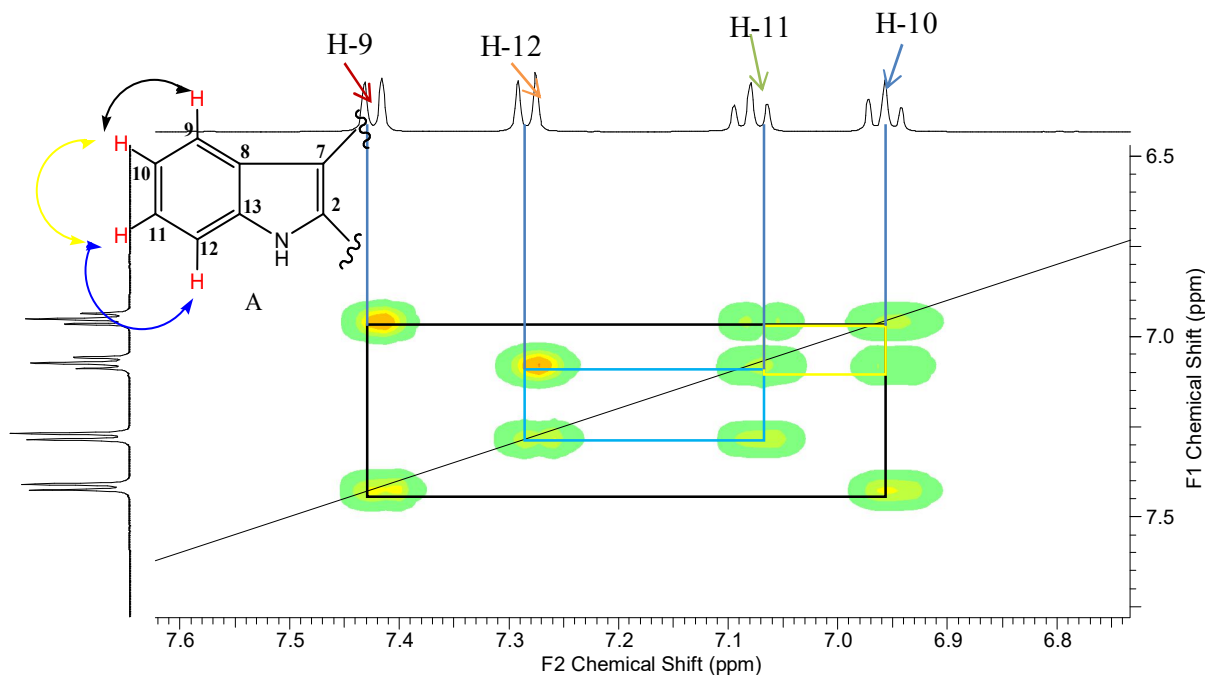


Figure 5: COSY Spectrum (DMSO-*d*₆) of TCO₃

The ¹H and COSY spectra reveals, in addition to the aromatic system of the indole alkaloid:

- the presence of an isolated methylene, characterized by two signals at δ_{H} 5.24 (1H, s, H-17a) and 5.33 (1H, s, H-17b) representing a terminal double bond;
- an N-CH₂-CH₂-CH spin system, characterized by signals at δ_{H} 3.20 (1H, m, H-3b) and 3.22 (1H, m, H-3a); 1.71 (1H, m, H-14a) and 1.80 (1H, m, H-14b); 4.22 (d, 5.3 Hz, H-14) characteristic of the N/C-3/C-14/C-15 fragment of the aspidospermatan-series of monoterpene indole alkaloids (Van beek *et al.*, 1984);
- a =CH-CH₃ spin system characterized by signals at δ_{H} 1.89 (3H, d, 6.8 Hz, H-18) and 6.03 (1H, q, 6.8 Hz, H-19) corresponding to the C18-C19 unit;
- an isolated methylene characterized by signals at δ_{H} 5.07 (d, 16.5 Hz, H-6b) and 4.29 (d, 16.5 Hz, H-6a).

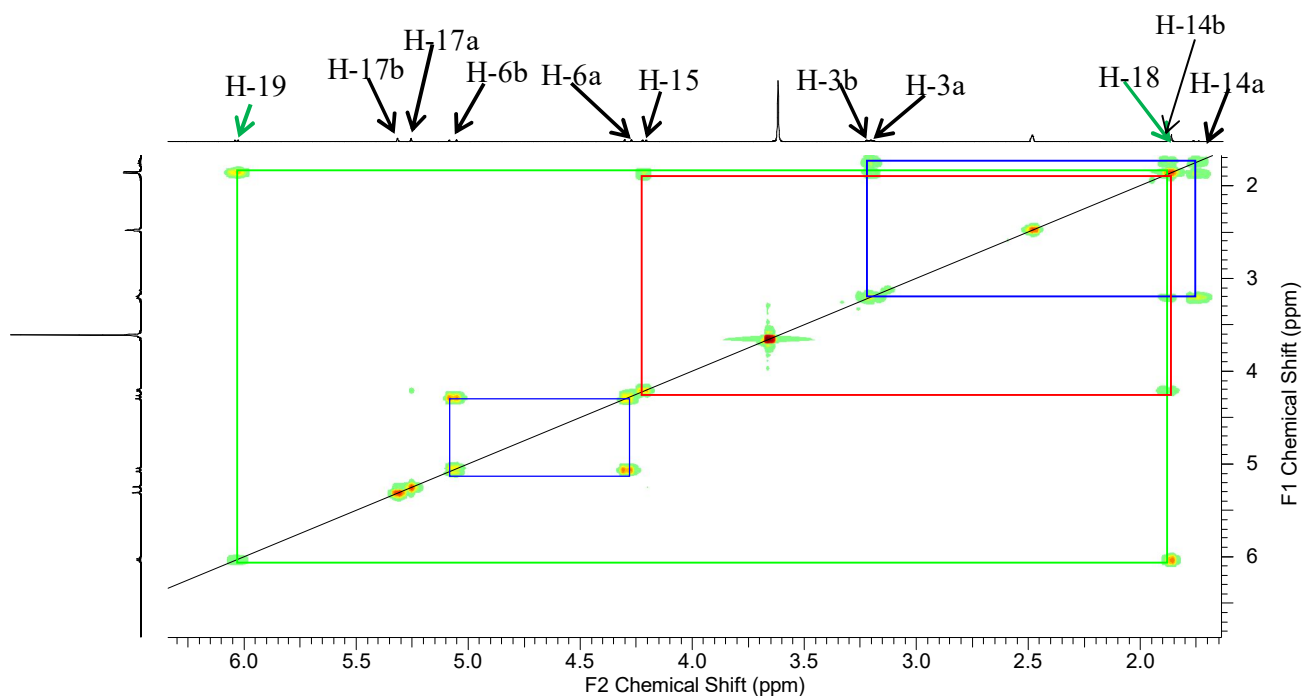


Figure 6: COSY Spectrum (DMSO- d_6) of TCO₃

Its ¹³C NMR spectrum (Figure 7) accounted for 18 carbon resonances, including one methyl at δ_c 13.4 (C-18), four methylene at δ_c 27.2 (C-14), 44.8 (C-3), 47.6 (C-6), 119.7 (C-17), a carbonyl signal at δ_c 176.2 (C-21), belonging to the amide functional group and eight aromatic carbon signals at δ_c 132.5 (C-2), 111.5 (C-7), 127.2 (C-8), 118.8 (C-9), 119.2 (C-10), 136.3 (C-13), 111.5 (C-12), 122.6 (C-11) confirming the indole alkaloid moiety of TCO₃.

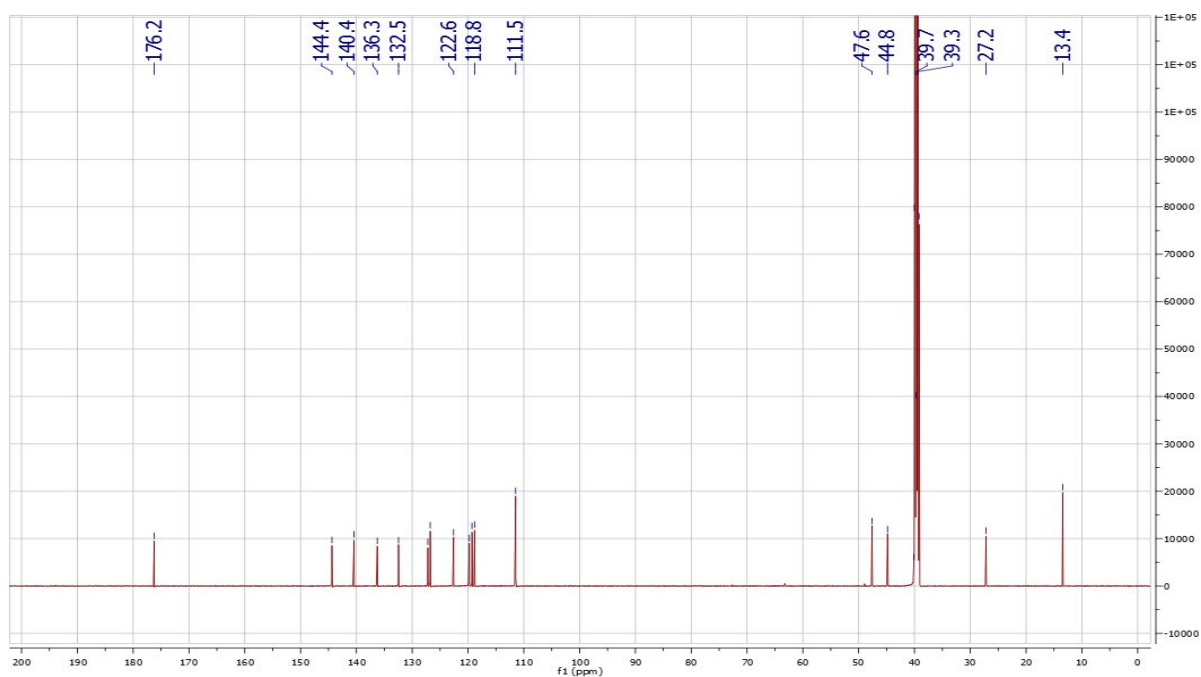


Figure 7: ^{13}C NMR spectrum (DMSO- d_6 , 150 MHz) of TCO $_3$

The structure of TCO $_3$ was confirmed using its HMBC (Figure 8) spectrum where correlations of the monoterpene part are observed between H-18 and C-19, C-20 and the carbonyl signal at δ_C 176.2 (C-21); between H-15 and C-16, C-14, C-3, C-20 and the carbonyl signal at δ_C 176.2 (C-21). This led to the establishment of the carbonyl group at position 21.

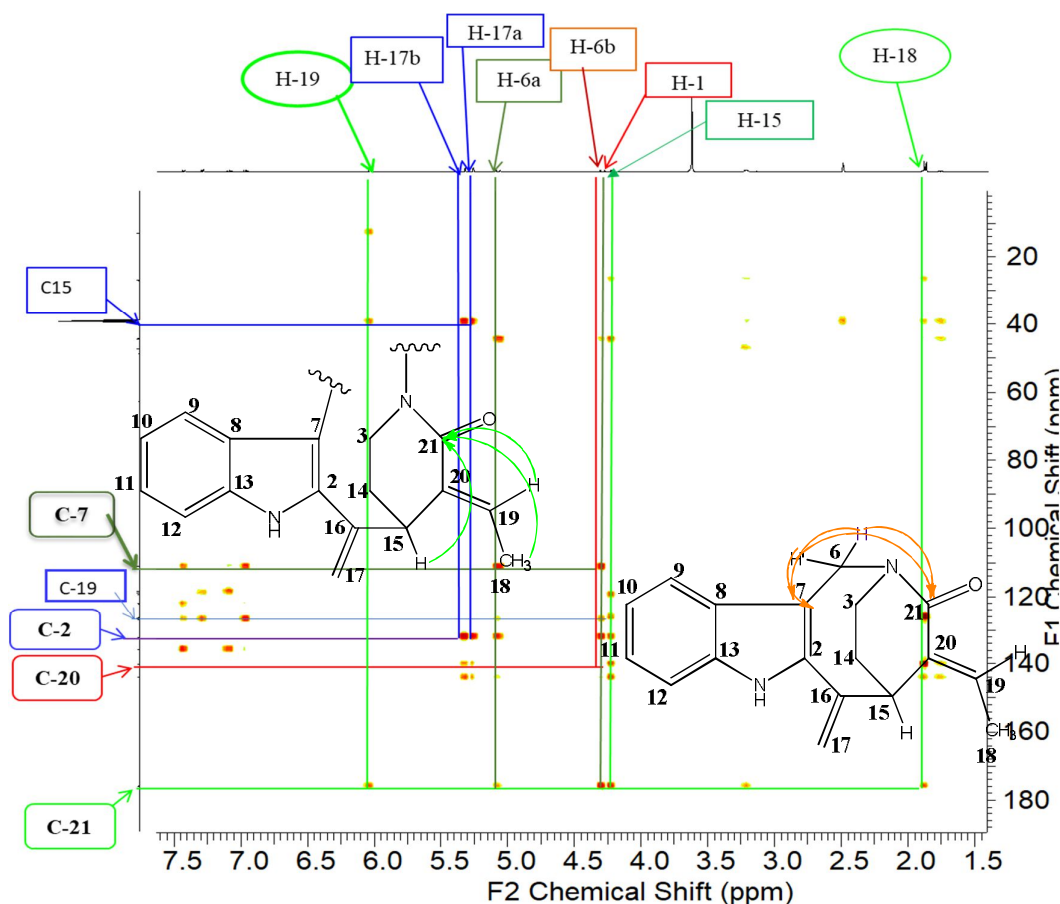


Figure 8: HMBC spectrum (DMSO- d_6) of TCO₃

Its NMR values were generally similar to those of apparicine (**73**) (Bennasar *et al.*, 2009) except for the presence of a carbonyl group at position 21 (δ_c 176.2).

Based on spectral interpretations and by comparison of its spectral data to those of apparicine (**73**) in the literature (Bennasar *et al.*, 2009), the structure of TCO₃ was found to be that of a new monoterpene indole alkaloid derivative of which the name apparicin-21-one (**74**) was attributed. Its relative configuration was deduced from the NOESY experiment where cross-peaks are observed between H-18 and H-15/H-17a this suggests that H-15 is β -oriented. These correlations also indicates that the configuration of the double bond between C-19 and C-20 is E.

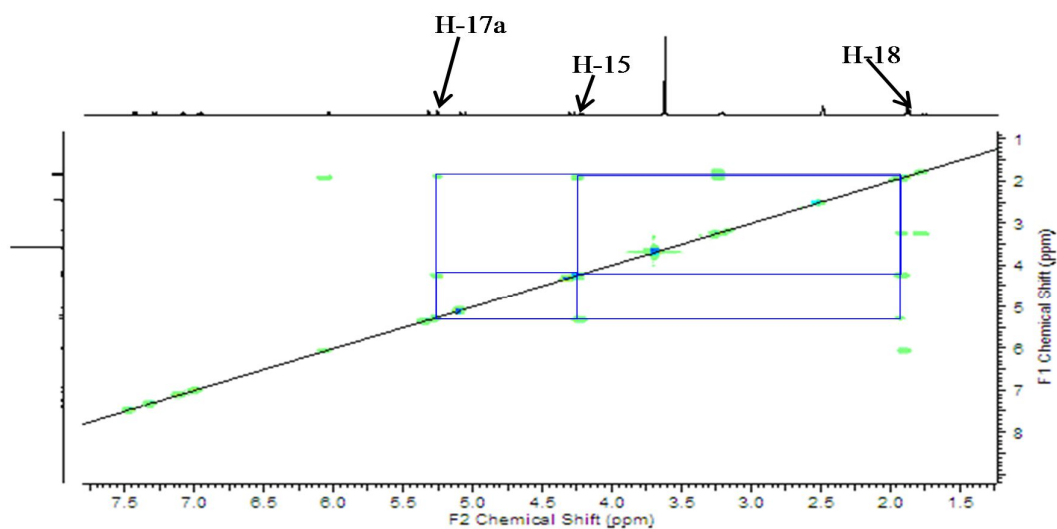


Figure 1: NOESY Spectrum (DMSO- d_6) of TCO₃

Figure 9: NOESY Spectrum (DMSO- d_6) of TCO₃

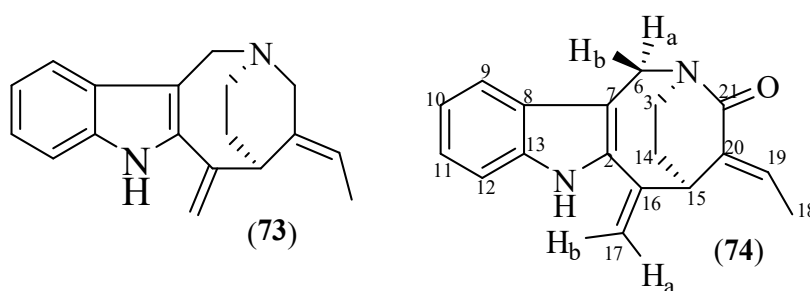


Table VI: NMR data (DMSO- d_6) of TCO₃

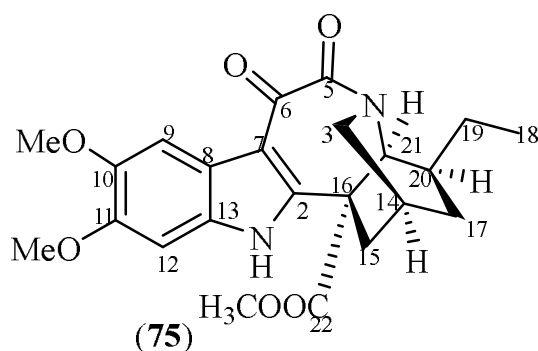
Position	TCO ₃	
	¹ H (H, m, J)	¹³ C
1	-	/
2	-	132.5
3	3.20 (1H, m); 3.22 (1H, m)	44.8
4	-	/
5	-	/
6	5.07 (d, 16.5); 4.29 (d, 16.5);	47.6
7	-	111.5
8	-	127.2
9	7.42 (1H, d, 7.8)	118.8
10	6.95 (1H, t, 7.5)	119.2
11	7.08 (1H, t, 7.5)	122.6
12	7.28 (1H, d, 7.8)	111.5
13	-	136.3
14	1.71 (1H, m); 1.80 (1H, m)	27.2
15	4.22 (1H, d, 5.3)	39.8
16	-	144.3
17	5.24 (1H ; brs); 5.33 (1H ; brs)	119.7

18	1.89 (1H, d, 6.8)	13.4
19	6.03 (2H, q, 7.01)	126.7
20	-	140.4
21	-	176.2

II.2.1.2. Characterization of TCO₅

TCO₅ was obtained from the fruits of *Tabernaemontana contorta* as a yellow powder in a mixture of Hex/AE 80/10. It is soluble in CHCl₃ and DMSO and responds positively to the Meyer's test giving a yellowish white precipitate and also to the Draggendorf's test giving a dark-red color characteristic of alkaloids.

From the spectroscopic data of TCO₅ such as HRESIMS, NMR 1D and 2D (including ¹H, ¹³C, COSY, HSQC and HMBC), its structure was determined to be that of a monoterpene indole alkaloid:



On the basis of HRESI-MS (m/z 427.1861 [M+H]⁺ calcd for 427.1869) (Figure 10), the molecular formula of TCO₅ was determined to be C₂₃H₂₆O₆N₂ indicating 12 double bond equivalents.

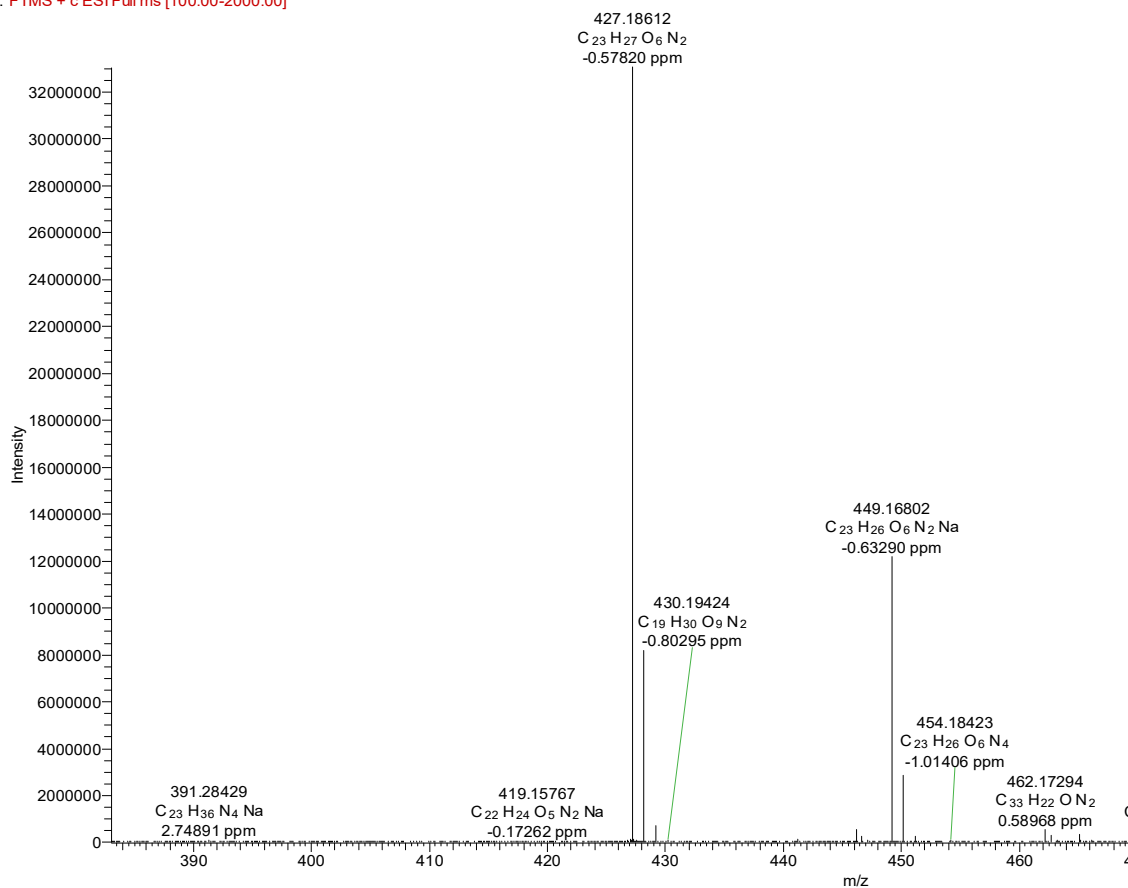


Figure 10: HRESI-MS of TCO₅

The ¹H NMR spectrum (Figure 11) of TCO₅ shows two aromatic proton signals at δ_{H} 6.90 (1H, s, H-12) and 7.32 (1H, s, H-9); two signals corresponding to three methoxy groups at δ_{H} 3.74 (6H, s) and 3.59 (3H, s); a bridgehead proton adjacent to nitrogen at δ_{H} 4.15 (1H, brs, H-21) and an ethyl group characterized by signals of a methyl at δ_{H} 0.84 (3H, t, 7.1 Hz, H-18) and a methylene δ_{H} 1.35 (1H, m, H-19a) and 1.44 (1H, m, H-19b).

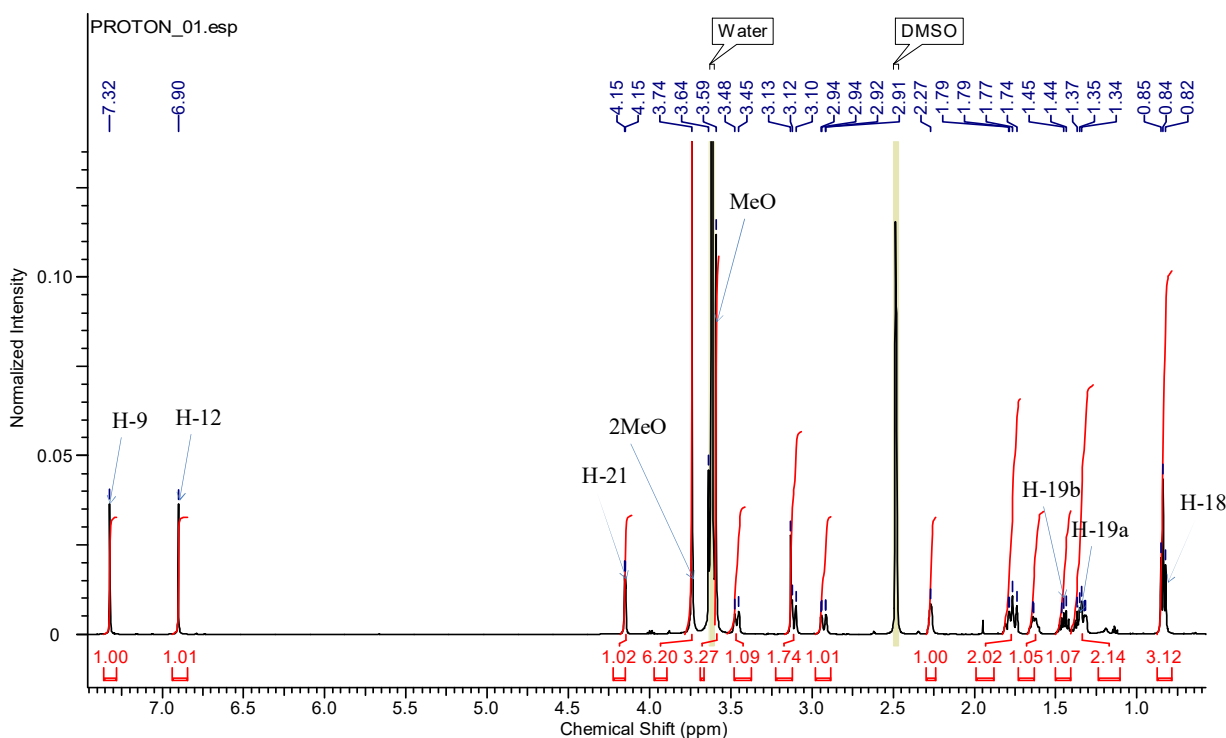


Figure 11: ^1H NMR spectrum (600 MHz, $\text{DMSO-}d_6$) of TCO_5

The COSY spectrum (Figure 12) of TCO_5 shows no correlation between the two aromatic protons meaning that the aromatic unit is *ortho* disubstituted. In addition to the aromatic unit, the main partial structures revealed by the COSY and HSQC data are:

- a $\text{CH}_2\text{CH}(\text{CH}_2)_2$ unit characterized by signals at δ_{H} 3.12 (1H, d, 12.2 Hz, H-3a), 3.46 (1H, d, 12.2 Hz, H-3b), 2.27 (1H, br s, H-14), 2.94 (1H, dd, 13.7, 1.5 Hz, H-15a); 1.79 (1H, dd, 13.7, 1.5 Hz, H-15b), 1.32 (1H, m, H-17a); 1.76 (1H, m, H-17b);
- a $\text{CHCHCH}_2\text{CH}_3$ unit characterized by signals at δ_{H} 4.15 (1H, d, 2.9 Hz, H-21), 1.64 (1H, m, H-20), 1.35 (1H, m, H-19a); 1.32 (1H, m, H-19b) and 0.84 (3H, t, 7.1 Hz, H-18). These two units are characteristic of the C-3/C-14/C-15/C-17 and C-21/C-20/C-19/C-18 fragments of the ibogan type indole alkaloid (Van Beek *et al.*, 1984).

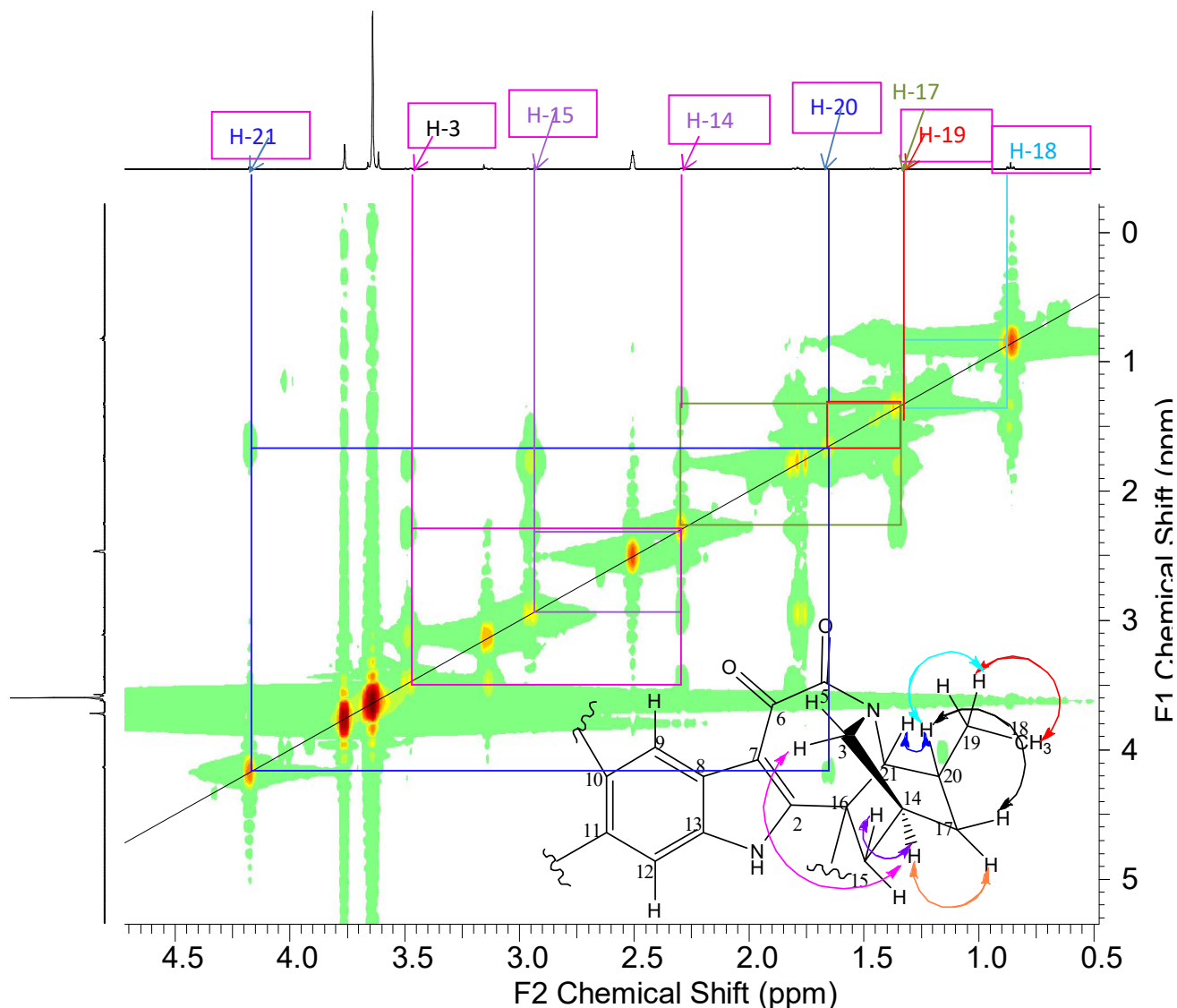


Figure 12: COSY Spectrum (DMSO- d_6) of TCO₅

The ^{13}C NMR spectrum (Figure 13) of TCO₅ reveals eight unsaturated carbon signals at δ_{C} 95.9 (C-12), 101.9 (C-9), 110.8 (C-7), 118.4 (C-8), 130.3 (C-13), 147.2 (C-11), 148.1 (C-10), 149.4 (C-2); three carbonyl signals at δ_{C} 168.3 (amide group C-5), 172.1 (ester group C-22), 185.4 (conjugated ketone C-6); four methylene signals at δ_{C} 27.9 (C-19), 28.6 (C-17), 33.2 (C-15), and 48.2 (C-3); three methyne signals at δ_{C} 28.2 (C-14), 35.4 (C-20) and 56.1 (C-21); a methyl signal at δ_{C} 11.9 (C-18) and three methoxy signals at δ_{C} 53.7, 56.1 and 56.2.

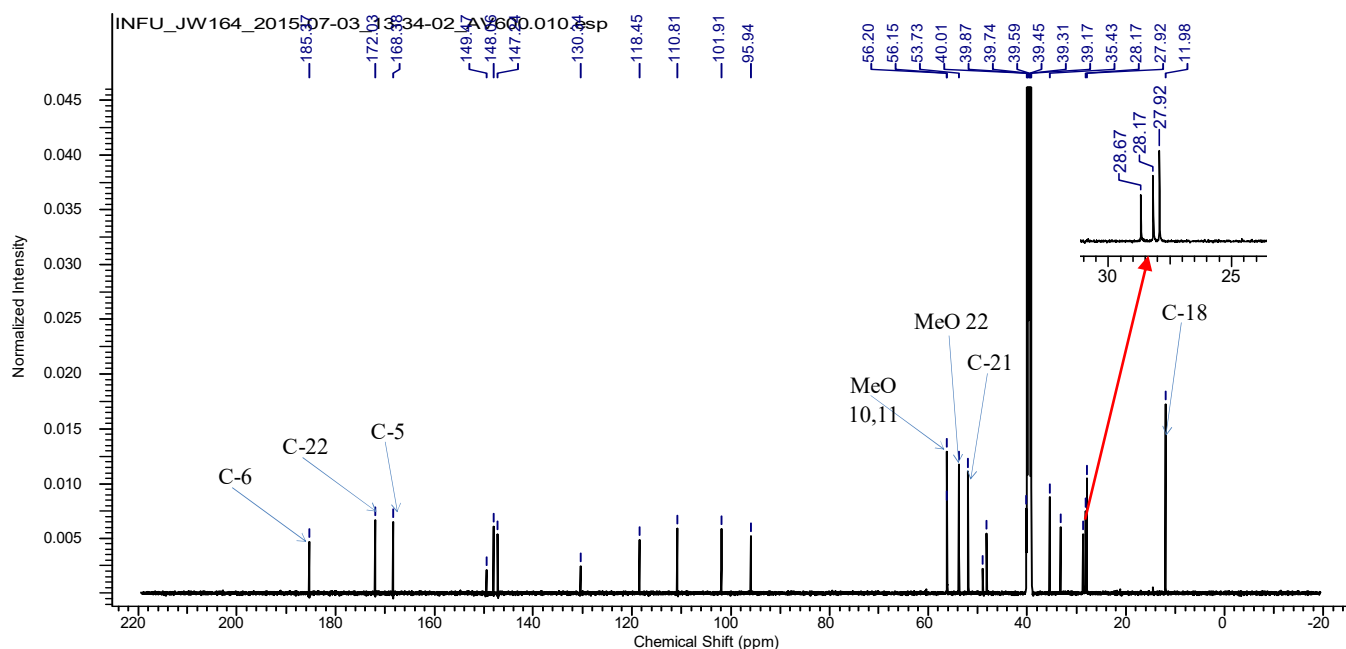
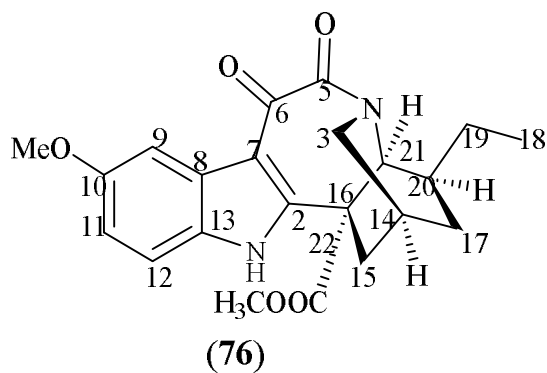


Figure 13: ^{13}C NMR spectrum (150 MHz, $\text{DMSO-}d_6$) of TCO_5

In the HMBC spectrum (Figure 14) of TCO_5 , the correlation between the proton of the two methoxy groups at δ_{H} 3.74 (6H, s) and the carbons C-10 (δ_{C} 148.1) and C-11 (δ_{C} 147.2) indicate their attachment to these carbons. It also shows correlations of the monoterpene part of the alkaloid between H-21 and C-20, C-19, C-5 and C-2; between H-15 and C-22, C-3 and C-16 and between H-17 and C-14, C-20 and C-2. The HMBC correlations between H-21 and the amide carbonyl group at δ_{C} 168.3 led to the establishment of the carbonyls at δ_{C} 168.3 and 185.4 to the carbons 5 and 6 respectively. The structure was closely similar to that of ibogamine-16-carboxylic acid,17,20-didehydro-5,6-dicarboxy-10-methoxy-methyl ester (**76**) (Chen *et al.*, 2016) (see Table 7) with the only difference being the presence of a methoxy group at position 11.



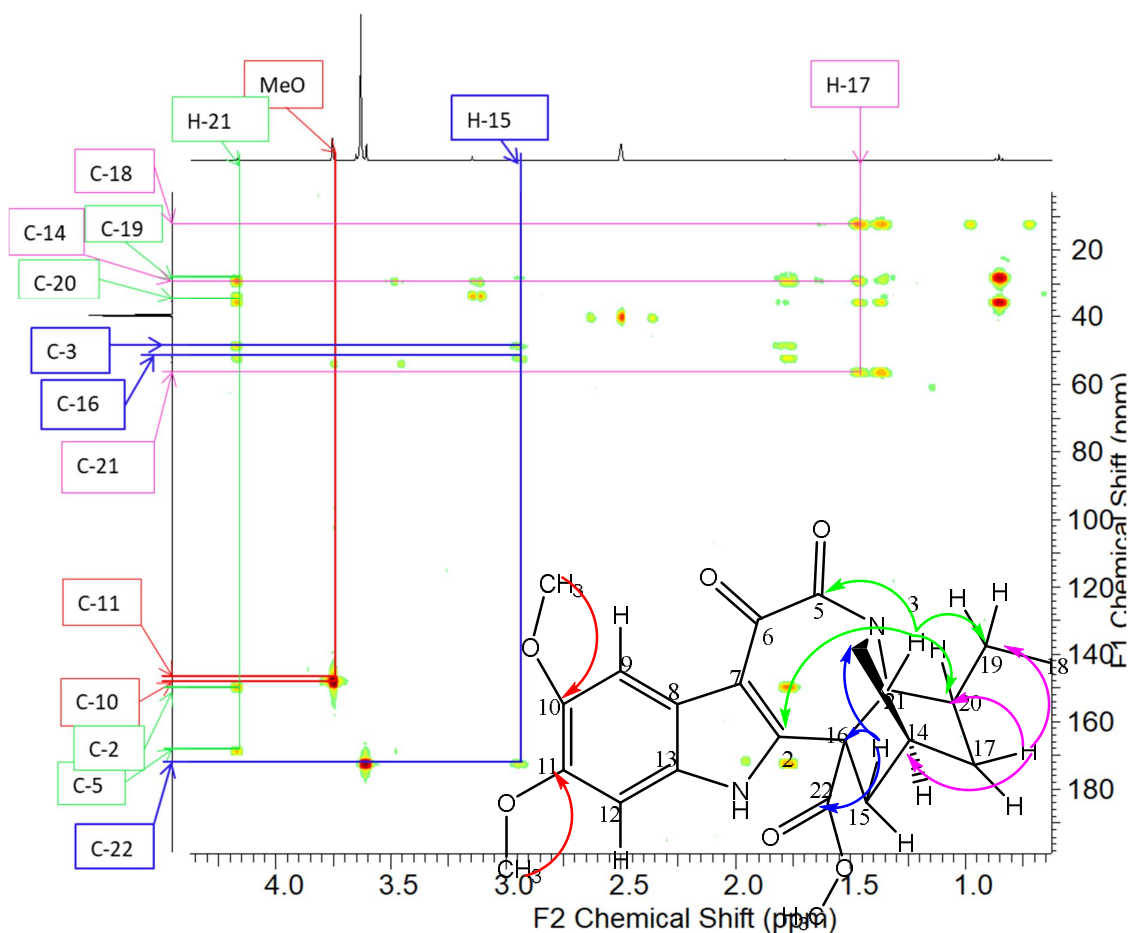


Figure 14: HMBC spectrum (DMSO- d_6) of TCO₅

Based on the HRESI-MS and the interpretation of the spectroscopic data and by comparison of these data with those of ibogamine-16-carboxylic acid, 17,20-didehydro-5,6-dicarboxy-10-methoxy-methyl ester (**76**) (Chen *et al.*, 2016), the structure of TCO₅ was determined to be that of a new monoterpene indole alkaloid derivative which was named 5,6-dioxo-11-methoxy voacangine (**75**). The relative stereochemistry at C-14, C-16 and C-21 of iboga type is reported to be the same because of the existence of the C-14/C-3/N-4 bridge (Van Beek *et al.*, 1984). Biogenetically, the H-21 of iboga type monoterpene indole alkaloid derivatives isolated from Apocynaceae species is α -oriented (Van Beek *et al.*, 1984) thereby β -orientating the C-14/C-3/N-4 bridge. The NOESY correlations (Figure 15) observed between H-20, H-21 and H-14 indicate that they are all α -orientated thereby confirming the β -orientation of the C(14)-C(3)-N(4) bridge as described by the literature (Van Beek *et al.*, 1984)

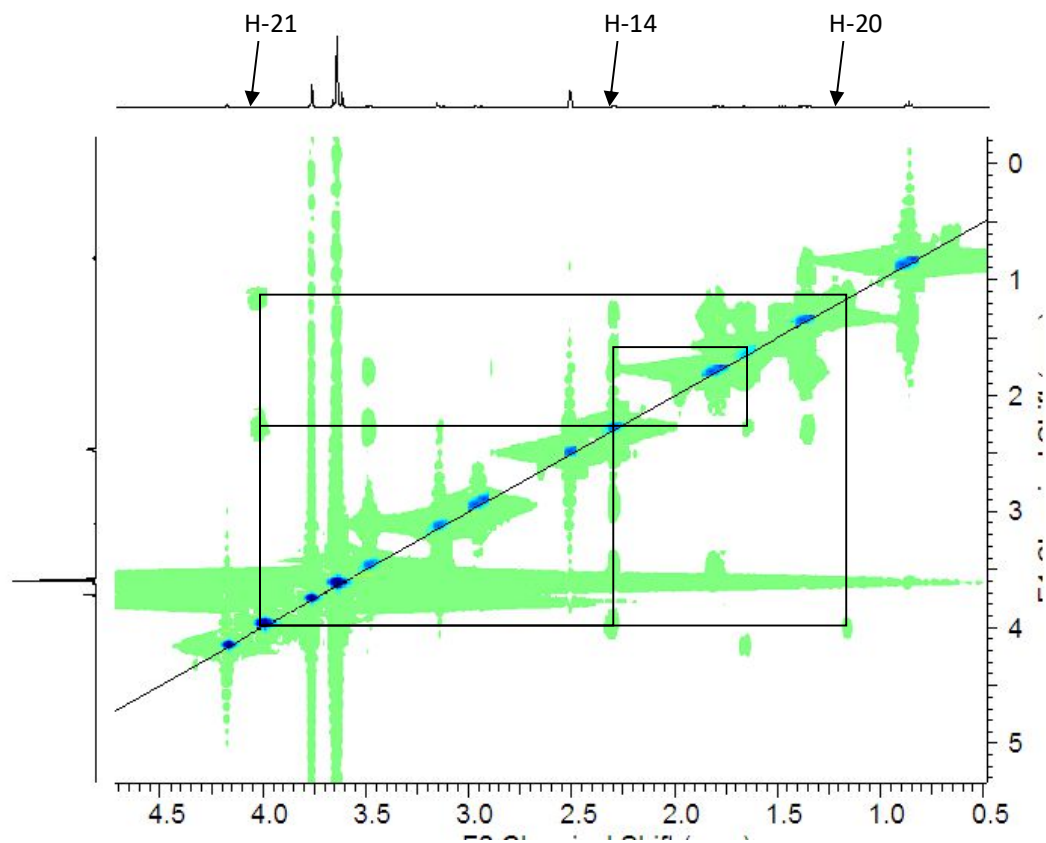


Figure 15: NOESY Spectrum (DMSO-*d*₆) of TCO₅

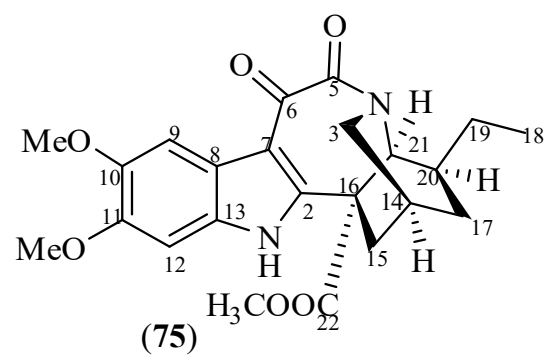


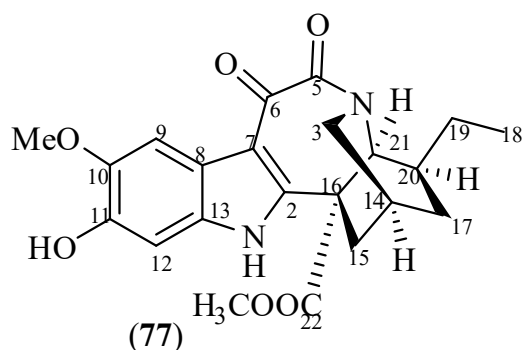
Table VII: ^1H and ^{13}C NMR data (DMSO- d_6) of TCO₅

Position	^1H (nH, m, J)	^{13}C
	TCO ₅	TCO ₅
1NH	-	-
2	-	149.4
3	3.12 (1H, d, 12.2) 3.46 (1H, d, 11.2)	48.2
4NH	-	-
5	-	168.3
6	-	185.4
7	-	110.8
8	-	118.4
9	7.32 (1H, s)	101.9
10	-	148.1
11	-	147.2
12	6.90 (1H, s)	95.9
13	-	130.3
14	2.27 (1H, br s)	28.2
15	2.94 (1H, dd, 13.7, 1.5) 1.79 (1H, dd, 13.7, 1.5)	33.2
16	-	51.8
17	1.32 (1H, m) 1.76 (1H, m)	28.6
18	0.84 (3H, t, 7.1)	11.9
19	1.35 (1H, m) 1.32 (1H, m)	28.2
20	1.64 (1H, m)	35.4
21	4.15 (1H, d, 2.9)	56.1
22COOMe	3.59 (3H, s)	172; 53.7
MeO 10, 11	3.74 (6H, s)	56.2

II.2.1.3. Characterization of TiS₅

TiS₅ was obtained from the stem of *Tabernaemontana inconspicua* as a yellow powder in a mixture of Hex/AE 40/60. It is soluble in CHCl₃ and DMSO and responds positively to the Meyer's test and also to the Dragendorff's test characteristic of alkaloids.

From the spectroscopic data of TiS₅ such as HRESI-MS, NMR 1D and 2D (including ^1H , ^{13}C , COSY, HSQC and HMBC) and by comparison of these data to those of TCO₅, its structure was determined to be that of a monoterpene indole alkaloid:



The molecular formula of TiS_5 was determined to be $C_{22}H_{24}O_6N_2$ on the basis of HRESI-MS (m/z 413.1704 $[M+H]^+$ calcd for 413.1713), (Figure 16) indicating 12 double bond equivalents.

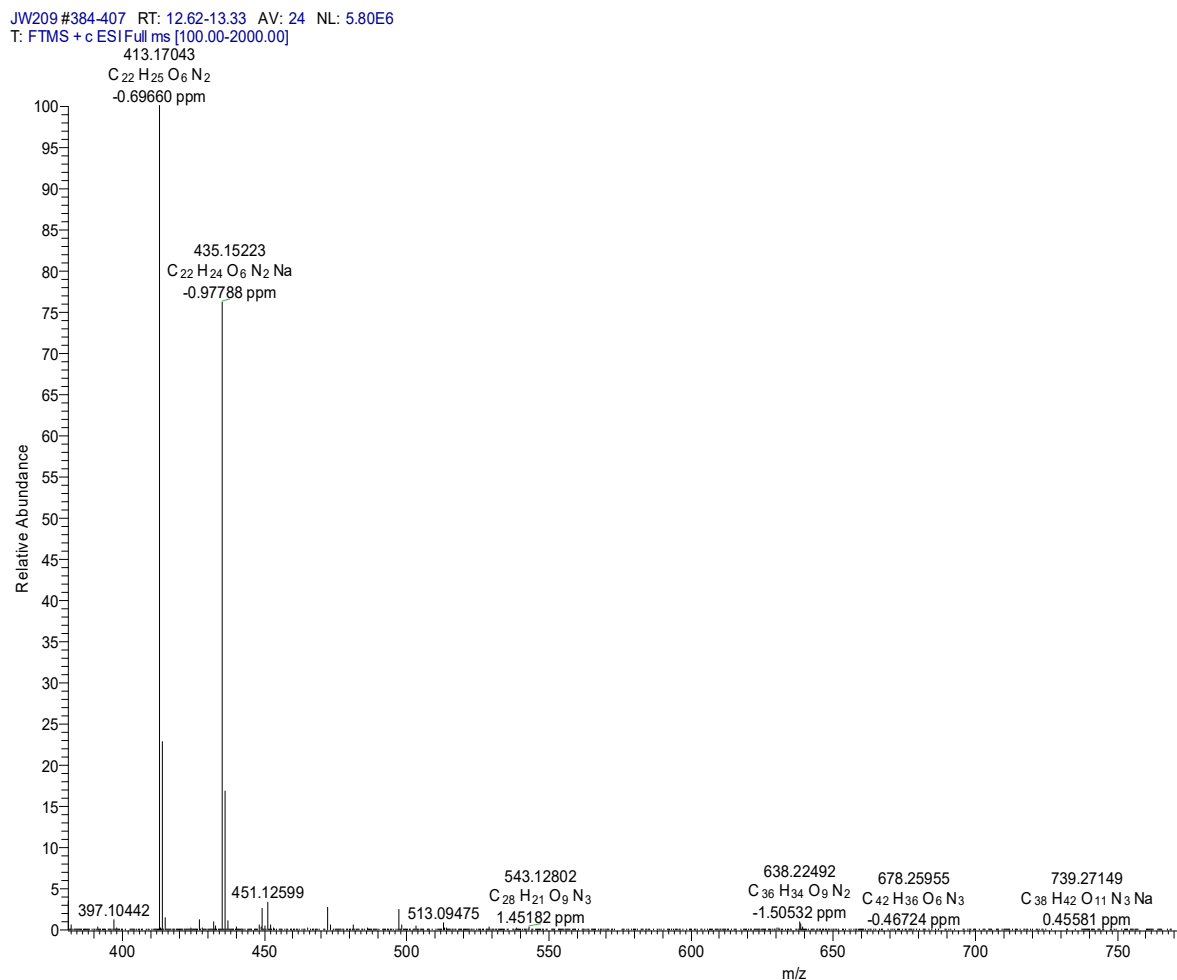


Figure 16: HRESI-MS of TiS_5

The 1H NMR spectrum of TiS_{12} (Figure 17), is readily comparable to that of TCO_5 with the difference being the presence of only two methoxy groups at δ_H 3.69 (3H, s) and 3.85 (3H, s) instead of three in the 1H NMR spectrum of TCO_5 . Moreover, there is the

appearance of a phenolic hydroxy proton at δ_H 9.07 (1H, s) suggesting that one methoxy group either at position 10 or 11 has been replaced by a hydroxy group.

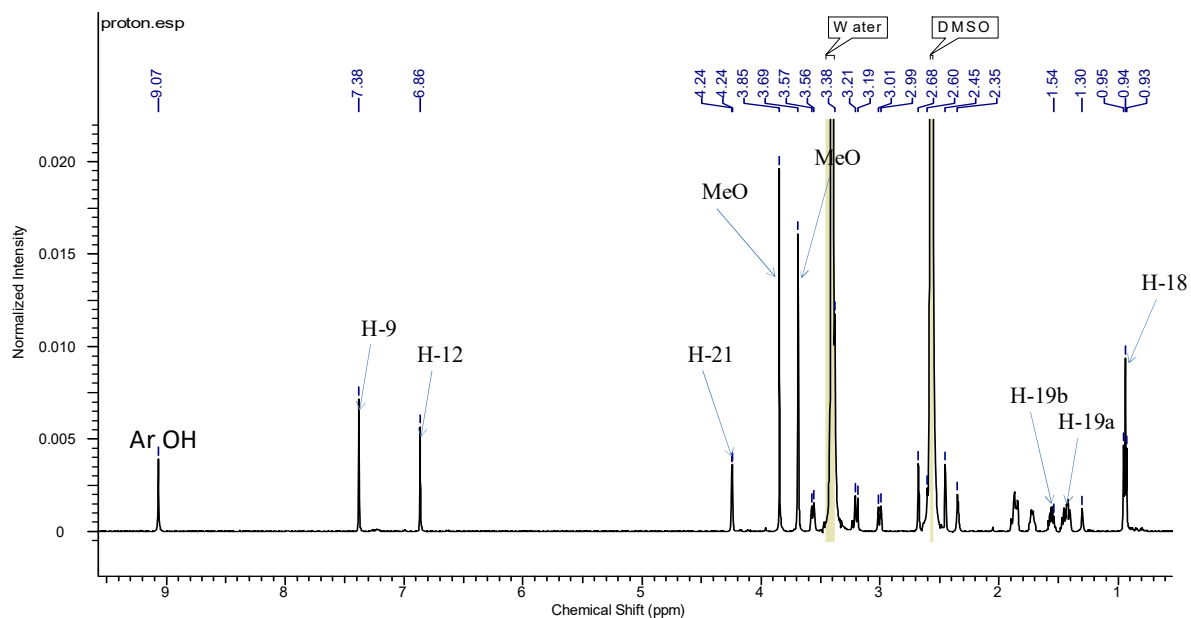


Figure 17: ^1H NMR (600 MHz, $\text{DMSO-}d_6$) of TiS_5

The COSY and NOESY spectra (Figures 18 and 19) of TiS_5 are identical to that of TCO_5 .

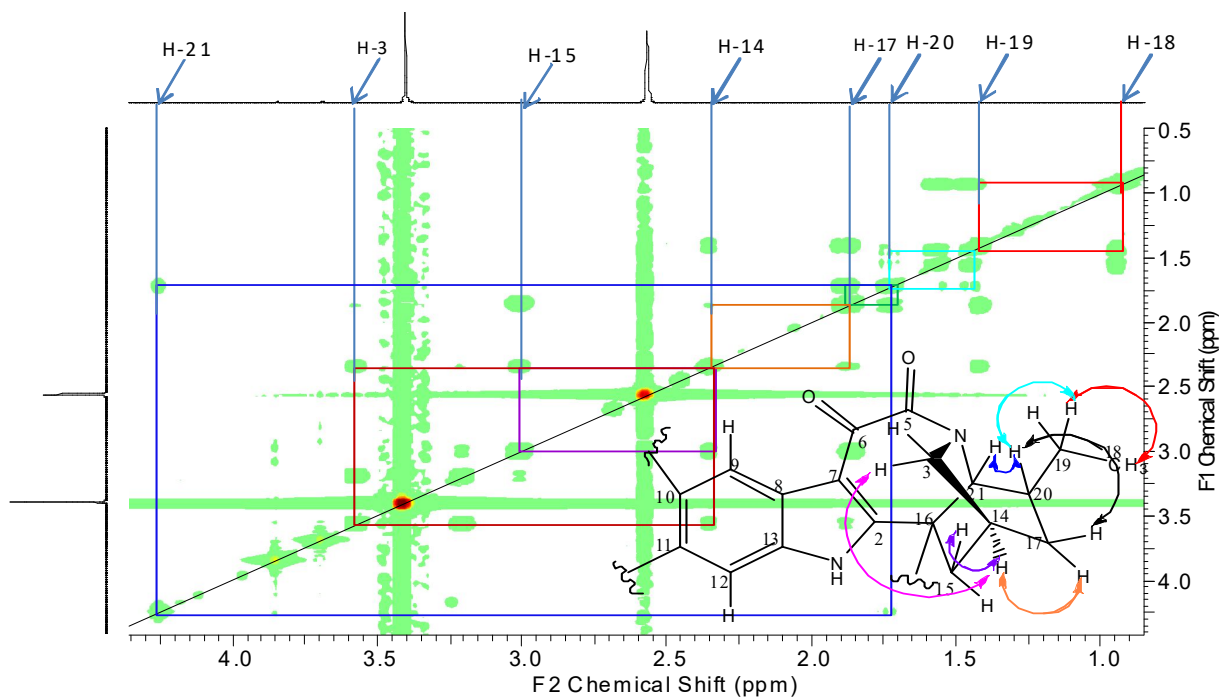


Figure 18: COSY Spectrum ($\text{DMSO-}d_6$) of TiS_5

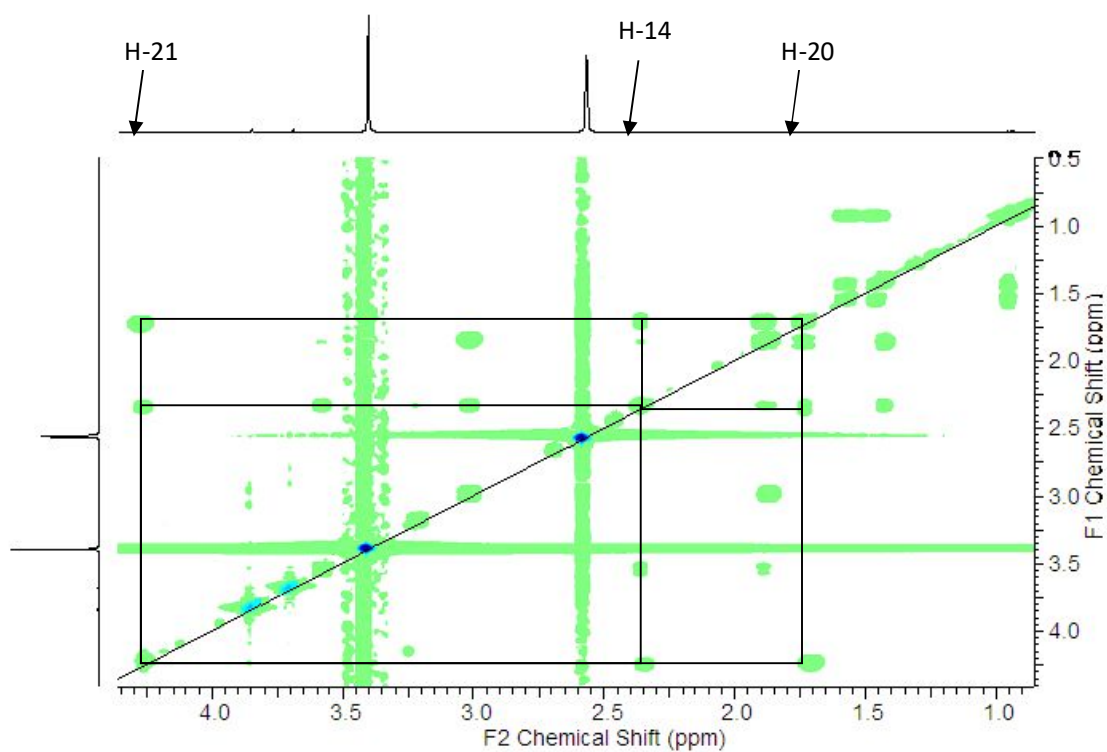


Figure 19: NOESY Spectrum (DMSO- d_6) of TiS_5

The ^{13}C NMR spectrum (Figure 20) of TiS_5 reveals 22 carbon signals instead of 23 like in TCO_5 confirming the absence of a methoxy group.

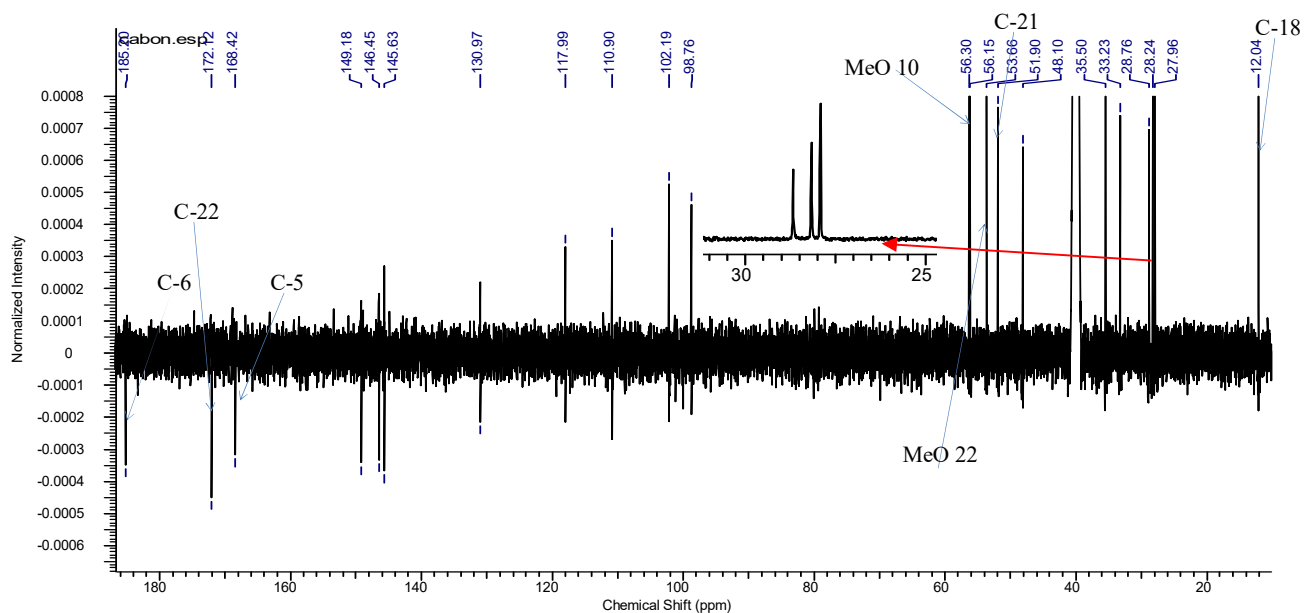


Figure 20: ^{13}C NMR spectrum (150 MHz, DMSO- d_6) of TiS_5

The position of the hydroxy group was confirmed by HMBC correlation from the hydroxy proton δ_H 9.07 to C-11 and C-12.

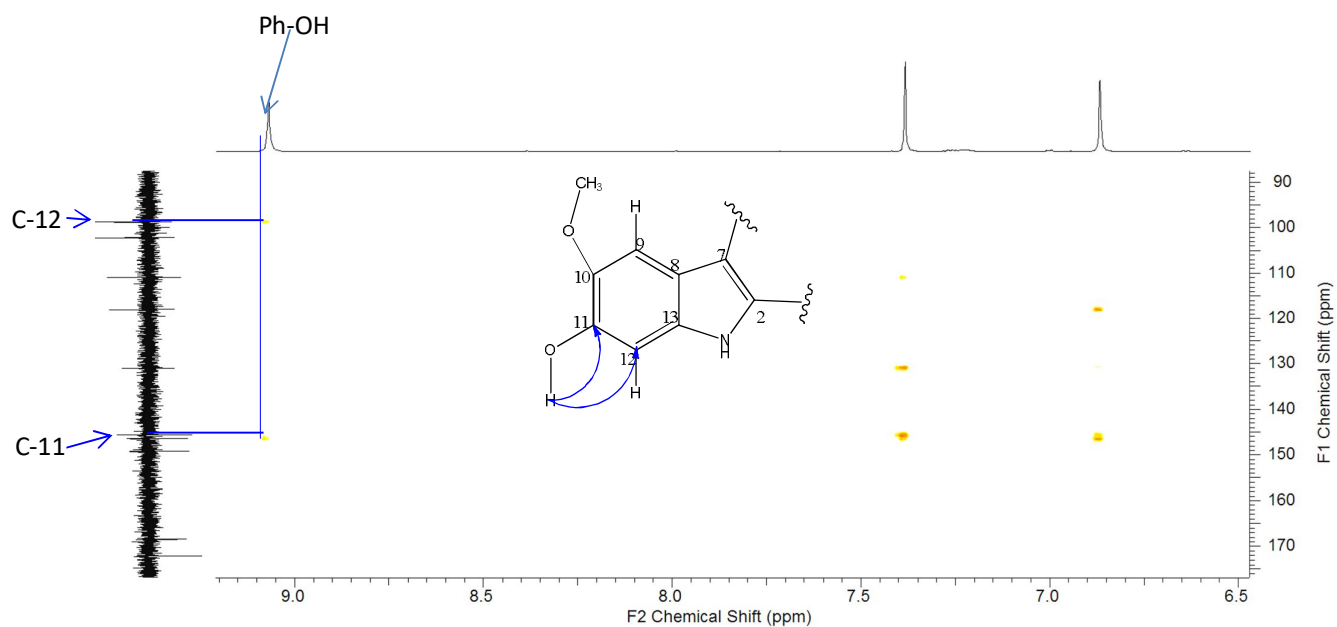


Figure 21: HMBC spectrum (DMSO- d_6) of TiS₅

Based on the HRESI-MS, the interpretation of the spectroscopic data and by comparison of these data with those of TCO₅, the structure of TiS₅ was determined and found to be a new voacangine derivative to which the name 5,6-dioxo-11-hydroxy voacangine (**77**) was given.

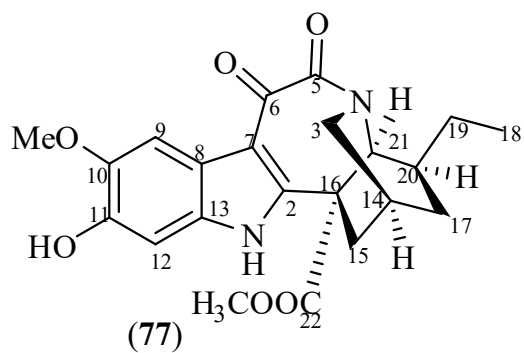


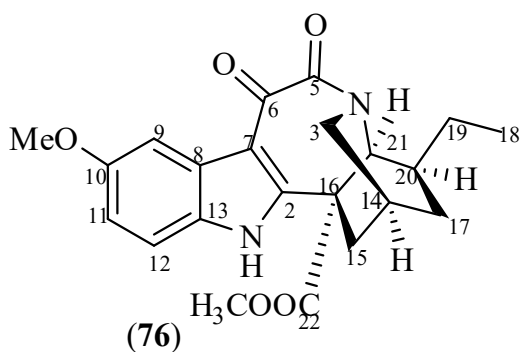
Table VIII: ^1H and ^{13}C NMR data (DMSO- d_6) of TiS_5

Position	TiS_5	
	^1H (nH, m, J)	^{13}C
1NH	-	-
2	-	149.2
3	3.20 (1H, d, 11.3); 3.56 (1H, d, 11.3)	48.1
4NH	-	-
5	-	168.4
6	-	185.2
7	-	110.9
8	-	118.0
9	7.32 (1H, s)	102.2
10	-	146.4
11	-	145.6
12	6.90 (1H, s)	98.7
13	-	130.9
14	2.35 (1H, br s)	28.7
15	3.00 (1H, d, 12.1); 1.87 (1H, d, 12.1)	33.2
16	-	51.9
17	1.42 (1H, m); 1.86 (1H, m)	28.7
18	0.94 (3H, t, 7.1)	12.0
19	1.45 (1H, m); 1.42 (1H, m)	28.2
20	-	35.5
	1.64 (1H, m)	
21	4.15 (1H, d, 2.9)	56.1
COOMe	3.69 (3H, s)	172.1; 53.7
10-MeO	3.85 (3H, s)	56.3
11-OH	9.07 (1H, s)	-

II.2.1.4. Identification of TiS_{10}

TiS_{10} was obtained from the stem of *Tabernaemontana inconspicua* as a yellow powder in a mixture of Hex/AE 40/60. It is soluble in CHCl_3 and DMSO and responds positively to the Meyer's test and also to the Dragendorff's test characteristic of alkaloids.

From the spectroscopic data of TiS_{10} such as HRESI-MS, NMR 1D and 2D (including ^1H , ^{13}C , COSY, HSQC and HMBC) and by comparison of these data to those described in the literature, its structure was determined to be that of a monoterpene indole alkaloid:



The molecular formula of TiS_{10} was determined to be $C_{22}H_{24}O_5N_2$ on the basis of HRESIMS (m/z 397.1756 $[M+H]^+$ calcd for 397.1763) (Figure 19), being indicative of 12 double bond equivalents.

JW155 150618153447 #709-754 RT: 10.97-11.64 AV: 46 NL: 4.90E7
 F: FTMS + c ESI Full ms [100.00-2000.00]

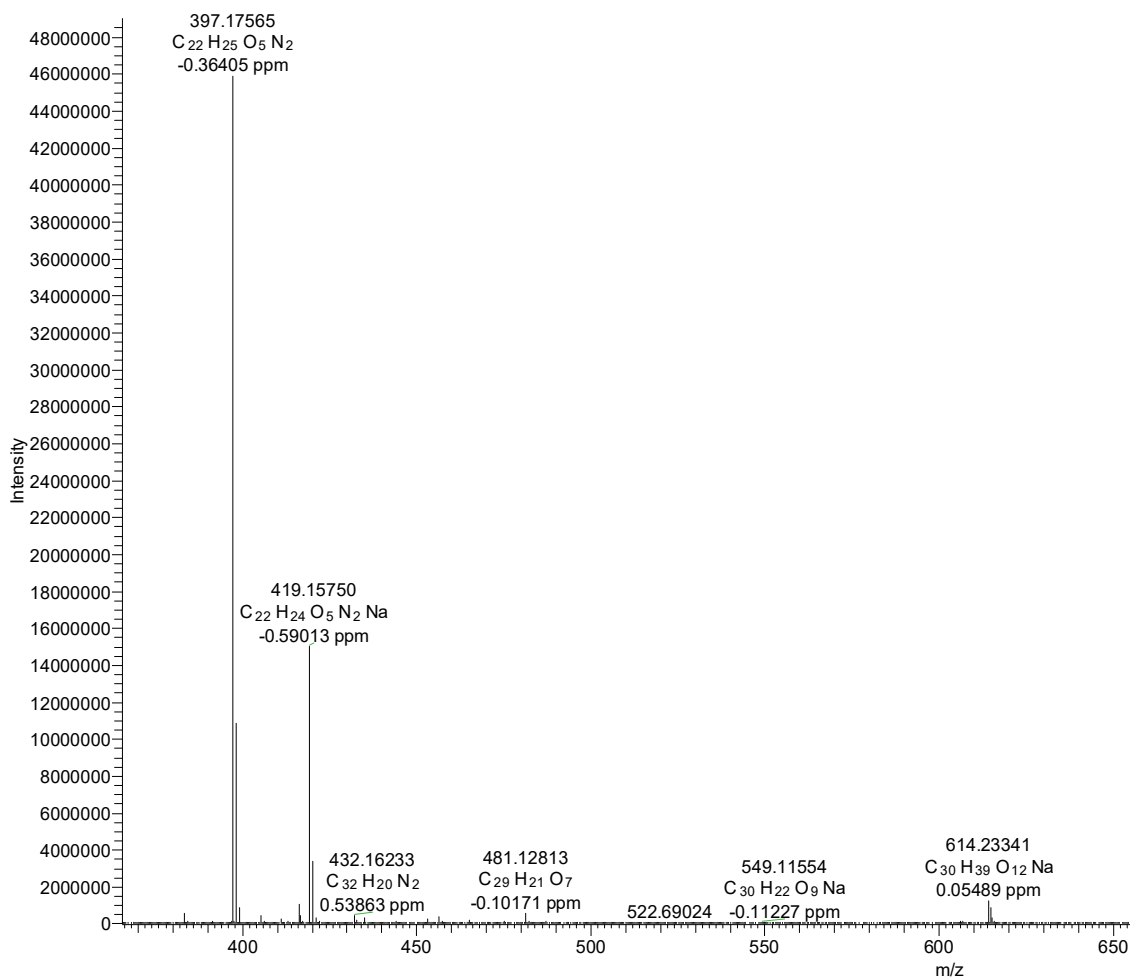


Figure 22: HRESI-MS of TiS_{10}

Its 1H NMR spectrum (Figure 23), is also comparable to that of TCO_5 with the main difference being the presence of two methoxy groups at δ_H 3.16 (3H, s) and 3.76 (3H, s)

instead of three in the ^1H NMR spectrum of TCO_5 . In addition, there is the appearance of three aromatic protons at δ_{H} 6.86 (1H, d, 8.4 Hz), 7.31 (1H, d, 8.4 Hz) and 7.38 (1H, d, 2.3 Hz) on the proton spectrum of TiS_{10} instead of two in that of TCO_5 suggesting the absence of one methoxy group either at position 10 or 11.

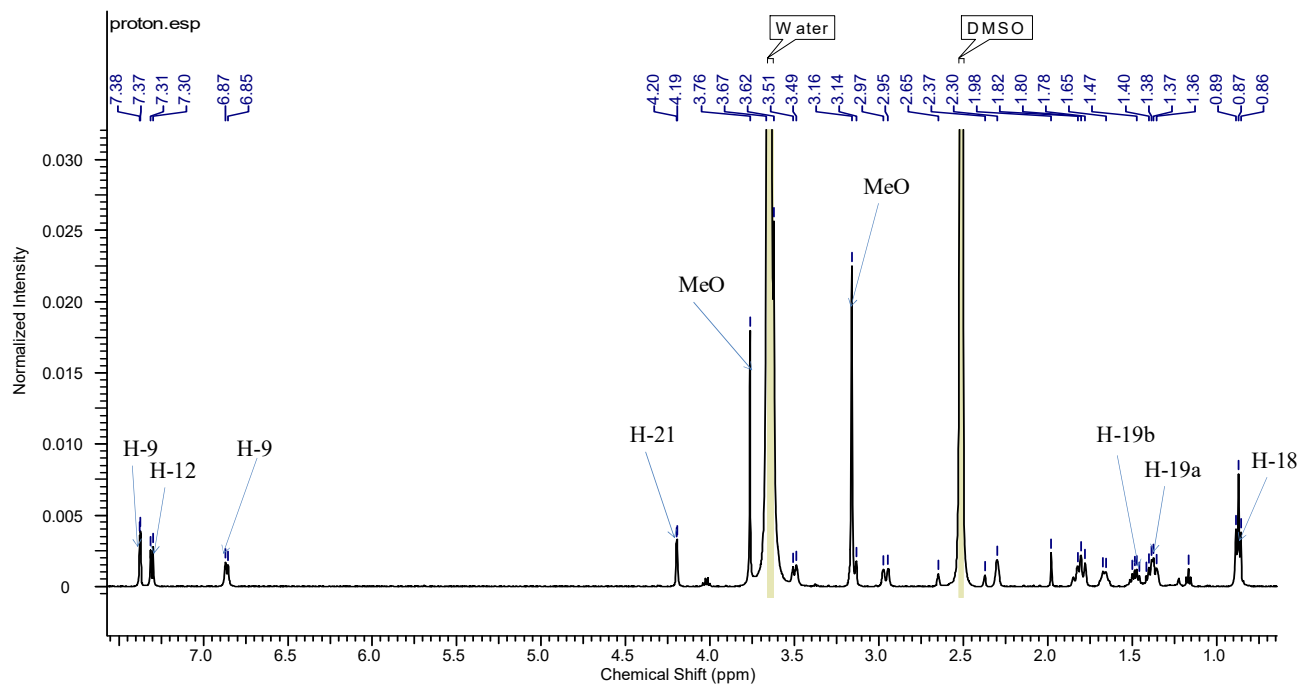


Figure 23: ^1H NMR spectrum ($\text{DMSO-}d_6$, 600 MHz) of TiS_{10}

The COSY spectrum (Figure 24) of TiS_{10} unlike in TCO_5 shows correlation between the aromatic protons between H-12 (δ_{H} 7.31) and H-11 (δ_{H} 6.86).

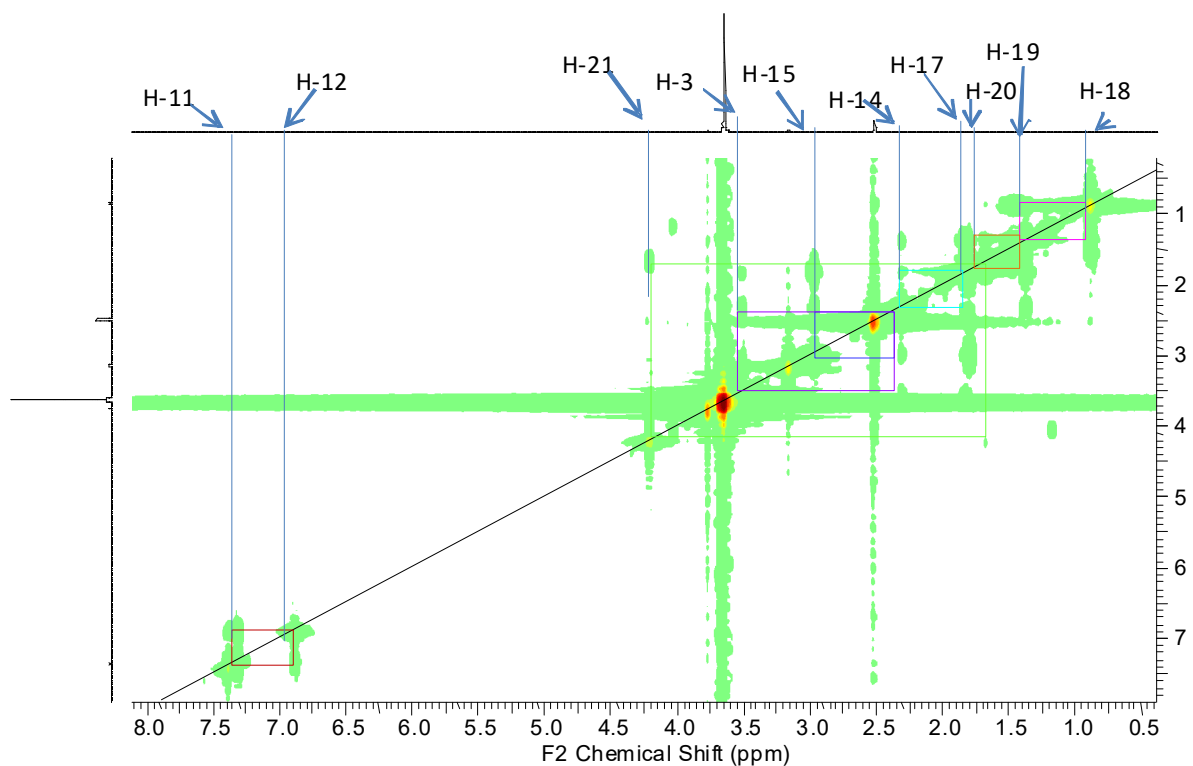


Figure 24: COSY Spectrum (DMSO-*d*₆, 600 MHz) of TiS₁₀

The ¹³C NMR spectrum of TiS₁₀ (Figure 25) is also very close to that of TCO₅ with the difference being the drop of displacement shift of C-11 from 147, 2 to 113.6 confirming the absence of a methoxy group at that position.

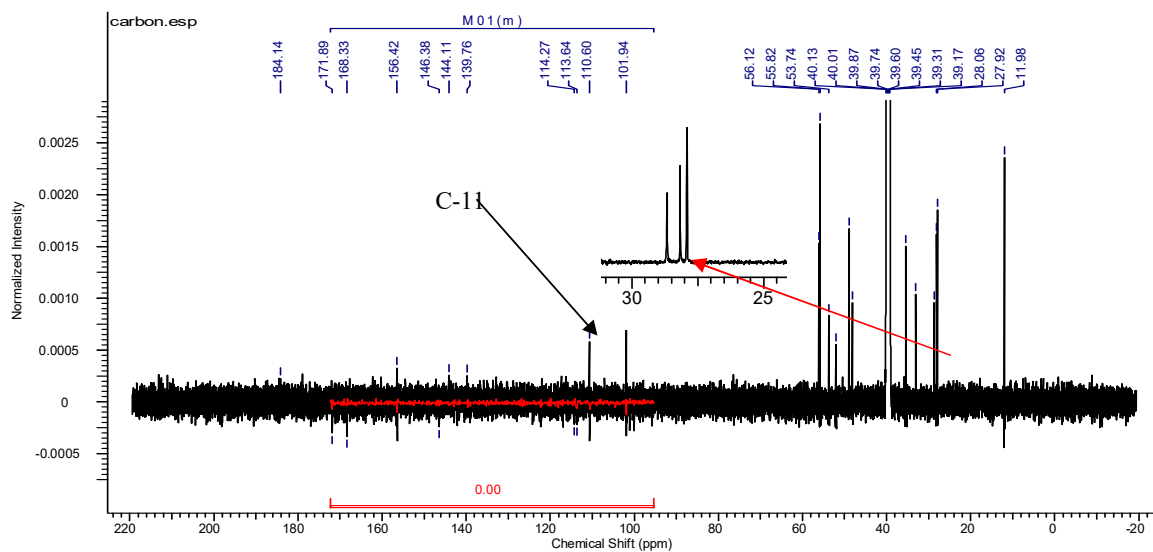


Figure 25: ¹³C NMR spectrum (DMSO-*d*₆, 150 MHz) of TiS₁₀

The HMBC spectrum (Figure 26) of TiS₁₀ enabled the positioning of the methoxy group at position 10 thanks to the correlation between the proton at δ_H 3.76 (3H, s) and C-10 (δ_C 156.4).

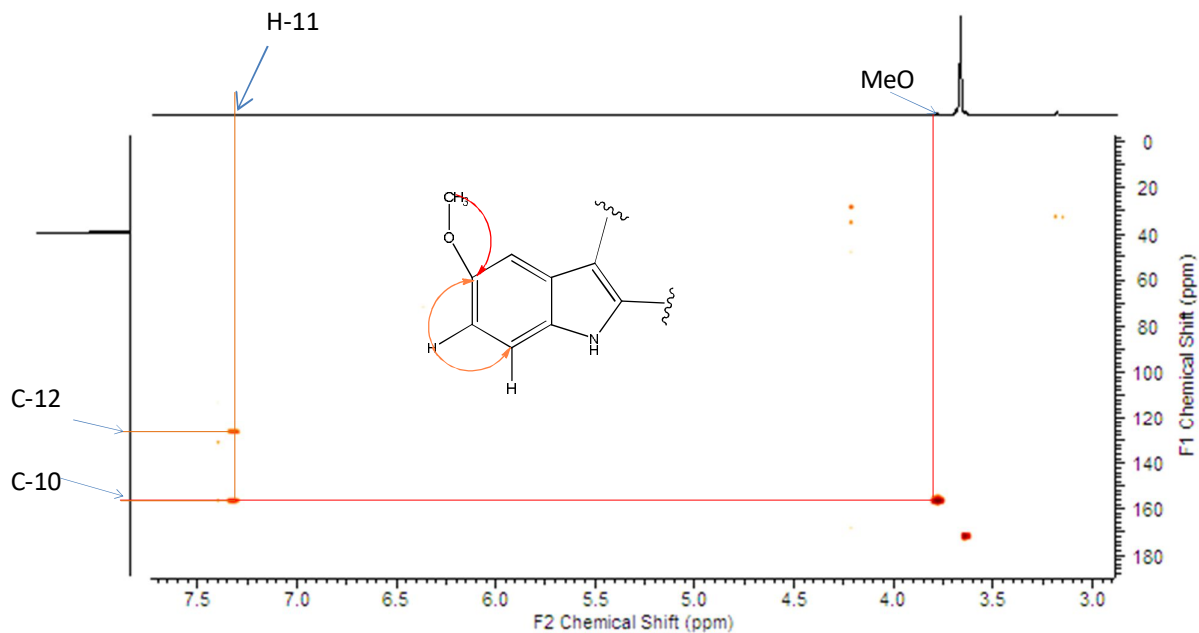


Figure 26: HMBC spectrum (DMSO-*d*₆) of TiS₁₀

Based on the analysis of the physical and spectroscopic data of TiS₁₀ and by comparison of these data to those described in the literature, the structure of TiS₁₀ was identified to be that of ibogamine-16-carboxy,17,20-didehydro-5,6-dicarboxo-10-methoxy-methyl ester (**76**) (Chen *et al.*, 2016).

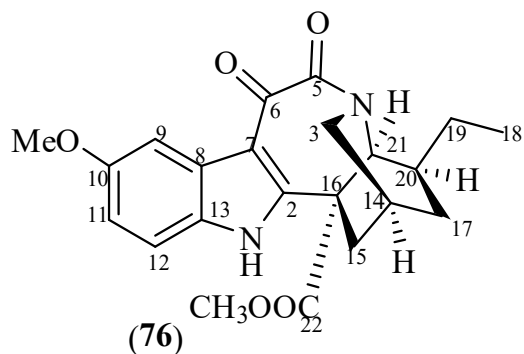


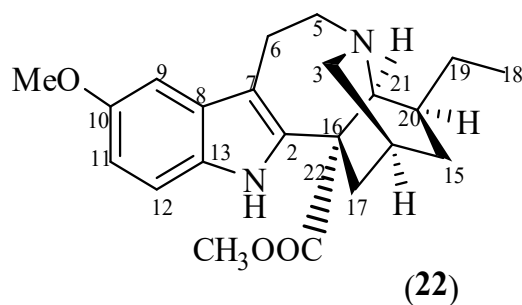
Table IX: ¹H and ¹³C NMR (DMSO-*d*₆) data of TiS₁₀ compared to the literature (Chen *et al.*, 2016)

Position	¹ H (nH, m, J)		¹³ C	
	TiS ₁₀	(Chen <i>et al.</i> , 2016)	TiS ₁₀	(Chen <i>et al.</i> , 2016)
1NH	-	-	-	-
2	-	-	151.4	151.7
3	3.50 (1H, d, 11.5); 3.12 (1H, d, 11.6)	3.50 (1H, d, 11.4); 3.14 (1H, d, 11.6)	48.2	48.1
4NH	-	-	-	-
5	-	-	168.3	168.4
6	-	-	184.1	185.1
7	-	-	110.6	110.6
8	-	-	127.8	126.6
9	7.38 (1 H d, 2.3)	7.39 (1H, d, 2.3)	101.9	101.9
10	-	-	156.4	156.4
10-OCH3	3.76 (3H, s)	3.77 (3H, s)	55.8	55.7
11	6.86 (1H, d, 8.8)	6.85 (1H, dd, 8.8, 2.4)	113.6	113.7
12	7.31 (1H, d, 8.8)	7.29 (1H, d, 8.8)	114.2	113.7
13	-	-	131.9	131.1
14	2.30 (1H, s)	2.29 (1H, s)	28.1	28.1
15	1.82 (1H, m); 2.96 (1H, d, 12.6)	1.81 (1H, m); 2.96 (1H, m)	33.1	33.1
16	-	-	52.0	52.1
17	1.40 (1H, m) 1.82 (1H, m)	1.37 (1H, m) 1.82 (1H, m)	28.7	28.8
18	0.87 (3H, t, 7.3) 1.50 (1H, m);	0.88 (3H, t, 7.3) 1.52 (1H, m);	12.0 28.0	12.0 28.0
19	1.38 (1H, m)	1.39 (1H, m)		
20	1.67 (1H, brs)	1.67 (1H, m)	35.4	35.5
21	4.20 (1H, d, 1.9)	4.20 (1H, brs)	56.2	56.1
22COOCH3	3.62 (3H, s,)	3.63 (3H, s,)	172.0; 53.7	172.0; 53.5

II.2.1.5. Identification of TiS₆ = TCO₇

TiS₆ was obtained from the stem of *Tabernaemontana inconspicua* and stem-bark of *Tabernaemontana contorta* as greyish needlets in a mixture of Hex/AE 36/64. It is soluble in CHCl₃ and DMSO and responds positively to the Meyer's and Dragendorff's test characteristic of alkaloids.

From the spectroscopic data of TiS₆ such as HRESI-MS, NMR 1D and 2D (including ¹H, ¹³C, COSY, HSQC and HMBC) and by comparison of these data to those described in the literature, its structure was identified to be that of a monoterpene indole alkaloid:



Its molecular formula was determined to be $C_{22}H_{28}O_3N_2$ on the basis of HRESI-MS (m/z 369.21763[M+H]⁺ calcd for 368.2094) (Figure 27), indicating 10 double bond equivalents.

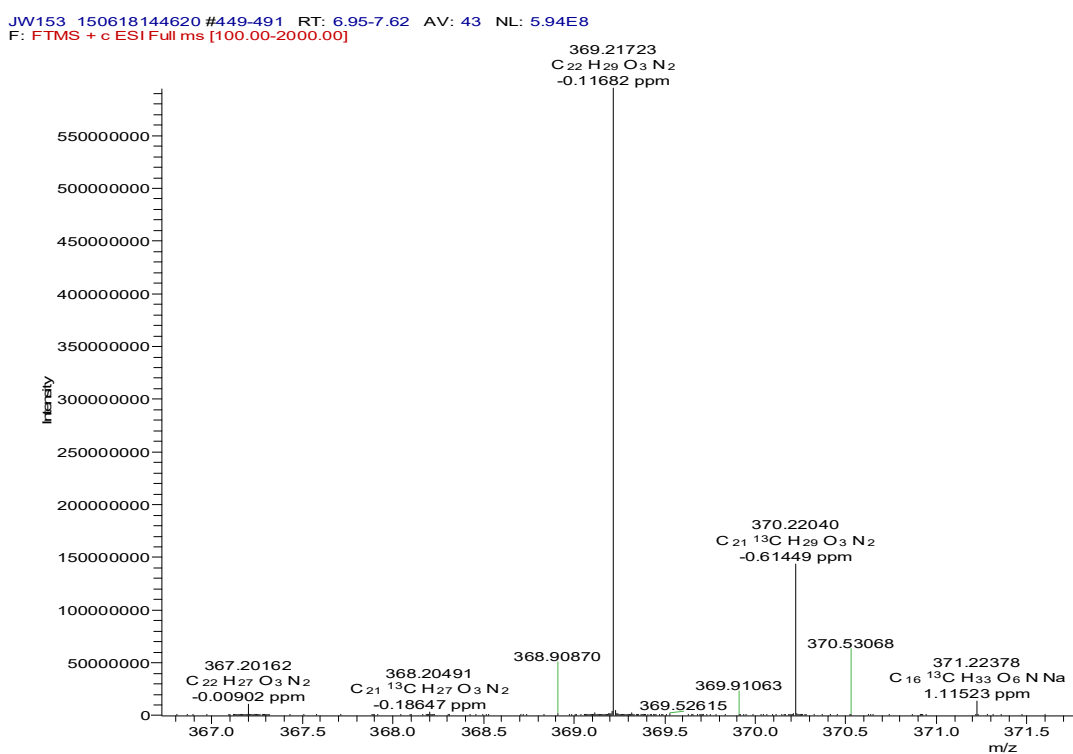


Figure 27: HRESI-MS of TiS_6

Its ¹H NMR spectrum (Figure 28) is comparable to that of TiS_{10} . The main difference here is the appearance of four signals corresponding to two diastereotopic methylene groups at δ_H 2.97 (1H, m, H-6a); 3.15 (1H, m, H-6b) and 3.22 (1H, m, H-5a); 3.39 (1H, m, H-5b) which are absent in the spectrum of TiS_{10} . This finding suggests the absence of the two carbonyls at positions 6 and 5 in the structure of TiS_{10} .

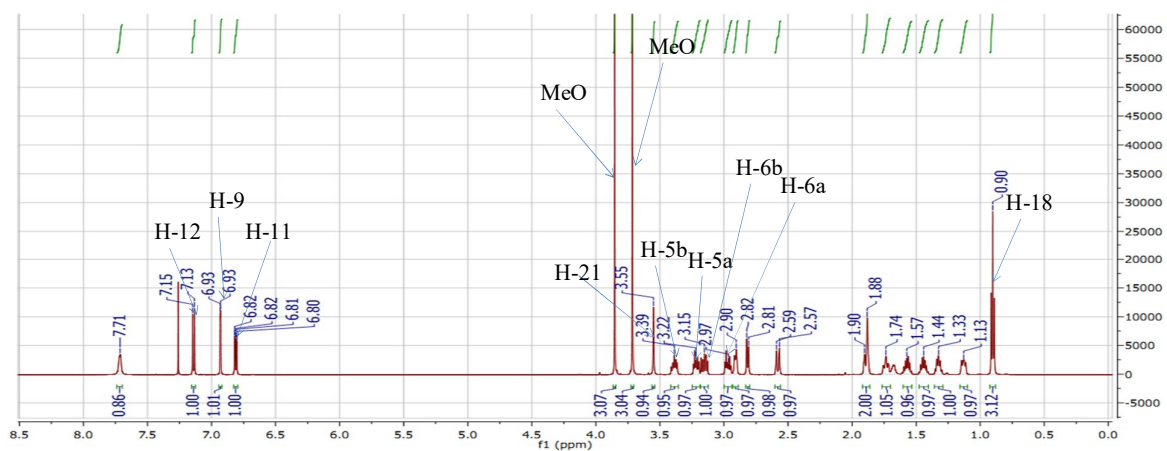


Figure 28: ^1H NMR spectrum (CDCl_3 , 600 MHz) of TiS_6

The COSY spectrum (Figure 29) shows a correlation between the protons H-6 and H-5 which serves as a confirmation to the suggestion above.

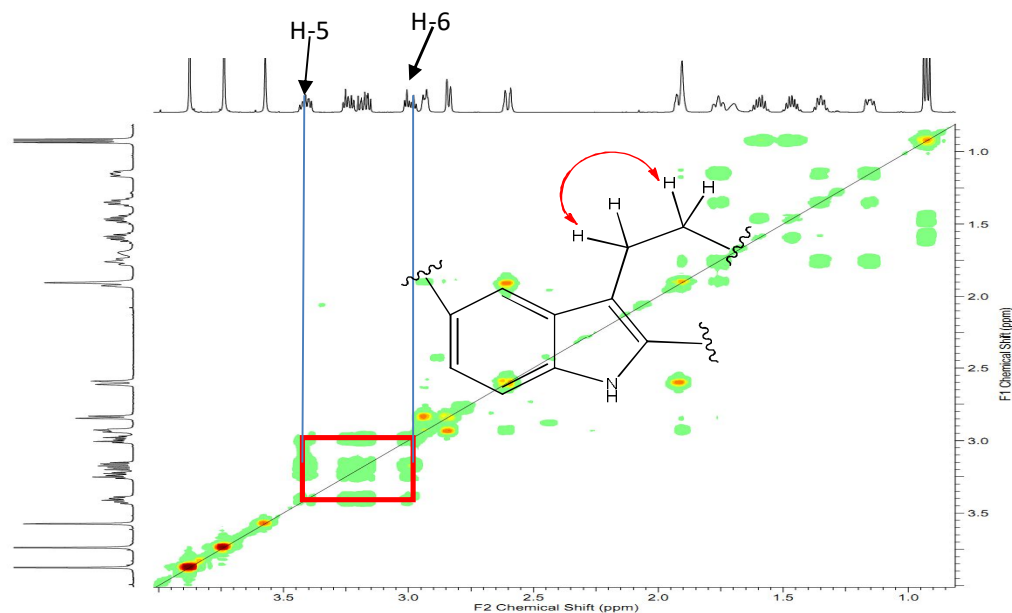


Figure 29: COSY Spectrum (CDCl_3 , 600 MHz) of TiS_6

The ^{13}C NMR spectrum of TiS_6 (Figure 30) is also very close to that of TiS_{10} with the marked difference being the absence of two carbonyl signals and the presence of two methylene signals at δ_{C} 55.3 and 22.3.

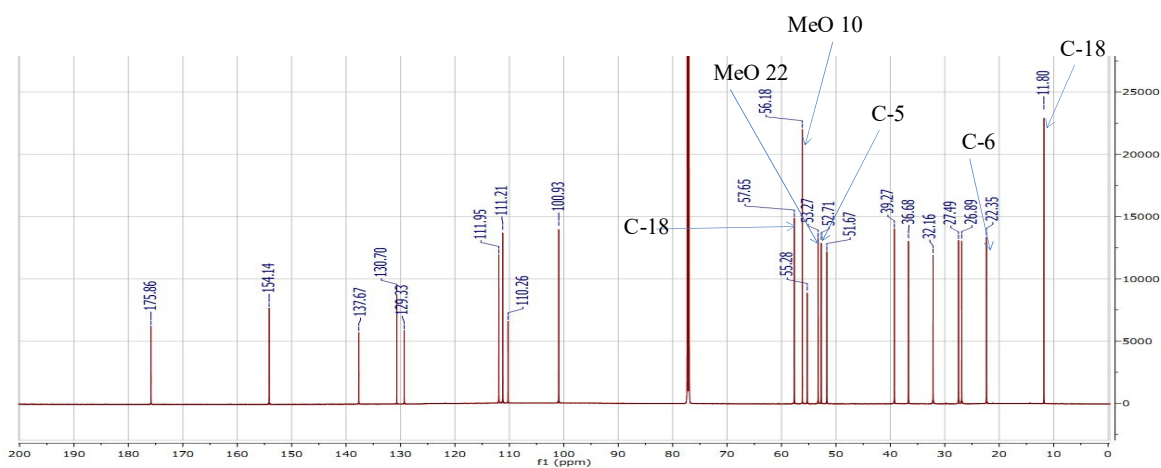


Figure 30: ^{13}C NMR Spectrum (CDCl_3 , 150 MHz) of TiS_6

The structure of TiS_6 was confirmed by analyzing its HMBC spectrum (Figure 31) where correlations were observed arising from H-18 to C-19, C-20, C-21 and C-14.

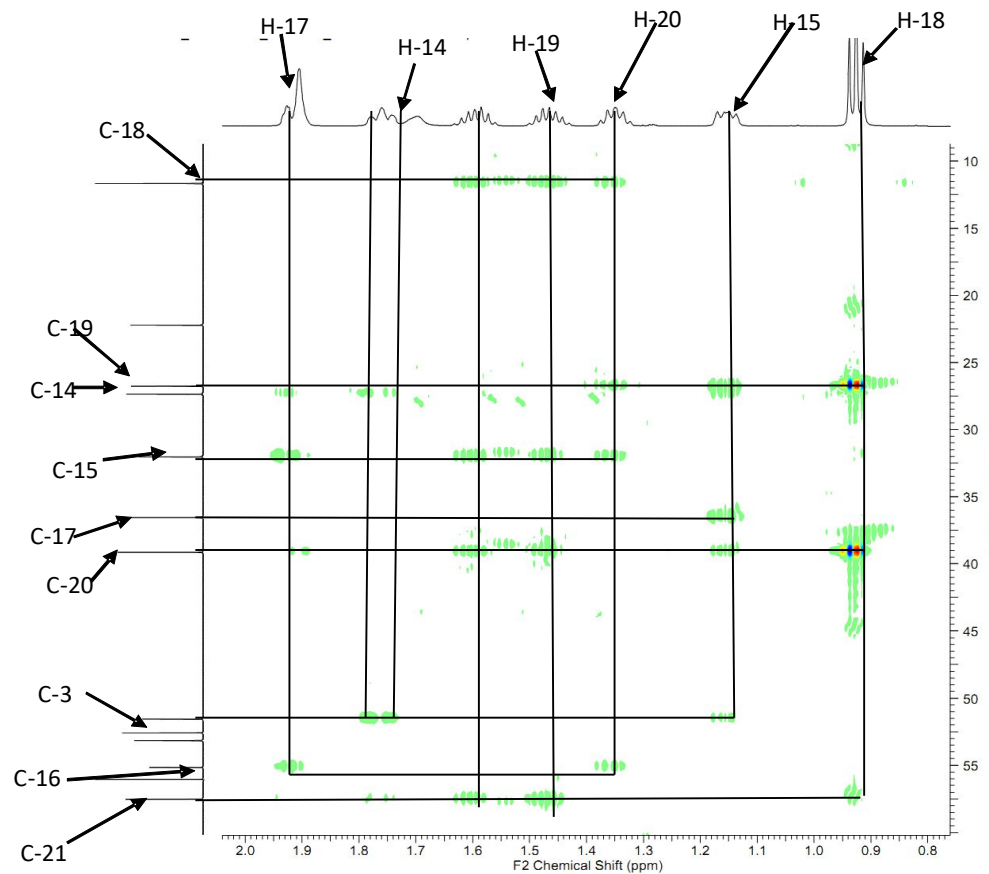


Figure 31: HMBC Spectrum (CDCl_3 , 600 MHz) of TiS_6

Based on spectroscopic analysis and by comparison of the spectral data of TiS₆ to those described in the literature (Pereira *et al.*, 2008), its structure identified to be that of voacangine (**22**)

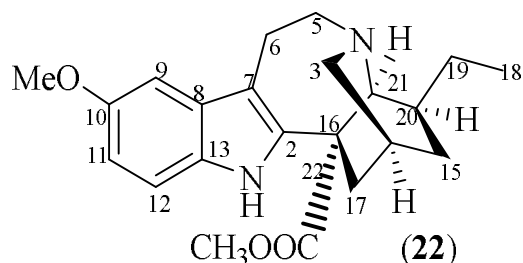


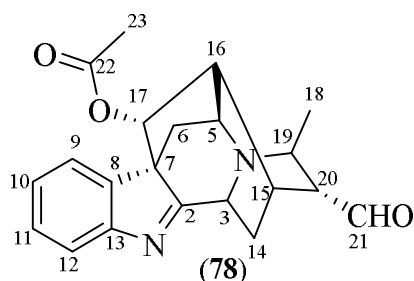
Table X: ¹H and ¹³C NMR (CDCl₃) data of TiS₆ compared to the literature (Pereira *et al.*, 2008)

Position	¹ H (nH, m, J)		¹³ C	
	TiS ₆	(Pereira <i>et al.</i> , 2008)	TiS ₆	(Pereira <i>et al.</i> , 2008)
1NH	7.71 (1H, s)	7.90 (1H, s)	-	-
2	-	-	137.7	137.3
3	2.81 (1H, d, 11.5); 2.82 (1H, d, 11.5)	2.90 (1H, d, 11.4) 2.82 (1H, d, 11.4)	51.6	51.6
4NH	-	-	-	-
5	3.22 (1H, m); 3.33 (1H, m)	3.25 (1H, m); 3.32 (1H, m)	52.7	52.6
6	2.97 (1H, m); 3.15 (1H, m)	2.92 (1H, m); 3.16 (1H, m)	22.3	22.2
7	-	-	110.3	109.9
8	-	-	129.3	129.0
9	6.93 (1H, d, 2.3)	6.91 (1H, d, 2.6)	100.9	100.7
10	3.85(3H, s)	3.85 (3H, s)	154.2; 56.2	154.0; 56.0
OCH ₃				
11	6.86 (1H dd, 8.8; 2.3)	6.80 (dd, 8.6; 2.6)	111.9	111.8
12	7.14 (1 H d, 8.8)	7.13 (d, 8.6)	111.1	111.1
13	-	-	130.7	130.5
14	1.88 (1H, s)	2.89 (1H, s)	27.5	26.9
15	1.30 (1H, m); 1.74 (1H, m)	1.31 (1H, m); 1.74 (1H, m)	32.2	31.6
16			55.3	55.7
17	1.90 (1H, m); 2.59 (1H, m)	2.02 (1H, m); 2.60 (1H, m)	36.7	36.4
18	0.90 (3H, t, 7.4)	0.90 (t, 7)	11.8	11.5
19	1.44 (1H, m); 1.57 (1H, m)	1.45(1H, m); 1.60 (1H, m)	26.9	26.4
20	1.33(1 H, m)	1.32 (1H, m)	39.3	38.9
21	3.55 (1H, brs)	3.54 (1H, brs)	57.6	57.5
22COOCH3	3.71 (3H, s,)	3.73 (3H, s)	175.8;53.3	175.4; 52.6

II.2.1.6. Identification of TC₅

TC₅ was obtained from the stem-bark of *Tabernaemontana contorta* as yellowish crystals in a mixture of Hex/AE (44/76). It is soluble in CHCl₃ and DMSO and responds positively to the Meyer's test and also to the Draggendorf's test characteristic of alkaloids.

From the spectroscopic data of TC₅ such as NMR 1D (including ¹H, ¹³C) and by comparison of these data to those described in the literature, its structure was determined to be that of a monoterpene indole alkaloid:



On the basis of spectral analysis, the molecular formula of TC₅ was determined to be C₂₁H₂₂O₃N₂ indicating 12 double bond equivalents.

Its ¹H NMR spectrum (Figure 29) reveals four aromatic signals at δ_H 7.23 (1H, t, 7.3 Hz), 7.38 (1H, t, 7.3 Hz), δ_H 7.52 (1H, d, 7.3 Hz) and 7.54 (1H, d, 7.3 Hz) suggesting an unsubstituted indole moiety. It also reveals, two methyl signals at δ_H 1.20 (3H, d, 6.6 Hz, H-21) and 2.17 (3H, s, H-23); two methylene signals at δ_H 2.80 (1H, dd, 11.7; 4.8 Hz, H-6b), 1.66 (1H, d, 11.7 Hz, H-6a) and 1.63 (1H, m, H-14a); 1.58 (1H, dd, J = 4.0; 4.9, H-14b) and seven methine signals δ_H 2.28 (1H, d, 9.2 Hz, H-19), 2.48 (1H, t, 6.1 Hz, H-16), 2.68 (1H, t, 4.8 Hz, H-15), 3.33 (1H, m, H-20), 3.64 (1H, t, 5.7 Hz, H-3), 4.02 (1H, d, 9.2 Hz, H-3), 4.96 (1H, s, H-17).

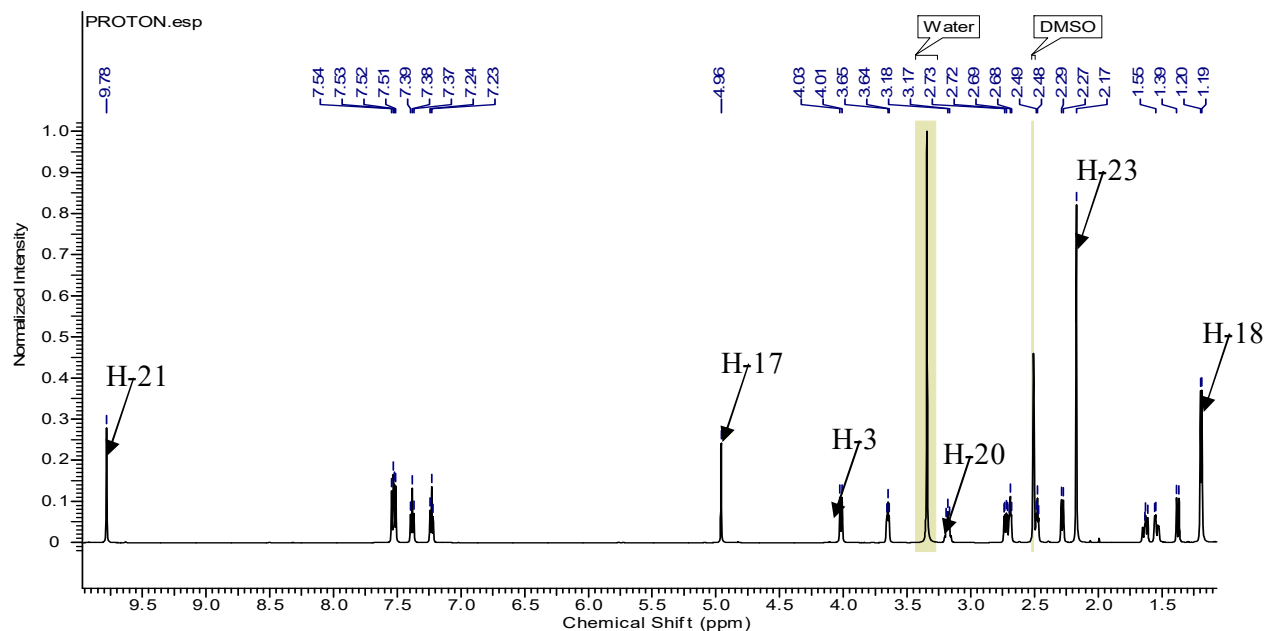


Figure 32: ^1H NMR Spectrum (DMSO- d_6 , 600 MHz) of TC₅

The ^{13}C NMR spectrum of TC₅ (Figure 33) accounts for twenty-one carbon signals with eleven sp^2 amongst which six aromatic at δ_{C} 120.8, 124.4, 125.8, 128.8, 137.1, 156.9 characteristic of a partially aromatic indole moiety, three carbonyl signals at δ_{C} 170.1 (C-22), 183.8 (C-2) and 204.3 (C-21). The ^{13}C NMR coupled with the HSQC spectrum reveals two methylene signals at δ_{C} 37.7 (C-6) and 22.6 (C-14); seven methyne signals at δ_{C} 26.0 (C-15), 48.2 (C-16), 49.8 (C-19), 51.4 (C-5), 55.2 (C-20), 56.5 (C-3), 77.6 (C-17) and two methyl signals at δ_{C} 19.0 (C-21), 21.3 (C-23).

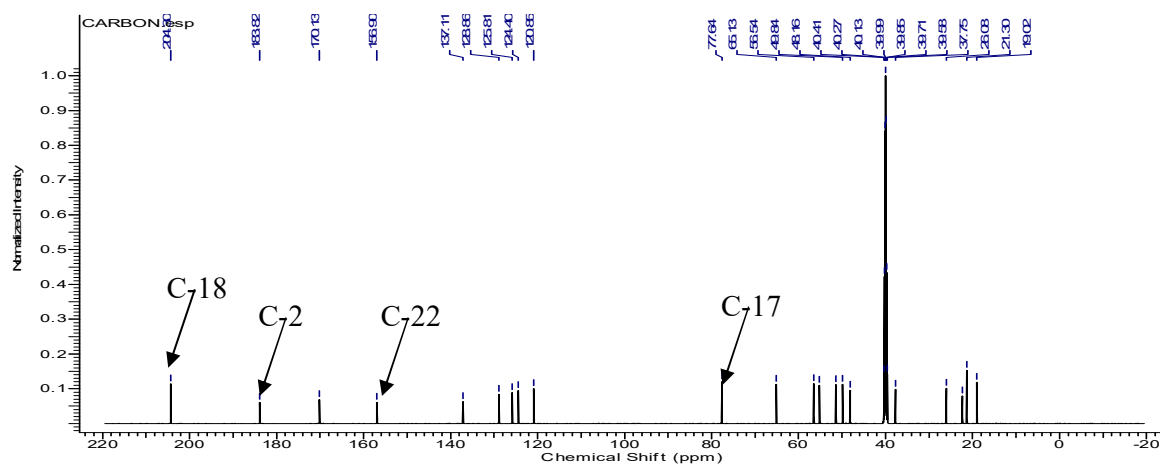


Figure 33: ^{13}C NMR Spectrum (DMSO- d_6 , 150 MHz) of TC₅

Based on the spectroscopic analysis and by comparison of the spectral data of TC₅ with those described in the literature, the structure of TC₅ was identified to be that of perakine (**78**) (Gao *et al.*, 2015).

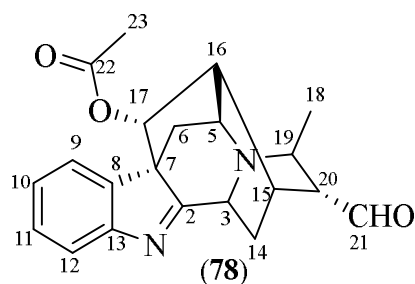


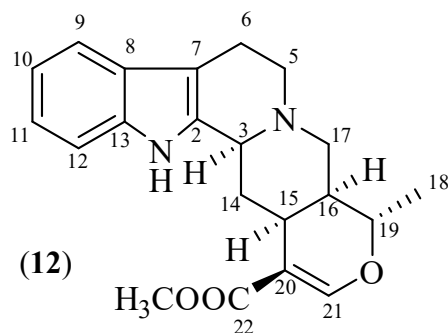
Table XI: ¹H and ¹³C NMR (DMSO-*d*₆) data of TC₅ compared to the literature (Gao *et al.*, 2015)

Position	¹ H (nH, m, <i>J</i>)		¹³ C	
	TC ₅	(Gao <i>et al.</i> , 2015)	TC ₅	(Gao <i>et al.</i> , 2015)
1NH	-	-	-	-
2	--	-	183.8	183.2
3	4.02(1H, d, 9.2)	4.14 (d, 9.7)	56.5	56.8
4NH	/	/		
5	3.65 (1H, t, 5.7)	3.64 (dd, 6.6, 4.9)	51.4	50.7
6	1.60 (1H, d, 11.7); 2.73 (1H, dd, 11.7, 4.8)	1.60 (1H, d, 11.9); 2.79 (dd, 11.9, 4.9)	37.7	37.6
7	/	/	65.1	64.8
8	/	/	137.1	136.3
9	7.52(1H, d, 7.3)	7.47 (1H, d, 7.3)	124.4	123.8
10	7.23(1H t, 7.3)	7.22 (1H, dd, 7.6, 7.3)	125.8	125.4
11	7.38(1H t, 7.3)	7.39 (1H, dd, 7.7; 7.6)	128.8	128.6
12	7.54(1H, d, 7.3)	7.61 (1H, d, 7.7)	120.8	120.9
13	/	/	156.9	156.5
14	1.76 (1H, m); 1.58 (1H, dd, 14.0, 4.9)	1.89 (1H, dd, 14.7, 9.7); 1.52 (1H, dd, 14.7, 4.7)	22.3	22.0
15	2.68 (1H, t, 4.8) 2.48 (1H, t, 6.1)	2.62 (1H, m) 2.34 (1H, dd, 6.6, 5.0)	26.0 48.2	27.2 49.2
16				
17	4.96 (1H, s)	4.99 (1H, s)	77.6	78.3
18	1.19 (3H, d, 6.6)	1.29 (3H, d, 6.5)	19.2	20.4
19	3.17 (1H, m)	2.65 (1H, m)	49.8	49.4
20	2.28 (1H, d, 9.2)	1.25 (1H, m)	55.2	53.1
21	9.28 (1H, s)	9.20 (1H, s)	204.3	208.5
22	/		170.1	171.2
23	2.17 (3H, s)	2.09 (3H, s)	21.3	21.5

II.2.1.7. Identification of TiS₇

TiS₇ was obtained from the stem of *Tabernaemontana inconspicua* as yellow needles in a mixture of Hex/AE (45/65). It is soluble in CHCl₃ and DMSO and responds positively to the Meyer's test and also to the Dragendorff's test characteristic of alkaloids.

From the spectroscopic data of TiS₇ such as NMR 1D (including ¹H, ¹³C) and by comparison of these data to those described in the literature, its structure was identified to be that of a monoterpene indole alkaloid:



On the basis of EI-MS ($m/z = 352$ [M]⁺) (Figure 31) and spectral analysis, the molecular formula of TiS₇ was determined to be C₂₁H₂₅O₃N₂ indicating 11 double bond equivalents.

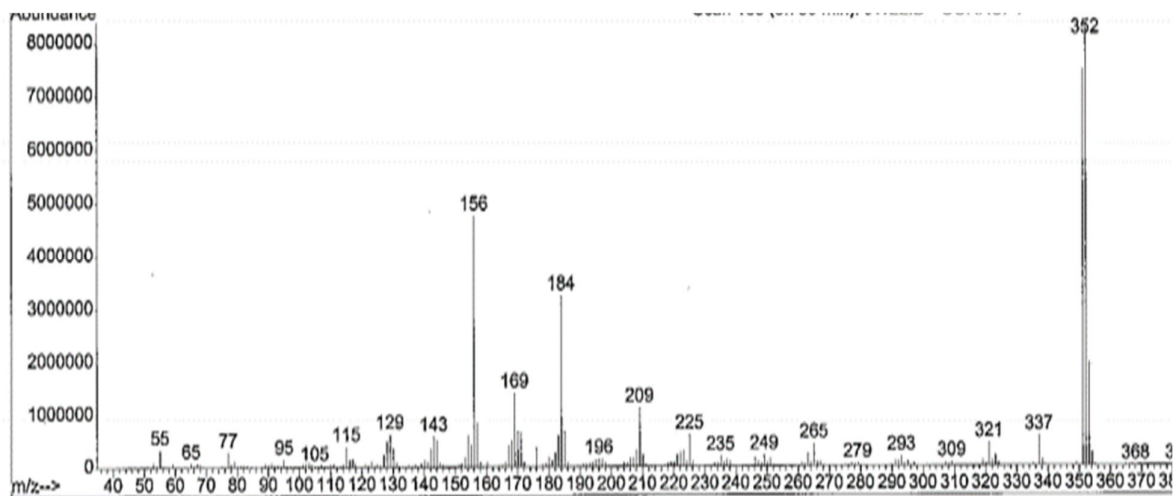


Figure 34: EI-MS of TiS₇

The ¹H NMR spectrum of TiS₇ (Figure 35) reveals four aromatic signals at δ_H 7.25 (1H, ddd, 7.2; 7.2; 1.4 Hz, H-10); 7.32 (1H, ddd, 7.2; 7.2; 1.4 Hz, H-11); δ_H 7.72 (1H, dd, 7.2; 1.4 Hz, H-12) and 7.58 (1H, dd, 7.2 Hz; 1.4, H-9) suggesting that the indole moiety of

TiS₇ is not substituted. In addition, two other signals at δ_{H} 7.66 (1H, s, H-21), 1.05 (3H, d, 6.5, H-18) and a methoxy signal at δ_{H} 3.54 (3H, s) were observed.

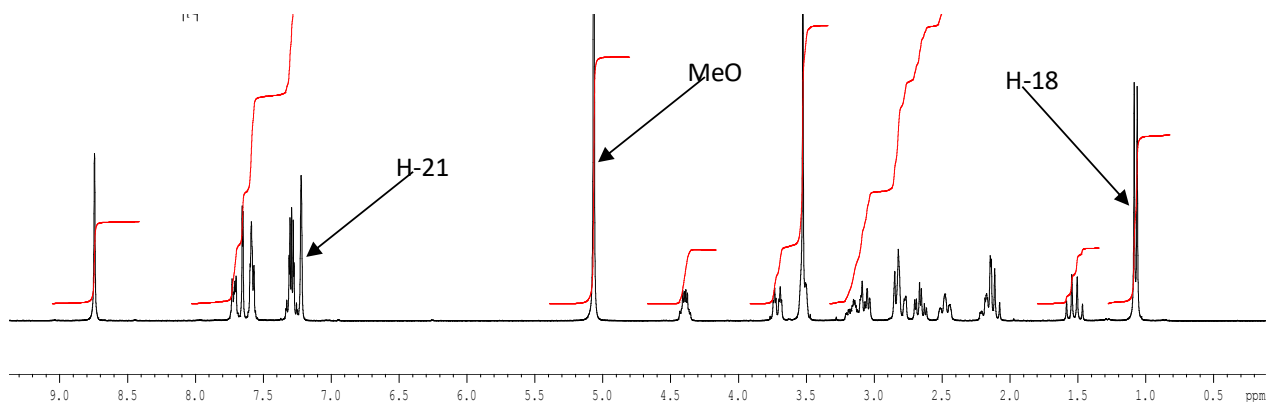


Figure 35: ¹H NMR Spectrum (Pyridine-*d*₆, 300 MHz) of TiS₇

The ¹³C NMR spectrum (Figure 36) accounts for twenty-one carbon signals including eleven *sp*² amongst which eight aromatic at δ_{C} 108.2 (C-20), 112.2 (C-12), 118.8 (C-9), 119.7 (C-10), 121.7 (C-11), 128.7 (C-28.7), 137.0 (C-13), 138.1 (C-2) attributed to an indole moiety, a double bond at δ_{C} 108.3 (C-20), 154.8 (C-21) and a carbonyl signal at δ_{C} 167.5 (C-22) of the ester group. The ¹³C NMR coupled with the DEPT 135 spectrum reveals four methylene signals at δ_{C} 23.1 (C-6), 31.6 (C-14), 51.0 (C-5), 57.4 (C-17), four methyne signals at δ_{C} 34.6 (C-15), 42.2 (C-16), 54.0 (C-3), 74.5 (C-19), a methyl signal at δ_{C} 15.4 (C-18) and a methoxy signal at δ_{C} 61.1.

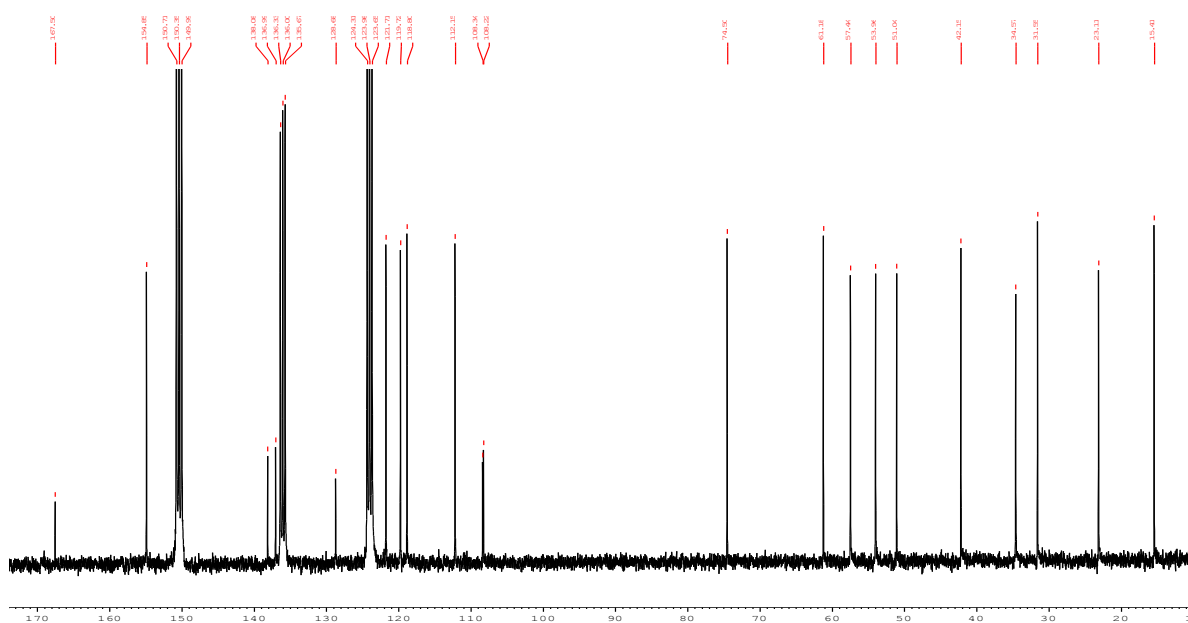


Figure 36: ¹³C NMR Spectrum (Pyridine-*d*₆, 75 MHz) of TiS₇

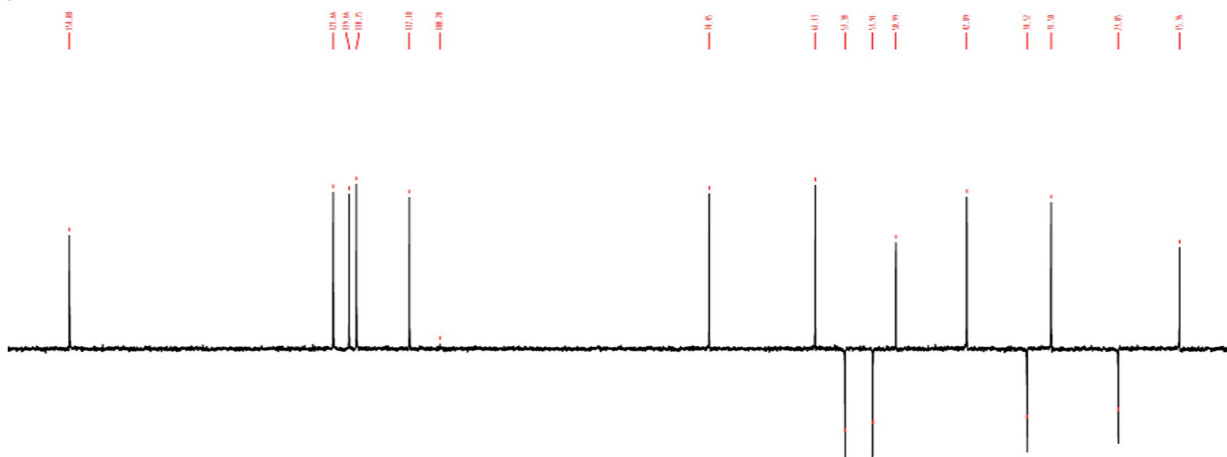


Figure 33: DEPT 135 (Pyrridine- d_6 , 75 MHz) of TiS₇

Based on the analysis of the physical and spectroscopic data of TiS₇ and by comparison to those described in the literature (Sheludko *et al.*, 2002), the structure of TiS₇ was identified to be that of tetrahydroalstonine (**12**).

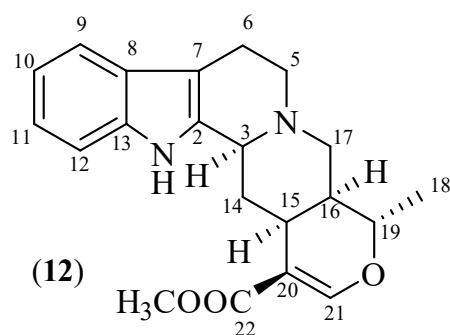


Table XII: ¹³C NMR data (Pyrridine- d_6) of TiS₇ compared to the literature (Sheludko *et al.*, 2002)

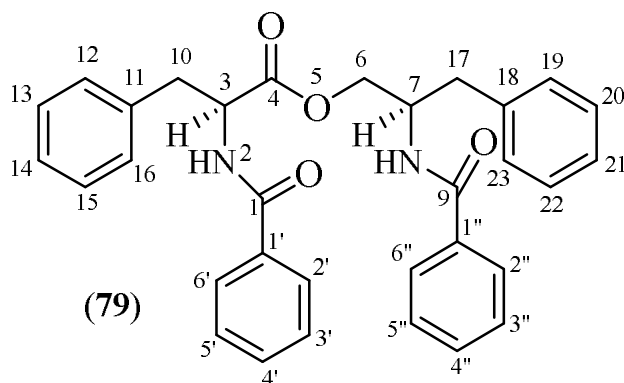
position	TiS ₇	(Sheludko <i>et al.</i> , 2002)
2	138.1	139.3
3	54.0	53.4
5	51.0	49.7
6	23.1	27.4
7	108.2	105.0
8	128.7	128.5
9	118.8	118.5
10	119.7	119.3
11	121.7	121.3
12	112.2	111.9

13	137.0	137.8
14	31.6	30.0
15	34.6	34.2
16	42.2	42.2
17	57.4	57.4
18	15.4	15.4
19	74.5	74.5
20	108.3	108.3
21	154.8	154.8
22	167.5	167.5

II.2.1.8. Identification of TC₆

TC₆ was obtained from the stem of *T. incondpicua* as a yellowish-white powder in a mixture of Hex/AE (50/50). It is soluble in CHCl₃ and responds positively to the Meyer's test and Dragendorff's test characteristic of alkaloids.

From the spectroscopic data of TC₆ such as HRESI-MS, NMR 1D and 2D (including ¹H, ¹³C, COSY, HSQC and HMBC) and by comparison of these data to those described in the literature, its structure was identified to be that of the alkaloid (**79**):



The molecular formula of TC₆ was determined to be C₃₂H₃₀O₄N₂ on the basis of HRESIMS (*m/z* 507.2276 [M+H]⁺ calcd for 507.2206) (Figure 34) being indicative of 19 double bond equivalents.

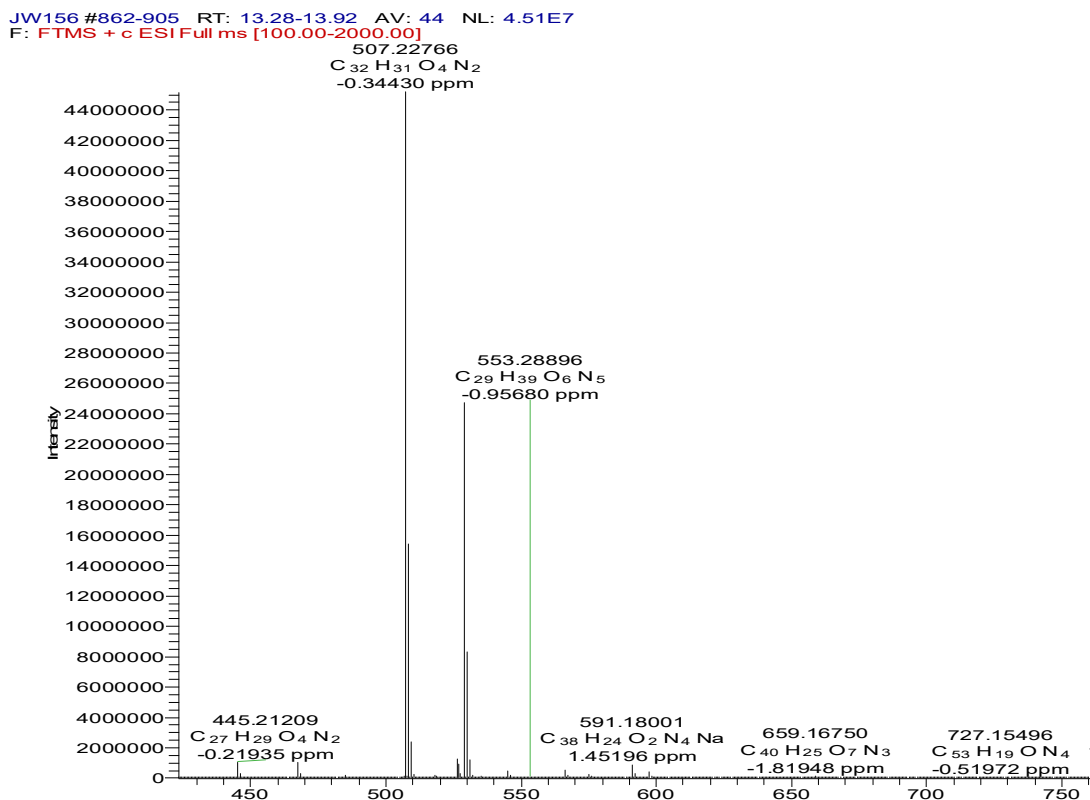


Figure 37: HRESI-MS of TC₆

The presence in its ¹H NMR spectrum (Figure 38) of four series of doublets at δ_{H} 2.92 (dd, 13.8, 8.2 Hz, H-17a), 3.03 (dd, 13.8, 6.4 Hz, H-17b); 3.24 (1H, dd, 13.8, 7.3 Hz, H-10a) and 3.32 (dd, 13.8, 6.3 Hz, H-10b); and of two signals at δ_{H} 4.93 (q, 6.6 Hz, H-3) and at δ_{H} 4.65 (m, H-7) showed that TC₆ is a quasi-symmetrical molecule. The integration of signals between δ_{H} 7.23 and 7.73 suggests the presence of twenty aromatics protons from four different phenyls groups in this compound. The presence of two signals at δ_{H} 6.61 (d, 5.2 Hz, H-2), and 6.69 (d, 5.9 Hz, H-8) which do not correlate in the HSQC spectrum but show COSY and HMBC correlations suggested the presence of two secondary amide groups. Furthermore, the presence of two other signals at δ_{H} 4.06 (dd, 11.3, 4.4 Hz, H-6a) and 4.57 (dd, 11.3, 3.2 Hz, H-6b) confirmed the quasi-symmetrical nature of this compound.

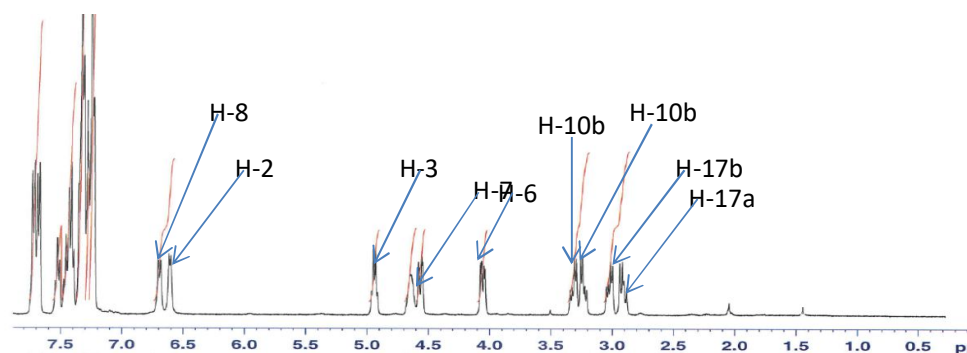


Figure 38: ^1H NMR spectrum (CDCl_3 , 400 MHz) of TC_6

Its ^{13}C NMR spectrum (Figure 36) reveals three carbonyl signals at δ_{C} 167.2 (C-9), 167.4 (C-1) and 171.9 (C-4). The presence of three methylene groups respectively at δ_{C} 37.2 (C-17), 37.5 (C-10) and 65.4 (C-6) suggested that the latter is close to the carbonyl ester.

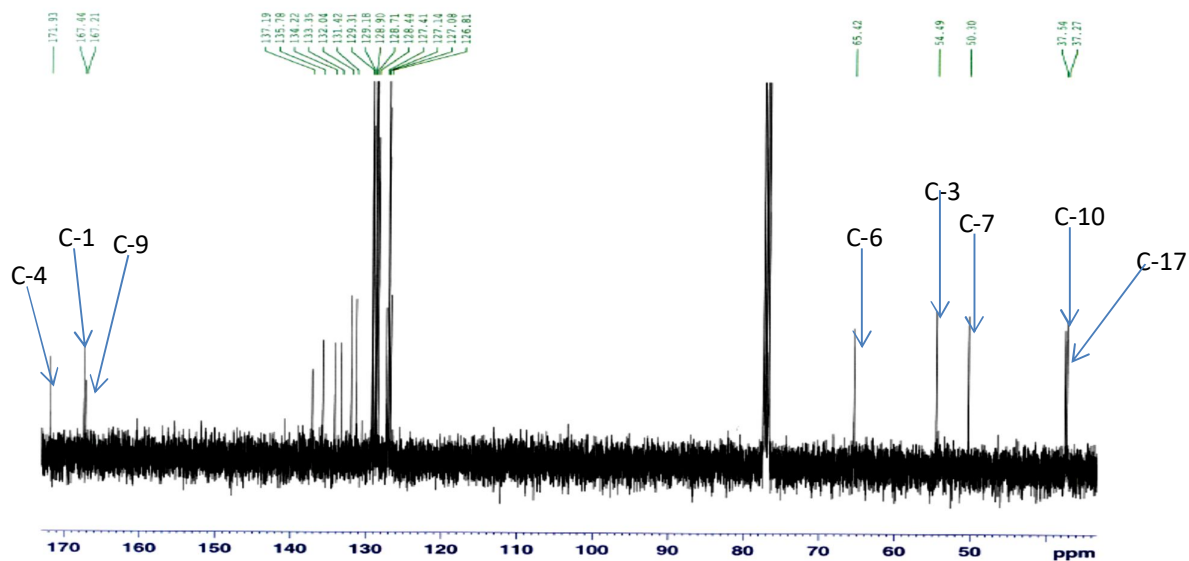


Figure 39: ^{13}C NMR spectrum (CDCl_3 , 100 MHz) of TC_6

Correlations observed in the COSY spectrum (Figure 40) between H-17a (δ_{H} 2.92), H-17b (δ_{H} 3.03) and H-7 (δ_{H} 4.65); between H-10a (δ_{H} 3.32), H-10b (δ_{H} 3.24) and H-3 (δ_{H} 4.93), and between H-7 (δ_{H} 4.65) and H-6a (δ_{H} 4.06) and H-6b (δ_{H} 4.57) showed the difference between the two parts of the molecule.

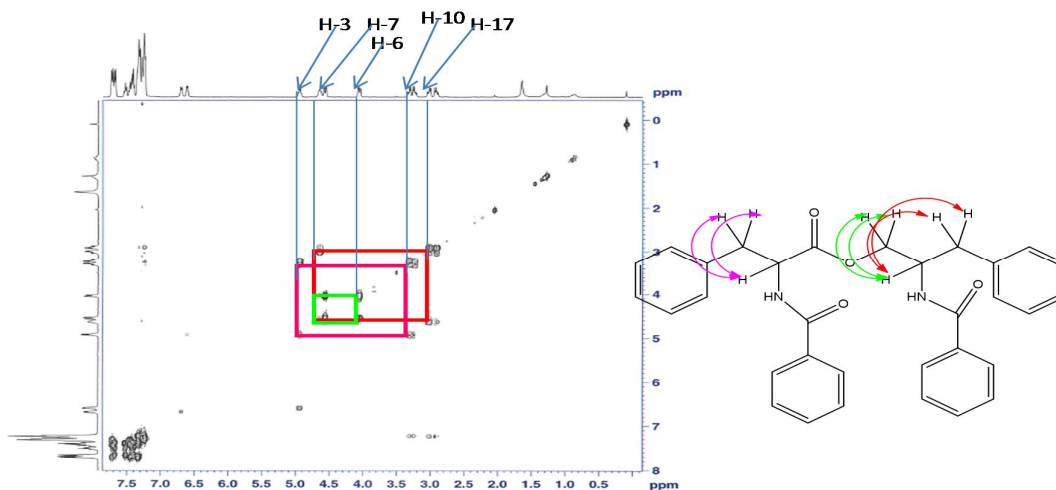


Figure 1: COSY spectrum (CDCl₃) of TC₆

Figure 40: COSY spectrum (CDCl₃) of TC₆

HMBC correlations (Figure 41) observed between H-10a/ H-10b, H-3 and C-4 (δ_C 171.9); between H-2 and C-1; and between H-8 and C-9 enabled the construction of the central part of the molecule which comprises two amides and one carbonyl ester groups. Moreover, correlations between H-6a and C-4, C-7, C-17 confirmed the quasideimeric nature of compound with the two moieties connected to the ester group (C-4).

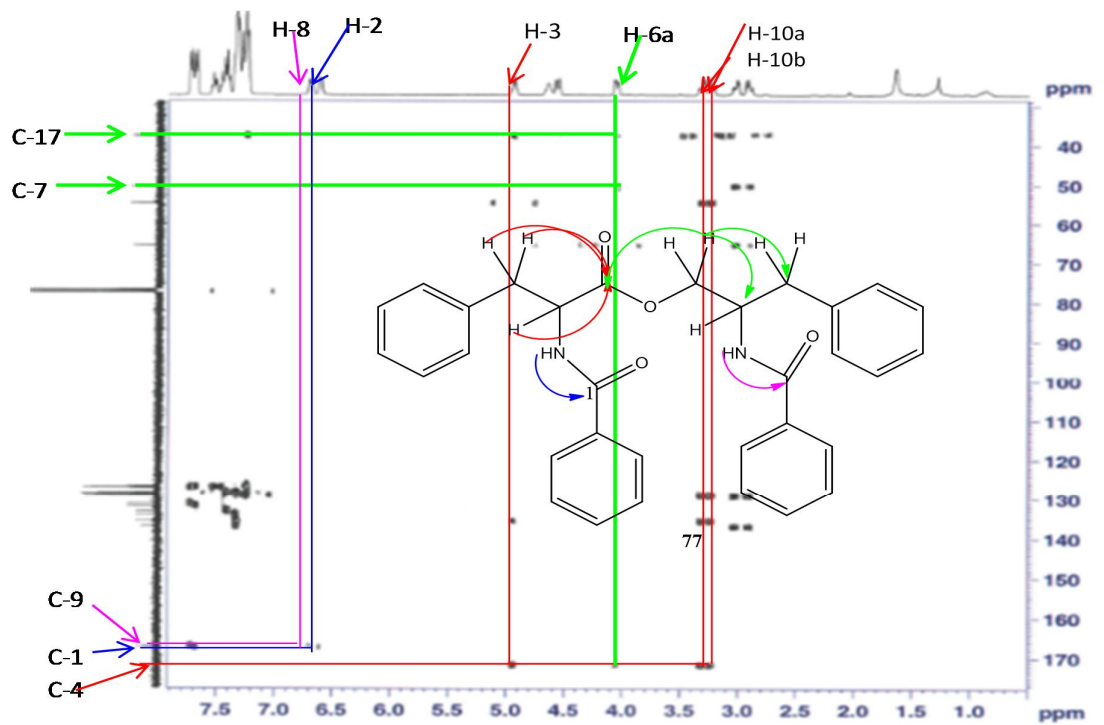


Figure 41: HMBC spectrum (CDCl_3) of TC_6

Based on physical and spectroscopic data compared to those described in the literature (Yaya *et al.*, 2014) the structure of TC_6 was identified to be that of asperphenamate (79).

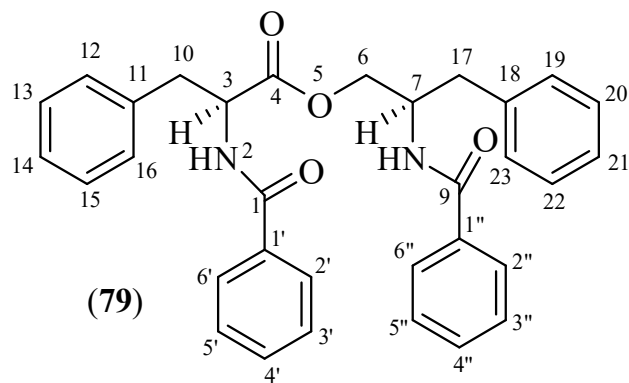


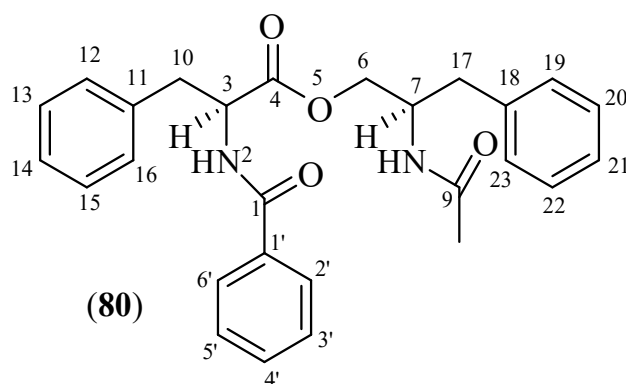
Table XIII: ^1H and ^{13}C NMR (CDCl_3) data of TC_6 compared to those of the literature (Yaya *et al.*, 2014)

position	^1H (nH, m, J)		^{13}C	
	TC_6	(Yaya <i>et al.</i> , 2014)	TC_6	(Yaya <i>et al.</i> , 2014)
1	-	-	167.4	167.4
2	6.61 (d, 5.2 Hz)	-	-	-
3	4.93 (q, 6.6)	4.92 (q, 6.6)	54.5	54.5
4	-	-	171.9	171.9
5	-	-	-	-
6	4.57 (1H, dd, 11.3; 3.2) 4.06 (1H, dd, 11.3; 4.2)	4.54 (1H, dd, 11.3; 3.2) 4.04 (1H, dd, 11.3; 4.4)	65.4	65.4
7	4.65 (m)	4.63 (m)	50.3	50.3
8	6.69 (d, 5.9 Hz)	-	-	-
9	-	-	167.2	167.2
10	3.32 (1H, dd, 13.8, 6.3) 3.24 (1H, dd, 13.8, 7.3)	3.29 (1H, dd, 13.8, 6.3) 3.21 (1H, dd, 13.8, 7.3)	37.5	37.5
11	-	-	135.8	135.7
12	7.25 (ov)	7.25 (ov)	128.9	128.9
13	7.25 (ov)	7.25 (ov)	128.7	128.7
14	7.29 (ov)	7.29 (ov)	127.1	127
15	7.25 (ov)	7.25 (ov)	128.7	128.7
16	7.25 (ov)	7.25 (ov)	128.9	128.9
17	3.03 (1H, dd, 13.8, 6.4) 2.92 (1H, dd, 13.8, 8.2)	2.99 (1H, dd, 13.8, 6.4) 2.91 (1H, dd, 13.8, 8.2)	37.2	37.2
18	-	-	137.2	137.1
19	7.48 (s)	7.48 (s)	129.3	129.3
20	7.21 (ov)	7.21 (ov)	127.1	127
21	7.31 (ov)	7.31 (ov)	126.8	126.8
22	7.21 (ov)	7.21 (ov)	127.1	127
23	7.48 (s)	7.48 (s)	129.3	129.3
1'	-	-	133.3	133.3
2'	7.71 (d, 0.9)	7.71 (d, 0.9)	128.4	128.4
3'	7.43 (tt, 7.8, 1.3)	7.43 (tt, 7.8, 1.3)	127.1	127.1
4'	7.50 (tt, 7.8, 1.2)	7.50 (tt, 7.8, 1.2)	132.0	132.4
5'	7.43 (tt, 7.5, 1.3)	7.43 (tt, 7.5, 1.3)	127.1	127.1
6'	7.71 (dd, 8.2, 1.2)	7.71 (dd, 8.2, 1.2)	128.4	128.4
1''	-	-	134.2	134.2
2''	7.69 (dd, 8.8, 1.3)	7.66 (dd, 8.8, 1.3)	127.4	127.4
3''	7.33 (ov)	7.33 (ov)	129.2	129.2
4''	7.43 (tt, 7.5, 1.3)	7.43 (tt, 7.5, 1.3)	131.4	131.4
5''	7.33 (ov)	7.33 (ov)	129.2	129.2
6''	7.69 (dd, 8.8, 1.3)	7.66 (dd, 8.8, 1.3)	127.4	127.4

II.2.1.9. Identification of TiS_8

TiS_8 was obtained from the stem of *Tabernaemontana inconspicua* as a yellowish white powder in a mixture of Hex/AE (50/50). It is soluble in CHCl_3 .

From the spectroscopic data of TiS₈ such as HRESI-MS, NMR 1D and 2D (including ¹H, ¹³C, COSY, HSQC and HMBC) and by comparison of these data to those described in the literature, its structure was determined to be that of an alkaloid:



On the basis of HRESI-MS (m/z 445.2120 [M+H]⁺ calcd for 445.2127), (Figure 39) the molecular formula of TiS₈ was determined to be C₂₇H₂₈O₄N₂ indicating 15 double bond equivalents.

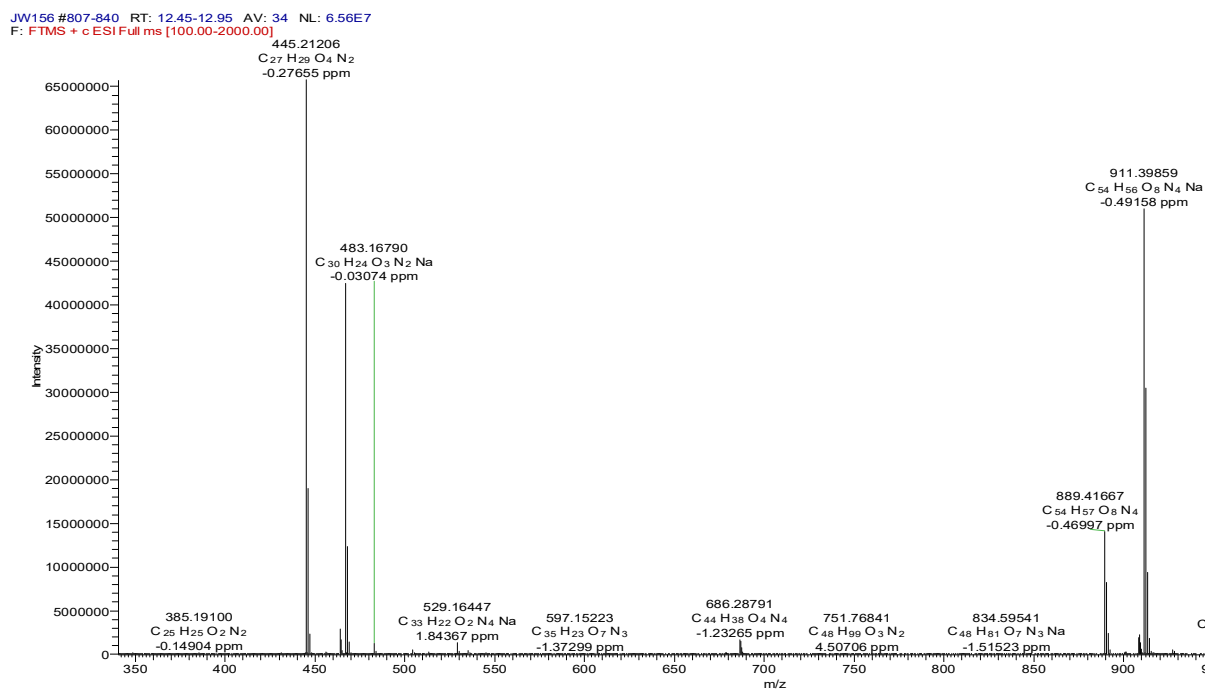


Figure 42: HRESI-MS of TiS₈

The ¹H NMR spectrum of TiS₈ (Figure 43) was closely similar to that of TC₆ with the difference being that the integration of signals between δ_H 7.26 and 7.75 suggests the presence of fifteen aromatic protons from three different phenyl groups in this compound instead of 20 in compound TC₆. Furthermore, the presence of a methyl singlet at δ_H 1.69

which is absent in the spectrum of TC₆ suggests that one of the a phenyl group of TC₆ has been replaced by a methyl group.

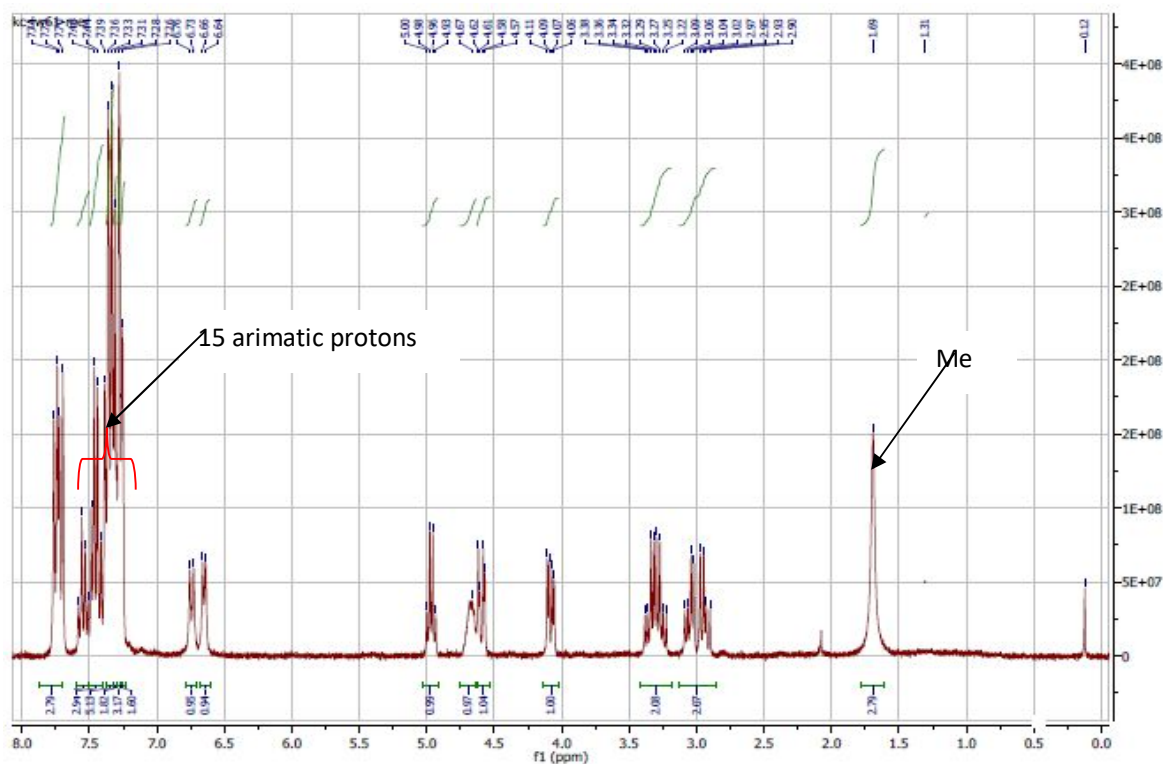


Figure 43: ¹H NMR spectrum (CDCl₃, 400 MHz) of TiS₈

The above suggestion is confirmed by the presence on the ¹³C NMR spectrum of TiS₈ (Figure 44), of a carbon signal at δ_C 25.2. The deshielding nature of this carbon indicates that the methyl group is linked to a carbonyl group.

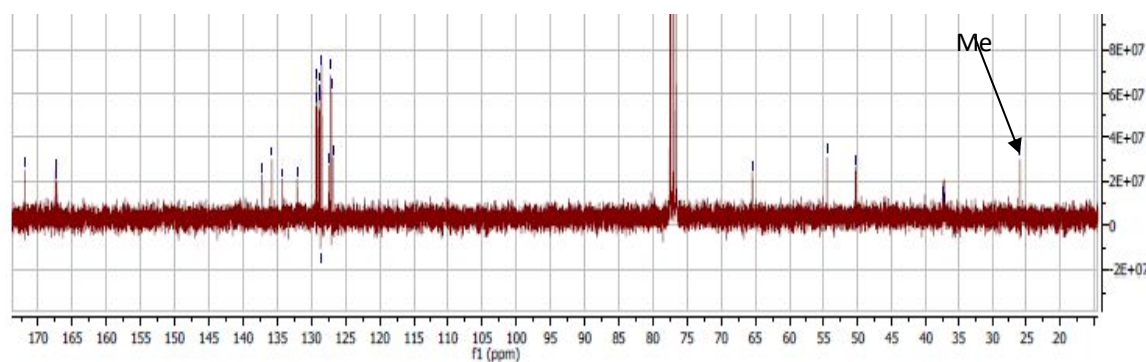


Figure 44: ¹³C NMR spectrum (CDCl₃, 100 MHz) of TiS₈

All these physical and spectroscopic data compared to those of literature (Hasnah *et al.*, 2010) led to the identification of the structure of TiS₈ to that of patriscabratine (**80**).

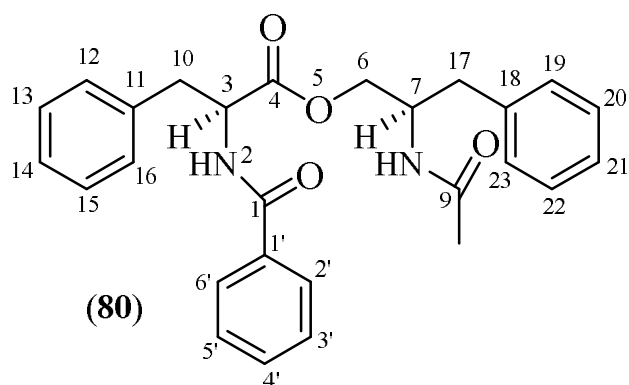


Table XIV: ^1H and ^{13}C NMR (CDCl_3) data of TiS_{11} compared to the literature (Hasnah *et al.*, 2010)

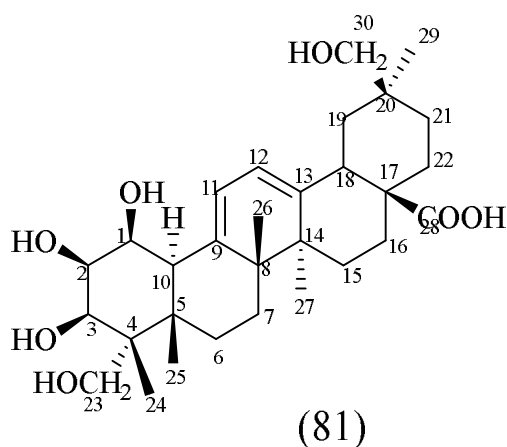
Position	^1H (m, J)		^{13}C	
	TiS_{11}	(Hasnah <i>et al.</i> , 2010)	TiS_{11}	(Hasnah <i>et al.</i> , 2010)
1	-	-	167.4	167.4
2	6.61 (d, 5.2)	-	-	-
3	4.93 (q, 6.6)	4.92 (q, 6.6)	54.5	54.5
4	-	-	171.9	171.9
5	-	-	-	-
6	4.57 (dd, 11.3, 3.2) 4.06 (dd, 11.3, 4.4)	4.54 (dd, 11.3, 3.2) 4.04 (dd, 11.3, 4.4)	65.4	65.4
7	4.65 (m)	4.63 (m)	50.3	50.3
8	6.67 (d, 5.6)	-	-	-
9	-	-	167.2	167.2
10	3.32 (dd, 13.8, 6.3) 3.24 (dd, 13.8, 7.3)	3.29 (dd, 13.8, 6.3) 3.21 (dd, 13.8, 7.3)	37.5	37.5
11	-	-	135.8	135.7
12	7.25 (ov)	7.25 (ov)	128.9	128.9
13	7.25 (ov)	7.25 (ov)	128.7	128.7
14	7.29 (ov)	7.29 (ov)	127.1	127
15	7.25 (ov)	7.25 (ov)	128.7	128.7
16	7.25 (ov)	7.25 (ov)	128.9	128.9
17	3.03 (dd, 13.8, 6.4) 2.92 (dd, 13.8, 8.2)	2.99 (dd, 13.8, 6.4) 2.91 (dd, 13.8, 8.2)	37.2	37.2
18	-	-	137.2	137.1
19	7.48 (s)	7.48 (s)	129.3	129.3
20	7.21 (ov)	7.21 (ov)	127.1	127
21	7.31 (ov)	7.31 (ov)	126.8	126.8
22	7.21 (ov)	7.21 (ov)	127.1	127
23	7.48 (s)	7.48 (s)	129.3	129.3
1'	-	-	134.2	134.2
2'	7.69 (dd, 8.8, 1.3)	7.66 (dd, 8.8, 1.3)	127.4	127.4
3'	7.33 (ov)	7.33 (ov)	129.2	129.2
4'	7.43 (tt, 7.5, 1.3)	7.43 (tt, 7.5, 1.3)	131.4	131.4
5'	7.33 (ov)	7.33 (ov)	129.2	129.2
6'	7.69 (dd, 8.8, 1.3)	7.66 (dd, 8.8, 1.3)	127.4	127.4

II.2.2. Triterpenoids

II.2.2.1. Characterisation of TCO₉

Compound TCO₉ was obtained as a white powder from the fruits of *T. contorta* in a mixture of CH₂Cl₂-MeOH (98:02). It is soluble in methanol and responds positively to the Liebermann-Burchard's test giving a red purple color characteristic of triterpenes.

From the spectroscopic data of TCO₉ such as HRESI-MS, NMR 1D and 2D (including ¹H, ¹³C, COSY, HSQC and HMBC and NOESY), its structure was determined to be that of a triterpene:



The molecular formula of TCO₉ was found on the basis of HRESI-MS (m/z 517.3112[M-H]⁻ calcd for 517.3165) (Figure 42) to be C₃₀H₄₆O₆ indicating 8 double bond equivalents.

20180905-TC109_18090513444#70-72 RT: 0.79-0.81 AV: 3 NL: 2.36E6
T: FTMS - p ESI Full ms [100.00-2000.00]

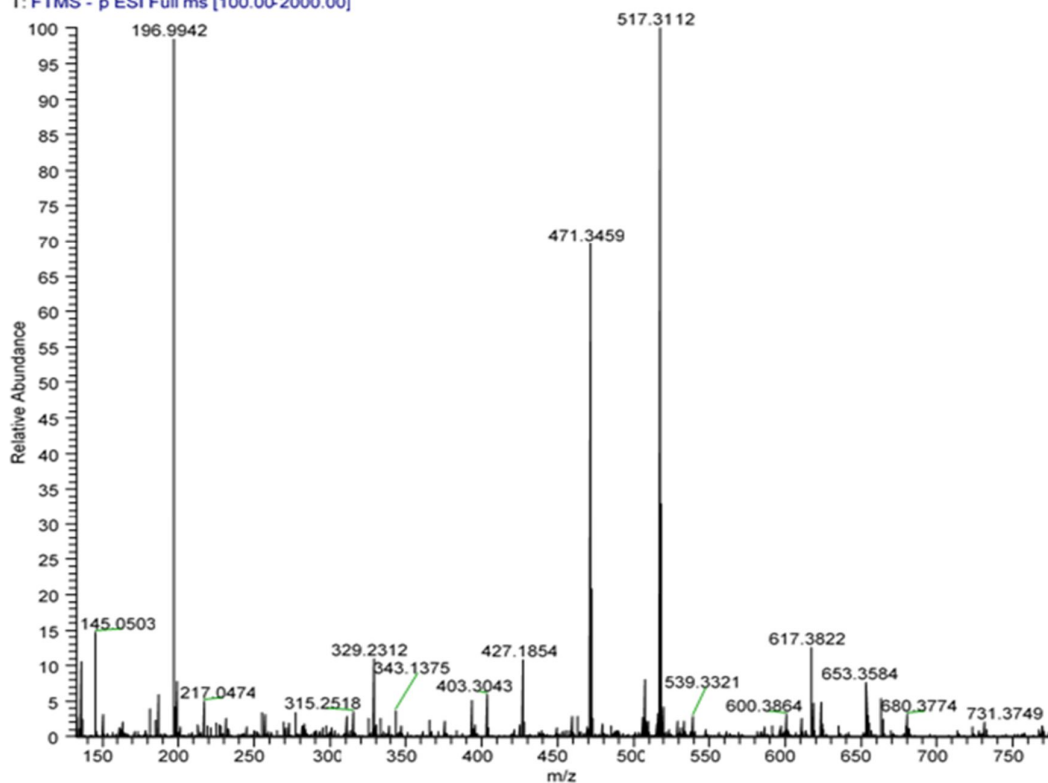


Figure 45: HRESI-MS of TCO₉

Its ¹H NMR spectrum (Figure 46) reveals between δ_{H} 0.70 and 1.16 six methyl singlets instead of eight indicating that two of them have been oxidized. The absence of methyl doublets between δ_{H} 1.2 and 1.4 suggests an oleanan skeleton (Mahato and Kundu, 1994). This spectrum also reveals two diastereotopic oxymethylenes at δ_{H} 3.28 (1H, d, 11.1 Hz, H-23a), 3.52 (1H, d, 11.2 Hz, H-23b) and 4.21 (1H, d, 5.4, H-30b), 4.22 (1H, d, 5.4, H-30a); three oxymethylenes at δ_{H} 2.90 (1H, brd, 9.3 Hz, H-2), 3.62 (1H, m, H-3), 3.63 (1H, m, H-1) and two olefinic protons at δ_{H} 5.21 (2H, brs H-11; H-12).

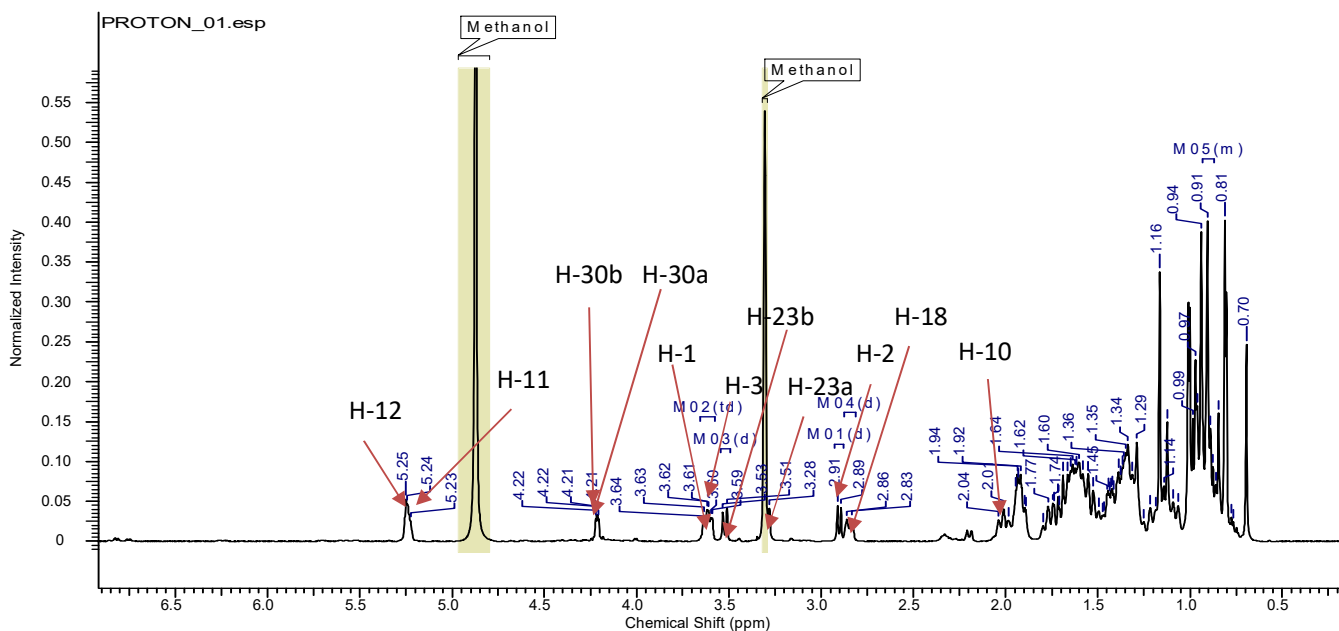


Figure 46: ^1H NMR spectrum (MeOD, 500 MHz) of TCO_9

Its ^1H - ^1H COSY spectrum (Figure 47) shows correlations between protons at δ_{H} 2.90 (H-2)/3.62 (H-3) and 3.63 (H-1); 1.91 (H-10)/3.63 (H-1) and 5.25; 2.84 (H-18)/1.68 (H-19).

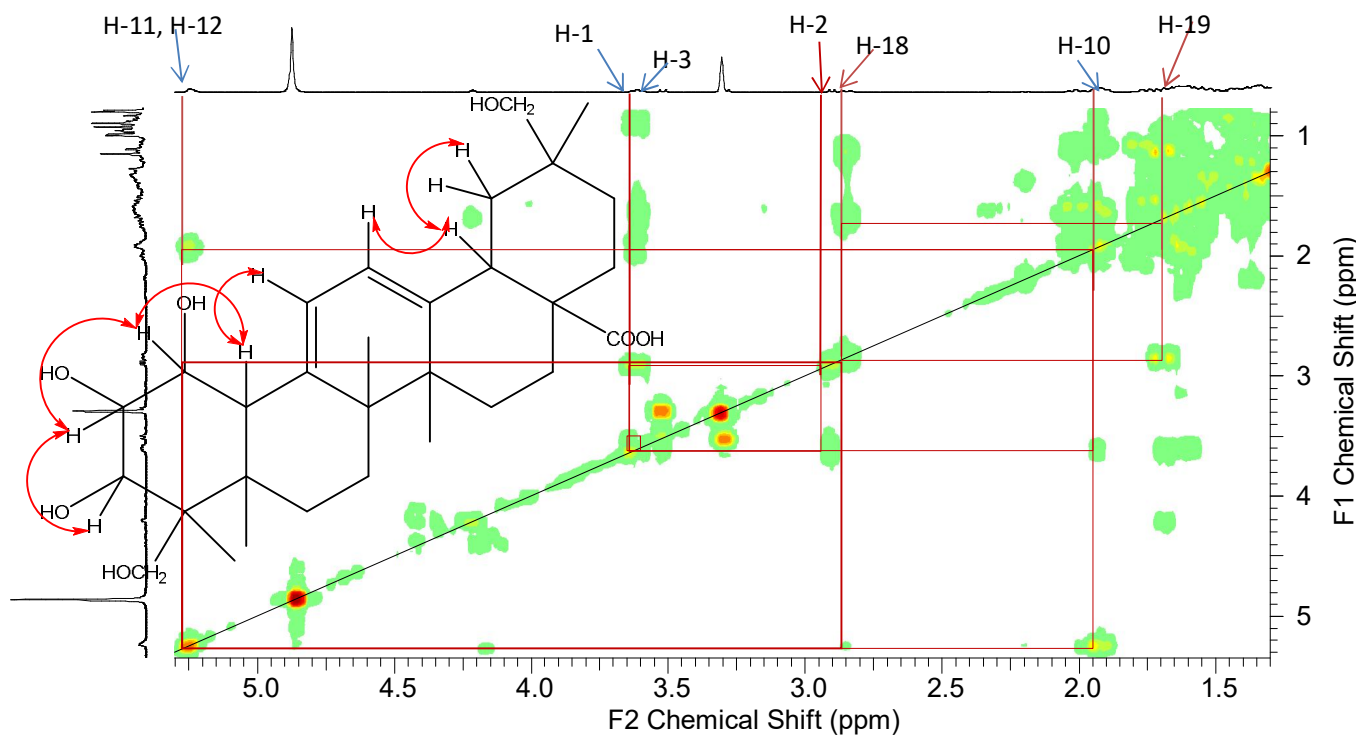


Figure 47: COSY spectrum (MeOD) of TCO_9

The ^{13}C NMR spectrum (Figure 48) of TCO_9 reveals an acid carbonyl signal at δ_{C} 180.4 (C-28); olefinic carbons at δ_{C} 143.9 (C-13) and 122.0 (C-12) confirming the olean-12-

ene nature of triterpene; the appearance of another pair of olefinic carbons at δ_c 143.8 (C-9) and 122.1 (C-11) reveals the existence of a second double bond. This spectrum also reveals three oxymethynes at δ_c 83.0 (C-2), 72.4 (C-3), 68.0 (C-1); two oxymethylenes at δ_c 65.9 (C-23) and 67.6 (C-30).

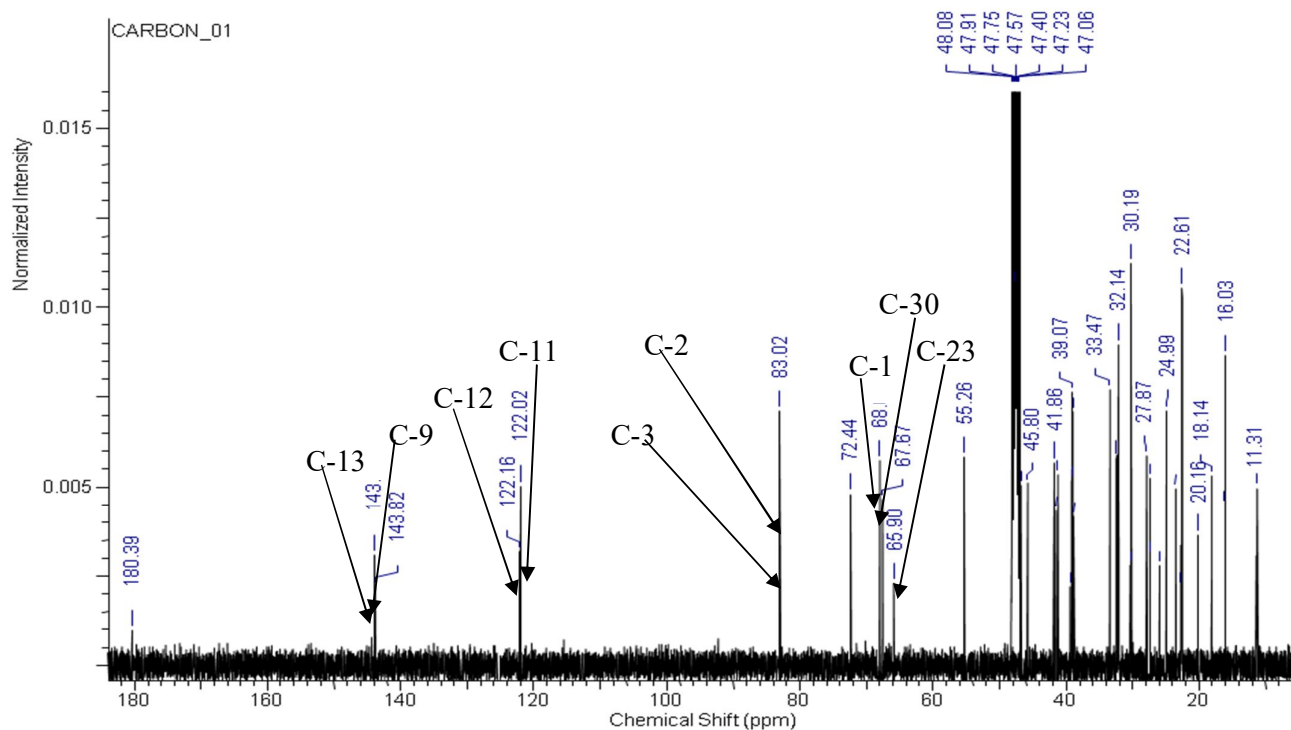


Figure 48: ^{13}C NMR spectrum (MeOD, 125 MHz) of TCO_9

In the HMBC spectrum (Figure 46) of TCO_9 , correlations were observed between H-10 and C-1, C-2, C-9, C-11 confirming the two hydroxy groups at positions 1 and 2 and also the position of the second double bond. In addition, correlations were observed between the oxymethylene protons and C-3 (δ_c 72.4), C-4 (δ_c 46.7), C-5 (δ_c 41.7), C-24 (δ_c 11.3) confirming one of the hydroxymethylene group at position 23; between H-18 and C-12, C-13, and the acid carbonyl carbon confirming this double bond a position 12 and the acid group at position 28 and finally between the second hydroxy-methylene at position 30 and H-19, H-21.

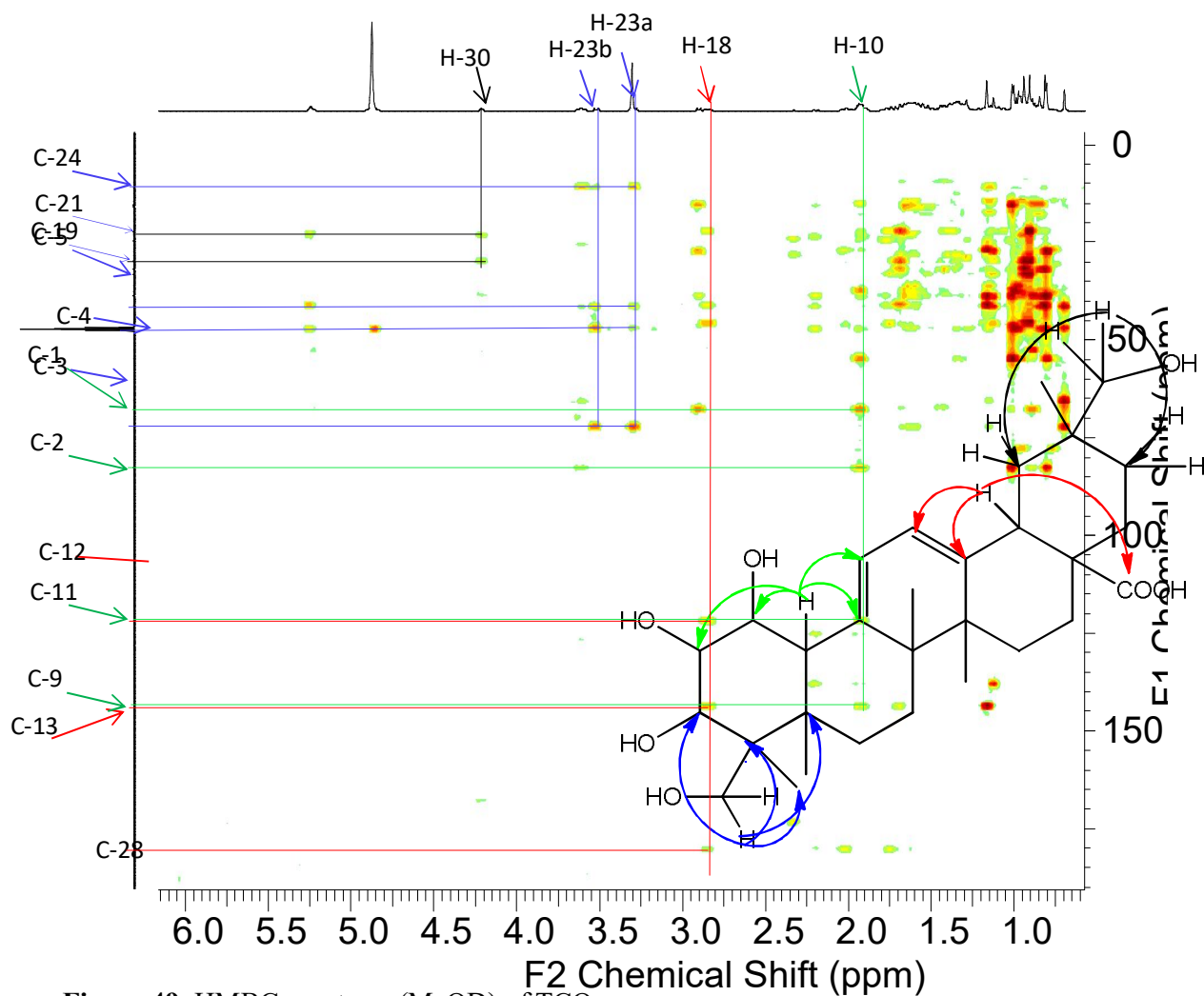


Figure 49: HMBC spectrum (MeOD) of TCO₉

The NOESY spectrum (Figure 47) shows correlations between H-3 and H-24 confirming the position of CH₂OH at 23 and not 24 and the β -orientation of OH-2. The absence of correlation between H-1 and H-3 shows that H-1 is α -orientated. The correlations observed between CH₂OH-29 and H-18 confirms its position at 30 and not 29.

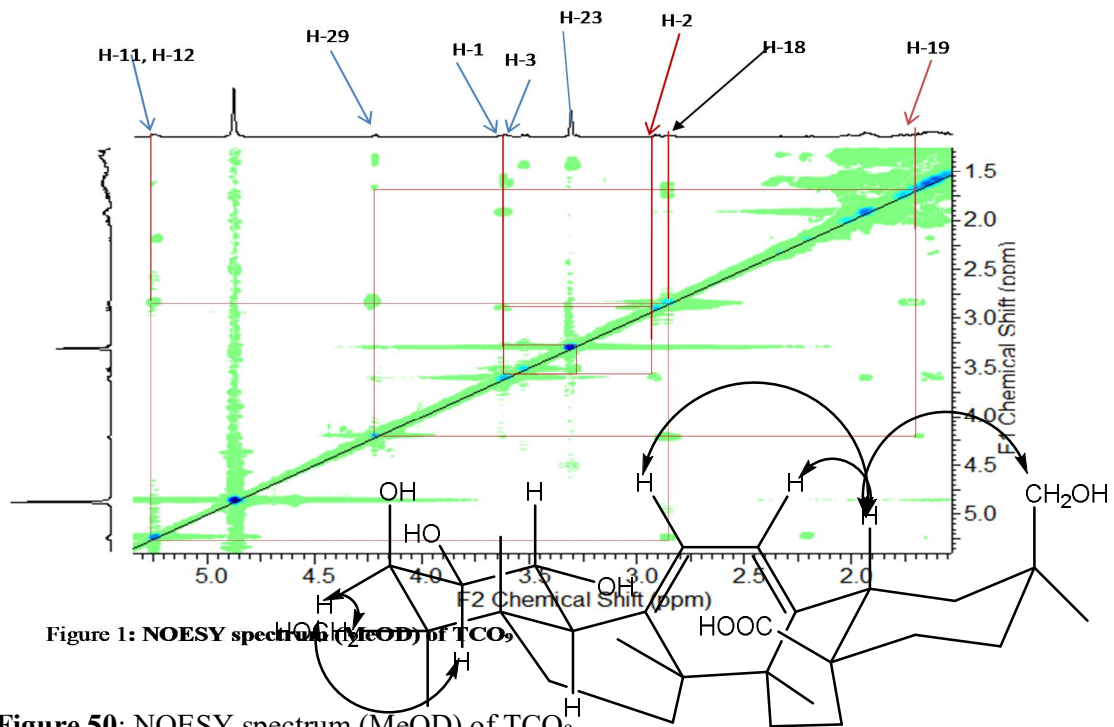


Figure 50: NOESY spectrum (MeOD) of TCO₉

The structure of TCO₉ was determined based on spectral analysis to be that of 1 α ,2 β ,3 β ,23,30-pentahydroxymimusopa-9(11),12-dien-28-oic acid of which the name contortic acid (**81**) was given.

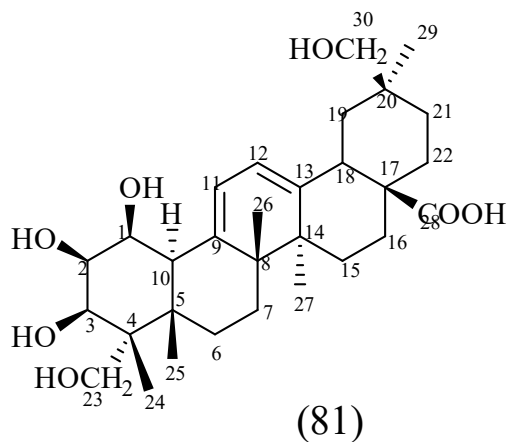


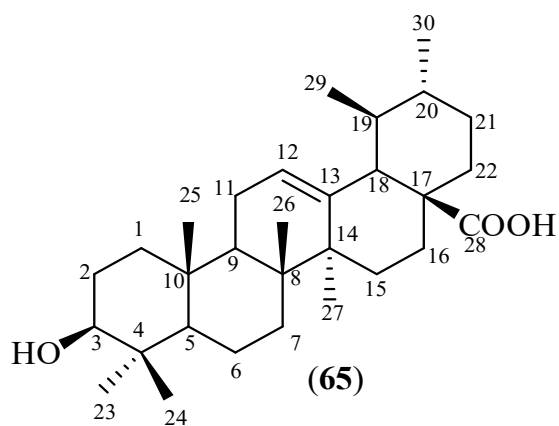
Table XV: ^1H and ^{13}C NMR data (MeOD) of TCO₉

Position	^1H (nH, m, J)	^{13}C
1	3.63 (1H, dd, 10.3; 2.3)	68.0
2	2.90 (1H, d, 9.3)	83.0
3	3.62 (1H, dd, 10.3; 3.9)	72.4
4	-	46.7
5	-	41.8
6	1.08 (2H, m)	26.0
7	1.78 (2H, m)	27.3
8	-	39.0
9	-	143.9
10	1.91 (1H, d, 2.3)	55.2
11	5.23 (1H, brs)	122.1
12	5.25 (1H, brs)	122.0
13	-	143.9
14	-	41.5
15	1.59 (2H, m)	25.0
16	1.56 (1H, m); 1.42 (1H, m)	18.1
17	-	45.8
18	2.85 (1H, d, 13.7)	41.3
19	1.68 (1H, m); 1.36 (1H, m)	38.9
20	-	30.1
21	2.01 (2H, m)	22.7
22	1.75 (2H, m)	32.1
23	0.70 (3H, s)	11.3
24	3.52 (1H, d, 11.2); 3.29 (1H, d, 11.2)	65.9
25	0.80 (3H, s)	16.0
26	0.93 (3H, s)	22.6
27	1.01 (3H, s)	27.8
28	-	180.4
29	1.65 (3H, s)	24.9
30	4.21 (1H, d, 5.4); 4.22 (1H, d, 5.4)	67.6

II.2.2.2. Identification of TC₄=TCO₄

Compound TC₄ was obtained as a white powder from the fruits and stem-bark of *T. conotorta* and the stem of *T. inconspicua* in a mixture of Hex/AE 30%. It is soluble in DMSO and pyridine. It responds positively to the Liebermann-Burchard's test giving a red purple color characteristic of triterpenes.

From the spectroscopic data of TiS₈ such as ^1H , ^{13}C NMR and by comparison of these data to those described in the literature, its structure was identified to be that of a triterpene:



On the basis of the interpretations of its NMR spectra, the molecular formula of TC₄ was determined to be C₃₀H₄₈O₃ (double bond equivalents 7).

Its ¹H NMR spectrum (Figure 51) shows signals at: δ_{H} 2.90 (1H, dd, 6.0; 12.0 Hz, H-3) an oxymethine proton. This coupling constants show that the hydroxy group has a β orientation; δ_{H} 5.15 (1H, d, 12.0 Hz, H-12) an olefinic proton suggesting a pentacyclic triterpene of the urs-12-ene type (Mahato and Kundu., 1994); δ_{H} 1.80 (1H, m, H-19) and δ_{H} 1.49 (1H, m, H-20) an information which is directly linked to the presence of two signals at δ_{H} 1.25 (3H, d, 6.0 Hz, H-29) and δ_{H} 1.23 (3H, d, 6.0 Hz, H-30) characteristics of the two methyl groups at position 29 and 30 of the ursane series. In addition, the presence of five singlets instead of six between 0.63 and 1.0 ppm proofs that one of the angular methyl groups of the pentacyclic triterpene has been oxidized.

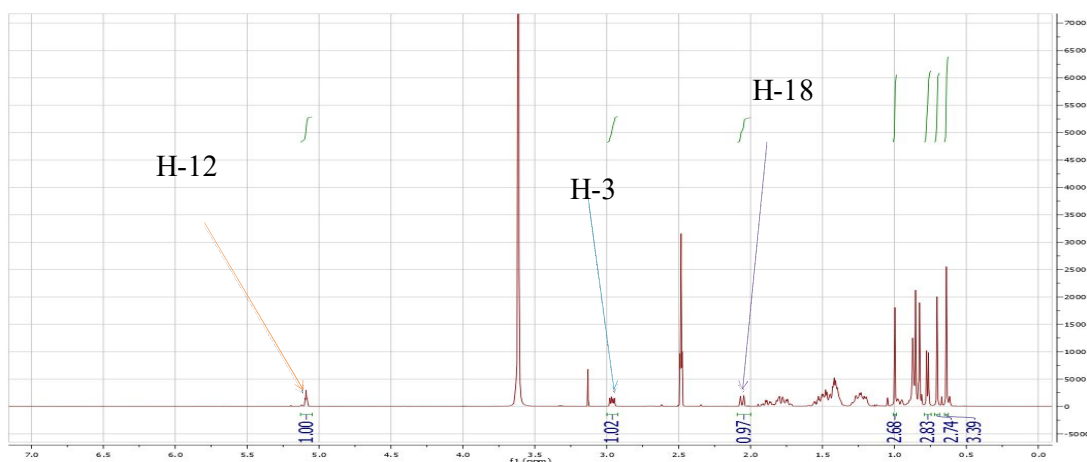


Figure 51: ¹H NMR spectrum (DMSO-*d*₆, 500 MHz) of TC₄

The ¹³C NMR spectrum (Figure 52) shows carbon signals at: δ_{C} 125.0 (C-12) and 138.6 (C-13) characteristic of the Δ^{12} ursenes (Mahato and Kundu, 1994) confirming the

above suggestions; δ_C 77.3 (C-3) a hydroxyl carbon atom in relation with the biosynthesis of triterpenes and the carbonyl signal at δ_C 178.9 confirms the oxidation of one of the methyl groups which is most likely at position 28.

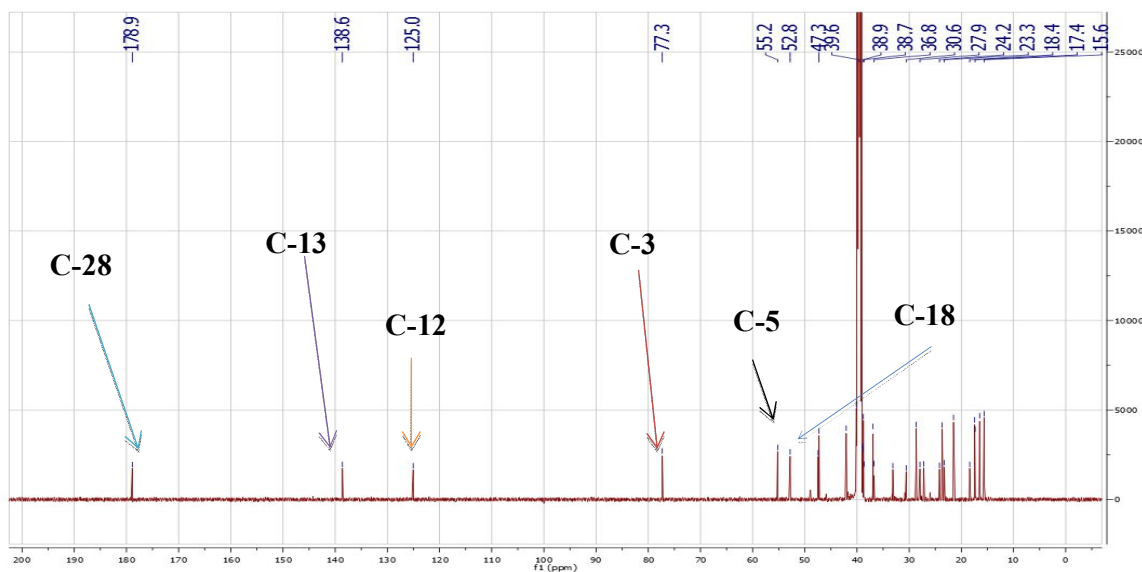


Figure 52: ^{13}C NMR spectrum (DMSO- d_6 , 125 MHz) of TC₄

Based on the physical and spectroscopic data of TC₄ and by comparison of these data with those described in the literature (Seebacher *et al.*, 2003), its structure was identified to that of 3 β -hydroxyurs-12-en-28-oic acid commonly called usolic acid (**65**).

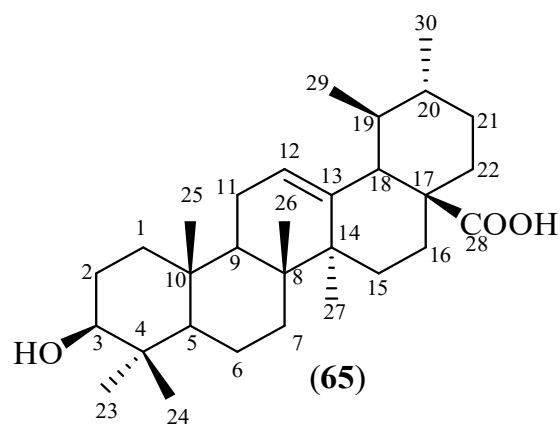


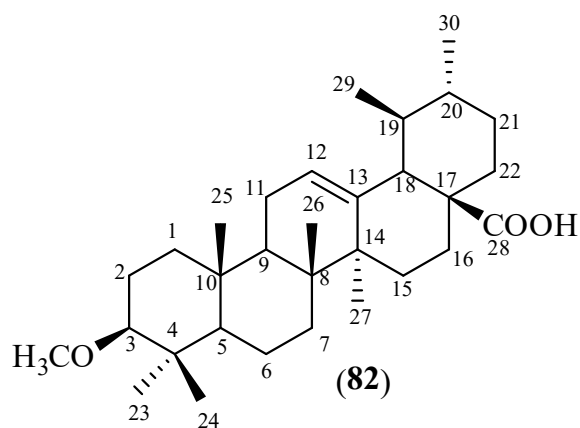
Table XVI: ^{13}C NMR (DMSO- d_6) data of TC₄ compared to the literature (Seebacher *et al.*, 2003)

Position	TC ₄	Seebacher <i>et al.</i> , 2003
1	30.6	39.2
2	24.2	28.2
3	77.3	78.2
4	36.8	39.6
5	55.2	55.9
6	19.5	18.8
7	27.9	33.7
8	38.9	40.1
9	47.3	48.1
10	31.8	37.5
11	23.3	23.7
12	125.0	125.7
13	138.6	139.3
14	38.9	42.6
15	28.8	28.8
16	17.8	25.0
17	40.7	48.1
18	52.8	53.6
19	38.1	39.5
20	39.8	39.4
21	24.4	31.1
22	29.2	37.4
23	25.3	28.8
24	17.7	16.5
25	15.6	15.7
26	17.4	17.5
27	19.5	24.0
28	178.9	179.7
29	17.4	17.5
30	17.7	21.4

II.2.2.3. Identification of TiS₃

Compound TiS₃ was obtained as a white powder from the stem of *T. inconspicua* in a mixture of Hex/AE 30%. It is soluble in pyridine and responds positively to the Liebermann-Burchard's test characteristic of triterpenes.

From the spectroscopic data of TiS₃ such as ^1H , ^{13}C NMR, COSY, HSQC, HMBC and by comparison of these data to those described in the literature, its structure was determined to be that of a triterpene:



On the basis of the interpretations of its NMR (1D and 2D) spectra, the molecular formula of TiS_3 was determined to be $\text{C}_{31}\text{H}_{50}\text{O}_3$ (double bond equivalents 7).

Its ^1H NMR spectrum (Figure 53) is readily similar to that TC_4 with the only difference being the presence of an intense methoxy signal at δ_{H} 3.61 (3H, s).

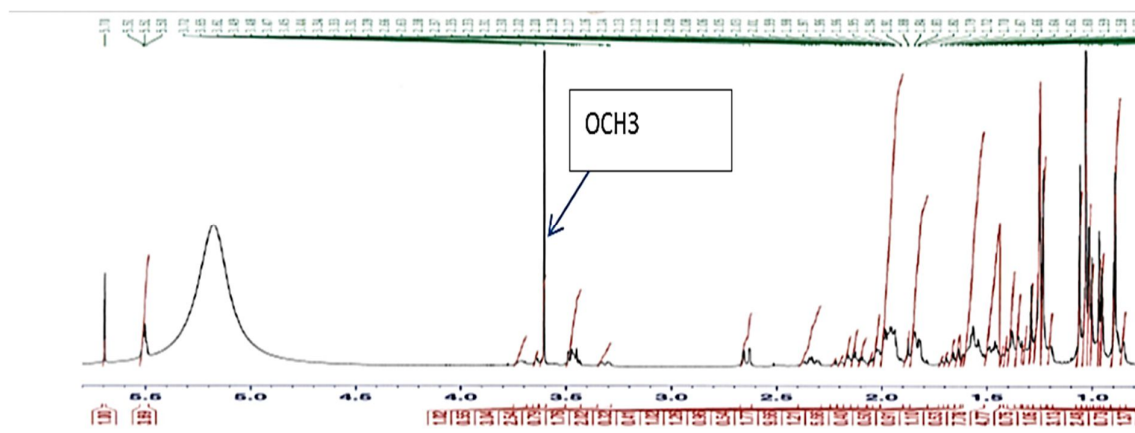


Figure 53: ^1H NMR spectrum (pyridine- d_5 , 400 MHz) of TiS_3

The ^{13}C spectrum (Figure 54) of TiS_3 is also very closed that of TC_4 but the appearance of a signal at δ_{C} 50.0 which correlates with the above methoxy protons in the HSQC spectrum (Figure 55) makes the difference between the two structures. The HMBC spectrum (Figure 56) shows a correlation between the methoxy protons and C-3 (δ_{C} 77.9) to confirm its position.

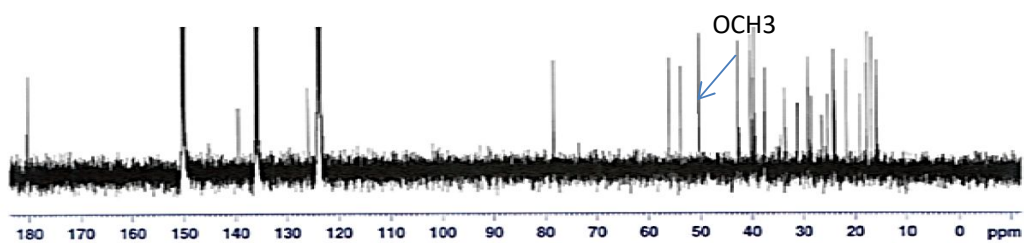


Figure 54: ^{13}C NMR spectrum (pyridine- d_5 , 100 MHz) of compound TiS_3

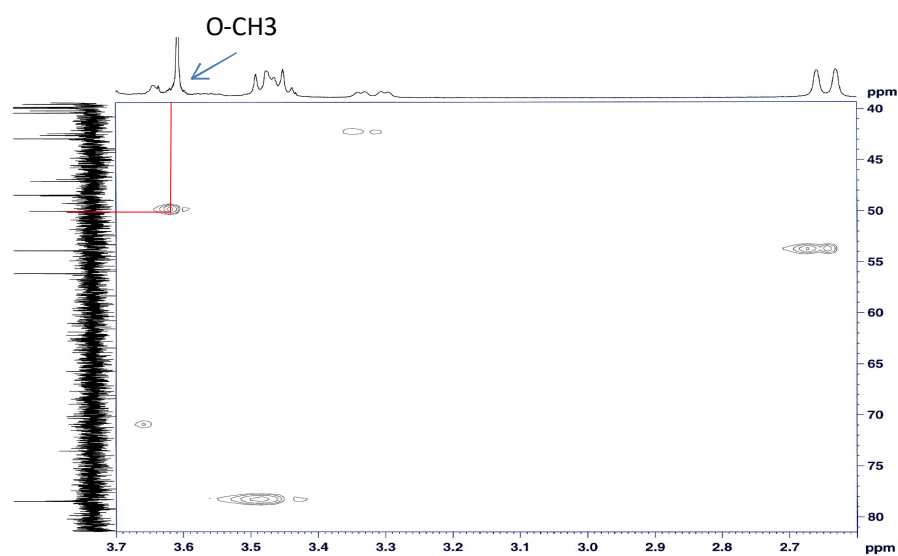


Figure 55: HSQC spectrum (pyridine- d_5) of TiS_3

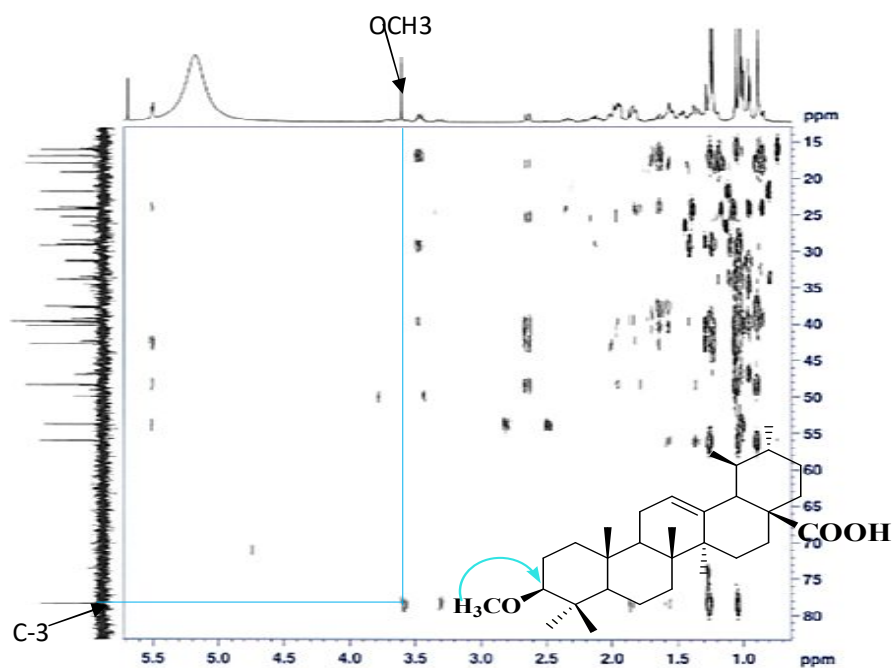


Figure 56: HMBC spectrum (pyridine- d_5) of TiS_3

On the basis of the sphysical and spectral data of TiS₃ and by comparison of these data with those described in the literature (Kwon *et al.*, 2009), its structure was identified to be that of 3 β -methoxyurs-12-en-28-oioque acid commonly called 3-methoxyusolic acid (**82**).

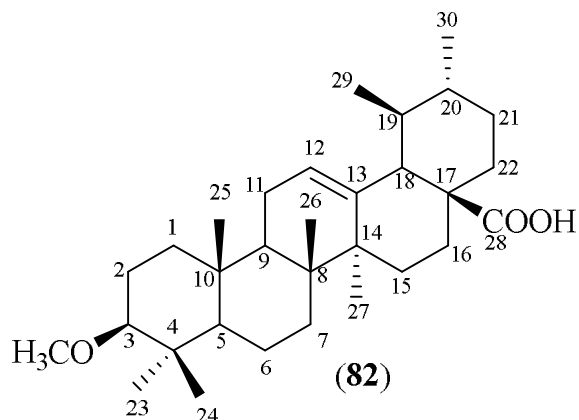


Table XVII: ¹³C NMR (pyridine-*d*₅) data of TiS₃ compared to those of the literature (Kwon *et al.*, 2009)

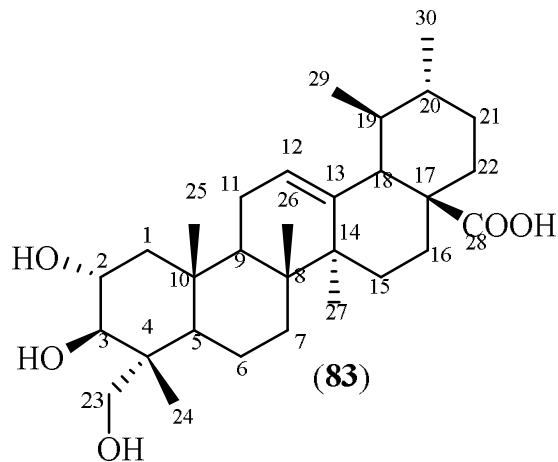
Position	TiS ₃	(Kwon <i>et al.</i> , 2009)
1	30.6	39.2
2	24.2	28.1
3	77.3	88.0
4	36.8	39.3
5	55.2	55.7
6	19.5	18.3
7	27.9	33.3
8	38.9	39.7
9	47.3	47.8
10	31.8	37.2
11	23.3	23.7
12	125.0	125.4
13	138.6	139.3
14	38.9	42.3
15	28.8	28.4
16	17.3	24.7
17	40.7	47.7
18	52.8	53.3
19	38.1	38.3
20	39.8	38.7
21	24.4	30.8
22	29.2	36.9
23	25.3	23.7
24	17.7	16.6
25	15.6	15.3
26	17.4	17.3
27	19.5	23.4
28	178.9	179.6

29	17.4	17.2
30	17.7	21.2
O-CH3	52.3	56.8

II.2.2.4. Identification of TCO₈

Compound TCO₈ was obtained as a white powder from the fruits, stem-bark of *T. conotrta* and the stem of *T. inconspicua* in a mixture of Hex/AE 20/80. It is soluble in DMSO and pyridine and responds positively to the Liebermann-Burchard's test characteristic of triterpenes.

From the spectroscopic data of TCO₈ such as ¹H, ¹³C NMR and by comparison of these data to those described in the literature, its structure was identified to be that of a triterpene:



Its molecular formula was determined to be C₃₀H₄₈O₅ on the basis of HRESIMS (m/z 489.3576 [M+H]⁺ calcd for 489.3580) (Figure 57), indicating 7 double bond equivalents.

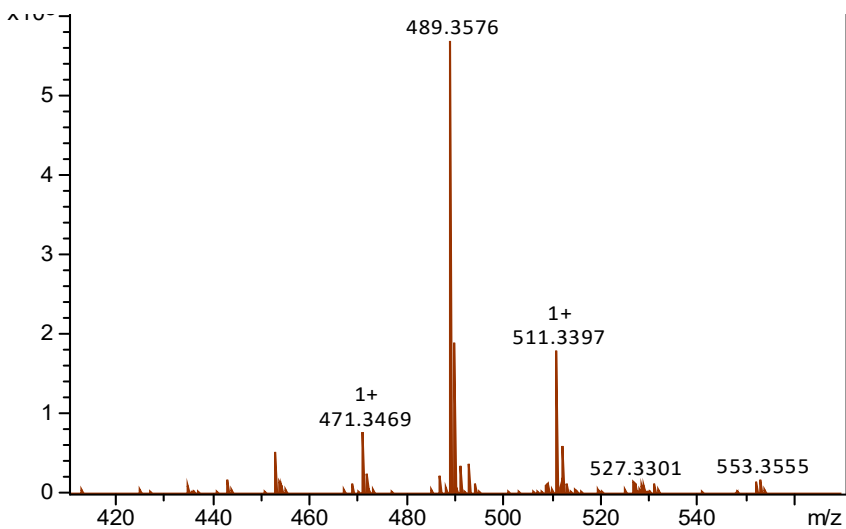


Figure 57: HRESIMS of TCO₈

Its ¹H NMR spectrum (Figure 58) reveals signals at: δ_{H} 5.29 (1H, brs, H-12), four methyl singlets (δ_{H} 0.70, 0.74, 1.04, and 1.23); two methyl doublets at δ_{H} 0.81 (6.3 Hz, H-29) and 0.97 (6.3 Hz, H-30) and a methyne at δ_{H} 2.11 (1H, d, 11.2 Hz, H-18) characteristic of the urs-12-ene skeleton. In addition, it reveals two oxymethynes δ_{H} 3.84 (1H, m, H-2 α), 3.48 (d, 9.3 Hz, H-3 β) and an oxymethylene at δ_{H} 3.20 (d, 11.5 Hz, H-23a) and 3.41 (d, 11.5 Hz, H-23b).

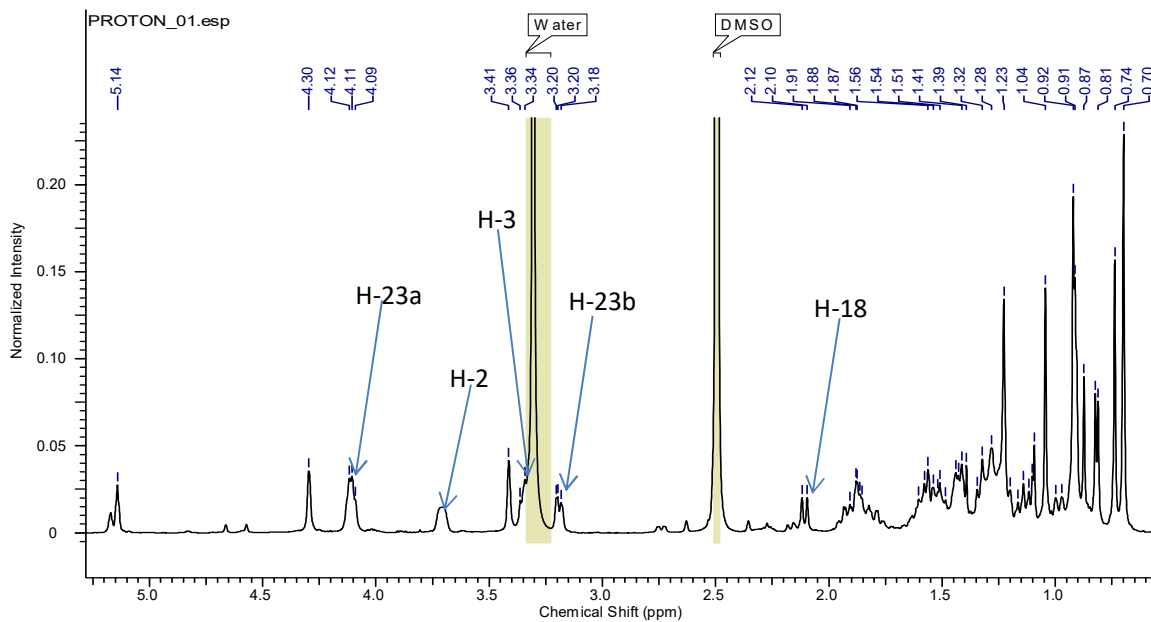


Figure 58: ¹H NMR spectrum (DMSO-*d*₆, 600 MHz) of TCO₈

The ^{13}C NMR of TCO_8 (Figure 59) shows carbon signals at: δ_{C} 124.9 (C-12) and 138.7 (C-13) characteristic of the Δ^{12} ursenes (Mahato and Kundu, 1994); δ_{C} 76.3 (C-3) a hydroxyl carbon atom in relation with the biosynthesis of triterpenes and a carbonyl signal at δ_{C} 180.2. The appearance of signals at δ_{C} 69.6 and 65.1 confirms the presence of hydroxyl groups at positions C-2 and C-23.

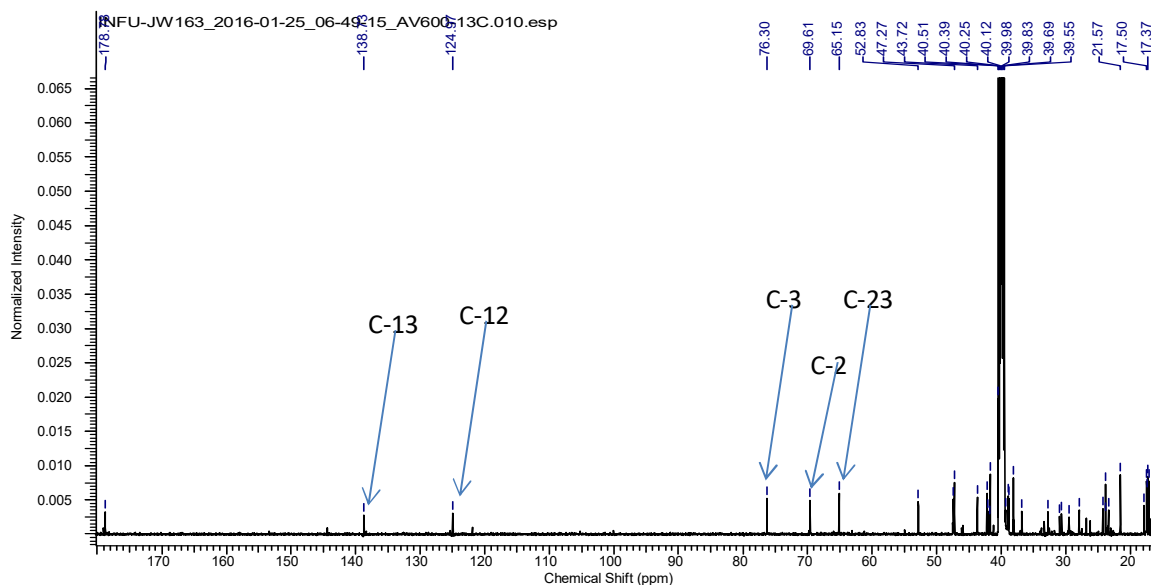


Figure 59: ^{13}C NMR spectrum (DMSO- d_6 , 150 MHz) of TCO_8

On the basis of physical and spectroscopic data of TCO_8 and by comparison of these data with those described in the literature (Collins *et al.*, 1992), its structure was identified to be that of 2 α ,3 β ,23-trihydroxy-urs-12-en-28-oic acid commonly called asiatic acid (**83**).

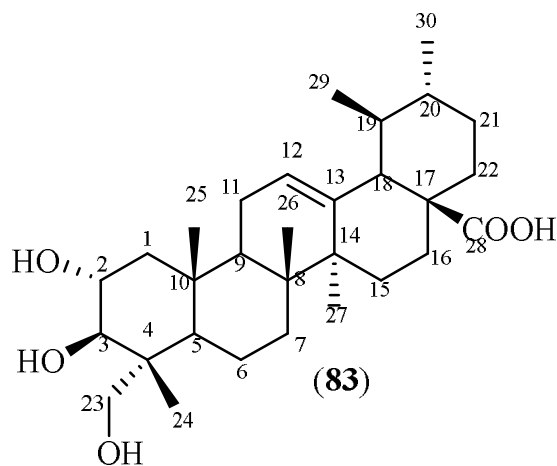


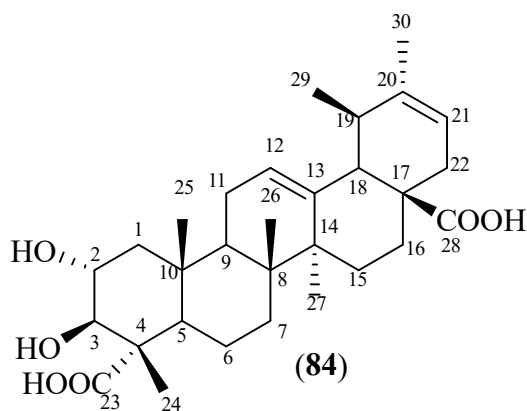
Table XVIII: ^{13}C NMR (DMSO- d_6) data of TCO₈ compared to those of the literature (Collins *et al.*, 1992)

Position	TCO ₈	(Collins <i>et al.</i> , 1992)
1	43.7	46.4
2	69.6	68.0
3	76.3	78.8
4	42.2	42.7
5	47.4	48.0
6	17.9	18.1
7	32.8	32.4
8	39.5	39.4
9	43.7	47.3
10	38.1	38.0
11	23.4	23.3
12	124.9	125.2
13	138.7	138.2
14	42.2	42.0
15	27.9	27.9
16	23.9	24.1
17	47.2	47.9
18	52.8	52.8
19	38.9	39.0
20	38.8	38.8
21	30.6	30.6
22	36.7	36.6
23	65.2	68.6
24	17.1	13.1
25	17.3	16.8
26	17.4	17.0
27	23.8	23.7
28	178.7	178.5
29	17.7	17.2
30	21.5	21.2

II.2.2.5. Identification of TiS₉

Compound TiS₉ was obtained as a white powder from the stem of *T. inconspicua* in a mixture of Hex/AE (10/90). It is soluble in chloroform and pyridine and responds positively to the Liebermann-Burchard's test giving a red purple color characteristic of triterpenes.

From the spectroscopic data of TiS₉ such as ^1H , ^{13}C NMR and by comparison of these data to those described in the literature, its structure was determined to be that of a triterpene:



Its molecular formula was determined on the basis of interpretation of its NMR spectra to be $C_{30}H_{44}O_6$ indicating 9 double bond equivalents.

Its 1H NMR spectrum (Figure 60) reveals two methyne signals at δ_H 5.47 (1H, brs, H-12) and 5.48 (1H, brs, H-21) suggesting the presence of two double bonds, four methyl singlets at δ_H 0.95, 0.98, 1.04, and 1.27; a methyl doublet at δ_H 0.99 (6.3 Hz, H-29) and a vinyl methyl singlet at δ_H 2.01 (H-30). In addition it reveals a doublet at δ_H 2.11 (1H, d, 11 Hz, H-18) characteristic of the ursene skeleton which is dihydroxylated in positions 2α (δ_H 4.10, 1H, dt, 11.2; 3.6 Hz) and 3β (δ_H 3.41, dd, 10.8; 3.8 Hz).

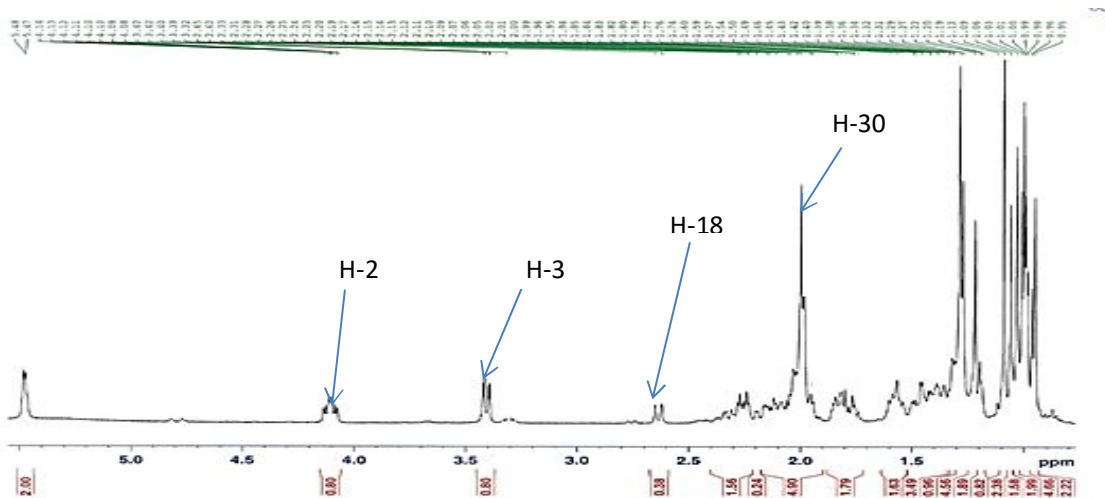


Figure 60: 1H NMR spectrum (pyridine- d_5 , 400 MHz) of TiS_9

The ^{13}C NMR of TiS_9 (Figure 61) shows four olefinic carbon signals with two at: δ_C 122.8 (C-12) and 145.2 (C-13) characteristic of the Δ^{12} ursenes (Mahato and Kundu, 1994) and the other two are attributed to C-20 (δ_C 139.6) and C-19 (δ_C 125.9). It also reveals two hydroxylated carbon signals at δ_C 84.1 attributed to C-3 in relation with the biosynthesis of triterpenes and δ_C 68.9 attributed to C-2. Two carbonyl signals at δ_C 180.2 and 180.5

attributed to C-23 and C-28 respectively in comparison with reported data (Mahato and Kundu, 1994).

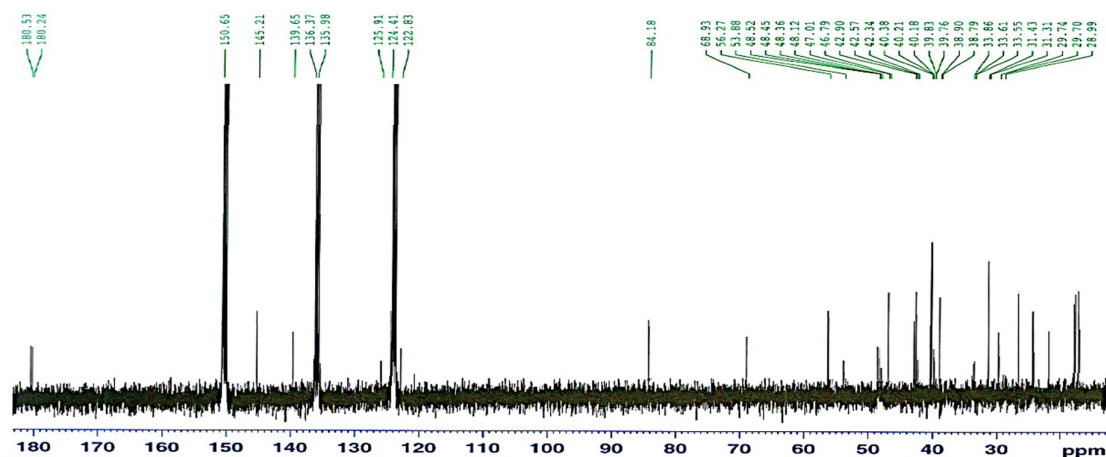


Figure 61: ^{13}C NMR spectrum (pyridine- d_5 , 100 MHz) of TiS_9

The comparison of its physical and spectroscopic data to those reported in literature (Khan *et al.*, 1991) led to the identification of the structure of TiS_9 to that of $2\alpha,3\beta$ -dihydroxyurs-12,20-diene-24,28-dioic acid commonly called cordepressenic acid (**84**).

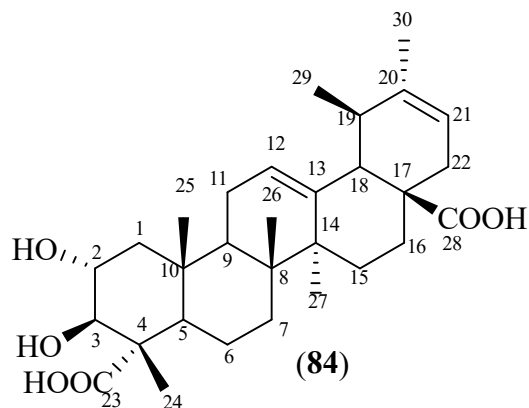


Table XIX: ^{13}C NMR (DMSO- d_6) data of TiS_9 compared to the literature (Khan *et al.*, 1991)

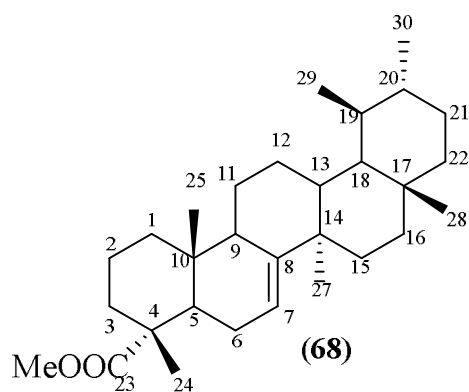
Position	TiS_9	(Khan <i>et al.</i> , 1991)
1	48.4	47.0
2	68.9	67.0
3	84.1	82.5
4	46.7	46.5
5	53.5	53.5
6	18.0	20.66
7	33.5	32.4
8	39.7	39.4
9	48.5	49.5
10	39.8	38.0

11	24.1	23.0
12	122.8	129.5
13	139.6	138.5
14	42.5	42.0
15	29.7	27.5
16	24.1	25.5
17	47.0	47.2
18	56.8	55.5
19	40.2	36.3
20	145.2	145.0
21	125.9	125.5
22	38.9	37.6
23	180.5	180.0
24	17.2	15.4
25	17.3	16.8
26	17.4	17.0
27	24.2	23.7
28	180.2	181.5
29	17.8	17.2
30	26.5	26.0

II.2.2.6. Identification of TC₃

Compound TC₃ was obtained as a white powder from the stem of *T. inconspicua* in a mixture of Hex/AE (80/20). It is soluble in chloroform and pyridine and responds positively to the Liebermann-Burchard's test characteristic of triterpenes.

From the spectroscopic data of TC₃ such as ¹H, ¹³C NMR and by comparison of these data to those described in the literature, its structure was determined to be that of a triterpene:



Its molecular formula was determined to be C₃₂H₅₂O₂ (double bond equivalents 6), based on interpretation of its NMR spectra.

Its ^1H NMR spectrum (Figure 62) reveals six methyl singlets at δ_{H} 0.76, 0.85, 0.93, 0.94, 0.99 and 1.25 two methyl doublets at δ_{H} 0.93 (5.9 Hz, H-29) and 1.04 (5.9 Hz, H-30) characteristic of the ursane skeleton. Moreover it shows signals at δ_{H} 4.52 (1H, dd, 11.2; 6.9 Hz, H-3); a methylketone singlet at δ_{H} 2.05 (3H, s) and an sp^2 methyne at δ_{H} 5.40 (1H, brs).

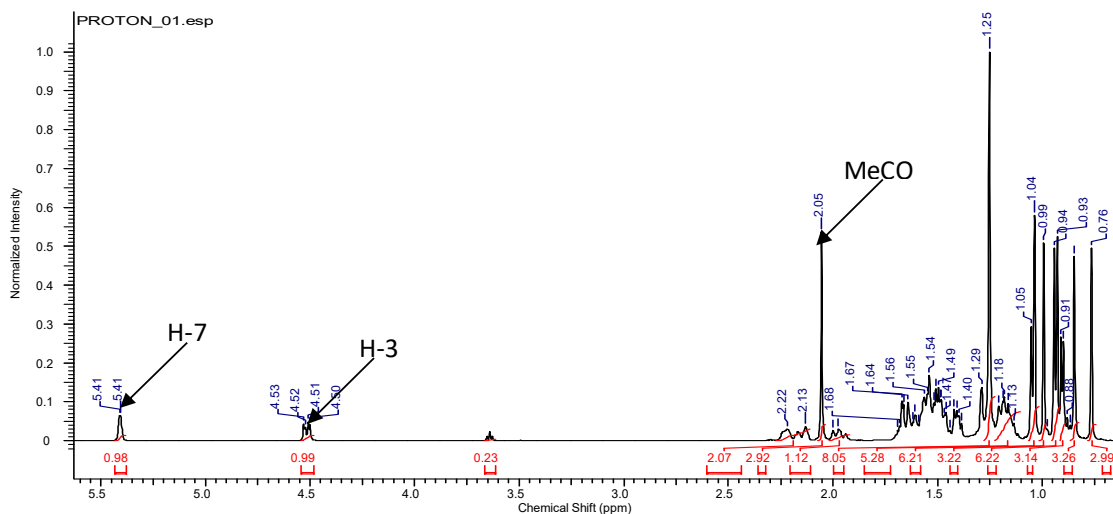


Figure 62: ^1H NMR spectrum (CDCl_3 , 600 MHz) of TC_3

The carbon spectrum (Figure 63) of TC_3 shows carbon signals at: δ_{C} 116.2 (C-7) and 45.4 (C-8) characteristic of the Δ^7 ursenes (Mahato and Kundu, 1994); δ_{C} 81.1 (C-3) an oxymethine carbon atom in relation with the biosynthesis of triterpenes and an ester carbonyl signal at δ_{C} 171.0.

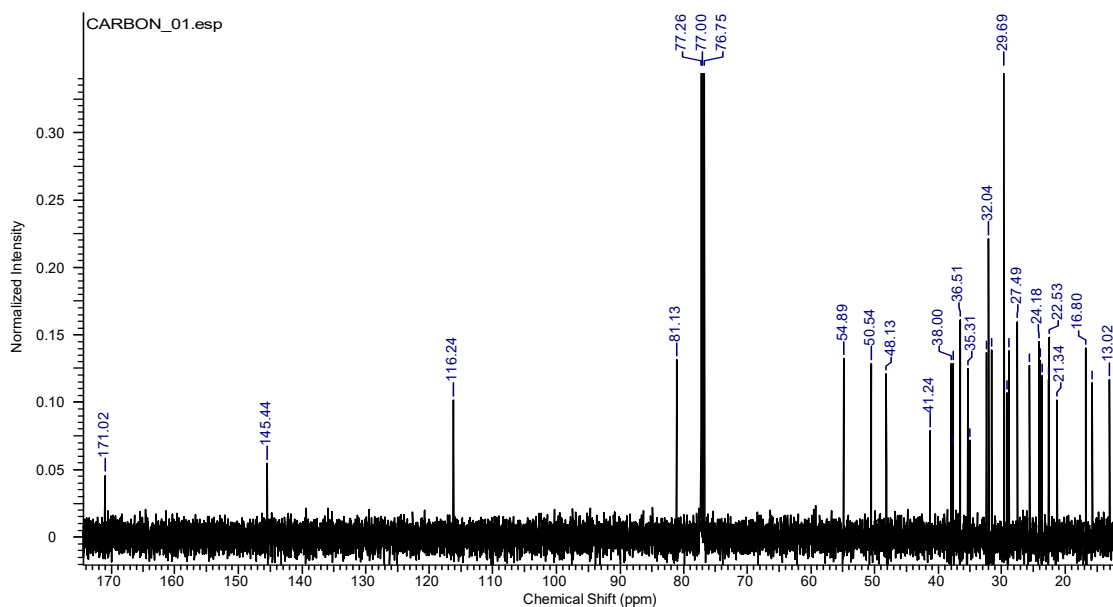


Figure 63: ^{13}C NMR spectrum (CDCl_3 , 150 MHz) of TC_3

Based on the physical spectral data of TC₃ and by comparison of these data with those described in the literature (Mahato and Kundu, 1994), its structure was identified to that of Bauerenyl acetate (**68**).

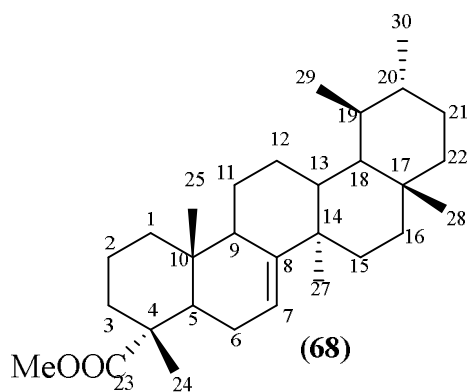


Table XX: ¹³C NMR (CDCl₃) data of TC₃ compared to the literature (Mahato and Kundu, 1994)

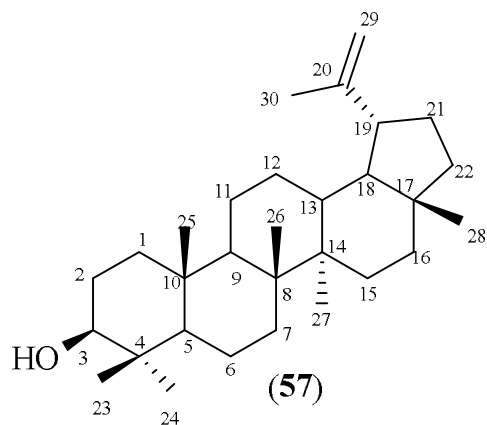
Position	TC ₃	(Mahato and Kundu, 1994)
1	36.5	36.5
2	24.2	24.2
3	81.1	81.1
4	37.7	37.8
5	50.5	50.0
6	24.0	24.0
7	116.5	116.2
8	145.4	145.4
9	48.1	48.2
10	35.1	35.1
11	16.8	16.9
12	122.8	32.5
13	139.6	37.8
14	41.2	41.3
15	28.9	28.9
16	31.5	31.5
17	32.0	32.1
18	54.9	55.0
19	35.3	35.4
20	38.0	38.0
21	29.2	29.2
22	37.7	37.8
23	27.5	27.5
24	15.8	15.8
25	13.0	13.0
26	23.6	23.6
27	22.7	22.7
28	32.3	32.1
29	25.6	25.6

30	22.5	22.5
C=O	171.0	171.0

II.2.2.7. Identification of TiS₂

Compound TiS₂ was obtained as a white powder from the stem of *T. inconspicua* in a mixture of Hex/AE (80/20). It is soluble in chloroform and pyridine and responds positively to the Liebermann-Burchard's test characteristic of triterpenes.

From the spectroscopic data of TiS₂ such as ¹H, ¹³C NMR and by comparison of these data to those described in the literature, its structure was identified to be that of a triterpene:



Its molecular formula was determined to be C₃₀H₅₀O (double bond equivalents 6), on the basis of interpretation of its NMR spectra.

Its ¹H NMR spectrum (Figure 64) reveals signals at: δ_H 3.20 (1H, dd, 6.2 Hz; 11.9, H-3); angular methyl singlets between δ_H 0.80 and 1.10 (H-23, 24, 25, 26, 27, 28); δ_H 1.70 (3H, s, H-30) probably a vinyl methyl group; δ_H 4.55 et 4.70 (each 1 H, brs, CH₂-29) suggesting a lup 20(29) series of pentacyclic triterpenes (Mahato and Kundu, 1994).

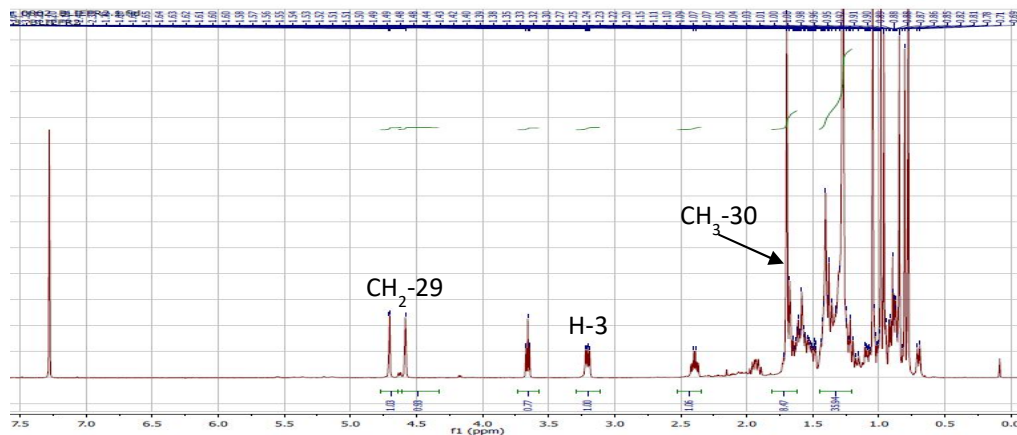


Figure 64: ^1H NMR spectrum (CDCl_3 , 400 MHz) of TiS_2

The ^{13}C NMR spectrum of TiS_2 (Figure 65) shows carbon signals at: δ_{C} 109.3 (C-29), 150.9 (C-20) and 79.0 (C-3), characteristic of the lup 20(29) series of pentacyclic triterpenes (Mahato and Kundu, 1994).

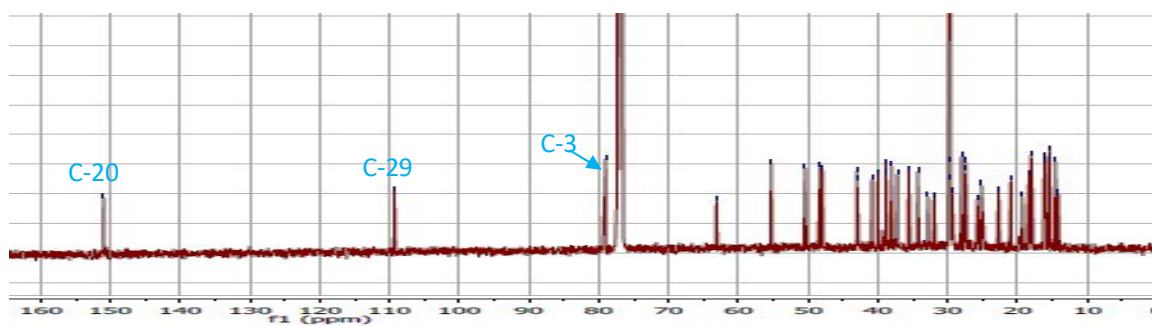
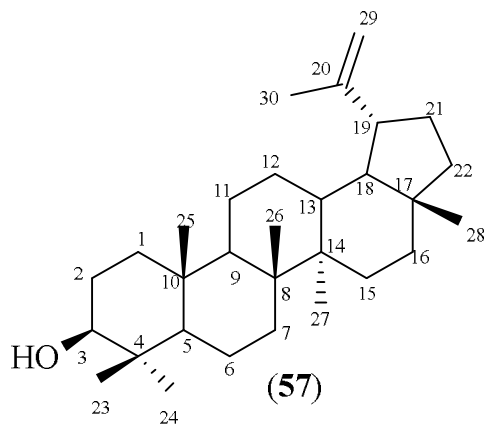


Figure 65: ^{13}C NMR spectrum (CDCl_3 , 100 MHz) of TiS_2

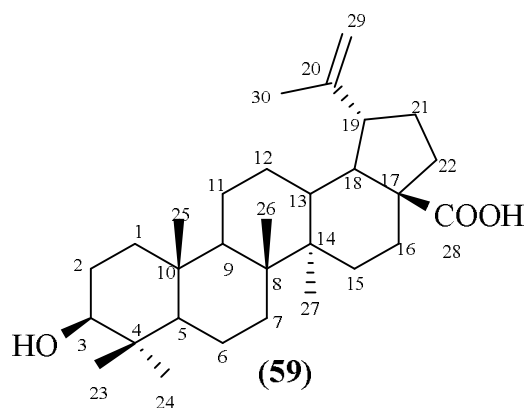
On the basis of the physical and spectral data of TiS_2 and by comparison of these data to those described in the literature (Mahato and Kundu, 1994), its structure was identified to be that of lupeol (**57**).



II.2.2.8. Identification of TiS₄

Compound TiS₄ was obtained as a white powder from the stem of *T. inconspicua* in a mixture of Hex/AE (78/22). It is soluble in chloroform and pyridine and responds positively to the Liebermann-Burchard's test giving a red purple colour characteristic of triterpenes.

From the spectroscopic data of TiS₄ such as ¹H, ¹³C NMR and by comparison of these data to those described in the literature, its structure was identified to be that of a triterpene:



Its molecular formula was determined to be C₃₀H₄₈O₃ (double bond equivalents 7), on the basis of interpretation of its NMR spectra.

The ¹H NMR spectrum (Figure 66) of TiS₄ is relatively similar to that of TiS₂ with the difference being that it reveals between δ_H 0.72 and 95 five angular methyls (s, H-23, 24, 25, 26, 27) instead of six, suggesting that one of them has been oxidized.

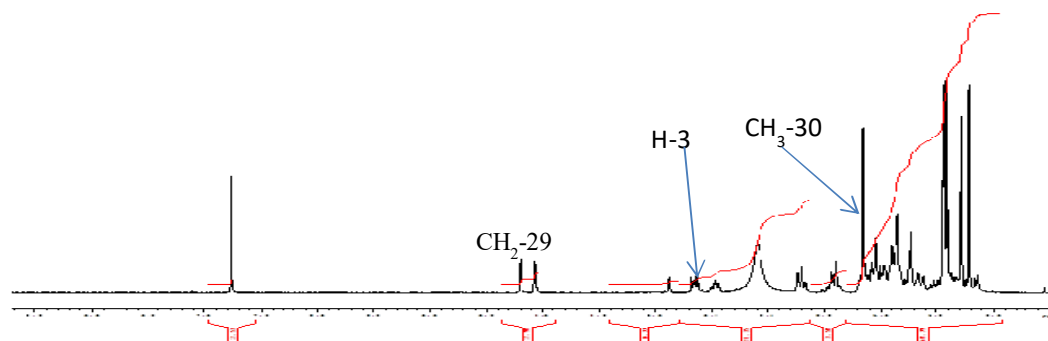


Figure 66: ¹H NMR spectrum (CDCl₃, 400 MHz) of TiS₄

The ^{13}C NMR spectrum of TiS_4 (Figure 67) is also similar to that of TiS_2 with the difference being the presence of an additional signal of an acid functional group at $\delta_{\text{C}} 179.2$ (C-28) confirming the above oxidation.

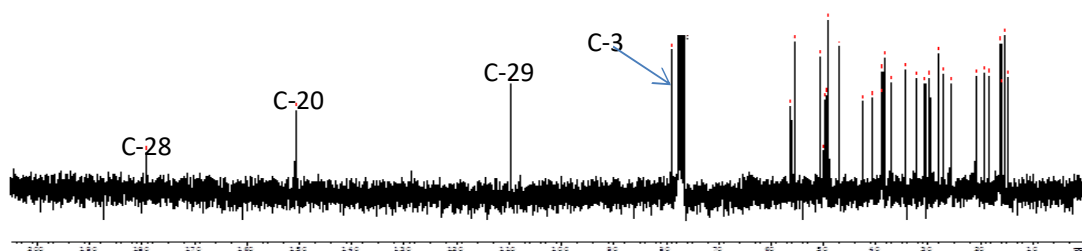
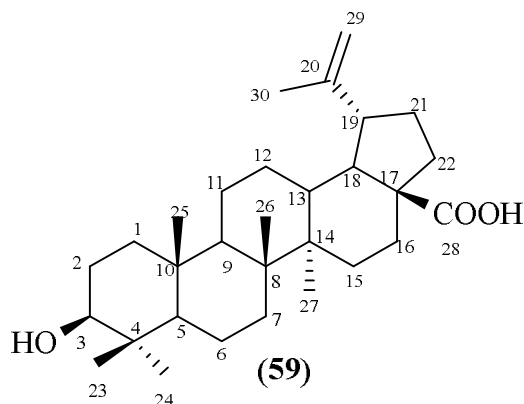


Figure 67: ^{13}C NMR spectrum (CDCl_3 , 100 MHz) of TiS_4

On the basis of the spectral data of TiS_4 and by comparison of these data to those described in the literature (Mahato and Kundu, 1994), its structure was identified to be that of 3β -hydroxylup-20, 29-en-28-oic acid or butelinic acid (**59**).



II.2.3 Steroids

II.2.3.1 Identification of $\text{TCO}_1=\text{TC}_2=\text{TiS}_1$

TCO_1 was obtained as white crystals, from fruits and stem-bark of *T. contorta* and stem of *T. inconspicua*. It is soluble in CHCl_3 and gives a positive response to the Liebermann-Burchard test giving a green colour, characteristic of steroids.

Its molecular formula was determined on the basis of the interpretation of its NMR spectra to be $\text{C}_{29}\text{H}_{48}\text{O}$

Its ^1H NMR spectrum (Figure 68) shows signals at $\delta_{\text{H}} 5.15$ (1H, m), $\delta_{\text{H}} 5.03$ (1H, dd) and $\delta_{\text{H}} 5.36$ corresponding to H-23, H-22 and H-6 respectively. This was confirmed by the

four olefinic carbon resonances observed in the ^{13}C NMR spectrum (Figure 69). The two signals at δ_{C} 129.2 and 138.3 are typical of C-23 and C-22 of a Δ^{22} sterol skeleton (Rubinstein *et al.*, 1976). The two other signals that appear at δ_{C} 121.7 and 140.7 are characteristic of C-6 and C-5 of a Δ^5 sterol frame work (Tandon *et al.*, 1990). Furthermore, a signal at δ_{C} 72.8 is attributed to an oxymethine carbon which is assigned to C-3; this information is confirmed by a multiplet at δ_{H} 3.52 on the proton spectrum.

The comparison of its physical and spectroscopic data to those reported in literature (Goad, 1991) led to the identification of TCO₁ as stigmasterol (**85**).

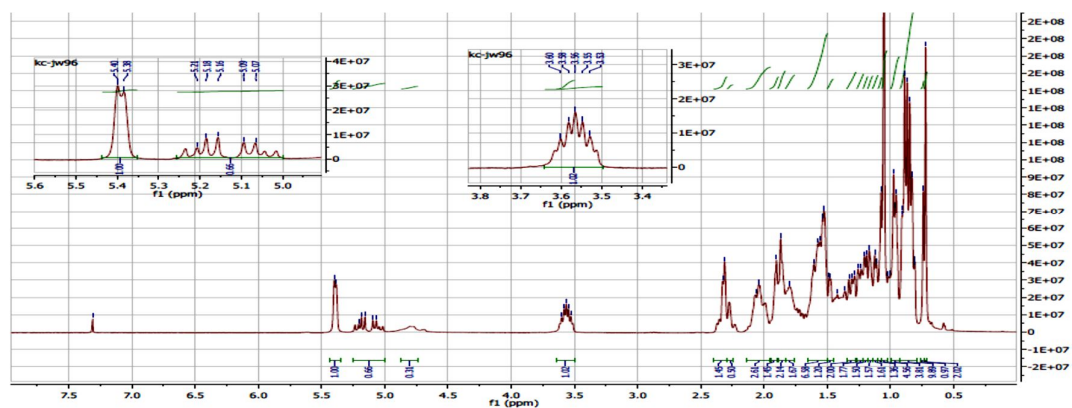
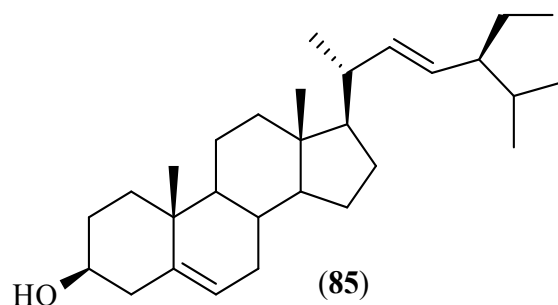


Figure 68: ^1H NMR spectrum (CDCl_3 , 400 MHz) of TCO₁

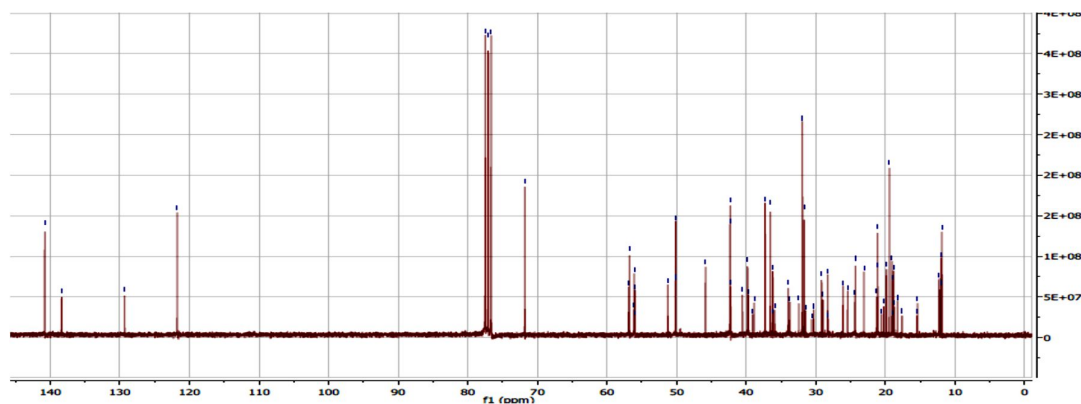


Figure 69: ^{13}C NMR spectrum (CDCl_3 , 100 MHz) of TCO₁

II.2.3.2. Identification of TCO₁₈ =TC₁₆

TCO₁₈ was obtained as a white powder, from the fruits and stem-bark of *T. contorta* in a mixture of hex/AE (25/75) It is soluble in pyridine and gives a positive response to the Liebermann-Burchard test giving a green color, characteristic of steroids and to the molish's test giving a purple color, characteristics of sugars.

Its molecular formula was determined on the basis of the interpretation of its NMR spectra to be C₃₅H₆₀O₆.

The ¹H NMR (Figure 70) spectrum reveals signals at δ_H 4.01 (1H, m, H-3); 5.09 (2H, d, H-6) characteristics of sterol (Tandon *et al.*, 1990). Also, a large triplet is observed at δ_H 4.33 belonging to the H-6' of glucose with its anomeric proton at δ_H 4.10. This leads to a suggestion that the TCO₁₈ is a steroid glycoside.

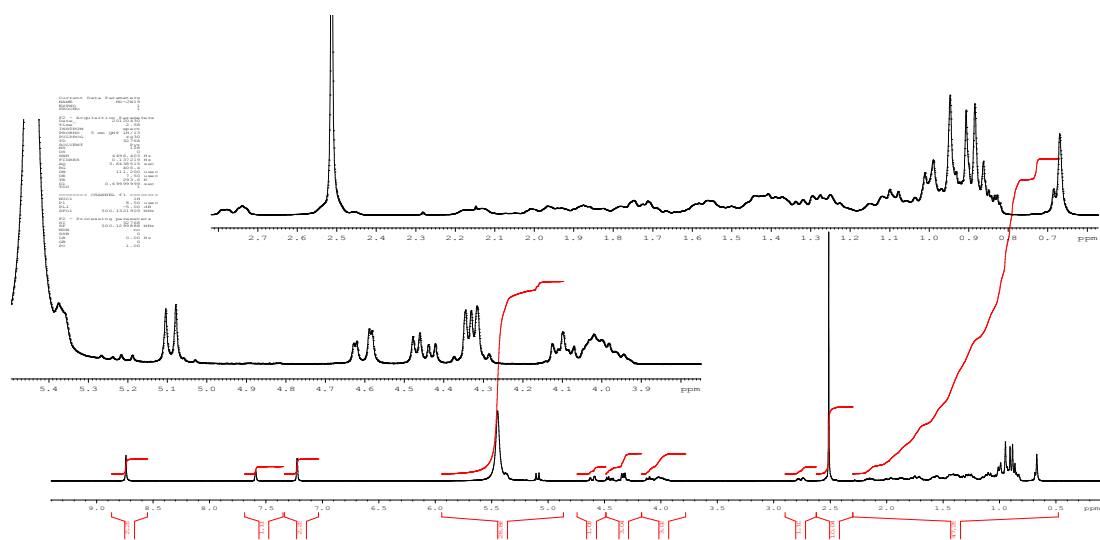


Figure 70: ¹H NMR spectrum (pyridine-*d*₅, 300 MHz) of TCO₁₈

The structure of TCO₁₈ was confirmed by the ¹³C NMR (Figure 7168) which reveals two at δ_C 141.4 and 122.4 ppm belonging to *sp*² carbons of a Δ⁵⁽⁶⁾-sterol (Tandon *et al.*, 1990). An anomeric carbon is observed at δ_C 103.0 and six others between δ_C 63.3 – 79.1 belonging to the hydroxylated carbons of glucose.

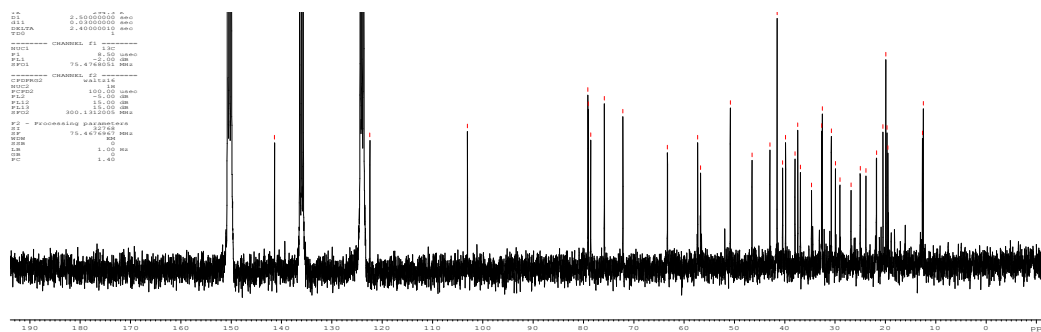
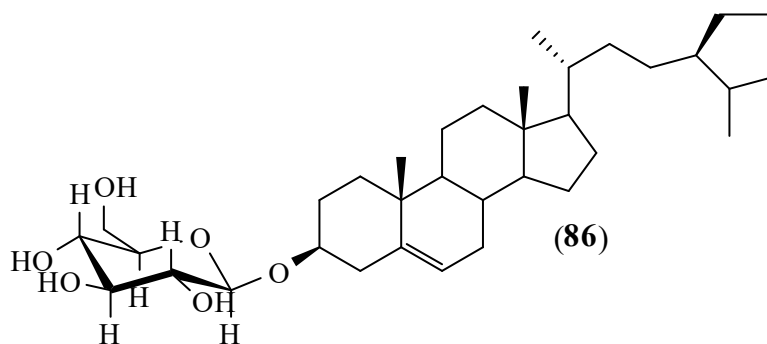


Figure 71: ^{13}C NMR spectrum (pyridine- d_5 , 75 MHz) of TCO_{18}

On the basis of the spectral data of TCO_{18} and by comparison of these data to those described in the literature (Villasenor *et al.*, 2002), its structure was identified to be that of sitosterol-3- O - β -D- glucopyranoside (**86**).



II.2.3.3. Identification of TiS_{14}

TiS_{14} was obtained as a white powder from the stem of *T. inconspicua* in a mixture of hex/AE (25/75). It is soluble in pyridine and gives a positive response to the Liebermann-Burchard and to the molish's test.

Its molecular formula was determined on the basis of the interpretation of its NMR spectra to be $\text{C}_{35}\text{H}_{58}\text{O}_6$

Its ^1H NMR (Figure 72) spectrum is similar to that of TCO_{18} but its ^{13}C NMR spectrum (Figure 73) reveals the presence of additional two sp^2 carbon signal at δ_{C} 125.4 and 148.2 showing the presence of an additional double bond.

On the basis of spectral data and by comparison of these data to those described in the literature (Ngouela. 1990), the structure of TiS_{14} was identified to be that of stigmasterol 3- O - β -D-glucopyranoside (**87**).

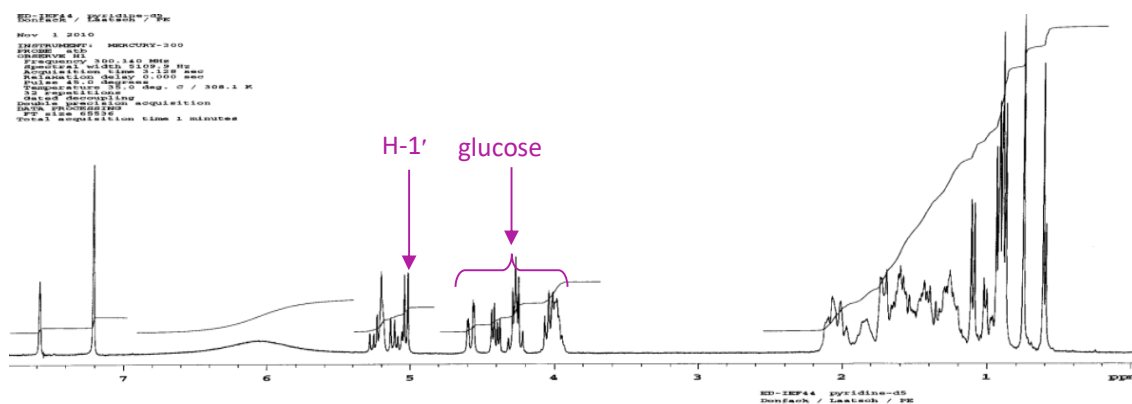
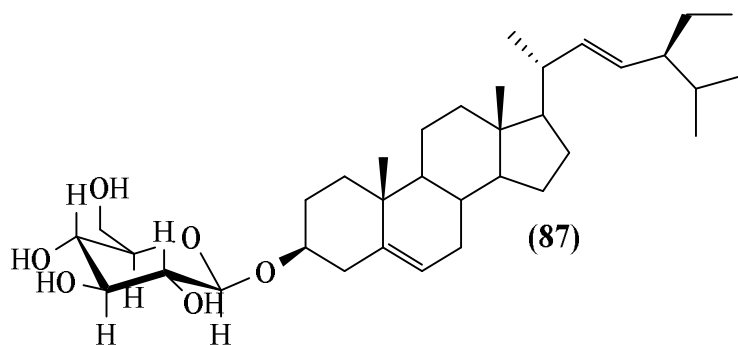


Figure 72: ^1H NMR spectrum (pyridine- d_5 , 400 MHz) of TS_{14}

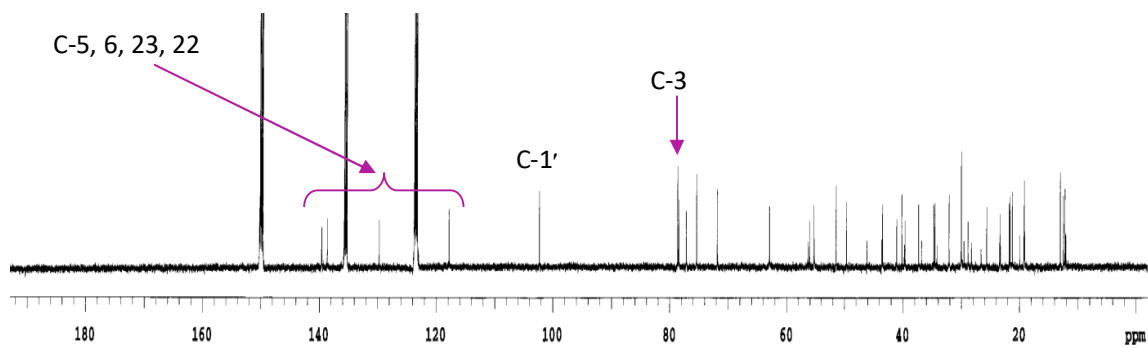


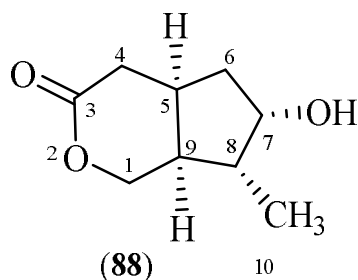
Figure 73: ^{13}C NMR spectrum (pyridine- d_5 , 100 MHz) of TS_{14}

II.2.4. Monoterpenes

II.2.4.1. Identification of TCO_2

TCO_2 was obtained from the stem-bark of *Tabernaemontana contorta* as colorless crystals in a mixture of Hex/AE 70/30. It is soluble in CHCl_3 .

From the spectroscopic data of TCO₂ such as ¹H, ¹³C NMR and by comparison of these data to those described in the literature, its structure was identified to be that of a monoterpene:



On the basis of EI-MS ($m/z = 170[M]^+$) (Figure 74) and spectral analysis, its molecular formula was determined to be C₉H₁₄O₃ indicating three double bond equivalents.

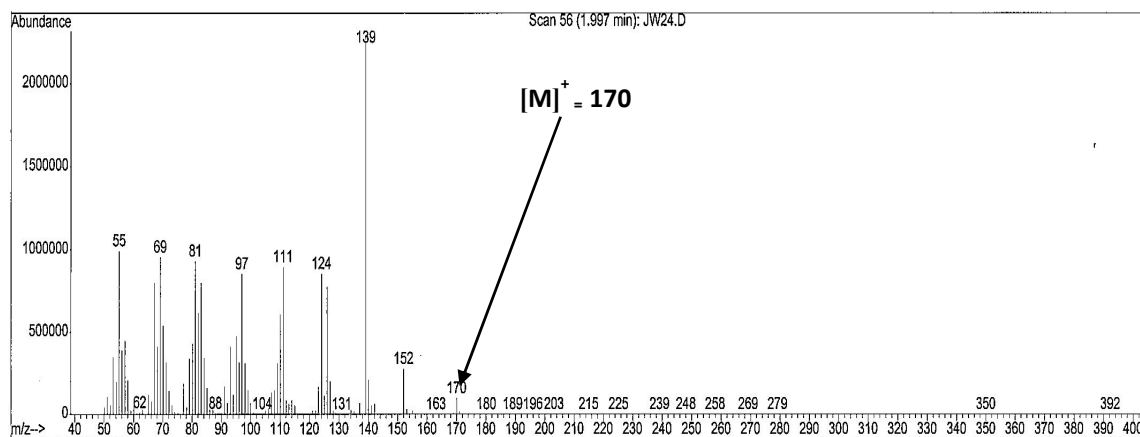


Figure 74: EIMS of TCO₂

The ¹H NMR spectrum of TCO₂ (Figure 75) reveals signals of: an oxymethylene at δ_H 4.35 (1H, dd, 12.0, 4.0 Hz, H-1b) and 4.15 (1H, dd, 12.0, 3.0 Hz, H-1a); an oxymethyne at δ_H 4.20 (1H, m, H-7); two methylenes at δ_H 2.74 (1H, dd, 16.0, 8.0 Hz, H-4b), 2.43 (1H, dd, 16.0, 4.0 Hz, H-4a), 2.15 (1H, m, H-6b), 1.43 (1H, ddd, 14.0, 11.0, 3.5 Hz, H-6a); three methyenes at δ_H 3.10 (1H, m, H-5); 2.22 (1H, m, H-9) and 1.89 (1H, m, H-8) and a methyl at δ_H 1.15 (1H, d, 7.5 Hz, H-10).

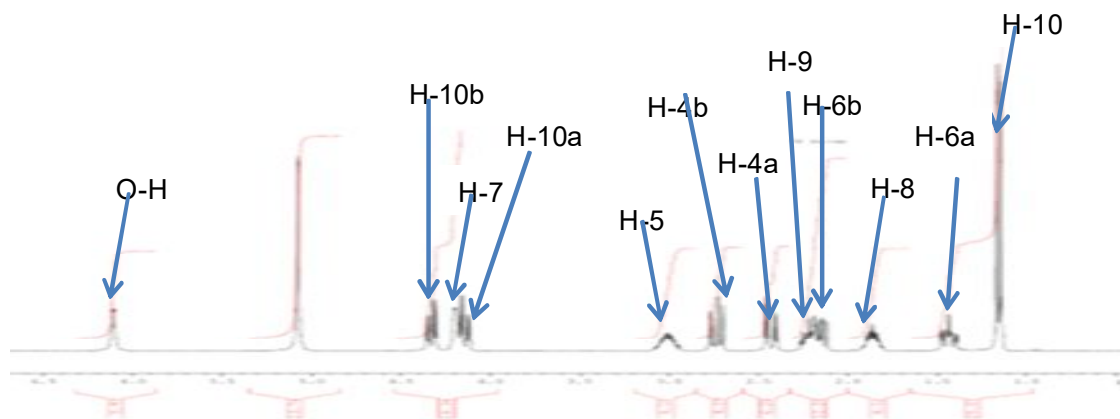


Figure 75: ^1H NMR spectrum (Pyridine- d_5 , 400 MHz) of TCO_2

Its ^{13}C NMR spectrum (Figure 76) shows 9 signals. Coupled with the DEPT spectrum (Figure 74) reveals signals that comprise: one methyl at δ_{C} 13.7 (C-10); three methylenes at δ_{C} 69.2 (C-1), 33.5 (C-4), 42.8 (C-6); four methynes at δ_{C} 35.3 (C-5), 74.4 (C-7), 42.8 (C-8), 42.6 (C-9) and a carbonyl signal at δ_{C} 173.9 (C-2).

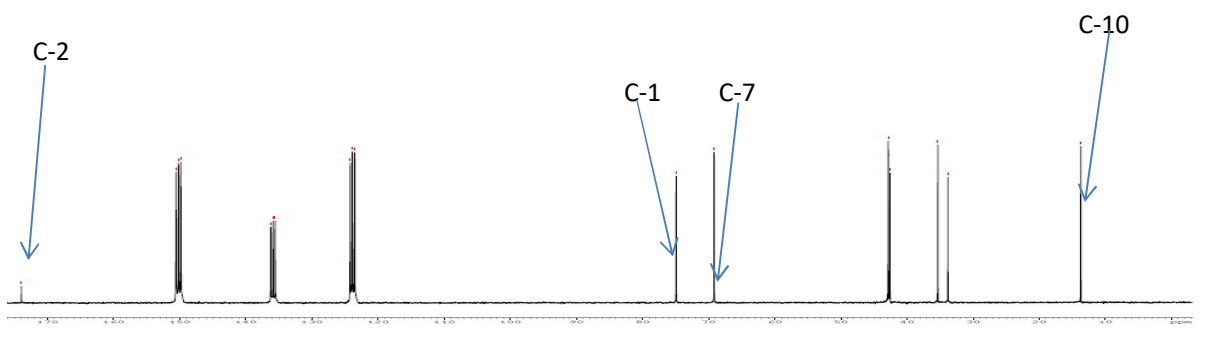


Figure 76: ^{13}C NMR spectrum (Pyridine- d_5 , 100 MHz) of TCO_2

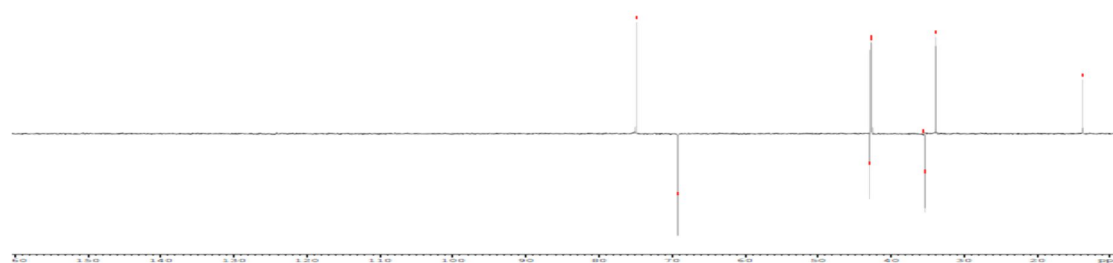


Figure 77: DEPT-135 spectrum (Pyridine- d_5 , 100 MHz) of TCO_2

Based on spectral analysis and by comparison of spectral data to those described in the literature (Bianco *et al.*, 1994) the structure of TCO_2 was identified to be that of isoboonein (**88**).

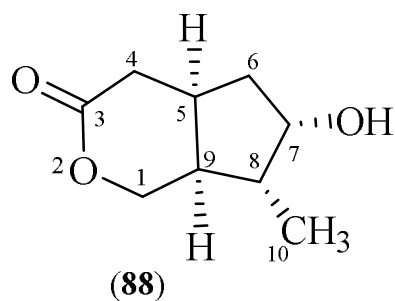


Table XXI: ^1H and ^{13}C NMR (Pyridine- d_5) data of TCO₂ compared to the literature (Bianco *et al.*, 1984)

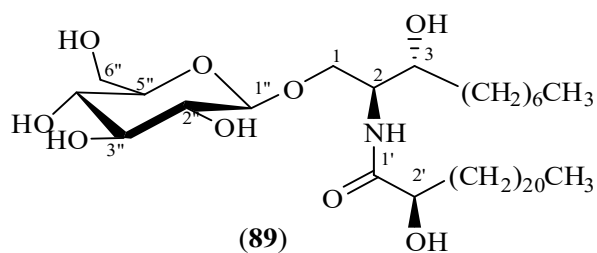
Position	^1H (nH, m, J)		^{13}C	
	TCO ₂	(Bianco <i>et al.</i> , 1994)	TCO ₂	(Bianco <i>et al.</i> , 1994)
1	4.35 (1 H, dd, 12.0, 4.0) 4.15 (1 H, dd, 12.0, 3.0)	4.32 (1 H, dd, 12.0, 4.0) 4.16 (1 H, dd, 12.0, 3.0)	69.2	67.5
2	-	-	-	-
3	-	-	173.9	172.3
4	2.74 (1H, dd, 16.0, 8.0) 2.43 (1H, dd, 16.0, 4.0)	2.66 (1H, dd, 15.5, 7.5) 2.39 (1H, dd, 15.5, 4.0)	33.5	31.6
5	3.10 (1H, m)	2.95 (1H, m)	35.3	33.5
6	2.15 (1H, m) 1.43 (1H, ddd, 14.0, 11.0, 3.5)	2.06 (1H, ddd, 14.0, 8.0, 1.0) 1.43 (1H, ddd, 14.0, 11.0, 3.5)	42.8	40.6
7	4.20 (1 H, m)	4.15 (1 H, m)	74.9	74.4
8	1.89 (1 H, m)	1.94 (1 H, ddq, 4.0, 10.0, 8.0)	42.8	40.7
9	2.22 (1H, m, H-9)	2.16 (1H, m, H-9)	42.6	40.4
10	1.15 (1H, d, 7.5)	1.09 (1H, d, 8.0)	13.7	13.3

II.2.4 lipids

II.2.4.1. Characterization of TiS₁₅

TiS₁₅ was obtained as a white powder from the stem of *T. inconspicua*, in a mixture of CH₂Cl₂-MeOH (85:15). It is soluble in pyridine and DMSO.

From the spectroscopic data of TiS₁₅ such as HRESI-MS, HRESI-MSMS, NMR 1D and 2D (including ^1H , ^{13}C , COSY, HSQC and HMBC), its structure was determined to be that of a cerebroside:



Its molecular formula was established to be $C_{39}H_{77}NO_9$ based on its HRESI-MS (at m/z 705.5723 $[M+2H]^{2+}$ calcd for 705.5755), indicating two double bond equivalents.

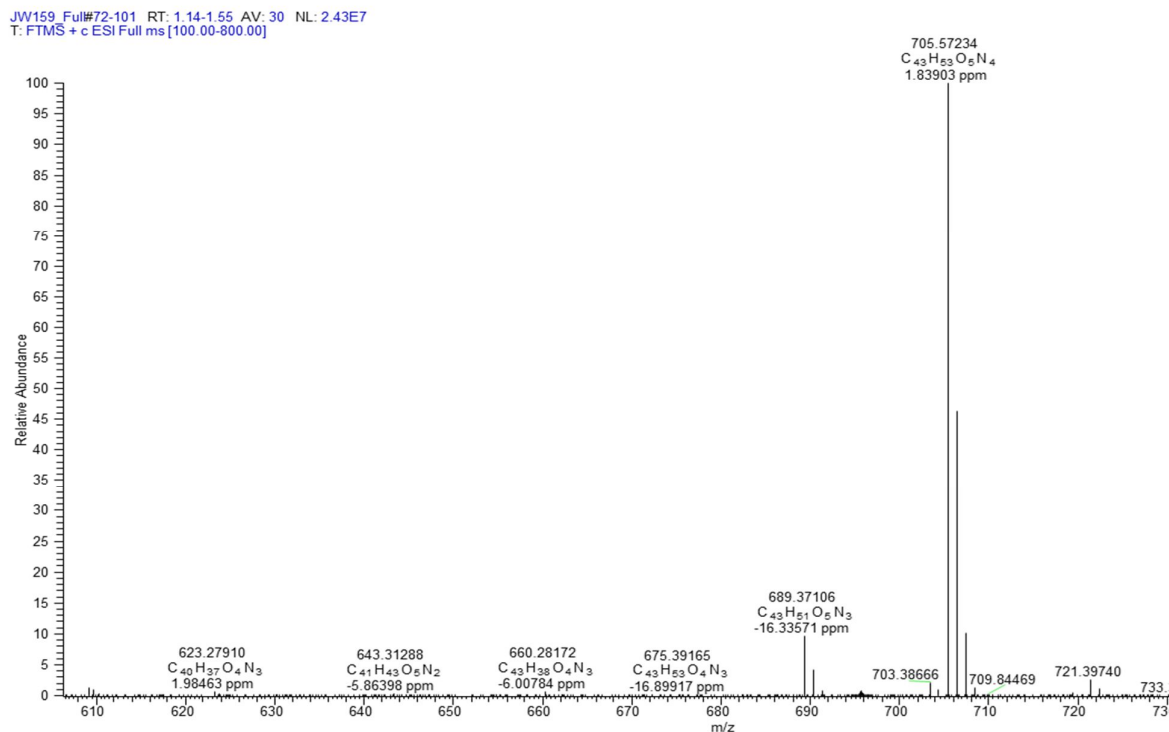


Figure 78: HRESI-MS of TiS_{15}

The 1H NMR spectrum of TiS_{15} (Figure 79) a group of proton signals δ_H 1.10–1.38 (m), 0.78 (6H, t, 5.9 Hz), which indicates that TiS_{15} might belong to the sphingolipid class of compounds. Its 1H NMR data suggests the glycolipid nature of the molecule with the anomeric proton at δ_H 4.13 (1H, d, 8.8 Hz). The characteristic signals of 2-amino-3-hydroxyl-1-ol of the hydrocarbon chain were observed at δ_H 3.98 (1H, m, H-2), 3.92 (1H, m, H-1); 3.53 (1H, m, H-1), and 3.33 (1H, m, H-3) and that of the 1'-carbonyl-2'-ol of the hydrocarbon chain was observed at δ_H 3.82 (1H, m, H-2').

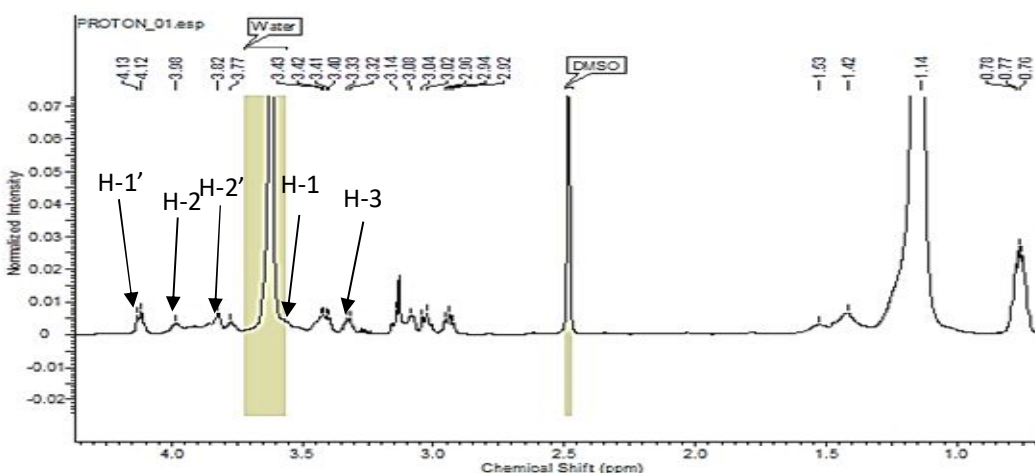


Figure 79: ^1H NMR spectrum (DMSO- d_6 , 600 MHz) of TiS $_{15}$

The ^{13}C NMR spectrum (Figure 80) reveals signals at δ_c 103.7, 77.0, 76.5, 73.7, 70.2 and 61.3 suggesting that the sugar in TiS $_{15}$ is of the β -D-glucopyranose form (Falk and Karlsson, 1979). The characteristic peaks of 2-amino-3-hydroxyl-1-ol of the hydrocarbon chain were observed at δ_c 50.3 (C-2), 61.3 (C-1) and 71.0 (C-3) and that of 1'-carbonyl-2'-ol of the hydrocarbon chain were observed at δ_c 174.8 (C-1) and 71.4 (C-2). The ^{13}C NMR spectrum shows signals of two terminal methyl groups in aliphatic hydrocarbon chains at δ_c 13.9.

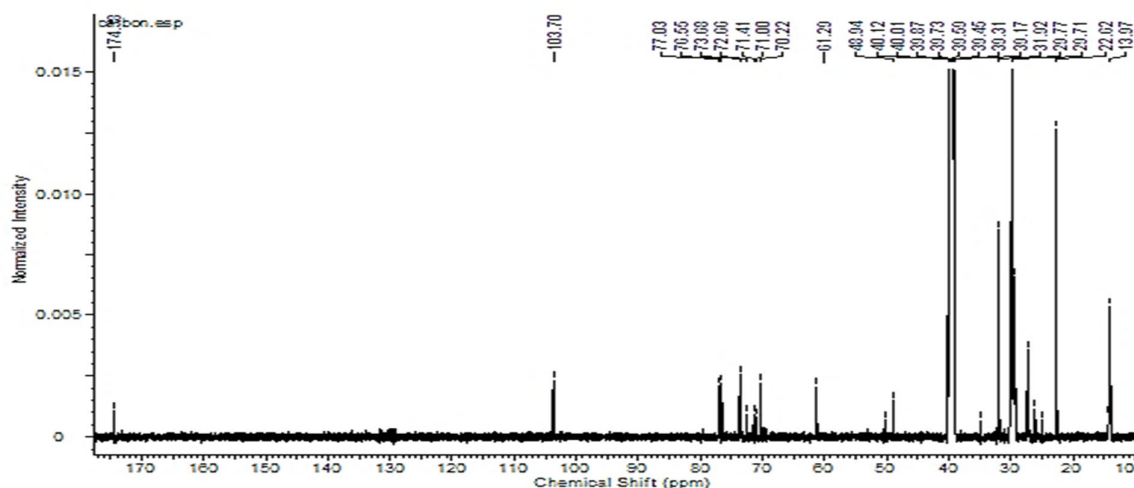


Figure 80: ^{13}C NMR spectrum (DMSO- d_6 , 150MHz) of TiS $_{15}$

Analysis of the 2D NMR spectra (^1H - ^1H COSY (Figure 78) and HMBC (Figure 81)) led to the assignment of proton and carbon signals for TiS $_{15}$. However, correlations were observed in the COSY spectrum between protons of the 2-amino-3-hydroxyl-1-ol of the

hydrocarbon chain H-1/ H-2, H-2/ H-3 and H-3/H-4. It also shows correlations of the 1'-carbonyl-2'-ol of the hydrocarbon chain between H-2' (δ_H 3.85) and H-3' (δ_H 1.42). The HMBC spectrum shows correlation arising from the anomeric proton at δ_H 4.14 and C-1 (δ_C 68.9). Furthermore, it shows correlations between H-2' and the carbonyl carbon (δ_C 174.3) and between H-1; H-3 and C-2.

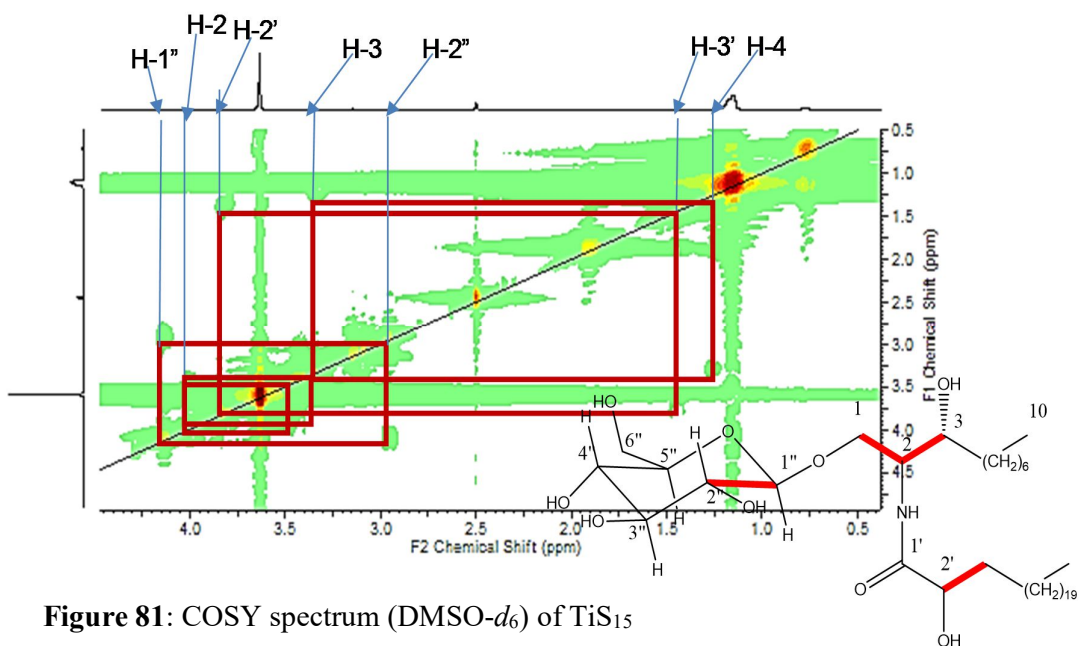


Figure 81: COSY spectrum (DMSO- d_6) of TiS₁₅

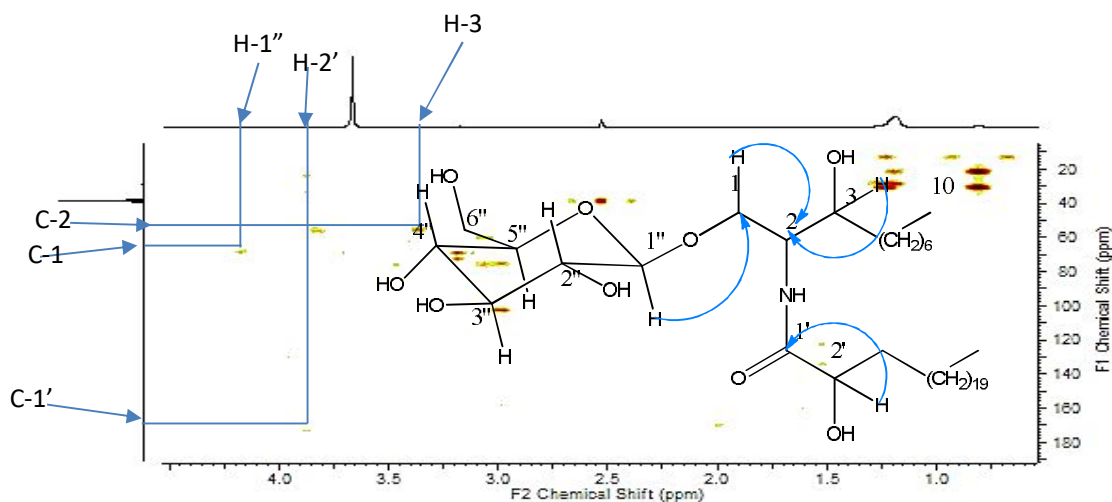


Figure 82: HMBC spectrum (DMSO- d_6) of TiS₁₅

Its ESI-MS/MS fragment analysis (Figure 83) shows one of the major fragments ions at m/z $[M + H]^+$ 369.2185 indicating that the 1'-carbonyl-2'-ol of the hydrocarbon chain the presence of a fatty chain of 19 carbon atoms.

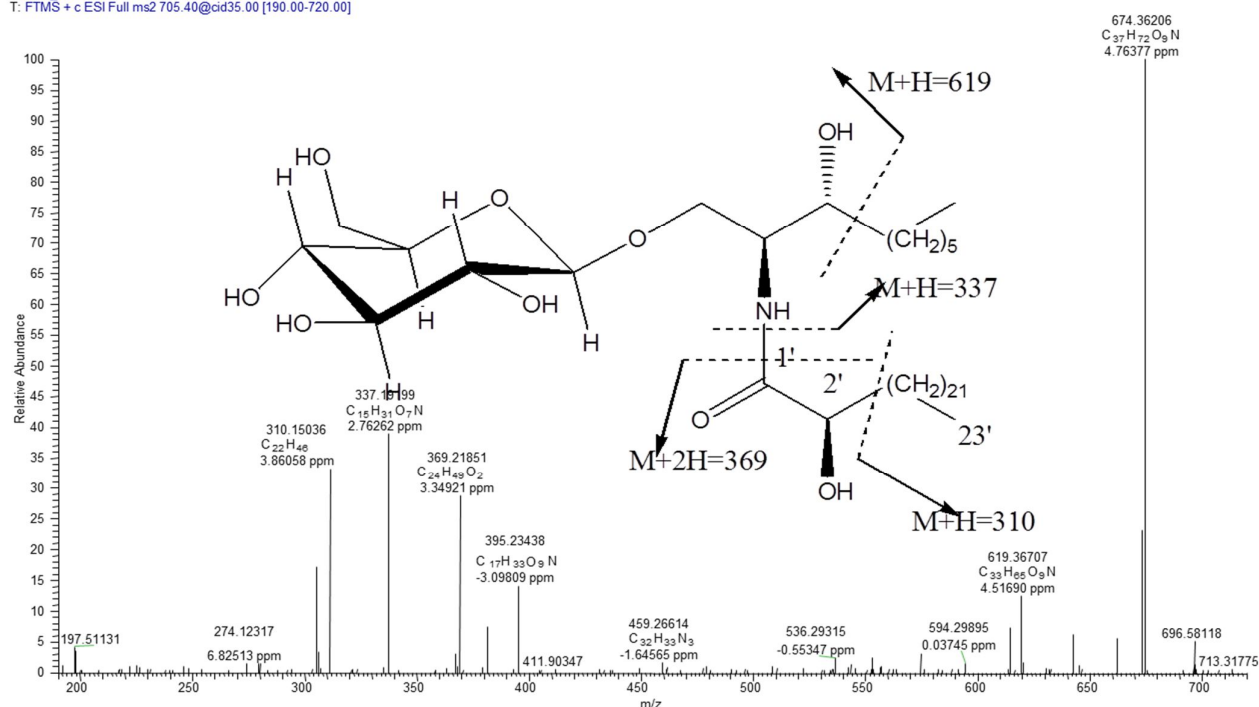


Figure 83: HRESI-MS/MS of compound TiS₁₅

It is reported that the absolute configurations of C-2 and C-3 in all sphingolipids isolated from natural plants were 2*S* and 3*R*, respectively (Hua and Pei, 2001), and the chemical shifts of C-2 (δ_c 50.3) and C-3 (δ_c 70.8) were very similar to those of ceramides, which have the same configuration (Kim *et al.*, 1997). Accordingly, the structure of TiS₁₅ was determined to be 1-*O*- β -D-glucopyranosyl-(2*S*,3*R*)-*N*-(2'-hydroxytricosanyl)-deca-sphinganine of which the name contortanoside (**89**) was given.

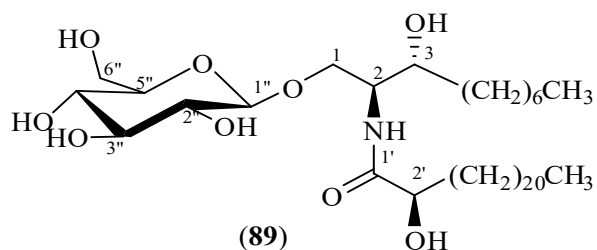


Table XXII: ¹³C and ¹H NMR data for TiS₁₅

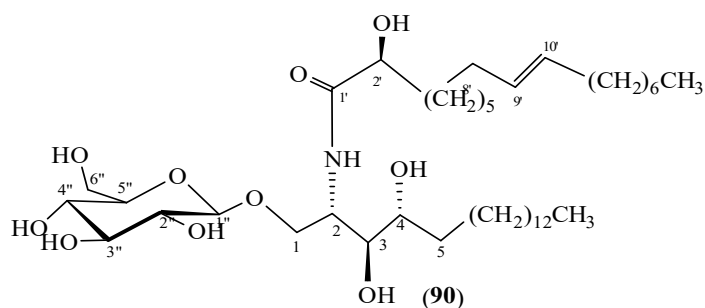
position	TiS	
	¹³ C	¹ H (nH, m, J)
1	69.4	3.92 (1H,m); 3.53 (1H,m)
2	50.3	4.01 (1H,m)
3	70.8	3.33 (1H, m)
4	24.9	1.24 (2H, m)
5-9, 4'-22'	22.9-29.8	1.12-1.31 (52H, brs)
10, 23'		0.78 (6H, t, 5.9)

1'	174.8	-
2'	71.2	3.82 (1H, m)
3'	26.0	1.42 (1H, m)
1''	103.5	4.13 (1H, d, 8.8)
2''	73.4	2.96 (1H, m)
3''	76.4	3.17 (1H, m)
4''	70.1	30.6 (1H, m)
5''	76.8	3.13 (1H, m)
6''	61.2	3.67 (1H, m); 3.45 (1H, m)

II.2.4.2.Characterisation of TCO₁₉

TCO₁₉ was obtained from the fruits of *Tabernaemontana contorta* as a white powder in a mixture of AE-MeOH (95:5). It is soluble in DMSO and pyridine.

From the spectroscopic data of TCO₁₉ such as HRESI-MS, NMR 1D (including ¹H, ¹³C), its structure was suggested to be that of a cerebroside:



Its molecular formula was determined to be C₄₁H₇₉NO₁₀ based on its HRESI-MS (at *m/z* 747.5817 [M+2H]²⁺ calcd for 747.5860), indicating two double bond equivalents.

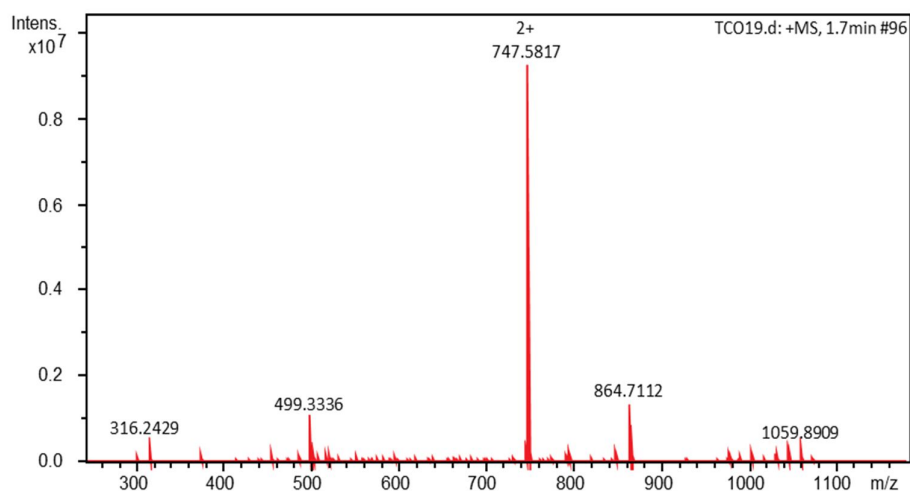


Figure 84: HRESI- MS of TCO₁₉

The ^1H NMR spectrum (Figure 85) of TCO_{19} is very similar to that of TiS_{15} with the main difference being the presence of a multiplet at δ_{H} 5.67 (2H, m) suggesting the presence of a double bond in the molecule.

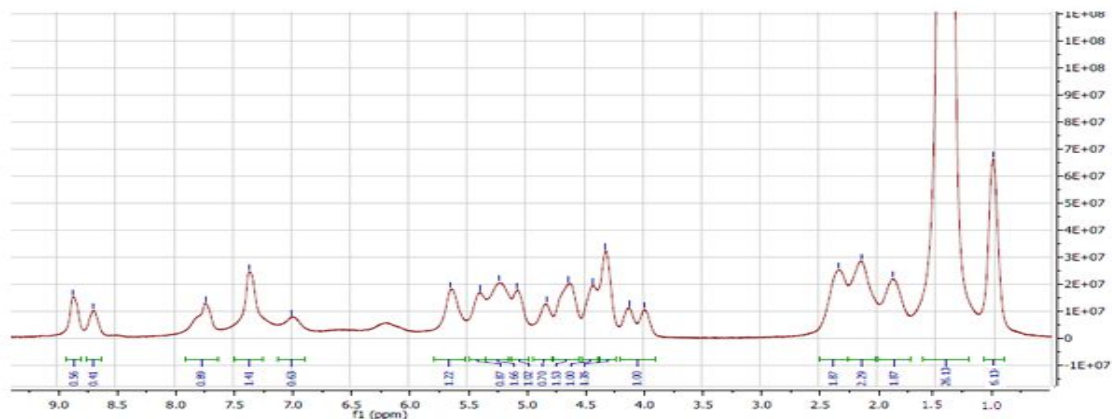


Figure 85: ^1H NMR spectrum (Pyridine- d_5 , 400 MHz) of TCO_{19}

The ^{13}C NMR spectrum (Figure 86) of TCO_{19} is also very similar to that of TiS_{15} with the main difference being a double bond at δ_{C} 131.5 and 131.6 confirming the suggestion above.

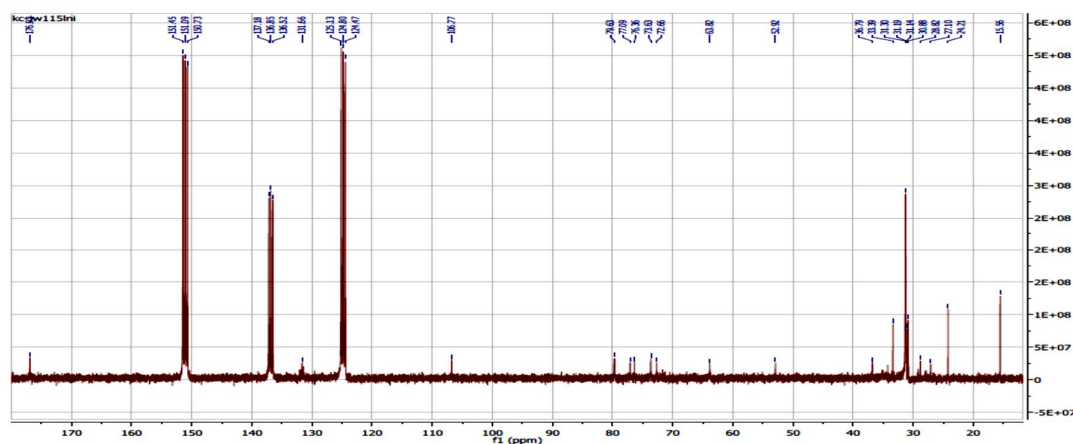
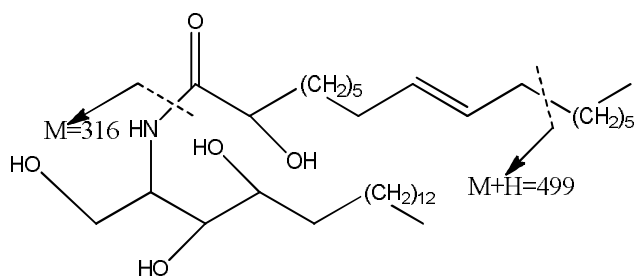
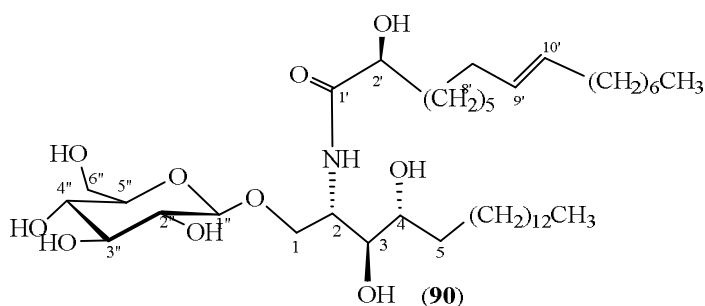


Figure 86: ^{13}C NMR spectrum ((Pyridine- d_5 , 100 MHz) of TCO_{19}

Its ESI-MS fragment analysis (Figure 84) shows one of the major fragment ions at m/z $[\text{M}]^+$ 316 indicating that the 2-amino-3,4-hydroxyl-1-ol hydrocarbon chain presents a fatty chain of 14 carbon atoms. The fragment at 499 indicates an allylic fragment confirming that the double bond is at position 9'.



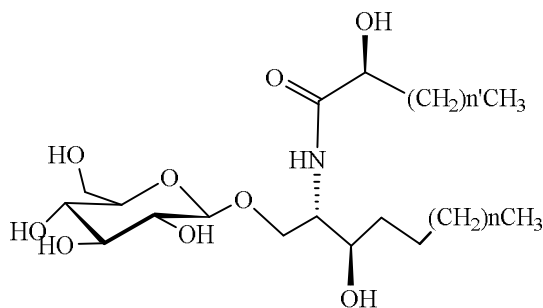
Based on spectral analysis, the structure of TCO₁₉ was suggested to be that of that of 1-*O*- β -D-glucopyranosyl-(2*S*,3*S*,4*R*)-*N*-(2-hydroxyheptadec-9-enoyl)-octadecasphegine. (**90**).



II.2.4.3. Characterisation of TCO₂₀

TCO₂₀ was obtained from the fruits of *T. contorta* as a white powder in a mixture of CH₂Cl₂-MeOH (85:15). It is soluble in DMSO and pyridine.

From the spectroscopic data of TCO₂₀ such as HRESIMS, NMR 1D (including ¹H, ¹³C), its structure was partially determined to be that of a cerebroside:



Its molecular formula was determined to be C₃₈H₇₁NO₁₀ based on its HRESI-MS (at *m/z* 703.5200 [M+2H]²⁺ calcd for 703.5234), indicating three double bond equivalents.

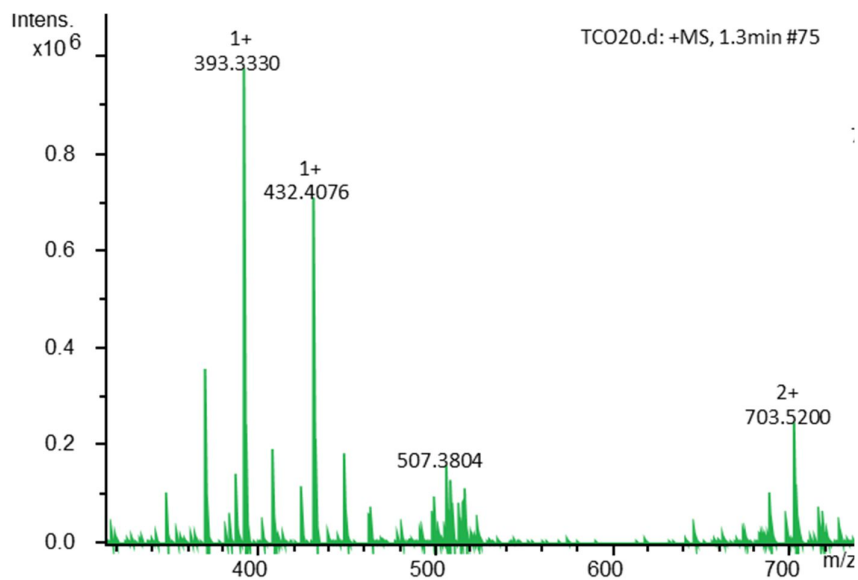


Figure 87: HRESI-MS of TCO₂₀

The ¹H NMR spectrum (Figure 88) of TCO₂₀ is also very similar to that of TiS₁₅. The difference is the presence of protons at δ c 6.12 (m) belonging to double bonds.

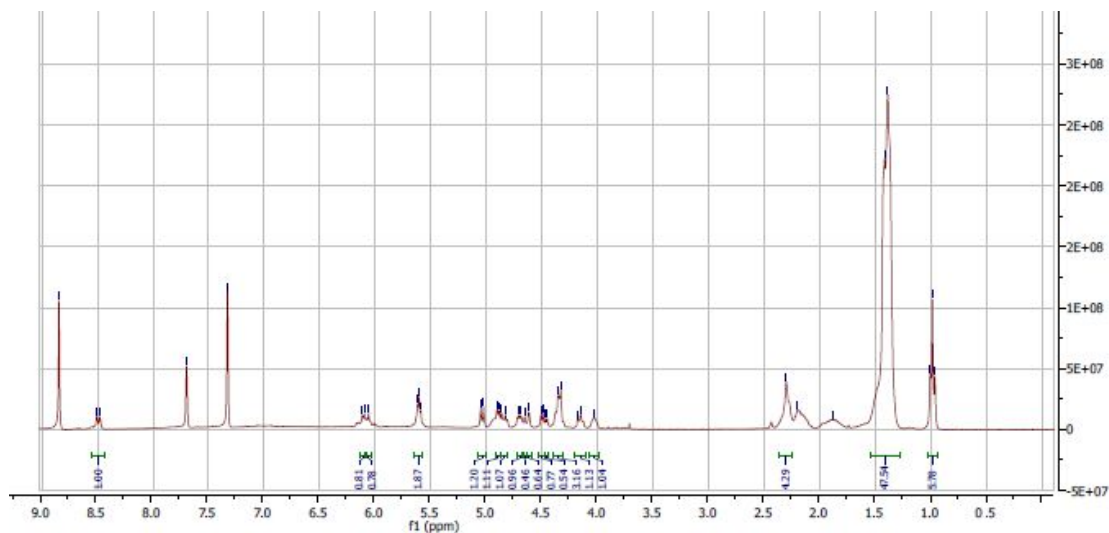


Figure 88: ¹H NMR spectrum (Pyridine-*d*₅, 400 MHz) of TCO₂₀

The ¹³C NMR spectrum (Figure 89) of TCO₂₀ is also like that of TiS₁₅ but the main difference is the appearance of two double bonds at δ c 130.3 and 130.5, 132.9 and 133.1.

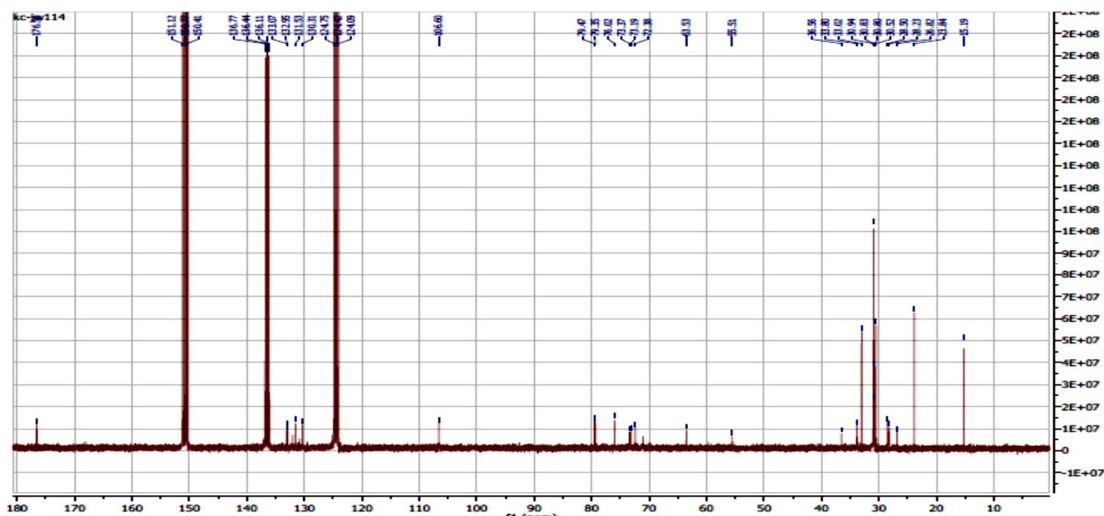
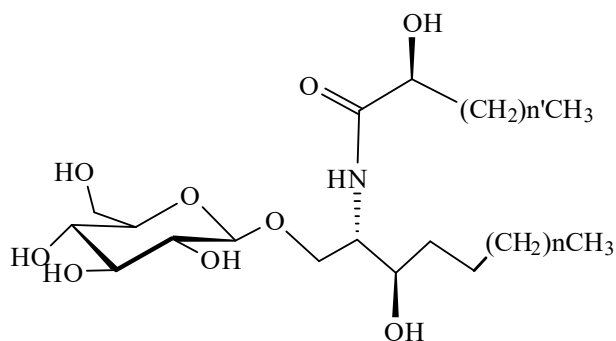


Figure 89: ^{13}C NMR spectrum (Pyridine- d_5 , 100 MHz) of TCO_{20}

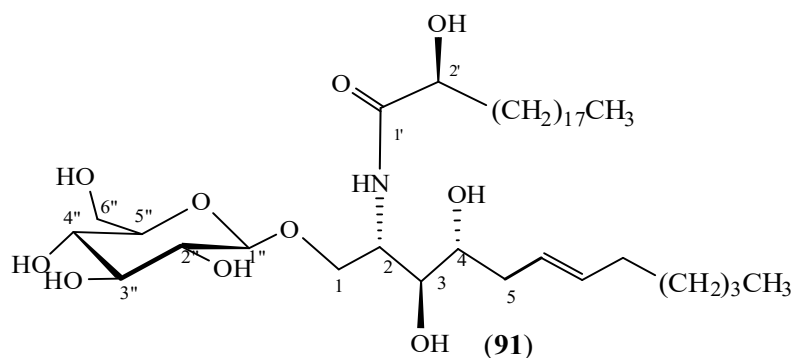
On the basis of spectral analysis, the structure of TCO_{20} was partially determined to be that of a phytocerebroside.



II.2.4.4 Characterisation of TC_{12}

TC_{12} was obtained from the stem-bark of *T. contorta* as a white powder in a mixture of CH_2Cl_2 -MeOH (96:4). It is soluble in DMSO and pyridine.

From the spectroscopic data of TC_{12} such as HRESI-MS, HRESIMSMS, NMR 1D (including ^1H , ^{13}C), its structure was suggested to be that of a ceramide:



Its molecular formula was determined to be $C_{32}H_{62}NO_5$ based on its HRESI-MS (at m/z 563.4548 $[M+Na]^+$ calcd for 563.4526), indicating two double bond equivalents.

JW168#496-519 RT: 7.69-8.04 AV: 24 NL: 5.54E6
F: FTMS + c ESI Full ms [100.00-2000.00]

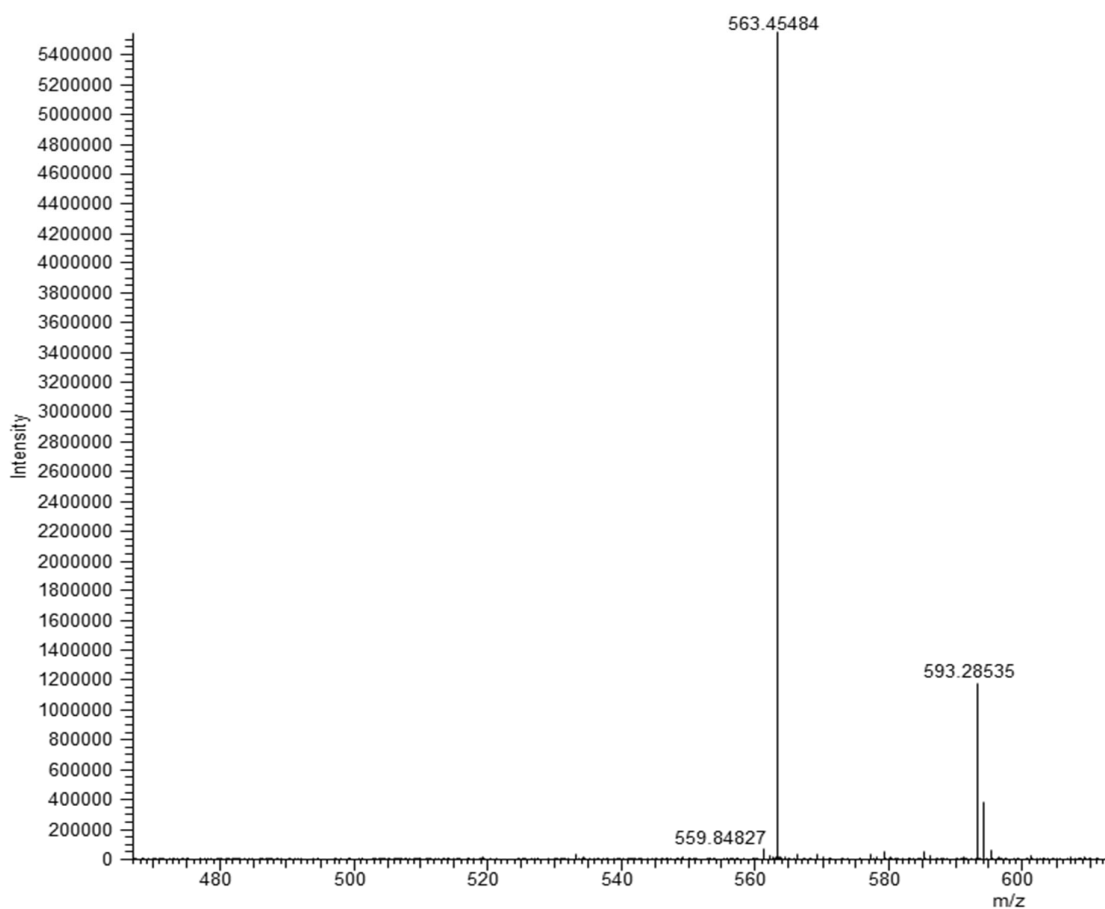


Figure 90: HRESI- MS of TC₁₂

The 1H NMR spectrum (Figure 91) of TC₁₂ reveals a group of proton signals between δ_H 1.15 and 1.35 (m) with a terminal methyl group at δ_H 0.88 (6H, t, 7.0 Hz), three oxymethines at δ_H 3.35 (1H, m), 3.37 (1H, m), 3.85 (1H, m); an oxymethylene at δ_H 3.53 (1H, m) and 3.58 (1H, m); four hydroxyl proton at δ_H 4.33 (d, 6.2 Hz), 4.58 (brs), 4.66 (d,

5.5 Hz), 5.49 (d, 7.7 Hz). This spectrum also reveals a doublet at 7.39 (d, 9.2 Hz) belonging to the NH group suggesting that TC₁₂ is a ceramide.

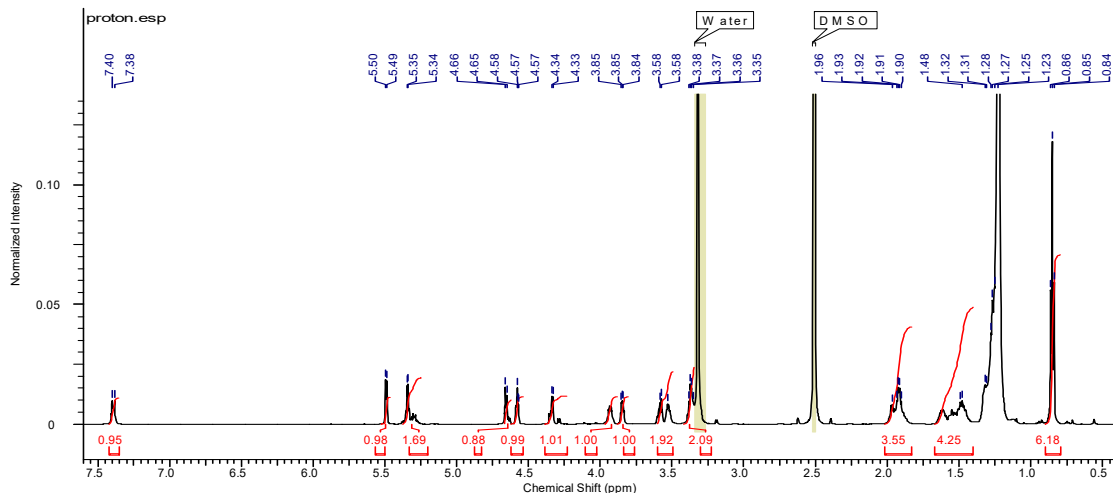


Figure 91: ¹H NMR spectrum (DMSO-*d*₆, 500 MHz) of TC₁₂

The ¹³C NMR spectrum (Figure 92) of TC₁₂ reveals characteristic signals of 2-amino-3,4-dihydroxyl-1-ol hydrocarbon chain at δ_c 51.5 (C-2), 60.9 (C-1), 71.4 (C-3) and 75.0 (C-4) those of 1'-carbonyl-2'-ol of the hydrocarbon chain were observed at δ_c 174.0 (C-1) and 71.5 (C-2) and two terminal methyl groups in aliphatic hydrocarbon chains at δ_c 14.3 confirming the ceramide nature of TC₁₂. In addition, it reveals a double bond at δ_c 130.1 and 130.6.

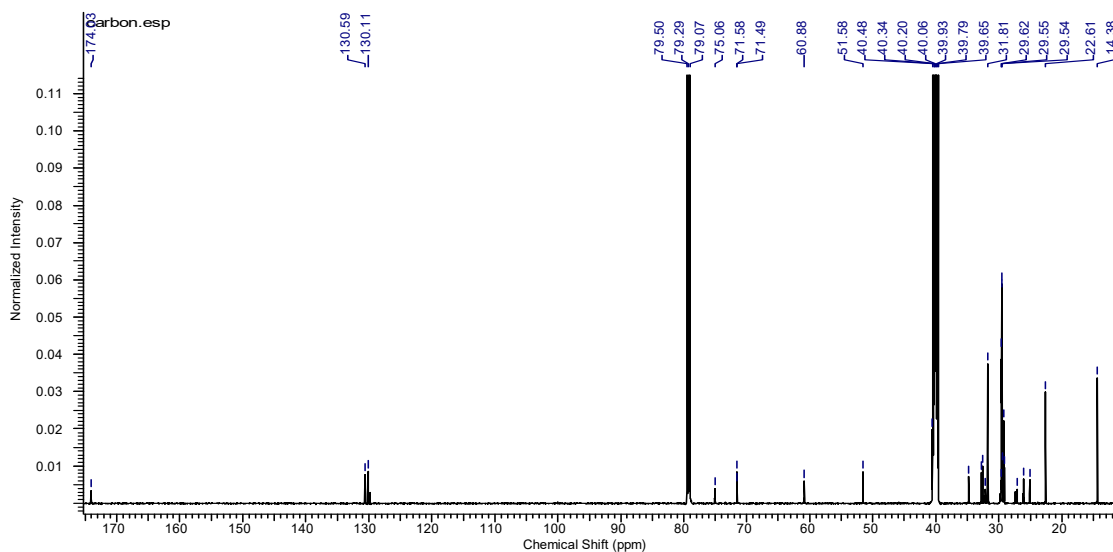


Figure 92: ¹³C NMR spectrum (DMSO-*d*₆, 125 MHz) of TC₁₂

Its ESI-MS/MS fragment analysis (Figure 93) shows one of the major fragments ions at m/z $[M]^+$ 326 indicating that the 1'-carbonyl-2'-ol hydrocarbon chain presents a fatty chain of 18 carbon atoms. The pic at 485 indicates an allylic fragment confirming that the double bond is at position 6.

JW168#573-613 RT: 7.70-8.22 AV: 41 NL: 1.29E4
T: FTMS + c ESI Full ms2 563.30@cid35.00 [155.00-570.00]

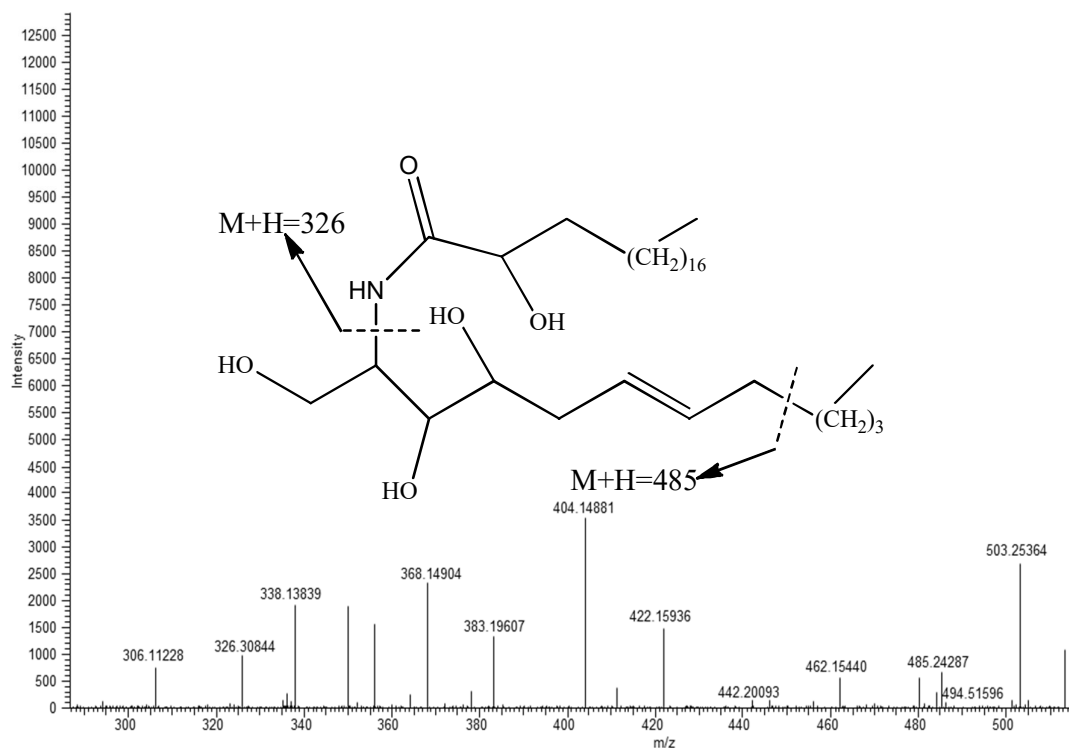
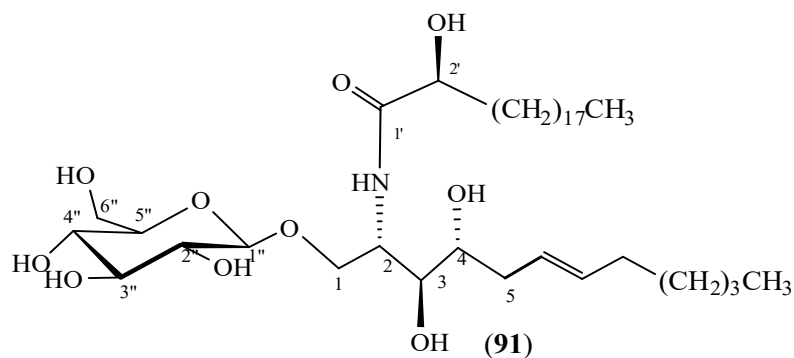


Figure 93: HRESI- MS/MS of TC₁₂

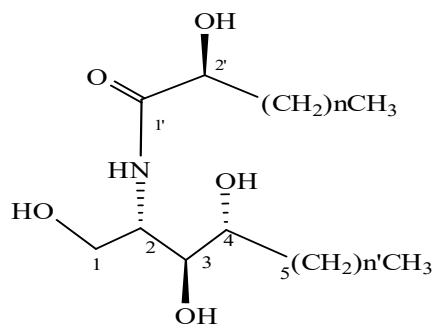
On the basis of spectral analysis the structure of TC₁₂ was suggested to be that of (R)-2-hydroxy-N-((2S,3S,4R,6E)-1,3,4-trihydroxydodec-6-en-2-yl)icosanamide (**91**).



II.2.4.5.Characterisation of TCO₁₄

TCO₁₄ was obtained from the fruits of *T. contorta* as a white powder in a mixture of CH₂Cl₂-MeOH (86:14). It is soluble in pyridine and responds positively to the nitrogene test.

From the spectroscopic data of TCO₁₅ such as HRESI MS, NMR 1D (including ¹H, ¹³C), its structure was partially determined to be that of a ceramide:



Its molecular formula was determined on the basis of interpretation of NMR spectra to be C₄₄H₈₉NO₅ indicating one double bond equivalent.

The ¹H NMR (Figure 94) spectrum of TCO₁₄ is similar to that of TC₁₂.

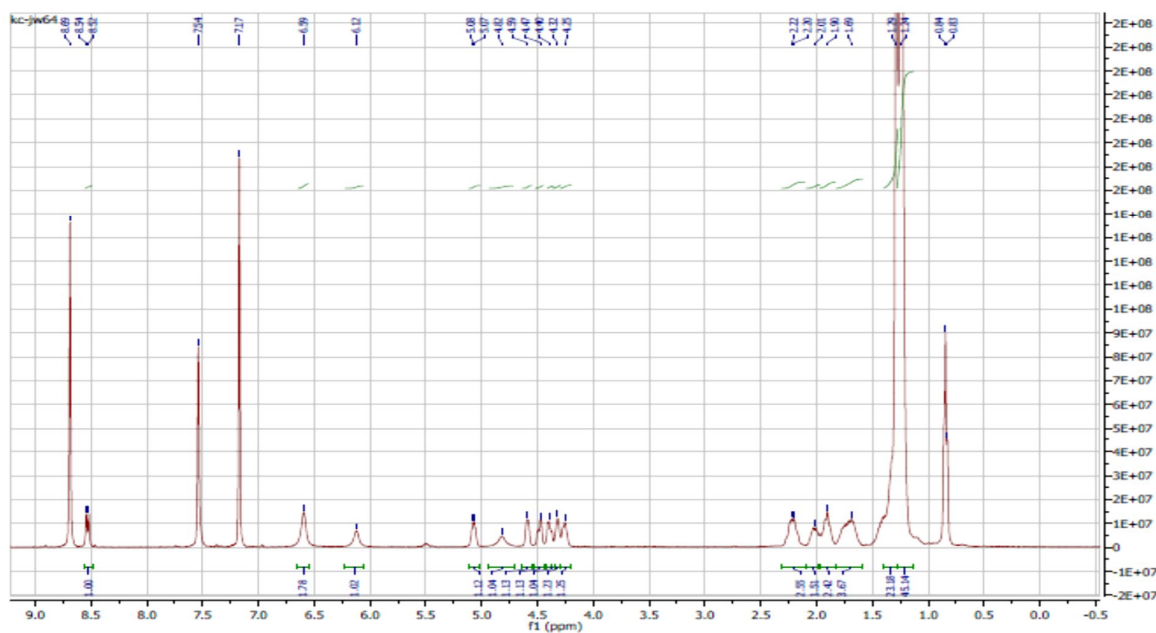


Figure 94: ¹H NMR spectrum (Pyridine-*d*₅, 400 MHz) of TCO₁₄

The ¹³C NMR spectrum (Figure 95) of TCO₁₄ is also like that of TC₁₂ with the difference being the absence of a double bond.

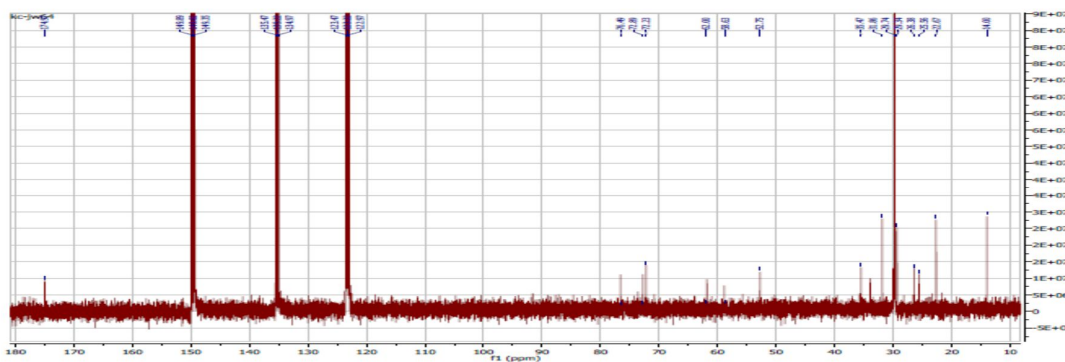
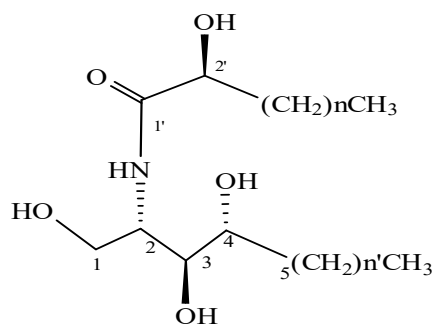


Figure 95: ^{13}C NMR spectrum (Pyridine- d_5 , 100 MHz) of TCO_{14}

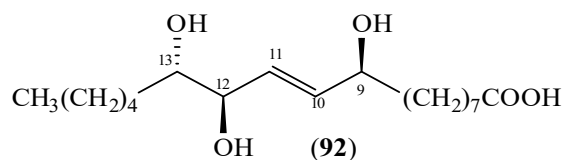
On the basis of spectral analysis, the structure of TCO_{14} was partially determined to be that of a phytoceramide.



II.2.4.6. Identification of $\text{TiS}_{13} = \text{TC}_7$

TiS_{13} was obtained from fruits of *T. contorta* and stem-bark of *T. inconspicua* as a gummy white solid in a mixture of Hex/AE 10/90. It is soluble in MeOH.

From the spectroscopic data of TiS_{13} such as ^1H and ^{13}C NMR, compared to published data, its structure was identified to be that of a fatty acid:



Its molecular formula was determined based on the interpretation of its NMR spectra to be $\text{C}_{18}\text{H}_{34}\text{O}_5$ being indicative of two double bond equivalents.

Its ^1H NMR spectrum (Figure 96) reveals a triplet at δ_{H} 0.91 (3H, 7.4 Hz, H-18) and a large singlet at δ_{H} 1.34 integrating for fourteen protons showing the presence of a hydrocarbon chain of about seven methylenes in the molecule. In addition, it reveals three

oxymethines at δ_{H} 3.41 (1H, brs, H-12), 3.90 (1H, t, 5.6 Hz, H-9), 4.05 (1H, q, 5.9 Hz, H-13) and two olefinic protons at δ_{H} 5.68 (1H, dd, 15.9; 5.6 Hz, H-10) and 5.70 (1H, dd, 15.9; 5.6 Hz, H-11).

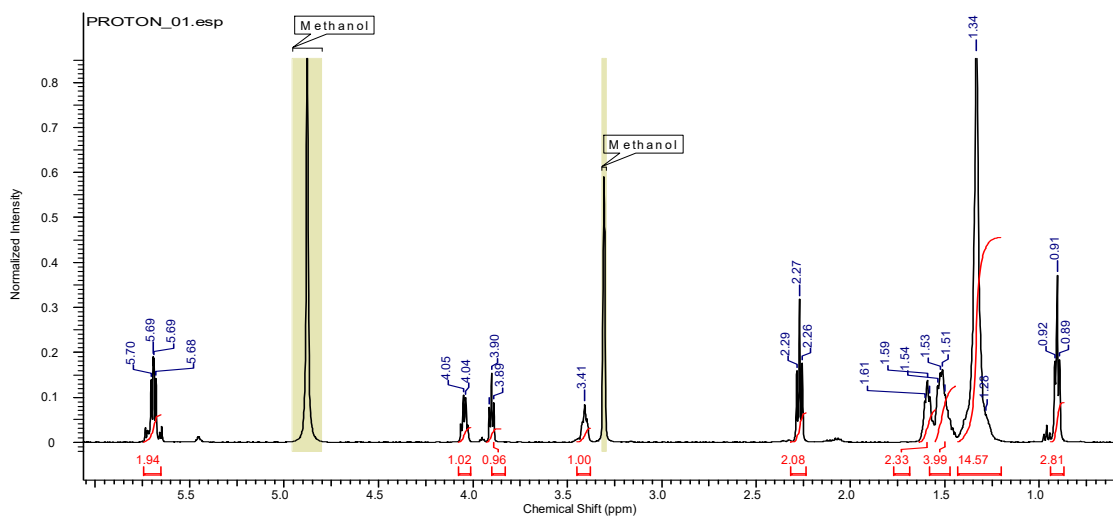


Figure 96: ^1H NMR spectrum (MeOD, 500MHz) of TiS_{13}

Its ^{13}C NMR spectrum (Figure 97) reveals eighteen carbon signals including an acid carbonyl signal at δ_{C} 176.7, two olefinic carbons at δ_{C} 129.6 and 135.1 and three oxymethines at δ_{C} 71.6, 74.3, 75.1.

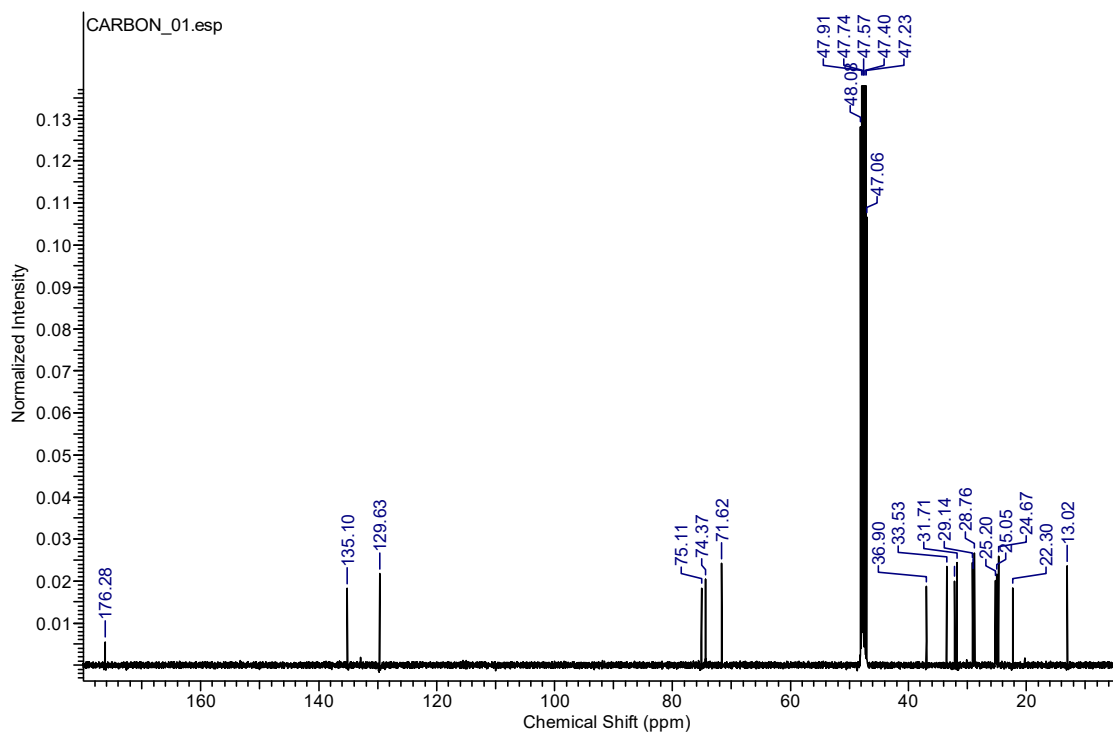


Figure 97: ^{13}C NMR spectrum (MeOD, 125 MHz) of TiS_{13}

Based on the spectral analysis and by comparison of its spectral data to those described in the literature (Choi *et al.*, 2012), the structure of TiS₁₃ was identified to be that of 9,12,13-trihydroxy-10(E)-octadecenoic acid commonly known as pinellic acid (**92**).

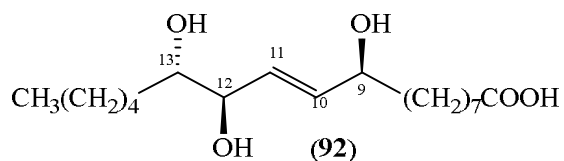


Table XXIII: ¹³C NMR (MeOD) data for TiS₁₃ compared to the literature (Choi *et al.*, 2012)

Position	¹³ C (ppm) of TS ₁₂	(Choi <i>et al.</i> , 2012)
1	176.3	177.9
2	33.5	35.1
3	25.1	26.2
4	28.5	29.9
5	28.9	30.1
6	29.1	30.3
7	25.2	26.3
8	36.9	38.8
9	71.6	72.7
10	129.6	130.4
11	135.1	136.4
12	75.1	76.2
13	74.4	75.5
14	32.1	33.2
15	24.6	25.9
16	31.7	32.8
17	22.4	23.5
18	13.0	14.3

II.2.4.7. Identification of TC₁

TC₁ was obtained from the stem-bark of *T. contorta* as a white powder in a mixture of Hex/AE 95/05. It is soluble in CHCl₃.

On the basis of spectral analysis, its molecular formula was determined to be C₂₅H₅₀O₂ indicating one double bond equivalents.

Its proton NMR spectrum (Figure 98) shows a triplet at δ_H 0.81 (6.0 Hz), attributable to a terminal methyl group which is linked to a methylene, another triplet at δ_H 2.28 (7.0 Hz) attributable to another methylene adjacent to a carbonyl group.

This spectrum also shows an intense pic integrating for forty-two protons at δ_H 1.30 indicating the presence of about twenty-one methylenes in a long hydrocarbon chain.

The ^{13}C NMR (Figure 99) spectrum reveals the presence of an acid carbonyl signal at δ_C 178.4.

Based on spectroscopic analysis and by comparison with the literature (Xian *et al.*, 2010), the structure of TC₁ was identified to be that of pentacosanoic acid (**93**) commonly known as hyenic acid.

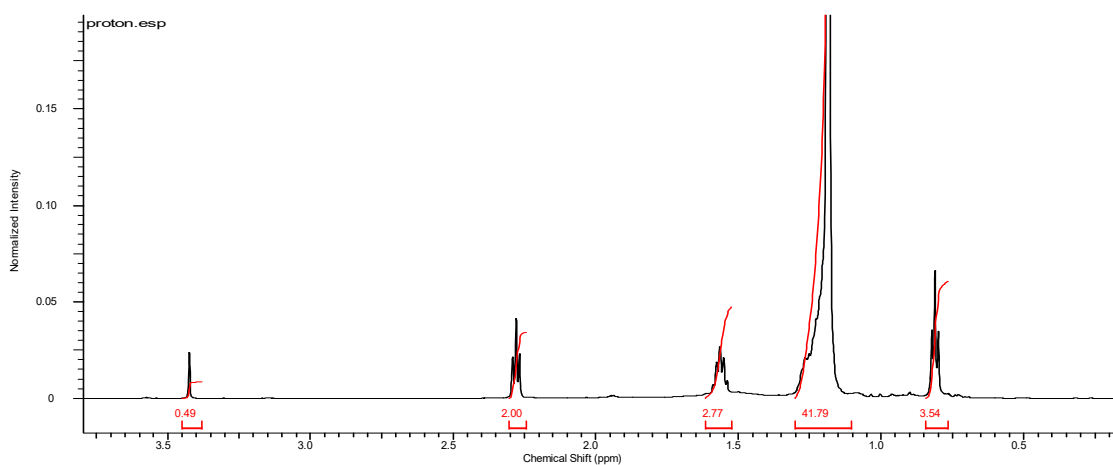
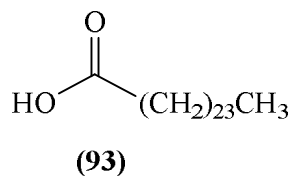


Figure 98: 1H NMR spectrum ($CDCl_3$, 500 MHz) of TC₁

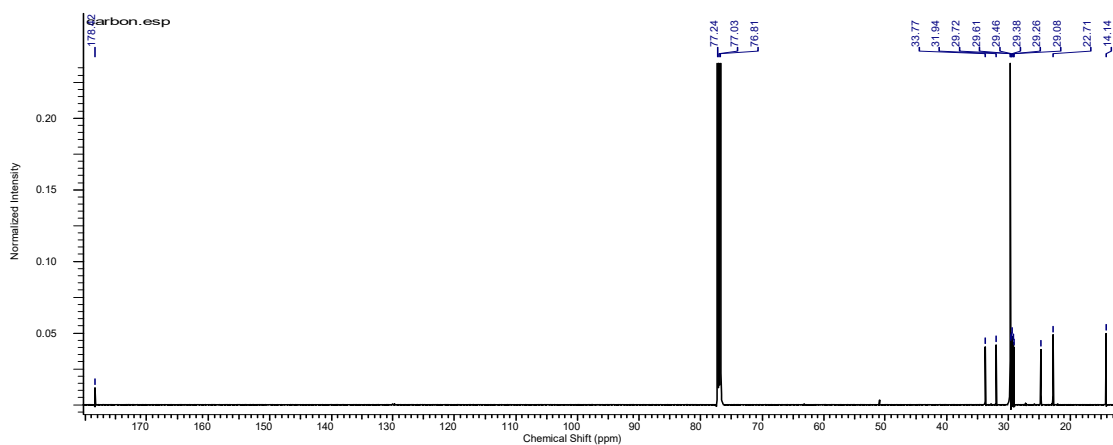


Figure 99: ^{13}C NMR spectrum ($CDCl_3$, 125 MHz) of TC₁

II.3. BIOLOGICAL TESTS ON SOME ISOLATED COMPOUNDS

II.3.1. Anticancer effect

Compounds TCO₈, TiS₅, TiS₃, TiS₁₃, TiS₈, TC₁, TCO₂ and TC₅ were tested for their anticancer effects on human breast cancer MDA-MB 231 cells. Figure 100 shows a plot the cell viability in percentage DMSO against concentration of all the compounds. TiS₅ reveals to be the most cytotoxic. For that reason, its cytotoxic effect on these same cells was measured over time (24 and 48 hours). The results (Figure 98) show that this compound is more cytotoxic when treated for 48h ($IC_{50} 2.19 \pm 0.15 \mu M$) than 24h ($IC_{50} 3.35 \pm 0.50 \mu M$). We also observed that the cell viability of breast cancer cells decreased as the concentration of the compound increases. These results indicate that TiS₅ inhibited the cell growth in both a concentration and time-dependent manner, and it therefore suggested that this compound can be used as a chemotherapeutic agent since it was found to be more effective overtime exposure.

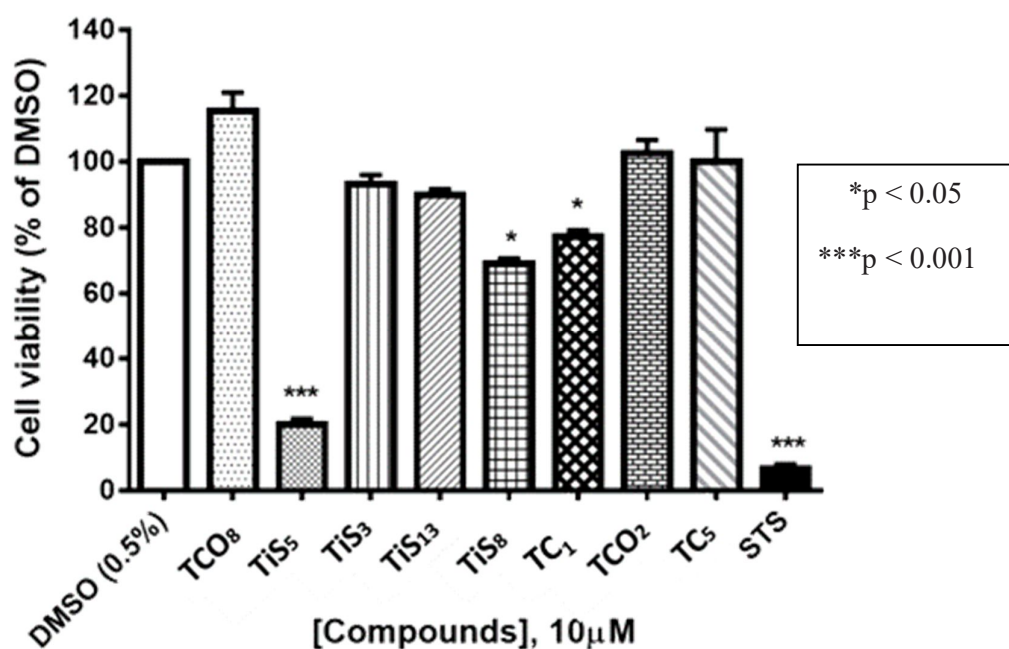


Figure 100: Anti cancer effect of some isolated compounds on human breast cancer MDA-MB 231 cells

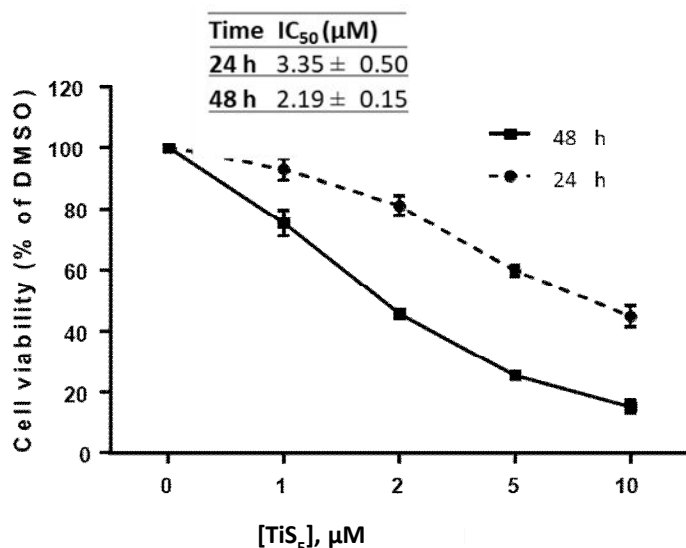


Figure 101: Anticancer effect of TiS₅ on human breast cancer MDA-MB 231 cells

II.3.2. Anti-inflammatory assay

Compounds TCO₅ (compound 1) and TCO₃ (compound 2) were evaluated for their ability to inhibit nitric oxide (NO) production in lipopolysaccharide-stimulated RAW264.7 macrophage cells, but did not exhibit significant NO inhibitory activity (Figure 102A). The cell viability was also determined using Cell Counting Kit-8 (CCK-8) and we found that compound TCO₅ significantly ($p < 0.05$) increased the proliferation of RAW 264 cells as compared to cells treated with LPS and DMSO used as solvent (Figure 102B). This increase in cell proliferation also correlates with the increased level of NO released by LPS-stimulated RAW 264.7 cells treated with compound TCO₅.

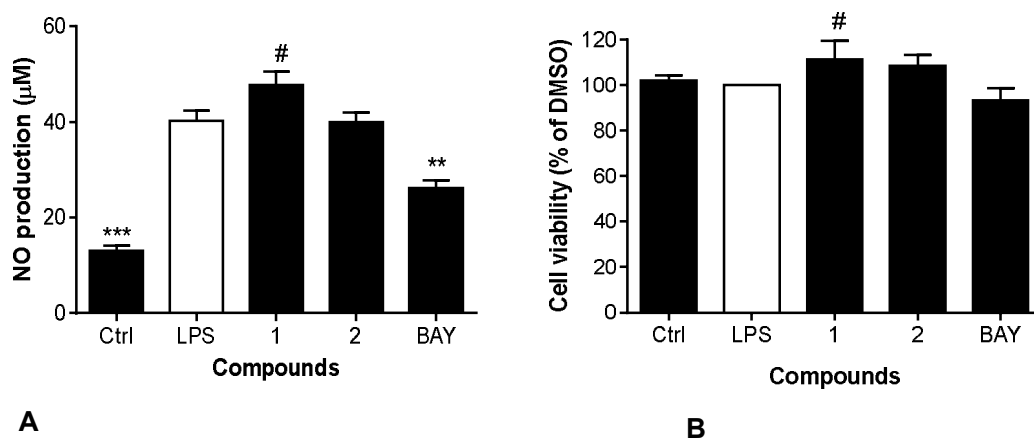


Figure 102: Effect of compounds on nitric oxide inhibitory activity (A) on lipopolysaccharide (LPS)-stimulated RAW 264.7 cells and their cell viability (B).

CONCLUSION AND PERSPECTIVES

This work led to the isolation of twenty compounds from the fruits of *T. contorta*, eighteen from the stem bark of *T. contorta* and fifteen from the stem of *T. inconspicua*. A total of twenty-eight compounds were isolated and twenty-six of them characterized and classified as nine alkaloids including three new derivatives (aparine-21-one (**74**), 5,6-dioxo-11-methoxy voacangine (**76**) and 5,6-dioxo-11-hydroxy voacangine (**77**)) and six known (ibogamine-16-carboxy-17,20-didehydro-5,6-dioxo-10-methoxymethyl ester (**75**), voacangine (**22**), perakine (**78**), tetrahydroalstonine (**12**), asperphenamate (**79**), patriscabratine (**80**)); eight triterpenoids with one new derivative (contortolic acid (**81**)) and seven known (usolic acid (**65**), 3-methoxy ursolic acid (**82**), asiatic acid (**83**), cordepressenic acid (**84**), baurenyl acetate (**68**), lupeol (**57**), butelinic acid (**59**)); 1 known monoterpene (isoboonein (**88**)); three steroids (stigmasterol (**85**), (24 R)-sito-5-ene-3-*O*- β -D-glucopyranoside (**86**) and stigmasterol 3-*O*- β -D-glucopyranoside (**87**)) and five lipids with one new cerebroside (contortanoside (**89**)) and six others (1-*O*- β -D-glucopyranosyl-(2S,3S,4R)-*N*-(2-hydroxyheptadec-9-enoyl)-octadecasphingene (**90**), (2R)-2-hydroxy-*N*-((2S,3S,4R,6E)-1,3,4-trihydroxydodec-6-en-2-yl)icosanamide (**92**), pinellic acid (**94**) and pentacosanoic acid (**95**)).

Aparine-21-one (**74**) and 5,6-dioxo-11-methoxy voacangine (**76**) were tested on lipopolysaccharide (LPS)-stimulated RAW 264.7 macrophage cells to determine their inhibitory effect on nitric oxide (NO) production and no significant inhibitory activity was found. Meanwhile, compound (5,6-dicarboxo-11-methoxy voacangine (**76**)) slightly increased the proliferation of RAW 264.7 cells which correlates well with the increased level of NO released by these cells.

The anticancer effect of pinellic acid (**92**), pentacosanoic acid (**93**), isoboonein (**88**), perakine (**78**), 5,6-dioxo-11-hydroxy voacangine (**77**), patriscabratine (**80**), asiatic acid (**83**) and 3-methoxy ursolic acid (**82**), was carried on human breast cancer MDA-MB 231 cells and 5,6-dioxo-11-hydroxy voacangine (**77**) showed a significant activity. This compound inhibited the cell growth in both a concentration and time-dependent manner, and it therefore suggested that this compound can be used as a chemotherapeutic agent since it was found to be more effective overtime exposure.

In order to complete this work, we hope in the future to characterize and test the rest of compounds, further our tests on 5,6-dioxo-11-hydroxy voacangine (**77**) which could be used as a chemotherapeutic agent. We also hope to extend our study to other parts of these

plans as well as other plants of the genus *Tabernaemontana*, to carry out other tests such as antibacterial, antiplasmodial, antifungi tests, for which plants of the the genus *Tabernaemontana* were active, on the crude extract and isolated compounds. We will carry out chemical transformations on the isolated compounds which may improve their activity.

We will now explain the procedures we followed to obtain the results given above.

CHAPTER III. GENERAL EXPERIMENT

III.1. GENERAL EXPERIMENTAL PROCEDURES

Masses were measured using Mettler 472 or Sartorius microbalance.

Mass spectra were registered on a micromass A-F instrument on a Nermag R10-10C spectrometer and the HP-5937 mass selective detector. EI (20 ev and 70 ev) with direct inlet. FAB+ with glycerol as matrix. NMR spectra were recorded using from 400 or 800 MHz Varian Gemini instrument and an NMR-Spectrospin Bruker AC from 400 or Advance 800. All spectra were recorded in CDCl₃, pyridine-*d*₅, MeOD or DMSO-*d*₆ as solvent unless otherwise stated. Tetramethyl silane was used as internal standard.

Micropipettes and glass columns ranging from 1 to 4 cm in diameter were used for column chromatography. Silica gel 60 (240-400 mesh), 60H (5-40 μm), 60 AC (20-45 μm), 60 AC (35-70 μm) were used as solid phase. Elution (gradient or isocratic) was allowed to proceed via gravity or under atmospheric pressure. The development of column chromatography and chemical reactions, were monitored by thin layer chromatography on pre-coated aluminium and glass sheets [Si gel 60 F254, 0.25 mm (Merck, Darmstadt, Germany)]. Compound spots were detected with UV light (254 and 365 nm, Spectroline Model ENF-240 CFE0) and/or by spraying with vanillin/sulphuric acid reagent, followed by heating at 150 °C. Fractions were bulked according to their retention factors. Eluents included hexane, ethyl acetate, dichloromethane and methanol in varying proportions depending on the polarity of the compounds involved.

III.2. CHARACTERISTIC ANALYTICAL TESTS

Phytochemical screening was realised by characteristic tests. About 25 mg of crude extracts were dissolved in 12 ml of CHCl₃. Portions of 5 ml were used for each test. For the isolated compounds, a pinch was dissolved in about 1 ml and similarly tested.

Liebermann-Burchard's Test

Objective: Identification of triterpenes and sterols

Reagents: Chloroform, acetic anhydride, concentrated sulphuric acid (50 ml/20 ml/1 ml).

To a chloroform solution of the sample to be analysed, a few drops of acetic anhydride is added, followed by concentrated sulphuric acid. Triterpenes and their saponins change colours from brick red, through purple, then blue and finally to green. Sterols give a blue colour that rapidly changes to green.

Molish's Test

Objective: Identification of sugars.

Reagents: Ethanol, α -naphthol, concentrated sulphuric acid.

In a test tube, the sample is dissolved in a solution of 1% ethanol in naphthol. Add a few drops of concentrated sulphuric acid, letting it flow down the side of the tube. The appearance of a purple-red ring at the interface, between the liquids indicates the presence of a sugar.

Ferric Chloride Test

Objective: Identification of phenols

Reagents: Iron (III) chloride, methanol

A few drops of Iron (III) chloride are added to an alcoholic solution of the compound. Phenols manifest a colour change from yellow to purple.

Meyer and Draggendorf's test

Objective: identification of alkaloids

Reagents: HCl, Meyer's reagent (potassiomercuric iodide solution) and Draggendorf's reagent (potassium tetraiodobismate)

To a test tube containing 8ml of extract, add 2ml of HCl (2%). Separate the mixture into two test tubes. To one, add 3 drops of Meyer's reagent and observe a yellowish white precipitate and to the other, add 2 drops of Draggendorf's reagent and observe brown-red precipitate.

III.3. MATERIALS

III.3.1. Plant material

The different parts of *T. contorta* (fruits and stem-bark) and *T. inconspicua* (stem) were collected in December 2013 at mount Elounden and Kalla respectively, locations of the

central region of Cameroon. These plants were identified by Mr NANA Victor (identification numbers NHC 45445 and NHC 61026 respectively).

III.4. EXTRACTION AND ISOLATION OF COMPOUNDS

III.4.1. Extraction

The air-dried and ground visible parts *T. contorta* (1000 g of fruits and 2000 g of stem-bark) and *T. inconspicua* (1200 g of stem) were macerated in a mixture of CH₂Cl₂/MeOH (1/1, 15 l) each for 48 h×3. After concentration at normal pressure using a rotary evaporator, total masses of 200 g, 176 g, and 180 g of crude extracts were obtained respectively.

III.4.2. Isolation

A part of the three extracts of *T. contorta* (180 g of fruits and 150 g of stem-bark) and *T. inconspicua* (90 g of stem) was fractionated in a chromatographic column using silica gel 60 (240-400 mesh, 500 g), at normal pressure, using a mixture of hexane-ethyl acetate and ethyl acetate-methanol in increasing polarity. The obtained fractions were concentrated and grouped according to their TLC profiles in 5 series A-F each as presented in the tables 24, 28 and 32.

Table XXIV: Chromatogram of the crud extract of the fruits of *T. contorta*

Eluent	Fraction	TLC	Series	Observation
Hex 100%	1-5	Hex	A	A mixture of at least 9 compounds including a white precipitate
Hex/AE 90/10	6-10			
Hex/AE 80/20	11-15	Hex/AE 90/10	B	A mixture of at least 6 compounds
Hex/AE 70/30	16-20			
Hex/AE 60/40	21-24			
Hex/AE 50/50	25-30	Hex/AE 50/50	C	A mixture of at least 6 compounds
Hex/AE 40/60	31-34			
Hex/AE 30/70	35-40			
Hex/AE 20/80	41-44			
Hex/AE 10/90	45-50			
AE 100%	51-54	AE/MeOH 95/5	D	A mixture of at least 4 compounds
AE/MeOH 90/10	55-60			
AE/MeOH 80/20	61-64			

AE/MeOH 70/30	65-70	AE/MeOH 90/10	E	Mixture of 2 compounds at least + tailing
---------------	-------	------------------	---	--

The different Fractions were allowed to rest for a few days after which:

- a precipitate in the form of white needles was observed in fractions 6-9. It was washed with hexane and indexed TCO₁;
- a precipitate in the form of white powder was observed in fractions 18-20, washed using a mixture of Hex/AE and indexed TCO₄;
- fractions 24, 38, 54 and 60 precipitated in the form of white powder, was washed using Hex/AE and indexed TCO₄, TCO₁₅, TCO₁₆, TCO₁₉.

Treatment of Series B

Series B was further chromatographed on silica gel (120 g) column using a mixture of *n*-hexane-EtOAc of increasing polarity. Fractions of 100 ml were collected, concentrated and grouped according to their TLC profiles in 3 sub-fractions, as presented in the following table.

Table XXV: Chromatogram of series B

Eluent	Fraction	TLC	Series	Observation
hexane	1-5	Hex/EA 95/05	1	Yellow oil containing TCO ₃
Hex/EA 95/05	6-11			
Hex/EA 90/10	12-17	Hex/EA 85/15	2	A mixture of, TCO ₅ and TCO ₆
Hex/EA 85/15	18-28			
Hex/EA 80/20	29-39	Hex/EA 75/35		
Hex/EA 75/35	40-47		3	A mixture of TCO ₇ , TCO ₈ and tailings
Hex/EA 70/30	48	CH ₂ Cl ₂		

Subfraction B1 was separated by column chromatography (CC) using *n*-hexane-EtOAc (95/15) as an eluent, to obtain compound TCO₃. B2 was separated by CC eluted with an isocratic system of MeOH-CH₂Cl₂ (2/98) to obtain TCO₅ and TCO₆. B3 was separated by CC eluted using *n*-hexane-EtOAc (72/38) to obtain TCO₇ and further eluted using *n*-hexane-EtOAc (70/30) to obtain TCO₈.

Treatment of Series C

Series C was separated by means of CC on silica gel (100 g) using a mixture of *n*-hexane-EtOAc of increasing polarity. Fractions of 50 ml were collected. These were concentrated and grouped according to their TLC profiles in 5 sub-fractions, as presented in table 25.

Table XXVI: Chromatogram of series C

Eluent	Fraction	TLC	Series	Observation
Hex/EA 75/25	1-6		1	A mixture containing TCO ₉
Hex/EA 70/30	7-21			
Hex/EA 65/35	12-17	Hex/EA 70/30	2	A mixture containing TCO ₁₀
Hex/EA 60/40	18-30			
Hex/EA 40/60	31-50	Hex/EA 60/40		
Hex/EA 45/55	51-68		3	A mixture containing TCO ₁₁
Hex/EA 50/50	69-80	CH ₂ Cl ₂		
Hex/EA 40/60	81-95		4	A mixture containing TCO ₁₂
Hex/EA 45/55	96-114	CH ₂ Cl ₂ /MeOH 95/05	5	A mixture containing TCO ₁₄
Hex/EA 40/60	115			

The different subfractions were purified using CC. However, C1 was eluted using a mixture of CH₂Cl₂-MeOH (98/02) to obtain TCO₉; C2 was eluted using a mixture of CH₂Cl₂-MeOH (95/05) to obtain TCO₁₀; C3 was eluted using a mixture of CH₂Cl₂-MeOH (92/08) to obtain TCO₁₁; C4 was eluted using a mixture of CH₂Cl₂-MeOH (90/10) to obtain TCO₁₂; C5 was eluted using a mixture of CH₂Cl₂-MeOH (90/10) to obtain TCO₁₄.

Treatment of Series D

Series D was also chromatographed on silica gel (100 g) column using a mixture of *n*-hexane-EtOAc in increasing polarity and a mixture of EA/MeOH. Fractions of 50 ml were collected. These were concentrated and grouped according to their TLC profiles in 3 sub-fractions, as presented in the following table.

Table XXVII: chromatogram of series D

Eluent	Fraction	TLC	series	Observation
Hex/EA 50/50	1-13	Hex/EA 60/40	1	A mixture containing TCO ₁₇
Hex/EA 40/60	14-32			
Hex/EA 35/65	33-43	CH ₂ Cl ₂		
Hex/EA 30/70	44-50		2	A mixture containing TCO ₁₈
Hex/EA 25/75	51-81			
Hex/EA 20/80	82-110	CH ₂ Cl ₂ /MeOH 95/05		
Hex/EA 15/85	111-131		3	A mixture containing TCO ₂₀
Hex/EA 10/90	132-142			
EA 100%	143-159	CH ₂ Cl ₂ /MeOH 90/10		
EA/MeOH 95/05	160-180			
EA/MeOH 90/10	181			tailings

The different subfractions were purified using CC. However, D1 was eluted using a mixture of CH₂Cl₂-MeOH (90:10) to obtain TCO₁₇; D2 was eluted using a mixture of CH₂Cl₂-MeOH (88:12) to obtain TCO₁₈; D3 was eluted using a mixture of CH₂Cl₂-MeOH (85:15) to obtain TCO₂₀.

Table XXVIII: Chromatogram of the crud extract of the stem-bark of *T. contorta*

Eluent	Fraction	TLC	Series	Observation
Hex 100%	1-5	Hex/AE 95/5	A	A mixture of at least 9 compounds including a white precipitate
Hex/AE 90/10	6-10			
Hex/AE 80/20	11-15	Hex/AE 90/10	B	A mixture of at least 6 compounds
Hex/AE 70/30	16-20			
Hex/AE 60/40	21-24			
Hex/AE 50/50	25-30	Hex/AE 50/50	C	A mixture of at least 6 compounds
Hex/AE 40/60	31-34			
Hex/AE 30/70	35-40			
Hex/AE 20/80	41-44			
Hex/AE 10/90	45-50			
AE 100%	51-54	CH ₂ Cl ₂ -MeOH	D	A mixture of at least 4 compounds

AE/MeOH 90/10	55-60	95/5		
AE/MeOH 80/20	61-64			
AE/MeOH 70/30	65-70	CH ₂ Cl ₂ -MeOH 90/10	E	Mixture of 2 compounds at least + tailing

The different Fractions were left to rest for a few days after which:

- a precipitate in the form of white needlets was observed in fractions 5-12. It was washed with hexane and indexed TC₁;
- a precipitate in the form of white powder was observed in fractions 12-14, washed using a mixture of Hex/AE and indexed TC₂;
- fractions 20-24, 26-30, 54-56 and 73 precipitated in the form of white powders, was washed using Hex/AE and indexed TC₆, TC₁₀, TC₁₃, TC₁₆.

Treatment of Series B

Series B was chromatographed on silica gel (150 g) column using a mixture of *n*-hexane-EtOAc in increasing polarity. Fractions of 100 ml were collected. These were concentrated and grouped according to their TLC profiles in 4 sub-fractions, as presented in the following table.

Table XXIX: Chromatogram of series B

Eluent	Fraction	TLC	series	Observation
hexane	1-6	Hex/EA 95/05	1	Yellow oil containing TC ₁
Hex/EA 95/05	6-12			
Hex/EA 90/10	13-17	Hex/EA 85/15	2	A mixture containing TC ₃
Hex/EA 85/15	18-30			
Hex/EA 80/20	31-39	Hex/EA 75/35	3	A mixture containing TC ₄
Hex/EA 75/25	40-56			
Hex/EA 70/30	57	CH ₂ Cl ₂		A mixture containing TC ₇

The different subfractions were purified using CC. However, B2 was eluted using a mixture of Hex-EA (75/25) to obtain TC₃; B3 was eluted using a mixture of Hex-EA (75/35) to obtain TC₄; B4 was eluted using a mixture of CH₂Cl₂ to obtain TC₇.

Treatment of Series C

Series C was chromatographed on silica gel (120 g) column using a mixture of *n*-hexane-EtOAc in increasing polarity. Fractions of 50 ml were collected. These were concentrated and grouped according to their TLC profiles in 5 sub-fractions, as presented in the following table.

Table XXX: Chromatogram of series C

Eluent	Fraction	TLC	series	Observation
Hex/EA 75/25	1-10		1	A mixture containing TC ₅
Hex/EA 70/30	11-17			
Hex/EA 65/35	18-24	Hex/EA 70/30	2	A mixture containing TC ₉
Hex/EA 60/40	25-30			
Hex/EA 40/60	31-37	Hex/EA 60/40		
Hex/EA 45/55	38-42		3	A mixture containing TC ₁₁
Hex/EA 50/50	43-48	CH ₂ Cl ₂		
Hex/EA 40/60	49-59		4	A mixture containing TC ₁₂
Hex/EA 45/55	60-71	CH ₂ Cl ₂ /MeOH 95/05	5	A mixture containing TC ₁₅
Hex/EA 40/60	72			

The different subfractions were purified using CC. However, C1 was eluted using CH₂Cl₂ to obtain TC₅; C2 was eluted using a mixture of CH₂Cl₂-MeOH (98/02) to obtain TC₉; C3 was eluted using a mixture of CH₂Cl₂-MeOH (92/08) to obtain TC₁₁; C4 was eluted using a mixture of CH₂Cl₂-MeOH (90/10) to obtain TC₁₂; C5 was eluted using a mixture of CH₂Cl₂-MeOH (90/10) to obtain TC₁₅.

Treatment of Series D

Series D was also chromatographed on a silica gel (100 g) column using a mixture of *n*-hexane-EtOAc of increasing polarity and a mixture of EA/MeOH. Fractions of 50 ml were collected. These were concentrated and grouped according to their TLC profiles in 3 sub-fractions, as presented in the following table.

Table XXXI: Chromatogram of series D

Eluent	Fraction	TLC	series	Observation
--------	----------	-----	--------	-------------

Hex/EA 50/50	1-13	Hex/EA 60/40	1	A brown mixture
Hex/EA 40/60	14-32			
Hex/EA 35/65	33-43	CH ₂ Cl ₂		
Hex/EA 30/70	44-50		2	A mixture containing TC ₁₇
Hex/EA 25/75	51-81			
Hex/EA 20/80	82-110	CH ₂ Cl ₂ /MeOH 95/05		
Hex/EA 15/85	111-131		3	A mixture containing TC ₁₈
Hex/EA 10/90	132-142			
EA 100%	143-159	CH ₂ Cl ₂ /MeOH 90/10		
EA/MeOH 95/05	160-180			
EA/MeOH 90/10	181			
				tailings

The different subfractions were purified using CC. However, D2 was eluted using a mixture of CH₂Cl₂-MeOH (85/15) to obtain TC₁₇; D3 was eluted using a mixture of CH₂Cl₂-MeOH (83/17) to obtain TC₁₈.

Table XXXII: Chromatogram of the crud extract of the stem of *T. inconspicua*

eluent	fraction	TLC	series	observation
Hex 100%	1-5	Hex/AE 95/5	A	A mixture of at least 9 compounds including a white precipitate
Hex/AE 90/10	6-10			
Hex/AE 80/20	11-15	Hex/AE 90/10	B	A mixture of at least 6 compounds
Hex/AE 70/30	16-20			
Hex/AE 60/40	21-24			
Hex/AE 50/50	25-30	Hex/AE 50/50	C	A mixture of at least 6 compounds
Hex/AE 40/60	31-34			
Hex/AE 30/70	35-40			
Hex/AE 20/80	41-44			
Hex/AE 10/90	45-50			
AE 100%	51-54	CH ₂ Cl ₂ -MeOH 95/5	D	A mixture of at least 4 compounds
AE/MeOH 90/10	55-60			
AE/MeOH 80/20	61-64			
AE/MeOH 70/30	65-70	CH ₂ Cl ₂ -MeOH 90/10	E	Mixture of 2 compounds at least + tailing

The different Fractions were left to rest for a few days after which:

- a precipitate in the form of white needles was observed in fractions 6-10. It was washed with hexane and indexed TiS₁;
- precipitate in the form of white powders were observed in fractions 16-20, and 22-28 washed using a mixture of Hex/AE and indexed TiS₂ and TiS₁₃ respectively.
- fractions 31-33, 35-40, 55 and 67 precipitated in the form of white powders, was washed using Hex/AE and indexed TiS₃, TiS₇, TiS₈.

Treatment of Series B

Series B was chromatographed on a silica gel (120 g) column using a mixture of *n*-hexane-EtOAc of increasing polarity. Fractions of 100 ml were collected. These were concentrated and grouped according to their TLC profiles in 3 sub-fractions, as presented in the following table.

Table XXXIII: Chromatogram of series B

Eluent	Fraction	TLC	Series	Observation
hexane	1-5	Hex/EA 95/05	1	Yellow oil
Hex/EA 95/05	6-11			
Hex/EA 90/10	12-17	Hex/EA 85/15	2	A mixture containing TiS ₄
Hex/EA 85/15	18-28			
Hex/EA 80/20	29-39	Hex/EA 75/35		
Hex/EA 75/35	40-47		3	A mixture containing TiS ₅
Hex/EA 70/30	48	CH ₂ Cl ₂		

Subfraction B2 was separated by column chromatography (CC) using *n*-hexane-EtOAc (95:15) as an eluent, to obtain compound TiS₄. B3 was separated by cc eluted using *n*-hexane-EtOAc (72:38) to obtain TiS₅.

Treatment of Series C

Series C was chromatographed on silica gel (150 g) column using a mixture of *n*-hexane-EtOAc in increasing polarity. Fractions of 50 ml were collected. These were concentrated and grouped according to their TLC profiles in 4 sub-fractions, as presented in the following table 33.

Table XXXIV: Chromatogram of series C

Eluent	Fraction	TLC	series	Observation
--------	----------	-----	--------	-------------

Hex/EA 75/25	1-8		1	A mixture containing TiS ₆
Hex/EA 70/30	9-18			
Hex/EA 65/35	19-22	Hex/EA 70/30	2	A mixture containing TiS ₉
Hex/EA 60/40	23-30			
Hex/EA 40/60	31-50	Hex/EA 60/40		
Hex/EA 45/55	51-68		3	A mixture containing TiS ₁₀
Hex/EA 50/50	69-80	CH ₂ Cl ₂		
Hex/EA 40/60	81-95		4	A mixture containing TiS ₁₁
Hex/EA 45/55	96-114	CH ₂ Cl ₂ /MeOH 95/05		

The different subfractions were purified using CC. However, C1 was eluted using a mixture of CH₂Cl₂-MeOH (94/06) to obtain TiS₆; C2 was eluted using a mixture of CH₂Cl₂-MeOH (95/05) to obtain TiS₉; C3 was eluted using a mixture of CH₂Cl₂-MeOH (92/08) to obtain TiS₁₀; C5 was eluted using a mixture of CH₂Cl₂-MeOH (90/10) to obtain TiS₁₁.

Treatment of Series D

Series D was also chromatographed on a silica gel (100 g) column using a mixture of *n*-hexane-EtOAc in increasing polarity and a mixture of EA/MeOH. Fractions of 50 ml were collected. These were concentrated and grouped according to their TLC profiles in 3 sub-fractions, as presented in the following table.

Table XXXV: Chromatogram of series D

Eluent	Fraction	TLC	Series	Observation
Hex/EA 50/50	1-13	Hex/EA 60/40	1	A mixture containing TiS ₁₂
Hex/EA 40/60	14-32			
Hex/EA 35/65	33-43	CH ₂ Cl ₂		
Hex/EA 30/70	44-50		2	A mixture containing TiS ₁₄
Hex/EA 25/75	51-81			
Hex/EA 20/80	82-110	CH ₂ Cl ₂ /MeOH 95/05		
Hex/EA 15/85	111-131		3	A mixture containing TiS ₁₅
Hex/EA 10/90	132-142			
EA 100%	143-159	CH ₂ Cl ₂ /MeOH 90/10		
EA/MeOH 95/05	160-180			
EA/MeOH 90/10	181			tailings

The different sub fractions were purified using CC. However, D1 was eluted using a mixture of CH₂Cl₂-MeOH (90/10) to obtain TiS₁₂; D2 was eluted using a mixture of CH₂Cl₂-MeOH (88/12) to obtain TiS₁₄; D3 was eluted using a mixture of CH₂Cl₂-MeOH (85/15) to obtain TiS₁₅.

III.5. BIOLOGICAL TESTS

0III.5.1. Anti cancer activity

MDA-MB 231 cells were grown at 37 °C with 5% CO₂ in a humidified environment in Dulbecco's Modified Eagle's Medium (DMEM) high glucose (4.5 g/L) containing L-glutamine (4 mM) supplemented with 10% (v/v) fetal bovine serum (FBS). The cells were seeded at a density of 10,000 cells per well in 96-well microtitre plate. After seeding, they were treated with 10 µM of the compounds dissolved in dimethyl sulfoxide (DMSO) and diluted in fresh culture medium. During each experiment, the maximal concentration of DMSO in the medium did not exceed 0.5%. Staurosporine (STS) at 2 µM was used as a positive control. After incubation for 48 h at 37 °C with 5% CO₂, the cell viability was determined by adding 10 µL of CCK-8 solution as described by the manufacturer. After incubation for 1 h at 37 °C with 5% CO₂, the absorbance was measured spectrophotometrically at 550 nm in a microplate reader. Each assay was done in triplicate and results are presented as means ± standard error. *p < 0.05, ***p < 0.001.

III.5.1.1. Anticancer effect of compound TiS₅

MDA-MB 231 cells were grown at 37 °C with 5% CO₂ in a humidified environment in Dulbecco's Modified Eagle's Medium (DMEM) high glucose (4.5 g/L) containing L-glutamine (4 mM) supplemented with 10% (v/v) fetal bovine serum (FBS). The culture medium was changed every 48h and the cells in a logarithmic increase phase were seeded at a density of 10,000 cells per well in 96-well microtiter plate. After seeding, the cells were allowed to attach overnight (at 37°C, 50% CO₂) after which they were treated with increasing concentrations of TiS₅ for 24 and 48 h respectively. The cell viability was measured by Cell Counting Kit-8 (CCK-8) assay, and the results are presented as percentage of DMSO (0.5%) used as negative control. The inhibitory rate at 50% (IC₅₀) was determined by using the non-linear regression analysis with GraphPad Prism 6.0. Each experiment was carried out in triplicate and data are presented as mean ± SEM, p < 0.05, ***p < 0.001.

III.5.2. Anti-inflammatory assay

III.5.2.1. Cell culture

RAW 267.4 cells were cultured in DMEM medium containing 10% FBS, 100 µg/mL streptomycin and 100units/mL penicillin at 37 °C in a humidified incubator with 5% CO₂.

III.5.2.2. Cell viability assay

Cell viability was measured by Am-Blue assay. In brief, 1×10^4 RAW 264.7 cells were seeded into 96-well plates, then treated with compounds at different concentrations or DMSO for 24 h, Am-Blue reagent (10 uL per well) was added to each well and detected by Thermo Scientific VarioskanFlash Multimode Reader with excitation at 544 nm and emission at 590 nm, respectively. Each sample was performed in triplicate.

III.5.2.3. Nitric Oxide measurement

RAW 264.7 cells were seeded in 48-well plates and treated with compounds for 2 h before exposure to LPS (1 µg/mL) for another 24 h. NO measurements were conducted in the cell culture medium by using commercially available kits based on the Griess reaction (Beyotime). Data reported are the mean values from triplicate analyses.

III.6. PHYSICO-CHEMICAL PROPERTIES OF COMPOUNDS DESCRIBED

CHARACTERISTICS

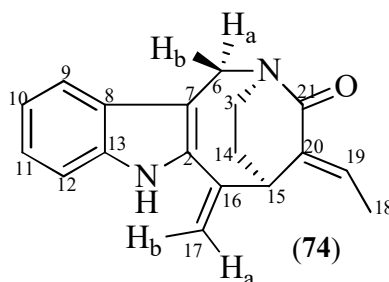
TCO₃: apparicine-21-one.

Physical appearance: black powder

Molecular formula: C₁₈H₁₈ON₂

¹H and ¹³C NMR data: see Table 6

STRUCTURES



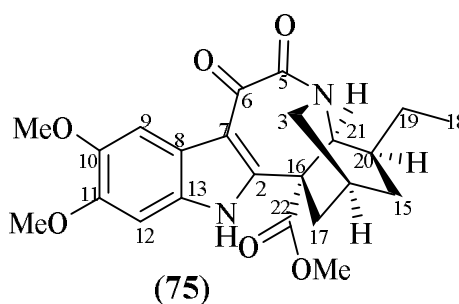
TCO₅: 5,6-dioxo-11-methoxy

voacangine Physical appearance:

yellow powder

Molecular formula: C₂₃H₂₆O₆N₂

¹H and ¹³C NMR data: see Table 7



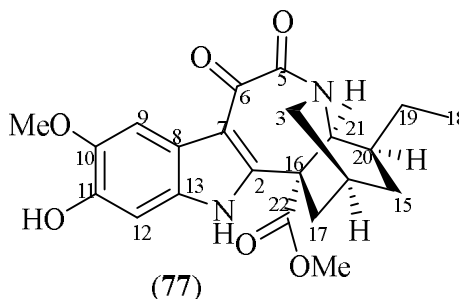
TiS₅: 5,6-dioxo-11-hydroxy

voacangine

Physical appearance: yellow powder

Molecular formula: C₂₂H₂₄O₆N₂

¹H and ¹³C NMR data: see Table 8

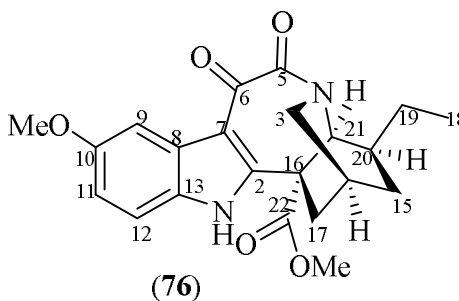


TiS₁₀: ibogamine-16-carboxy,17,20-didehydro-5,6-dioxo-10-methoxy-methyl ester

Physical appearance: yellow powder

Molecular formula: C₂₂H₂₄O₅N₂

¹H and ¹³C NMR data: see Table 9

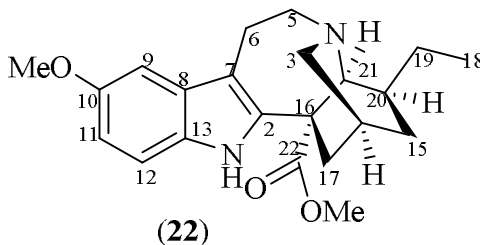


TiS₆ = TCO₇: voacangine

Physical appearance: greyish needles

Molecular formula: C₂₂H₂₈O₃N₂

¹H and ¹³C NMR data: see Table 10

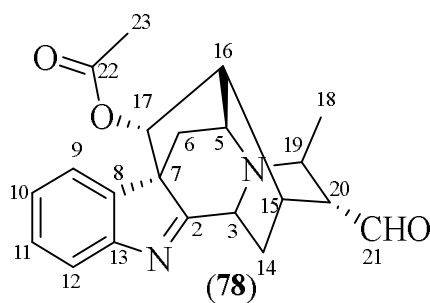


TC₅: perakine

Physical appearance: yellowish crystals

Molecular formula: C₂₁H₂₂O₃N₂

¹H and ¹³C NMR data: see Table 11

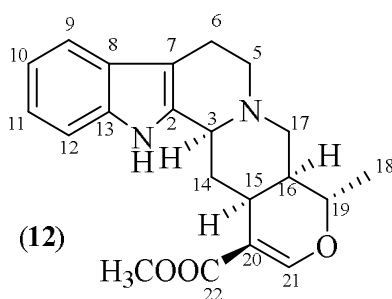


TiS₇: tetrahydroalstonine

Physical appearance: yellow needles

Molecular formula: C₂₁H₂₅O₃N₂

¹H and ¹³C NMR data: see Table 12

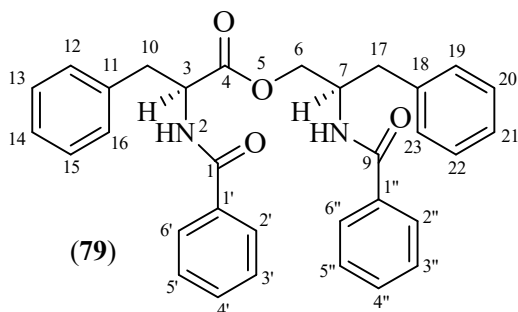


TC₆: asperphenamate

Physical appearance: yellowish-white powder

Molecular formula: C₃₂H₃₀O₄N₂

¹H and ¹³C NMR data: see Table 13

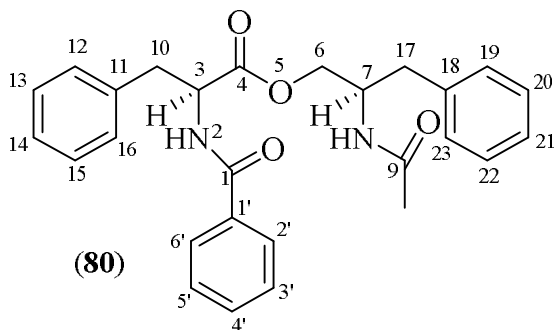


TiS₈: patriscabratine

Physical appearance: white powder

Molecular formula: C₂₇H₂₈O₄N₂

¹H and ¹³C NMR data: see Table 14

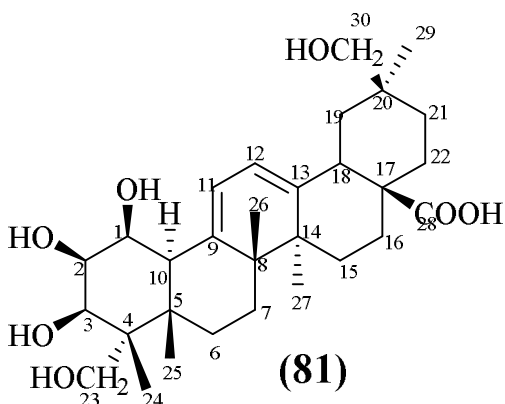


TCO₉: contortiac acid

Physical appearance: white powder

Molecular formula: C₃₀H₄₆O₆

¹H and ¹³C NMR data: see table 15

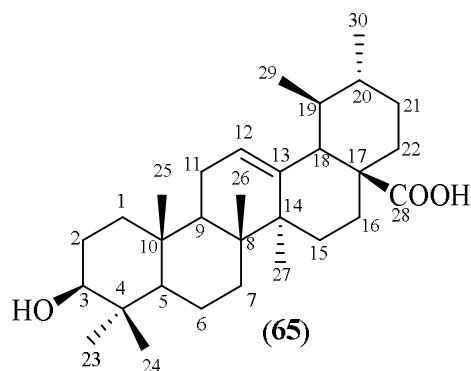


TC₄=TCO₄: ursolic acid

Physical appearance: white powder

Molecular formula: C₃₀H₄₈O₃

¹H and ¹³C NMR data: see Table 16

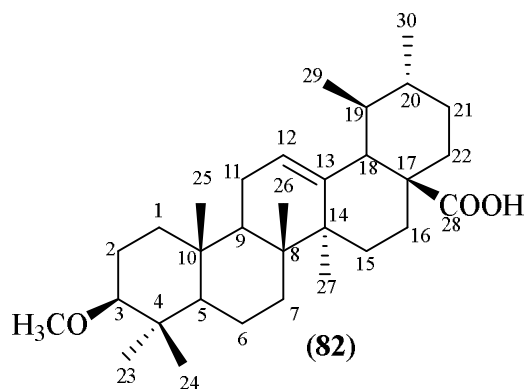


TiS₃: 3-methoxy ursolic acid

Physical appearance: white powder

Molecular formula: C₃₁H₅₀O₃

¹H and ¹³C NMR data: see Table 17

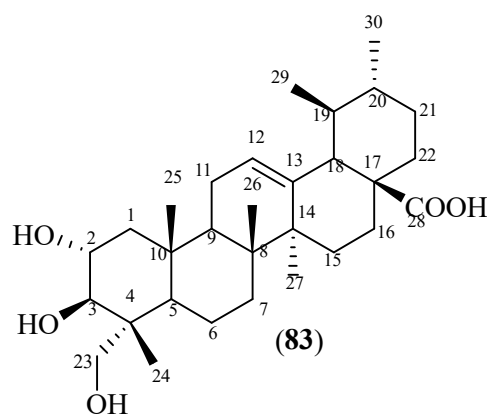


TCO₈: asiatic acid

Physical appearance: white powder

Molecular formula: C₃₀H₄₈O₅

¹H and ¹³C NMR data: see Table 18

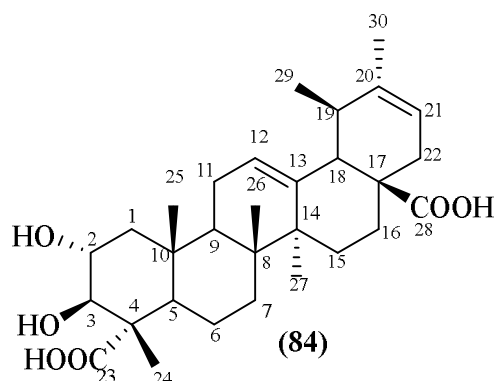


TiS₉: cordepressenic acid

Physical appearance: white powder

Molecular formula: C₃₀H₄₄O₆

¹H and ¹³C NMR data: see Table 19

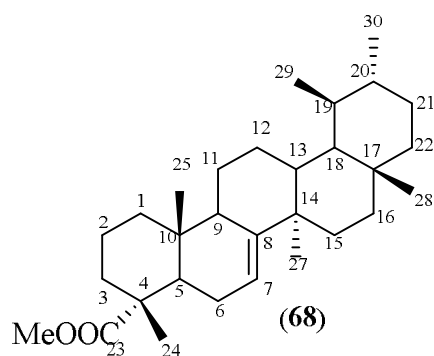


TC₃: baurenyl acetate

Physical appearance: white powder

Molecular formula: C₃₁H₅₂O

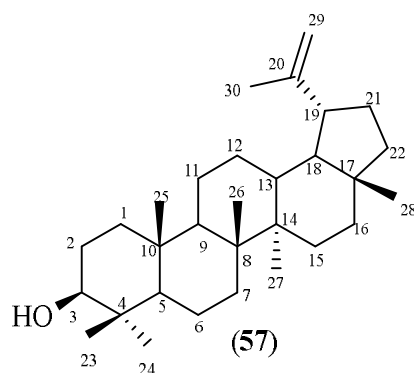
¹H and ¹³C NMR data: see Table 20



TiS₂: lupeol

Physical appearance: white powder

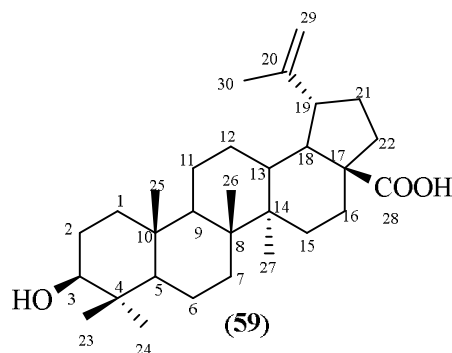
Molecular formula: C₃₀H₅₀O



TiS₄: butelinic acid

Physical appearance: white powder

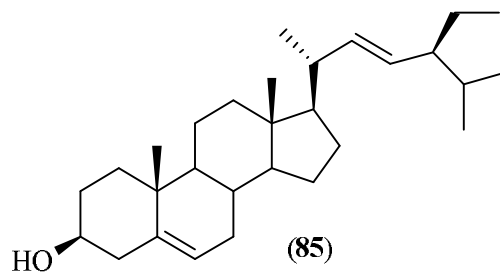
Molecular formula: C₃₀H₄₈O₃



TCO₁=TC₂=TS₁: stigmasterol.

Physical appearance: white needles

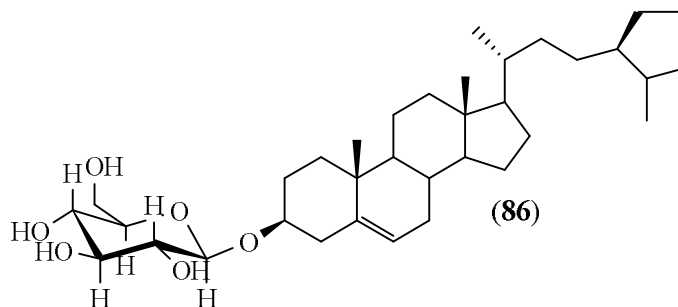
Molecular formula: C₂₉H₄₈O



TCO₁₈=TC₁₆: sitosterol-3- O-β-D-glucopyranoside

Physical appearance: white powder

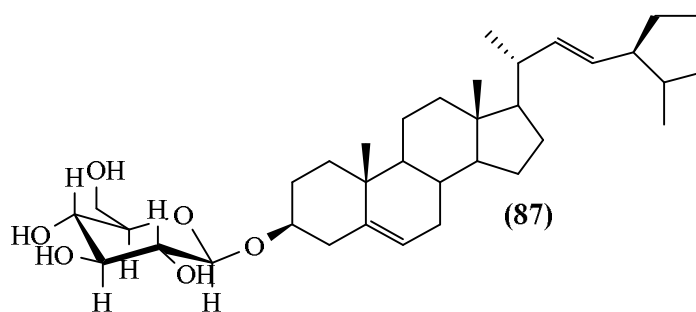
Molecular formula: C₃₅H₆₀O₆



TiS₁₄: stigmasterol-3-*O*- β -D-glucopyranoside

Physical appearance: white powder

Molecular formula: C₃₅H₅₈O₆

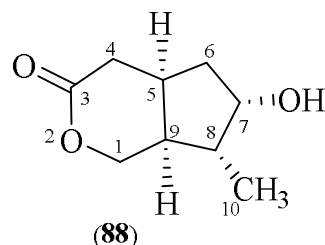


TCO₂: Isoboonein

Physical appearance: colorless crystals

Molecular formula: C₉H₁₄O₃

¹H and ¹³C NMR data: see table 21

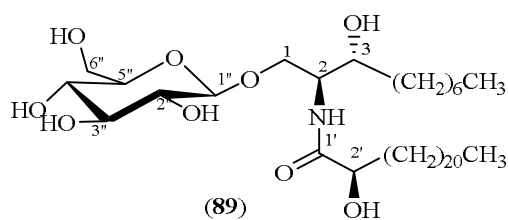


TiS₁₅: contortanoside

Physical appearance: white powder

Molecular formula: C₃₉H₇₇NO₉

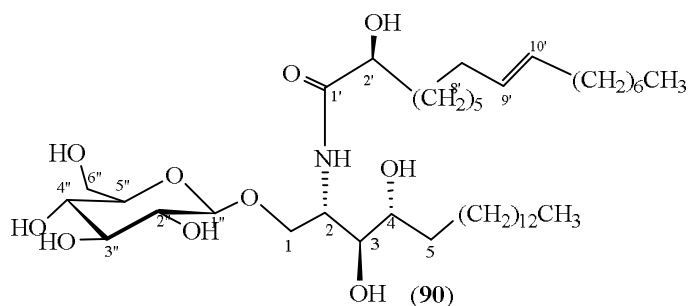
¹H and ¹³C NMR data: see table 22



TCO₁₉: 1-*O*- β -D-glucopyranosyl-(2*S*,3*S*,4*R*)-*N*-(2-hydroxyheptadec-9-enyl)-octadecaspingene.

Physical appearance: white powder

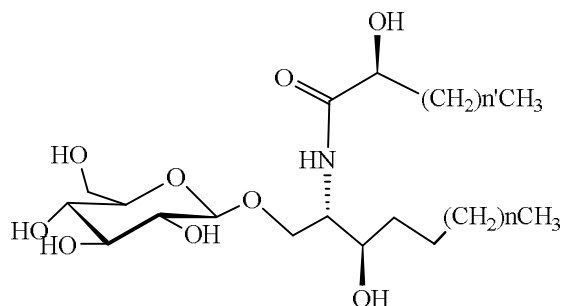
Molecular formula: C₂₈H₅₃NO₈



TCO₂₀: phytocerebroside

Physical appearance: white powder

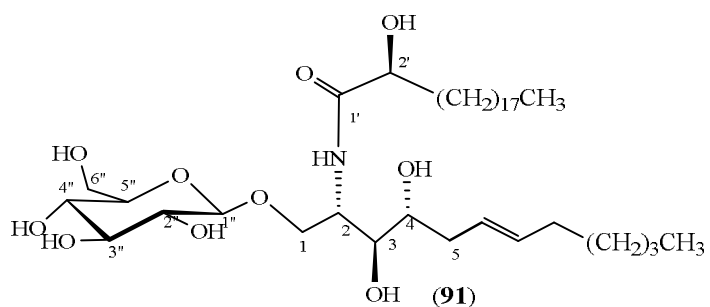
Molecular formula: C₃₂H₅₉NO₉



TC₁₂: (2R)-2-hydroxy-N-
((2S,3S,4R,6E)-1,3,4-
trihydroxydodec-6-en-2-
yl)icosanamide

Physical appearance: white powder

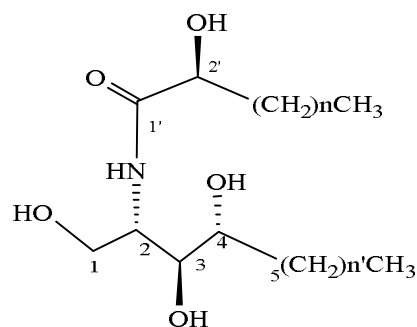
Molecular formula: C₃₇H₇₃NO



TCO₁₄: phytoceramide

Physical appearance: white powder

Molecular formula: C₄₄H₈₉NO₅

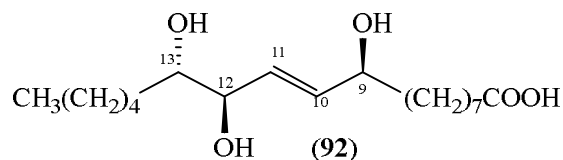


TiS₁₃=TCO₆: pinellic acid

Physical appearance: white powder

Molecular formula: C₁₈H₃₄O₅

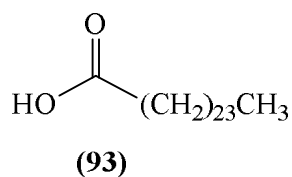
¹H and ¹³C NMR data: see table 23



TC₁: pentacosanoic acid

Physical appearance: white powder

Molecular formula: C₃₉H₇₇NO₂



REFERENCES

- Achenbach Hans, Benirschke Monika, Torrenegra Ruben. 1997. Alkaloids and other compounds from seeds of *Tabernaemontana cymosa*. *Phytochemistry*. **45**: 325-335. Doi: [10.1016/S0031-9422\(96\)00645-0](https://doi.org/10.1016/S0031-9422(96)00645-0)
- Aizawa Koichi, Liu Chun, Tang Sanyuan, Veeramachaneni Sudipta, Hu Kang-Quan K, Smith Donald E., WangXiang-Dong. 2016. Tobacco carcinogen induces both lung cancer and non-alcoholic steatohepatitis and hepatocellular carcinomas in ferrets which can be attenuated by lycopene supplementation. *International Journal of Cancer*. **139**: 1171-81. Doi:[10.1002/ijc.30161](https://doi.org/10.1002/ijc.30161)
- Andrade Marcelo T., Lima Josélia A., Pinto Angelo C., Rezende Claudia M., Carvalho Meriane P., Epifanio Rosângela A. 2005. Indole alkaloids from *Tabernaemontana australis* (Muell. Arg) Miars that inhibit acetylcholinesterase enzyme. *Bioorganic and Medicinal Chemistry*. **13**: 4092-4095. Doi: [10.1016/j.bmc.2005.03.045](https://doi.org/10.1016/j.bmc.2005.03.045)
- Aniszewski Tadeusz. 1994. The biological basis of quinolizidine alkaloids. *Science of Legumes*, **1**: 1-24.
- Aniszewski Tadeusz. 2007. Alkaloids - Secrets of Life: 1st Edition: Alkaloid Chemistry, Biological Significance, Applications and Ecological Role.
- Augustin Jörg M., Kuzina Vera, Andersen Sven B., Bak Søren. 2011. Molecular activities, biosynthesis and evolution of triterpenoid saponins. *Phytochemistry*, **72**: 435-57. Doi: [10.1016/j.phytochem.2011.01.015](https://doi.org/10.1016/j.phytochem.2011.01.015)
- Banthorpe D Derek. V. 1991. Classification of terpenoids and general procedures for their characterization, in *Terpenoids* (Charlwood, B. V. and Banthorpe, D. V., eds), *Methods in Plant Biochemistry* (Dey, P. M. and Harborne, J. B., eds.), vol. 7, Academic Press, San Diego, 1-41.
- Baron Andre, Brassell Stephen A., Shulman Lee P. 2005. Early cancer diagnosis: present and future; Advanced imaging techniques, molecular and protein biomarkers, and multimodal approaches are at the fore front of promising for detecting and diagnosing cancer at its earliest, most treatable stages. *Patient Care*, **35**: 22. Gale Academic Onefile, Accessed 2 November 2019.
- Bennasar Lluïsa M., Zulaica Ester, Sole Daniel, Alonso Sandra S. 2009. First total synthesis of apparicine. *Chemical Communications*, 1-31.
- Bernard Philippe, Scior Thomas, Didier Bruno, Hibert Marcel, Berthon Jean-Yves . 2001. Ethnopharmacology and bioinformatic combination for leads discovery: application to phospholipase A₂ inhibitors. *Phytochemistry*, **58**: 685-674. Doi: [10.1016/S0031-9422\(01\)00312-0](https://doi.org/10.1016/S0031-9422(01)00312-0).

Bhalla Triloki N., Gupta Mukut.B., Bhargava Krishna P. 1971. Antipyretic, analgesic activity of some natural products. *Indian Journal of Pharmacology*, **3**: 194-6.

Bianco Armandodoriano, De Luca Angelo, Mazzei Raffaele Antonio., Nicoletti Marcello, Passacantilli Pietro, De Lima Roberto Alves. 1994. Iridoids from *Rauvolfia grandifolia*. *Phytochemistry*, **35**: 1485-1487. Doi: [10.1016/S0031-9422\(00\)86881-8](https://doi.org/10.1016/S0031-9422(00)86881-8)

Biskup Edyta, Golebiowski Marek, Gniadecki Robert, Stepnowski Piotr, Lojkowska Ewa. 2012. Triterpenoid α -amyrine stimulates proliferation of human keratinocytes but does not protect them against UVB damage. *Acta Biochimica Polonica*, **59**: 255-260. Doi: [org/10.18388/abp.2012_2147](https://doi.org/10.18388/abp.2012_2147)

Boligon Aline Augusti, Athayde Margareth Linde. 2012. Phytochemical investigation and cytotoxic properties of *Tabernaemontana catharinensis* A. DC. Cultivated in Brazil. *Journal of Phytochemistry*, **6**: 127-131. Doi: [10.3923/rjphyto.2012.127.131](https://doi.org/10.3923/rjphyto.2012.127.131)

Burkill Humphrey M. 1985. Apocynaceae in The useful plants of west tropical Africa. **1** Kew: Royal Botanic Gardens.

Chaiyana Wantida, Rades Thomas, Okonogi Siriporn. 2013. Characterization and in vitro permeation study of microemulsions and liquid crystalline systems containing the anticholinesterase alkaloidal extract from *Tabernaemontana divaricata*. *International Journal of Pharmacology*, **452**: 201-210. Doi: [10.1016/j.ijpharm.2013.05.005](https://doi.org/10.1016/j.ijpharm.2013.05.005)

Chatterjee Tapan K. 2000. Medicinal plants with Hepatoprotective properties. In: herbal options, 3rd edn. Books and allied (P) Ltd. Calcutta, 135.

Chen Bing-Chang, Liao Chiao-Chun, Hsu Ming-Jen, Liao Yi-Ting, Lin Chia-Chin, Sheu Joen-Rong, Chien-Huang Lin. 2006. Peptidoglycan-induced IL-6 production in RAW 264.7 macrophage is mediated by cyclooxygenase -2, PGE2/PGE4 receptors, protein kinase AI- κ B and NF- κ B. *Journal of Immunology*. **177**: 681-693. Doi: [10.4049/jimmunol.177.1.681](https://doi.org/10.4049/jimmunol.177.1.681)

Chen Guang, Lu Huangwei, Wang Chunlei, Yamashita Koichi, Manabe Masanobu, Xu Suixu, Kodama Hiroyuki. 2002. Effects of five triterpenoid compounds isolated from leaves of *Diosyros kaki* on stimulus-induced superoxide generation and tyrosyl phosphorylation in human polymorphonuclear leukocytes. *Clinical Chimical Acta*, **320**: 11-6. Doi: [10.1016/S0009-8981\(02\)00021-9](https://doi.org/10.1016/S0009-8981(02)00021-9)

Chen Hong-Mei, Yang Yu-Ting, Li Hong-Xiang, CaoZhi-Xing, Dan Xiao-Mei, Mei Ling, GuoDa-Le, Song Chuan-Xia, Dai Yu, Hu Jia, & Deng Yun. 2016. Cytotoxic monoterpene indole alkaloids isolated from the barks of *Voacanga africana* Staph. *Natural Product Research*, **10**: 1144-9. Doi: [10.1080/14786419.2015.1046132](https://doi.org/10.1080/14786419.2015.1046132)

Choi Hyun Gyu, Park Yu Mi, Lu Yue, ChangHyeun Wook, Na Min Kyun, Lee Seung Ho. 2012. Inhibition of prostaglandine D2 production by trihydroxy fatty acids osolated from *Ulmus davidiana* Var. *Phytothertapy Research*, **27**: 1376-1380. Doi: [10.1002/ptr.4882](https://doi.org/10.1002/ptr.4882)

Chou Kang-Ju, Fang Hua-Chang, Chung Hsiao-Min, Cheng Jin-Shiung, Lee Kam-Chung, Tseng Li-Ling, Tang Kwong-Yui, Jan Chung-Ren. 2000. Effects of betulinic acid on

intramolecular-free Ca(2+) levels in Madin Darby canine kidney cells. *European Journal of Pharmacology*, **408**: 99-106. [Doi: 10.1016/S0014-2999\(00\)00750-0](https://doi.org/10.1016/S0014-2999(00)00750-0)

Collins David J., Pilotti Carmel A., Wallis Adrian F.A. 1992. Triterpene acids from some papua new Guinea terminalia Species, *Phytochemistry*, **31**: 881-884. [Doi: 10.1016/0031-9422\(92\)80031-9](https://doi.org/10.1016/0031-9422(92)80031-9)

Cos Paul, Vlietinck Arnold J., Berghe Dirk V., MaesLouis. 2006. Anti-infective potential of natural products: How to develop a stronger in vitro 'proof-of-concept'. *Journal of Ethnopharmacology*. **106**: 290-302. [Doi:10.1016/j.jep.2006.04.003](https://doi.org/10.1016/j.jep.2006.04.003)

Devita V.T., Hammond D.B., McLeod D.G. 2005. Follow-up care for survivors of breast and prostate cancer. *Patient Care*.

Dewick Paul M. 2002. The biosynthesis of C₅–C₂₅ terpenoid compounds, *Natural Product Report*, **19**: 181-222. [Doi: 10.1039/B002685I](https://doi.org/10.1039/B002685I)

Dewick Paul M. 2009 Medicinal Natural Products: A Biosynthetic Approach *3rd Edition* 311-336

Edith Gonzalez-Rocha, Rosa Cerros-Tlatilpa Y. 2015. The family Apocynaceae (Apocynoideae and Rauvolfioideae) in the State of Morelos, Mexico *Acta Botanica Mexicana*, **110**: 21-70

Elia John. 2006. Tabernaemontana pachysiphon Stapf. [Internet] Record from PROTA4U. Schmelzer G.H. & Gurib-Fakim A. (Editors). PROTA (Plant Resources of Tropical Africa), Wageningen, Netherlands. <<http://www.prota4u.org/search.asp>>. Accessed 18 November 2019.

Endress Mary E., Liede-Schumann S., Meve Ulrich. 2014. An updated classification for Apocynaceae, *Phytotaxa*, **159**: 175-194. [Doi: 10.11646/phytotaxa.159.3.2](https://doi.org/10.11646/phytotaxa.159.3.2)

Endress Mary E., and Bruyns Peter V. 2000. A revised classification of the Apocynaceae s. l. *The Botanica lReview*. (Lancaster), **66**: 1-56

Falk Karl-E., Karlsson Karl-A. and Samuelsson Bo E. 1979. Proton NMR analysis of anomeric structure of glycosphingolipids. Lewis-active and Lewis-like substances. *Archives of Biochemistry and Biophysics*, **192**: 191–202. [Doi: 10.1016/0003-9861\(79\)90084-5](https://doi.org/10.1016/0003-9861(79)90084-5)

Farina Carlo, Pinza Mmario, Pifferi Giorgio. 1998. Synthesis and anti-ulcer activity of glycyrrhetic oleanolic and ursolic acids. *Farmaco*, **53**: 22-32. [Doi: 10.1016/S0014-827X\(97\)00013-X](https://doi.org/10.1016/S0014-827X(97)00013-X)

Ferlay Jaques, Soerjomataram Isabelle, Dikshit Rajesh, Eser Sultan, Mathers Colin, Rebelo Marise, Parkin Donald M., Forman David, Bray Freddie. 2015. Cancer incidence and mortality worldwide: sources, methods and major patterns in GLOBOCAN 2012. *International Journal of Cancer*, **136**: 359-86. [Doi: 10.1002/ijc.29210](https://doi.org/10.1002/ijc.29210)

Field Ben, Fiston-Lavier Anna-S., Kemen Ariane, Geisler Katrin, Quesneville Hadi, Osbourn Anne E. 2011. Formation of plant metabolic gene clusters within dynamic

chromosomal regions. *Proceedings of the National Academy of Sciences USA*, **108**: 16116–21. Doi: [10.1073/pnas.1109273108](https://doi.org/10.1073/pnas.1109273108)

Field Ben, Osbourn Anne E. 2008. Metabolic diversification-independent assembly of operon-like gene clusters in different plants. *Science*, **320**: 543-47. Doi: [10.1126/science.1154990](https://doi.org/10.1126/science.1154990)

Fisher Rosalie, Pusztai Lajos, Swanton Charles. 2013. Cancer heterogeneity: implications for targeted therapeutics. *British Journal of Cancer*, **108**: 479-85. Doi: [10.1038/bjc.2012.581](https://doi.org/10.1038/bjc.2012.581)

Fuhrman Bianca, Aviram Michael. 2001. Flavonoid protects LDL from oxidation and attenuate atherosclerosis. *Current Opinion in Lipidology*, **12**: 41-48. Doi: [10.1097/00041433-200102000-00008](https://doi.org/10.1097/00041433-200102000-00008)

Gao Yuan, Zhou Dong-S., Hai Ping, Li Yan, Wang Fei. 2015. Hybrid Monoterpenoid Indole Alkaloids Obtained as Artifacts from *Rauvolfia tetraphylla*. *Natural Products and Bioprospecting*, **5**: 247–253.

Geetha Thiruvadantha, Varalakshmi Palaninathan, Latha Raja M. 1998. Effects of triterpenes from *Crataeva nurvala* stem bark on lipid peroxidation in adjuvant induced arthritis in rats. *Pharmacology Research*, **37**: 191-5. Doi: [10.1006/phrs.1997.0278](https://doi.org/10.1006/phrs.1997.0278)

Goad Lionel J. 1991. Phytosterols, in *Terpenoids* (B. V. Charlwood and D. V. Banthorpe, eds.), Vol. 7 of *Methods in Plant Biochemistry* (P. M. Dey and J. B. Harborne, eds.), *Academic Press, London*, 369-434,

Gorman Marvin, Neuss Norbert, Cone Nancy J., Deyrup James A. 1960. Alkaloids from Apocynaceae. III. Alkaloids of *Tabernaemontana* and *Ervatamia*. The Structure of Coronaridine, A New Alkaloid related to ibogamine. *Journal of American Chemical Society*, **82**: 1142-1145. Doi: [10.1021/ja01490a031](https://doi.org/10.1021/ja01490a031)

Gupta Malaya, Mazumdar Upal K., Gomathi Periyasamy. 2004. Antioxidant and protective effects of *Ervantamia coronaria* stapf leaves against CCl₄ induced liver injury. *European Bulletin of Drug Research*, **12**: 13-22.

Harvard Women's Health Watch. 2006. Recognizing and treating basal cell carcinoma. *Harvard Health Letter*.

Hasnah Sirat M., Deny Susanti, Farediah Ahmad, Hiromitsu Takayama, Mariko Kitajima. 2010. Amides triterpenes and flavonoids from the leaves of *Melastoma malabatricum* L. *Journal of Natural Medicines*, **64**: 492-495. Doi: [10.1007/s11418-010-0431-8](https://doi.org/10.1007/s11418-010-0431-8)

Heinecke Jay W. 1997. Mechanisms of oxidative damage of low density lipoprotein in human atherosclerosis. *Current Opinion on Lipidology*, **8**: 268-274. Doi: [10.1097/00041433-199710000-00005](https://doi.org/10.1097/00041433-199710000-00005)

Heinecke Jay W. 1998. Oxidants and antioxidants in the pathogenesis of atherosclerosis: implications for the oxidized low density lipoprotein hypothesis. *Atherosclerosis*, **141**: 1-15. Doi: [10.1016/S0021-9150\(98\)00173-7](https://doi.org/10.1016/S0021-9150(98)00173-7)

- Heinrich Michael C., Blanke Charles D., Druker Brian J., Corless Christopher L. 2002. Inhibition of KIT tyrosine kinase activity: a novel molecular approach to the treatment of KIT-positive malignancies. *Journal of Clinical Oncology*, **20**: 1692-703. Doi: [10.1200/JCO.2002.20.6.1692](https://doi.org/10.1200/JCO.2002.20.6.1692)
- Heywood Vernon H., Brummitt Richard K., Culham Alastair, Seberg Orpen B. 2007. Apocynaceae. 38- 40. In: Flowering Plant Families of the World. New. York, Firefly Books.
- Hill Robert A., Connolly Joseph D. 2012. Triterpenoids. *Natural Product Reports*, **29**: 780–818. Doi: [10.1039/c3np70032a](https://doi.org/10.1039/c3np70032a)
- Hua Huiming, Pei Yuehu. 2001. A survey of the study on cerebrosides. *Journal of Shenyang Pharmaceutical University*, **18**: 299–306
- Joensuu Heikki, Dimitrijevic Sasa. 2001. Tyrosine kinase inhibitor imatinib (STIS71) as an anticancer agent for solid tumours. *Annals of Medicine*, **33**: 451-455
- Kaelin Carolyn M., Neugut Alfred I. 2005. "Implementing the gains in cancer prevention: prevention experts share the news-good and bad-to help you counsel patients on minimizing their risk for cancer." *Patient Care for the Nurse Practitioner*. Gale Academic Onefile, Accessed 18 Nov. 2019.
- Kalyanaraman Balaraman, Joseph Joy., Parthasarathy Sampath. 1993. The use of spin traps to investigate site-specific formation of free radicals in lowdensity lipoprotein oxidation. *Biochemical Society Transactions*, **21**: 318-321. Doi: [10.1042/bst0210318](https://doi.org/10.1042/bst0210318)
- Kapil Aruna, Sharma Shalini. 1994. Anti-complement activity of oleanolic acid: an inhibitor of the classical complement pathway. *Journal of Pharmacy and Pharmacology*, **46**: 922-3. Doi: [10.1111/j.2042-7158.1994.tb05715.x](https://doi.org/10.1111/j.2042-7158.1994.tb05715.x)
- Kapil Aruna, Sharma Shalini. 1995. Effects of oleanolic acid on complement in adjuvant- and carrageenan-induced inflammation in rats. *Journal of Pharmacy and Pharmacology*, **47**: 585-7. Doi: [10.1111/j.2042-7158.1995.tb06719.x](https://doi.org/10.1111/j.2042-7158.1995.tb06719.x)
- Khan M Mohammad S.Y., Javed Kalim, Khan Hasnain M., Shamsi Mahtab A., Siddiqui Anis A. 1991. α -amyrine derivatives from *Corchorus Depressus*. *Phytochemistry*, **30**: 1989-1992. Doi: [10.1016/0031-9422\(91\)85053-3](https://doi.org/10.1016/0031-9422(91)85053-3)
- Kim Hee K., Cheon Bong S., Kim Young H., Kim Sung Y., Kim Hyun P., 1999. Effects of naturally occurring flavonoids on nitric oxide production in the macrophage cell line RAW 264.7 and their structure–activity relationships. *Biochemical Pharmacology*, **58**: 759-765. Doi: [10.1016/S0006-2952\(99\)00160-4](https://doi.org/10.1016/S0006-2952(99)00160-4)
- Kim Oe K., Murakami Akira, Nakamura Yoshimasa, Ohigashi Hajime, 1998. Screening of edible Japanese plants for nitric oxide generation inhibitory activities in RAW 264.7 cells. *Cancer Letters*, **125**: 199-207. Doi: [10.1016/S0304-3835\(97\)00513-2](https://doi.org/10.1016/S0304-3835(97)00513-2)
- Kim Sun Y, Choi Young-Hee, Huh Hoon, Kim Jinwoong, Kim Young C, Lee Heum S. 1997. New antihepatotoxic cerebroside from *Lycium chinense* fruits. *Journal of Natural Product*, **60**: 274-276

- King Richter C., Kraus Matthias H., Aaronson Stuart A. 1985. Amplification of a novel v-erb B-related gene in a human mammary carcinoma. *Science*, **229**: 974-7. Doi: [10.1126/science.2992089](https://doi.org/10.1126/science.2992089)
- Kliebenstein Daniel J., Osbourn Anne. 2012. Making new molecules-evolution of pathways for novel metabolites in plants. *Current Opinion in Plant Biology*, **15**: 415-23. Doi: [10.1016/j.pbi.2012.05.005](https://doi.org/10.1016/j.pbi.2012.05.005)
- Krokida Afrodite, Delis Costas, Geisler Katrin, Garagounis Constantine, Tsikou Daniela, Peña-Rodríguez Luis M., Katsarou Dimitra, Field Ben, Osbourn Anne E., Papadopoulou Kalliope K. 2013. A metabolic gene cluster in *Lotus japonicus* discloses novel enzyme functions and products in triterpene biosynthesis. *New Phytologist*, **200**: 675-90. Doi: [10.1111/nph.12414](https://doi.org/10.1111/nph.12414)
- Kukula-Koch Wirginia A., Widelski Jarosław. 2017. Alkaloids. *Pharmacognosy: Fundamentals, Applications and Strategies*, 163-198. Doi: [10.1016/B978-0-12-802104-0.00009-3](https://doi.org/10.1016/B978-0-12-802104-0.00009-3)
- Kwon Tae-H., Lee Bo-M, Chung Sung-H., Kim Dong-H., Lee Yong-S. 2009. Synthesis and NO Production Inhibitory Activities of Ursolic Acid and Oleanolic Acid Derivatives. *Bulletin Korean Chemical Society*, **30**: 119-123. Doi: 10.5012/bkcs.2009.30.1.119
- Leeuwenberg Anthonius Josephus M. 1991. A revision of *Tabernaemontana* **1**. The Old World species. *Royal Botanic Gardens, Kew*
- Lemmens Roeland Hendrikus Maria J. 2006. *Tabernaemontana stapfiana* Britten. In: Louppe, D., Oteng-Amoako, A.A. & Brink, M. (Editors). PROTA (Plant Resources of Tropical Africa), Wageningen, Netherlands. Accessed 11 October 2019.
- Lim Kuan-Hon H., Raja Vijay J., Brads_dhaw Tracey D., Lim Siew-Huah, LowYun-Yee, KamToh-Seok. 2015. Ibogan, tacaman, and cytotoxic bisindole alkaloids from *Tabernaemontana corymbosa*: Cononusine, an iboga alkaloid with unusual incorporation of pyrrolidne moety. *Journal of Natural Product*, **78**: 1129-38. Doi: [10.1021/acs.jnatprod.5b00117](https://doi.org/10.1021/acs.jnatprod.5b00117)
- Liu Jiangang, Liu Yadong, Madhu C., Klaassen C.D. 1993. Protective effects of oleanolic acid acetaminophen-induced hepatotoxicity in mice. *Journal of Pharmacology and Experimental Therapeutics*, **266**: 1607-13.
- Liu Jiangang, Liu, Yadong, Mao Q., Klaassen, C.D. 1994. The effects of ten triterpenoid compounds on experimental liver injury in mice. *Fundamental and Applied Toxicology*, **22**: 34-40.
- Liu Jie. 1995. Pharmacology of oleanolic acid and ursolic acid. *Journal of Ethnopharmacology*, **49**: 57-68. Doi: [10.1016/0378-8741\(95\)90032-2](https://doi.org/10.1016/0378-8741(95)90032-2)
- Mahato Shashi B., Kundu Asish P. 1994. ¹³C NMR Spectra of Pentacyclic Triterpenoids. A Compilation and Some Salient Features. *Phytochemistry*, **37**: 1517-1575. Doi: [10.1016/S0031-9422\(00\)89569-2](https://doi.org/10.1016/S0031-9422(00)89569-2)

Marathe Nachiket P., Rasane Mandar H., Kumar Himanshu, Patwardhan Ankur A., Shouche Yogesh S., Diwanay Sham S. 2013. In vitro antibacterial activity of *Tabernaemontana alternifolia* (Roxb) stem-bark aqueous extracts against clinical isolates of methicillin resistant *Staphylococcus aureus*. *Annals of Clinical Microbiology and Antimicrobials*, **12**: 26. Doi: [10.1186/1476-0711-12-26](https://doi.org/10.1186/1476-0711-12-26)

MarkowitzLauri E., DunneEileen F., SaraiyaMona, ChessonHarrell W., CurtisRobinette C., GeeJulianne, Bocchini Joseph A.Unger Elizabeth R. 2014. Human Papillomavirus Vaccination Recommendations of the Advisory Committee on Immunization Practices (ACIP). *Morbidity and Mortality Weekly Report*, **63**

Masudur Rhaman, Mohammed Aktar S., Kaishar Parvej B., Saiful Alan S. 2011. Antidiabetic and cytotoxic activities of methanolic extract of *Tabernaemontana divaricata* (L.) Leaves in alloxan induced mice. *Asian Journal of Pharmaceutical and Clinical Research*, **5**: 49-52.

Meacham Corbin E., Morrison Sean J. 2013. Tumour heterogeneity and cancer cell plasticity. *Nature*. **501**: 328-37.

Medeiros Maria R.F., Melo-Prado Luiz A., Fernandes Vanessa C., Figueiredo Sérgio S.F., Coppede Juliana, Martins Juliana, Fiori GiovanaMaria F, Martinez-Rossi Nilce Maria M., Belebony Rene O., Contini Silvia Helena C., Paulo Sérgio P., Ana Lúcia F.2011. Antimicrobial activities of indole alkaloids from *Tabernaemontana catharinensis*. *Natural Product Communication*, **6**: 193-196. Doi: [10.1177/1934578X1100600209](https://doi.org/10.1177/1934578X1100600209)

Milena Gonçalves S.G., Ivo Curcino Vieira J., Rodrigo Oliveira R., Raimundo Braz-Filho. 2011. Application of Preparative High-Speed Counter-Current Chromatography for the Separation of Two Alkaloids from the Roots of *Tabernaemontana catharinensis* (Apocynaceae). *Molecules*, **16**: 7480-7487.

Möhlau, Richard. 1882. "Ueber Diphenylidisoindol". *Chemische Berichte*. **15**: 2480. Doi: [10.1002/cber.188201502204](https://doi.org/10.1002/cber.188201502204).

Momna Heijmadi. 2010. Introduction to cancer biology, BooksBoon.com.

Moses Tessa, Pollier Jacob, Thevelein Johan M., Goossens Alain. 2013. Bioengineering of plant (tri)terpenoids: from metabolic engineering of plants to synthetic biology in vivo and in vitro. *New Phytologist*, **200**: 27-43. Doi: [10.1111/nph.12325](https://doi.org/10.1111/nph.12325)

Nakagawa Takako, Yokozawa Takako. 2002. Direct scavenging of nitric oxide and superoxide by green tea. *Food and Chemical Toxicology*, **40**: 1745-1750. Doi: [10.1016/S0278-6915\(02\)00169-2](https://doi.org/10.1016/S0278-6915(02)00169-2)

National Cancer Institute. "Common Cancer Types." Mar. 21, 2014.

Ndongo Joseph T., Ngo-MbingJoséphine, Tal Michel F., Monteillier Aymeric, Pegnyemb Dieudonné E., Cuendet Muriel, Laatsch Hartmut. 2017. Indoline alkaloids from *Tabernaemontana contorta* with chemopreventive activity. *Phytochemistry*, **144**: 189-196. Doi: [10.1016/j.phytochem.2017.09.013](https://doi.org/10.1016/j.phytochem.2017.09.013)

- Neidowicz Dana M, Daleke David L. 2005. The role of oxidative stress in diabetic complications. *Cell Biochemistry and Biophysics*, **43**: 289-330. Doi: [10.1385/CBB:43:2:289](https://doi.org/10.1385/CBB:43:2:289)
- Ness Andrew R., Powles John W. 1997. Fruit and vegetables, and cardiovascular disease: a review. *International Journal of Epidemiology*, **26**: 1-13. Doi: [10.1093/ije/26.1.1](https://doi.org/10.1093/ije/26.1.1)
- Ngouela Silvère A. 1990. Contribution à l'étude chimique des plantes médicinales du Cameroun, *Spathodea campanulata* (Bignoniaceae). Thèse de Doctorat de 3^{ème} Cycle, Université de Yaoundé, Cameroun, 45-48.
- Nielsen Helene B., Hazell Allan, Hazell Rita, Ghia Felipe, Torrsell Kurt B.G. 1994. Indole alkaloids and terpenoids from *Tabernaemontana markgrafiana*. *Phytochemistry*, **37**: 1729-1735. Doi: [10.1016/S0031-9422\(00\)89601-6](https://doi.org/10.1016/S0031-9422(00)89601-6)
- Oikawa Saeko T., Hiraku Yusuke, Kawanishi Michiko, Kawanishi Shosuke. 2003. Mechanism of generation of hydrogen peroxide and change of mitochondrial membrane potential during rotenone-induced apoptosis. *Life sciences*, **73**: 3277-3288. Doi: [10.1016/j.lfs.2003.06.013](https://doi.org/10.1016/j.lfs.2003.06.013)
- Osborn Anne., Goss Rebecca J.M., Field Robert A. 2011. The saponins-polar isoprenoids with important and diverse biological activities. *Natural Product Reports*, **28**: 1261-68. Doi: [10.1039/C1NP00015B](https://doi.org/10.1039/C1NP00015B)
- Otto Stapf. 1904. Flora of Tropical Africa, **4**: 24
- Oueslati Habib M., Jannet Hichem B., Mighri Zine, Chriaa J., Abreu Pedro M. 2006. Phytochemical Constituents from *Salsola tetrandra*. *Journal of Natural Product*, **69**: 1366-1369. Doi: [10.1021/np060222w](https://doi.org/10.1021/np060222w)
- Ourisson Guy, Albrecht Pierre. 1992. Hopanoids. 1. Geohopanoids-the most abundant natural products on Earth. *Accounts of Chemical Research*, **25**: 398-402. Doi: [10.1021/ar00021a003](https://doi.org/10.1021/ar00021a003)
- Pallant Chris, Cromarty Allan D., Steenkamp Vanessa. 2012. Effect of an alkaloidal fraction of *Tabernaemontana elegans* (Stapf.) on selected micro-organisms. *Journal of Ethnopharmacology*, **140**: 398-404. Doi: [10.1016/j.jep.2012.01.036](https://doi.org/10.1016/j.jep.2012.01.036)
- Park Eun-Jung, Min Hye-Young, Ahn Yong-Hyun, Bae Cheol-Man, Pyee Jae-Ho, Lee Sang-Kook. 2004. Synthesis and inhibitory effects of pinosylvins derivatives on prostaglandin E2 production in lipopolysaccharide-induced mouse macrophage cells. *Bioorganic and Medicinal Chemistry Letters*, **14**: 5895-5898. Doi: [10.1016/j.bmcl.2004.09.022](https://doi.org/10.1016/j.bmcl.2004.09.022)
- Pereira Paulo S., Ticli Fabio K., De Suzelei, França Suzelei C., Moniz Camila, Breves Moniz de Souza, Lourenço Miriam V. 2007. Enhanced triterpene production in *Tabernaemontana catharinensis* cell suspension cultures in response to biotic elicitors. *Química Nova*, **30**: 1849-1852. Doi: [10.1590/S0100-40422007000800010](https://doi.org/10.1590/S0100-40422007000800010)
- Pereira Paulo S., França Suzelei de Castro, Oliveira Paulo V.A., Breves Moniz de Souza C., Pereira Sarazetel.V. 2008. Chemical constituents from *Tabernaemontana catharinensis* root

bark: A brief NMR review of indole alkaloids and *in vitro* cytotoxicity. *Química Nova*, **31**: 20-24. Doi: [10.1590/S0100-40422008000100004](https://doi.org/10.1590/S0100-40422008000100004)

Prakash Chaturvedula S.V., J Schilling K., Randall Johnson K., D Kingston G.I. 2003. New Cytotoxic Lupane Triterpenoids from the Twigs of *Coussarea paniculata*. *Journal of Natural Product*, **66**: 419-422. Doi: [10.1021/np0204848](https://doi.org/10.1021/np0204848)

Prakash Chaturvedula V.S., Sprague Simon, Schilling Jennifer K., Kingston David G. 2005. New cytotoxic indole alkaloids from *Tabernaemontana calcarea* from the Madagascar rainforest. *Journal of Natural Product*, **66**: 528-31. Doi: [10.1021/np058092z](https://doi.org/10.1021/np058092z)

Qi Xiangbing, Bakht Saleha, Leggett Mike, Maxwell C., Melton Rachel, Osbourn Anne. 2004. A gene cluster for secondary metabolism in oat: implications for the evolution of metabolic diversity in plants. *Proceedings of the National Academy of Sciences, USA*, **101**:8233-38. Doi: [10.1073/pnas.0401301101](https://doi.org/10.1073/pnas.0401301101)

Quere Luc, Wenger Traudl, Schramm Hans J. 1996. Triterpenes as potential dimerization inhibitors of HIV-1 protease. *Biochemical and Biophysical Research Communications*, **227**: 484-8. Doi: [10.1006/bbrc.1996.1533](https://doi.org/10.1006/bbrc.1996.1533)

Ringbom Therese, Segura Laura, Noreen Ylva, Perera Premila, Bohlin Lars. 1998. Ursolic acid from *Plantago major*, a selective inhibitor of cyclooxygenase-2 catalyzed prostaglandin biosynthesis. *Journal of Natural Product*, **61**: 1212-5. Doi: [10.1021/np980088i](https://doi.org/10.1021/np980088i)

Rizo Wallace F., Ferreira Luis E., Colnaghi Vanessa, Martins Juliana S., Franchi Leonardo P., Takahashi Catarina S., Belebony Rene O., Marins Mozart, Pereira Paulo S., Fachin Ana L. 2013. Cytotoxicity and genotoxicity of coronaridine from *Tabernaemontana catharinensis* A.DC in a human laryngeal epithelial carcinoma cell line (Hep-2). *Genetics and Molecular Biology*, **36**: 105-110. Doi: [10.1590/S1415-47572013005000010](https://doi.org/10.1590/S1415-47572013005000010)

Rodney Croteau, Toni M. Kutchan, Norman G. Lewis. 2000. Natural products (secondary metabolites) in Biochemistry and Molecular Biology of plants by B. Buchanan, W. Gruissem, R. Jones, *American Society of Plant Physiologists* 1250-1318

Rodríguez Jaime A., Astudillo Luis, Schmeda-Hirschmann Guillermo. 2003. Oleanolic acid promotes healing of acetic acid-induced chronic gastric lesions in rats. *Pharmaceutical Research*, **48**: 291-4. Doi: [10.1016/S1043-6618\(03\)00155-5](https://doi.org/10.1016/S1043-6618(03)00155-5)

Rubinstein Ian, Goad JohnL, Clague A.D.H, Mulheirn Lawrence J. 1976. The 220 MHz NMR spectra of phytosterols. *Phytochemistry* **15**: 195-200. Doi: [10.1016/S0031-9422\(00\)89083-4](https://doi.org/10.1016/S0031-9422(00)89083-4)

Ruzica Leyla. 1953. The isoprene rule and the biogenesis of terpenic compounds *Experiential* 9:357. Doi:[10.1007/bf02167631](https://doi.org/10.1007/bf02167631)

Sawai Satoru, Saito Kazuki. 2011. Triterpenoid biosynthesis and engineering in plants. *Frontiers in Plant Science*, **2**: 25. Doi: [10.3389/fpls.2011.00025](https://doi.org/10.3389/fpls.2011.00025)

Schottenfeld David, Fraumeni Jr Joseph F. 2006. Cancer epidemiology and prevention: Oxford University Press.

Seebacher Werner, Simic Nebojsa, Weis Robert, Saf Robert, Kunert Olaf. 2003. Spectral Assignments and Reference Data: Complete assignments of ¹H and ¹³C NMR resonances of oleanolic acid, 18a-oleanolic acid, ursolic acid and their 11-oxoderivatives. *Magnetic Resonance Chemistry*, **41**: 636-638. Doi:[10.1002/mrc.1214](https://doi.org/10.1002/mrc.1214)

Sengbush Peter V. 2003. Alkaloids. *Botany online*. WEB: University of Hamburg.

Sheludko Yuri, Gerasimenko Irina, Kolshorm Heinz, Stokight Joachim. 2002. Isolation and structure elucidation of a new indole alkaloid from rauvilfia serpentine hairy root culture: The first naturally occurring alkaloid of the raumaciline group. *Planta Medica*, **68**: 435-439. Doi:[10.1021/np0200919](https://doi.org/10.1021/np0200919)

Sheu Fuu, Lai Hsi-Huai, YenGow-Chin. 2001. Suppression effect of soy isoflavones on nitric oxide production in RAW 264.7 macrophages. *Journal of Agricultural and Food Chemistry*. **49**: 1767-1772. Doi: [10.1021/jf001198+](https://doi.org/10.1021/jf001198+)

Siegel Rebecca L., Miller Kimberly D., Jemal Ahmedin. 2016. Cancer statistics, CA: *A Cancer Journal for Clinicians*, **66**: 7-30. Doi: [10.3322/caac.21332](https://doi.org/10.3322/caac.21332)

Steele J. C., Warhurst D.C., Kirby G.C., Simmonds M.S.J. 1999. Invitro and invivo evaluation of betulinic acid as an antimalarial. *Phytotherapy Research*, **13**: 115-9. Doi:[10.1002/\(SICI\)1099-1573\(199903\)13:2<115::AID-PTR404>3.0.CO;2-1](https://doi.org/10.1002/(SICI)1099-1573(199903)13:2<115::AID-PTR404>3.0.CO;2-1)

Subbaramaiah K., Michaluart Pedro, Sporn Michael B., Dannenberg Andrew J. 2000. Ursolic acid inhibits cyclooxygenase-2 transcription in human mammary epithelial cells. *Cancer Research*, **60**: 2399-404.

Surh Young-Joon, Chun Kyung-Soo, Cha Hyun-Ho, Han Seong Su, Keum Young-Sam, Park Kwang-Kyun, Lee Sang Sup. 2001. Molecular mechanisms underlying chemopreventive activities of anti-inflammatory phytochemicals: down-regulation of COX-2 and iNOs through suppression of NF-(B) activation. *Mutation Research*, **481**: 243-268. Doi:[10.1016/S0027-5107\(01\)00183-X](https://doi.org/10.1016/S0027-5107(01)00183-X)

Surya Shashikumar, Poornima Kannappan, Ravikumar Gurram Kalaiselvi, M, Duraisamy, Gomathi, Gopalakrishnan, Velliyur Kanniappan. 2011. In Vitro antioxidant activity and phytochemical screening of ethanolic extract of *Tabernaemontana coronaria* (L.). *Pharmacologyonline*, **2**: 212-218.

Suwito Hery, Heffen Wan Lelly, Cahyana Herry, Suwarso Wahyudi P. 2016. Isolation, transformation, anticancer and apoptosis activity of lupeyl acetate from *Artocarpus integra*. AIP Conference Proceedings 1718, 080004; Doi: [10.1063/1.4943339](https://doi.org/10.1063/1.4943339)

Tandon Rajiv, Goldman Robert S., Goodson Joann, Greden John F. 1990. Mutability and relationship between positive and negative symptoms during neuroleptic treatment. *Biological Psychiatry*, **27**: 1323-1326. Doi: [10.1016/0006-3223\(90\)90502-S](https://doi.org/10.1016/0006-3223(90)90502-S)

Tapondjou Leon A., Lontsi David, Sondengam Beibam L., Choi Jondwon, Lee Kyung-Tae, Jung Hyun-Jun, Park Hee-Juhn. 2003. In vivo anti-nociceptive and anti-inflammatory effects of the two triterpenes, ursolic acid and 23-hydroxyursolic acid from *Cussonia bancoensis*. *Archives Pharmacal Research*, **26**: 143-6. Doi: [10.1007/bf02976660](https://doi.org/10.1007/bf02976660)

Thambi Priya T., Kuzhivelil Bindu, Sabu MC. 2006. Antiooxidant and anti-inflammatory activities of the flowers of *T.coronaria*. *Indian Journal of Pharmaceutical Science*, **68**: 352-355. Doi:[10.4103/0250-474X.26675](https://doi.org/10.4103/0250-474X.26675)

Thimmappa Ramesha, Geisler Katrin, Louveau Thomas, O'Maille Paul, and Osbourn Anne. 2014. Triterpene Biosynthesis in Plants. *Annual Review of Plant Biology*, **65**: 16.1-16.33 Doi: [10.1146/annurev-arplant-050312-120229](https://doi.org/10.1146/annurev-arplant-050312-120229)

Thomas Roman K., Baker Alissa C., Debiassi Ralph M., Winckler Wendy, Laframboise Thomas, Lin William M., Wang Meng, Feng Whei, Zander Thomas, Mac Cornaill L., Lee Jeffrey C., Nicoletti Rock, Hatton Charlie, Goyette Mary, Girard Luc, Majmudar Kuntal, Ziaugra Liuda, Wong Kwok-Kin, Gabriel Stacey, Beroukhim Rameen, Peyton Michael, Barretina Jordi, Amit Dutt, Caroline Emery, Heidi Greulich, Kinjal Shah, Hidefumi Sasaki. 2007. High-throughput oncogene mutation profiling in human cancer. *Nature Genetics*, **39**: 347-51. Doi: [10.1038/ng1975](https://doi.org/10.1038/ng1975)

Van Beek Teris A., Verpoort Rob, Baerheim Svendsen A., Leeuwenberg Anthony J.M., Bisset Norman G., 1984. *Tabernaemontana* L. (Apocynaceae): A review of its taxonomy, phytochemistry, ethnobotany and pharmacology. *Journal of Ethnopharmacology*, **10**: 1-156. Doi: [10.1016/0378-8741\(84\)90046-1](https://doi.org/10.1016/0378-8741(84)90046-1)

Van Dyck Severine, Gerbaux Pascal, Flammang Patrick. 2010. Qualitative and quantitative saponin contents in five sea cucumbers from the Indian Ocean. *Marine Drugs*, **8**: 173-89 Doi: [10.3390/md8010173](https://doi.org/10.3390/md8010173).

Villasenor Irene M., Angelada Jennifer, Canlas Arlyn P., Echegoyen Deborah. 2002. Bioactivity Studies on β -Sitosterol and its Glucoside phytotherapy research, **16**: 417-421. Doi: [10.1002/ptr.910](https://doi.org/10.1002/ptr.910)

WHO, 2018. Latest global cancer data: Cancer burden rises to 18.1 million new cases and 9.6 million cancer deaths in 2018. *International Agency for Research on Cancer*. Press release n° **263**.

Wilcox Christopher S. 2005. Oxidative stress and nitric oxide deficiency in the kidney: a critical link to hypertension? *American Journal of Physiology-Regulatory Integrative and Comparative Physiology*, **289**: 913-935. Doi: [10.1152/ajpregu.00250.2005](https://doi.org/10.1152/ajpregu.00250.2005)

Winterstein E., Trier G. 1910. Die Alkaloide. Eine Monographie dernationalen, Base. Berlin

Xian Li-N., Qian Shi-Hui, Li Zhen-Lin. 2010. Studies of chemical constituents from the stems of *Acanthopanax gracilistylus*. *Zhong Yao cai*, **33**: 538-542.

Xu Ran, Fazio Gia C., Matsuda Seiichi P.T. 2004. On the origins of triterpenoid skeletal diversity. *Phytochemistry*, **65**: 261-91. Doi: [10.1016/j.phytochem.2003.11.014](https://doi.org/10.1016/j.phytochem.2003.11.014)

Yamashita Kochi, Lu Huangwei, Lu Jincui, Chen Guang, Yokoyama Takeshi, Sagara Yasuhiro, Manabe Masanobu, Kodama Hiroyuki. 2002. Effects of three triterpenoids, lupeol, betuline, and betulinic acid on the stimulus-induced superoxide generation and tyrosyl

phosphorylation of proteins in human neutrophils. *Clinica Chiica Acta*, **325**: 91-6. Doi: [10.1016/S0009-8981\(02\)00252-8](https://doi.org/10.1016/S0009-8981(02)00252-8)

Yaya A.J.G., Feumba R.D., Emmanuel R.D., Tiabo A.T., Frederich M., Oben J., Mbafor J.M. antioxidant activity of compounds isolated from *Erythrina droogmansiana*. *International Journal of Pharmaceutical Sciences and Drug Research*, **6**: 160-163.

Yoo Keun Y., Shin Hai R. 2003. Cancer epidemiology and prevention. *Korean Journal of Epidemiology*, **25**:1-15.